

UNRAVELING THE ROLE OF THE ENDOGENOUS COMPLEX GUT MICROBIOTA IN
THE PIRC RAT MODEL OF HUMAN COLON CANCER

A Dissertation

presented to

the Faculty of the Graduate School

at the University of Missouri-Columbia

In Partial Fulfillment

of the Requirements for the Degree

Doctor of Philosophy

by

SUSHEEL BHANU BUSI

Dr. James Amos-Landgraf, Dissertation Supervisor

DECEMBER 2018

© Copyright by Susheel Bhanu Busi 2018

All Rights Reserved

The undersigned, appointed by the dean of the Graduate School, have examined the dissertation entitled

UNRAVELING THE ROLE OF THE ENDOGENOUS COMPLEX GUT MICROBIOTA IN
THE PIRC RAT MODEL OF HUMAN COLON CANCER

presented by Susheel Bhanu Busi,

a candidate for the degree of doctor of philosophy

and hereby certify that, in their opinion, it is worthy of acceptance.

Dr. James Amos-Landgraf

Dr. Craig Franklin

Dr. Aaron Ericsson

Dr. Susan Deutscher

Dr. Sharad Khare

Dr. Michael Calcutt

ACKNOWLEDGEMENTS

“I shall be telling this with a sigh
Somewhere ages and ages hence:
Two roads diverged in a wood, and I—
I took the one less traveled by,
And that has made all the difference.”
~ The Road Not Taken, Robert Frost

I am grateful to God Almighty for his continued sustenance, patience and immeasurable love. You have been benevolent and omnipresent.

I would like to express my sincere gratitude to my advisor, Dr. James Amos-Landgraf whose constant encouragement, challenges, guidance and willingness to share from his abundant wealth of knowledge and experience made my story an easy one to tell. You have molded me into a better scientist and a critical thinker. You will always remain a source of encouragement and I feel well prepared for the next step in my scientific career, thanks to you.

A very special thanks to my committee members, Dr. Craig Franklin, Dr. Aaron Ericsson, Dr. Michael Calcutt, Dr. Susan Deutscher and Dr. Sharad Khare. It was wonderful learning from each and every one of you. I greatly appreciate your tremendous support and help. You have taught me many things about ways to approach science, but more importantly you have given me the desire to mentor someone, someday, the way you guided me.

Special thanks to my current and former lab colleagues and friends, Taybor Parker, Sarah Hansen, Jake Moskowitz, for all your suggestions and help. Sarah, you have been instrumental in improving my confidence and my ability to perform surgeries. Never did I imagine that my unsteady hands could hold a scalpel and make a straight incision, but you changed that. You have and will always be a good friend, one that I can count on always. Daniel Davis and Marcia Hart: thank you both for the innumerable conversations about science and the intricacies of life revolving around the complexities of science and graduate school. Our conversations have been great stimulants for my research and I've always looked forward to the Friday mornings where new ideas were forged.

The complexities and the travails of graduate school are not easy to navigate, until you have an awesome support team that includes Shelly Nail, Jana Clark, Shelly Crawford and Kathy LaMere. Shelly and Jana, you were always available and answered patiently my most trivial of questions. Thank you! I would also like to thank the entirety of Discovery Ridge and every one of its members including the IDEXX personnel. I would also like to thank Dr. Laura Page, the Office of Graduate Studies, and the MMI office team for always being there to address my concerns.

Last but by no means the least of all. My paramount love, appreciation and gratitude goes to my lovely wife. Runu Lata Busi; the one constant during my joyous times but most importantly my inspiration in the challenging moments. Her patience with me knows no boundaries. Runu, without you this would not have been possible. I thank God every day for you and for that moment of clarity in my life when He chose you to be my partner forever. I can't wait to go on several more adventures with you, tackling life's

challenges, one day at a time. I would also like to thank my parents, Rt. Rev. Dr. Suneel Bhanu Busi and Dr. Grace Bhanu. Throughout the years, as difficult as I have been, you were always supportive and encouraged my learning, starting from that day where you dropped me at school in Vizag. For your unconditional understanding and love, thank you! My brother, Santhosh Busi is the most hardworking, devoted and affectionate person I've known. Thank you for your constant support and motivation. My affection and gratitude also goes to the other half of my family, Meghanad and Pramila Bahadi, Rinku, Arvind and Manoj. Over the years, you have all been so reassuring and kind towards my absenteeism.

This journey would have been incomplete without key roles played by my extended family: the Lankapallis. Without the joy of growing up with, knowing and hanging out with you, my voyage would be inadequate. I also need to thank all my friends who have augmented my learning and development in various ways. The Phillips; thank you for teaching me that life is not about work alone, but rather duck-pin bowling needs a place in it. The Georges, the Pauls, the Coxs, the Greens, and the Silivas; thank you for making me a part of your family and for opening up your home to me. And finally, Varun Paul and Mohit Daber; for ages we have spent hours on the phone discussing life's minutiae and shared more than a moment of God's own time with each other. It has been a privilege to learn from both of you, and to know that in all of my mischievous, troubled, and joyful times I will have my best friends sticking it out with me. May history speak volumes of our friendship and may time commemorate the memories that we have shared. Thank you both for being a part of this journey, here's to many more endless experiences!

TABLE OF CONTENTS

ACKNOWLEDGEMENTS ii

LIST OF ABBREVIATIONSx

LIST OF FIGURES xiii

LIST OF TABLES xvii

ABSTRACT xix

CHAPTERS 1

 I. UNDERSTANDING THE ROLE OF THE MICROBIOME IN COLON
 CANCER 1

 1. Overview2

 2. Colon cancer: genetics and models4

 3. Gut microbiome and colon cancer susceptibility7

 4. Microbiota-induced inflammation/immune responses in CRC12

 5. Methods to unravel the complexity of the GM: Altered Schaedler Flora and
 Complex Microbiota Targeted Rederivation (CMTR)16

 6. Pirc rat model of colon cancer and differential susceptibility due to GM18

 7. Biofilms and colon cancer etiology19

 8. Beyond bacterial profiling and associations20

 9. Concluding remarks22

 II. EARLY TREATMENT WITH *FUSOBACTERIUM NUCLEATUM* SUBSP.
 POLYMORPHUM OR *PREVOTELLA COPRI* DECREASES TUMOR BURDEN
 IN THE PIRC RAT MODEL OF HUMAN FAMILIAL ADENOMATOUS
 POLYPOSIS24

1. Overview	25
2. Methods	26
3. Results	31
3.1. Early administration of <i>Fusobacterium nucleatum</i> subsp. <i>polymorphum</i> or <i>Prevotella copri</i> alleviates early tumor multiplicity in the Pirc rat	31
3.2. Average adenoma burden is not modulated by early bacterial treatment ..	32
3.3. GM population richness and diversity is unaffected by bacterial administration prior to disease onset	33
3.4. <i>Fn. polymorphum</i> treatment modulates the endogenous gut microbiota structure immediately after treatment	33
3.5. <i>Fn. polymorphum</i> treatment modulates the predicted microbiota metabolic capacity	33
3.6. GM structure maintains differences post-treatment at 2 months of age ...	34
3.7. GM profile and function modulated by <i>P. copri</i> treatment regardless of colonization	35
4. Discussion	35
5. Ethics Statement	40
6. Author Contributions and Acknowledgements	40
7. Figures	41
8. Tables	61
 III. UTILITY OF THE PIRC RAT MODEL OF HUMAN COLON CANCER TO TEST THE ROLE OF SPECIFIC BACTERIAL TAXA ON INTESTINAL ADENOMA DEVELOPMENT	 65

1. Overview	66
2. Methods	69
3. Results	79
3.1. Biofilm-competent <i>Desulfovibrio vulgaris</i> Hildenborough (DvH-MT) suppresses adenoma size in Pirc rats	79
3.2. DvH colonization modulates complex GM architecture	79
3.3. Type 1 secretion system (T1SS) ABC transporter is essential for colonization of Pirc rats	80
3.4. Endogenous complex GM community structure is modified due to DvH treatment	81
3.5. T1SS-competent DvH treatment is associated with decreased adenoma burden	82
3.6. Fecal sulfide levels are decreased in JWT733 treatment compared to the control and JWT716 groups	83
4. Discussion	85
5. Ethics Statement	93
6. Author Contributions and Acknowledgements	93
7. Figures	94
8. Tables	118
IV. SHIFT FROM A SIMPLIFIED TO COMPLEX GUT MICROBIOTA REDUCES ADENOMA BURDEN IN A PRECLINICAL RAT MODEL OF COLON CANCER	125
1. Overview	126

2. Methods	127
3. Results	132
3.1. Nominal taxa incursion in the Charles River Altered Schaedler Flora ...	132
3.2. Simplified gut microbiota increases susceptibility to colonic adenomas .	133
3.3. Altered Schaedler Flora alters the colonic adenoma phenotype and the physiology of the gastrointestinal tract	134
3.3. Conventional housing affects the GM architecture at 4 months of age	135
3.4. Barrier and conventional room diets have distinct GM populations	137
4. Discussion	138
5. Ethics Statement	143
6. Author Contributions and Acknowledgements	144
7. Figures	145
8. Tables	169
V. INTEGRATED METABOLOME AND TRANSCRIPTOME ANALYSES PROVIDE NOVEL INSIGHT INTO COLON CANCER MODULATION BY THE GUT MICROBIOTA	170
1. Overview	171
2. Methods	173
3. Results	181
3.1. Metabolite features at 1 month of age predict tumor susceptibility and severity at later developmental stages	181

3.2. Metabolomics analyses indicate differential metabolic profiles between GM:F344 and GM:LEW	181
3.3. Bile acid biosynthesis and aspirin-triggered resolvin E biosynthesis pathways are most affected due to putative fecal metabolomics features	182
3.4. Gut microbiota alters gene expression in both the normal epithelium and tumor tissues	183
3.5. Pathway analyses identify potential mechanisms contributing to high and low colonic tumor susceptibility	183
4. Discussion	185
5. Ethics Statement	190
6. Author Contributions and Acknowledgements	190
7. Figures	191
8. Tables	211
VI. CONCLUSIONS AND FUTURE DIRECTIONS	215
1. Conclusive Highlights	216
2. Future Directions	220
3. Graphical Abstract: effect of <i>Desulfovibrio vulgaris</i> Hildenborough on adenomas in Pirr rats	225
BIBLIOGRAPHY	226
VITA	282

LIST OF ABBREVIATIONS

ANOVA	Analysis of variance
AOM	Azoxymethane
APC	<i>Adenomatous polyposis coli</i>
<i>argH</i>	Argininosuccinate lyase
ASF	Altered Schaedler Flora
AT	Ambiguous taxa
ATCC	American Type Culture Collection
BD	Becton Dickinson
CA	California
CFU	Colony forming unit
CMTR	Complex microbiota targeted rederivation
CRASF	Charles River Altered Schaedler Flora
CRC	Colorectal cancer
CTLA	Cytotoxic T-lymphocyte-associated antigen
DEG	Differentially expressed gene(s)
DNA	Deoxyribonucleic acid
DSMZ	Deutsche Sammlung von Mikroorganismen und Zellkulturen
DSS	Dextran sodium sulfide
DvH	<i>Desulfovibrio vulgaris</i> Hildenborough
EDTA	Ethylenediaminetetraacetic acid
ETBF	Enterotoxigenic <i>Bacteroides fragilis</i>
F344	Fisher 344
F	Female
FAP	Familial adenomatous polyposis
FC	Fold-change
FDR	False discovery rate
FISH	Fluorescent In-Situ Hybridization
Fn	<i>Fusobacterium nucleatum</i>
GC	Gas chromatography
GF	Germ-free
GI	Gastrointestinal tract
GM	Gut microbiota/gut microbiome
GM-CSF	Granulocyte-macrophage colony-stimulating factor
GM:F344	F344/NHsd x F344/Ntac-Pirc gut microbiome
GM:LEW	Lewis gut microbiome
GWAS	Genome-wide association studies
HIF	Hypoxia-induced factor
HMP	Human microbiome project
HNPCC	Hereditary nonpolyposis colorectal cancer
HRM	High resolution melt
HUMAnN	HMP unified metabolic analysis network
IBD	Inflammatory bowel disease
IL	Interleukin
IN	Indiana

JWT716	Biofilm-deficient <i>Desulfovibrio vulgaris</i> Hildenborough
JWT733	Biofilm-competent <i>Desulfovibrio vulgaris</i> Hildenborough
KEGG	Kyoto Encyclopedia of Genes and Genomes
LC	Liquid chromatography
LDA	Linear discriminant analysis
LEW	Lewis rat
LPS	Lipopolysaccharide
M	Male
MA	Massachusetts
MAP	MYH-associated polyposis
MD	Maryland
ME	Maine
MMI	Molecular Microbiology and Immunology
MO	Missouri
MS	Mass spectrometry
MS/MS	Tandem mass spectrometry
MT	Montana
MU	University of Missouri
MUMC	MU Metagenomics Core
NA	Not applicable/available
NE	Normal epithelium
NF- κ B	nuclear factor kappa-light-chain-enhancer of activated B cells
NGS	Next-generation sequencing
NIH	National institute of health
NJ	New Jersey
NK	Natural killer
NKT	Natural killer T cell
NMDS	Non-metric dimensional scaling
NMR	Nuclear magnetic resonance
NOD	Non-obese diabetic
OTUs	Operational taxonomic unit(s)
PA	Pennsylvania
PAST	Paleontological statistics
PBS	Phosphate-buffered saline
PCA	Principal component analysis
PCoA	Principal coordinate analysis
PCR	Polymerase chain reaction
PD-L1	Programmed death-ligand 1
PERMANOVA	Permutational multivariate analysis of variance
PHD	prolyl hydroxylase domain
PICRUSt	Phylogenetic investigation of communities by reconstruction of unobserved states
PIRC	Polyposis in rat colon
PPE	Personal protective equipment
PRR	Pattern recognition receptor
qRT-PCR	Quantitative real-time polymerase chain reaction

RA	Rheumatoid arthritis
RB	Rumen bacterium
RBS	Ribosomal binding site
RGD	Rat genome database
RMD	Relative mass defect
RNA	Ribonucleic acid
RQI	RNA quality index
RTX	Repeat-in-toxin
SCFA	Short chain fatty acid
SD	Sprague-Dawley rat
SEM	Standard error of the mean
SI	Small intestine
SLIC	Sequence and ligation independent cloning
SNP	Single nucleotide polymorphism
SPE	Solid phase extraction
SPF	Specific-pathogen free
SRB	Sulfate-reducing bacteria
Subsp.	Subspecies
T	Tumor tissue
T1D	Type 1 diabetes
T1SS	Type 1 secretion system
TGCA	The Cancer Genome Atlas
TGF	Transforming growth factor
TLR	Toll-like receptor
TM	Trademark
TOPO	Topoisomerase
TSB	Tryptic soy broth
TSBA	Tryptic soy blood agar
TX	Texas
UB	Uncultured bacterium
UO	Uncultured organism
UCG	Uncultured Genus
USA	United States of America
WI	Wisconsin
WMGM	Wild mouse gut microbiota
WT	Wildtype

LIST OF FIGURES

CHAPTER II

Figure 1. Tumor multiplicity of rats treated with <i>Fusobacterium nucleatum</i> subsp. <i>polymorphum</i> or <i>Prevotella copri</i>	41
Figure 2. Early <i>Fn. polymorphum</i> treatment alleviates tumor multiplicity in the Pirc rat	42
Figure 3. Richness and diversity of the GM population	43
Figure 4. 16S rDNA sequencing analysis of <i>Fn. polymorphum</i> treated rats	44
Figure 5. 16S rDNA sequencing analysis of <i>Fn. polymorphum</i> treated rats at 2 months of age	48
Figure 6. 16S rRNA gene sequencing analysis of control and <i>P. copri</i> -treated rats	52
Supplementary figure 1. Pirc rat treatment with <i>F. nucleatum</i> subsp. <i>polymorphum</i> or <i>P. copri</i>	56
Supplementary figure 2. GM structure at 1 week post-treatment in rats treated with <i>F. nucleatum</i> subsp. <i>polymorphum</i>	58
Supplementary figure 3. PICRUS _t analysis of control and <i>P. copri</i> rats at 1 week post-treatment	60

CHAPTER III

Figure 1. Pirc rat treatment with Type 1 secretion system (T1SS) ABC transporter – competent (JWT733) and –deficient (JWT716) strains of DvH	94
--	----

Figure 2. 16S rRNA gene sequencing analysis of control, JWT733 and JWT716 groups	98
Figure 3. Tumor multiplicity, average tumor burden and OTU-tumor correlations in control and treated Piric rats	101
Figure 4 Sulfide assay and qRT-PCR gene expression of rat and bacterial sulfate reduction genes	104
Supplementary figure 1. Treatment of Piric rats with biofilm -competent and -deficient <i>Desulfovibrio vulgaris</i> Hildenborough (DvH)	106
Supplementary figure 2. Adenoma images via colonoscopy in DvH-treated Piric rats	108
Supplementary figure 3. 16S rRNA gene sequencing analysis of DvH treatment	109
Supplementary figure 4. Colonoscopy of fluorescent, T1SS-competent strain-treated rats	111
Supplementary figure 5. Fluorescent in-situ hybridization (FISH) and confocal microscopy assessing biofilm formation <i>in vivo</i> in the JWT733 treated rats	112
Supplementary figure 6. 16S rDNA analysis of fecal and biopsy samples from the control, JWT733 and JWT716 groups	113
Supplementary figure 7. Correlogram analysis of OTUs vs tumor multiplicity at 1 week post-treatment and 2 months of age	114
Supplementary figure 8. QRT-PCR analysis of gene expression in control, JWT733 and JWT716 groups	116

CHAPTER IV

Figure 1. 16S sequencing analysis of fecal microbiota in CRASF rats pre- and post-shipping	145
Figure 2. Colonic and small intestinal adenoma multiplicity of barrier and conventional rats at 4 months of age	148
Figure 3. Effect of Altered Schaedler Flora on the colonic adenoma phenotype and the physiology of the gastrointestinal tract	149
Figure 4. 16S sequencing analysis of fecal microbiota in F1-Pirc rats at weaning	152
Figure 5. Effect of conventional housing on the GM at 4 months of age	155
Figure 6. Correlation analysis of OTUs from barrier and conventional rooms with colonic tumor count at 4 months of age	158
Supplementary figure 1. Experimental design	161
Supplementary figure 2. GM profile and predicted metabolic function of barrier and conventional rats at 4 months of age	162
Supplementary figure 3. Correlation analysis of OTUs with colonic tumor count	164
Supplementary figure 4. Bacterial population analysis of barrier and conventional room feed via 16S rDNA sequencing	165
Supplementary figure 5. 16S analysis of cultured feed from barrier and conventional rooms	167

CHAPTER V

Figure 1. Experimental design	191
Figure 2. Metabolite features at 1 month of age predict tumor susceptibility and severity...	192
Figure 3. Metabolomics analyses indicate differential features between GM:F344 and GM:LEW	195
Figure 4. Bile acid biosynthesis and aspirin-triggered resolvin E biosynthesis pathways are most affected by metabolite features	198
Figure 5. GM modulates differential gene expression in the normal epithelium and tumor tissues	199
Figure 6. Pathway and correlation analyses identify potential mechanisms, differential factors contributing to low, and high tumor susceptibility	202
Supplementary figure 1. Serum metabolomics profiles and pathway analyses in Pirc and WT rats	204
Supplementary figure 2. Differentially expressed genes (DEGs) and pathways altered due to GM in the normal epithelium and tumor tissues	206
Supplementary figure 3. Analysis flowchart	209
Supplementary figure 4. Bile acid biosynthesis pathway	210

LIST OF TABLES

CHAPTER II

Table 1. Operational taxonomic units (OTUs) contributing to phenotype in control and <i>Fn. polymorphum</i> treated rats at one week post-treatment	61
Table 2. Operational taxonomic units (OTUs) contributing to phenotype in control and <i>Fn. polymorphum</i> treated rats at 2 months of age	62
Table 3. Operational taxonomic units (OTUs) contributing to phenotype in control and <i>P. copri</i> -treated rats at one week post-treatment	63
Table 4. Operational taxonomic units (OTUs) contributing to phenotype in control and <i>P. copri</i> -treated rats at 2 months of age	64

CHAPTER III

Table 1. Primer and probes used in this study	118
Table 2: Two-Way PERMANOVA post-hoc analysis of GM community profile in fecal and biopsy samples collected at 4 months of age	120
Table 3: One-Way PERMANOVA post-hoc analysis of GM community profile in fecal samples from DvH-treated rats	121
Table 4: Two-Way PERMANOVA post-hoc analysis of GM community profile in fecal and biopsy samples collected at 4 months of age	121
Table 5: Bacterial strains and plasmids used in the study	122

CHAPTER IV

Table 1. Altered Schaedler Flora alters the colonic adenoma phenotype and the physiology of the gastrointestinal tract	169
--	-----

CHAPTER V

Table 1. Compound class, RMD and putative identification of metabolites features in the METLIN databases	211
--	-----

Table 2. Normal epithelium genes involved in the bile acid biosynthesis and aspirin-triggered resolving E biosynthesis pathways	212
---	-----

Table 3. Putative metabolites contributing to bile acid and aspirin-triggered resolving E biosynthesis	213
--	-----

Supplementary Table 1. Summary of data processing results	214
---	-----

ABSTRACT

The gut microbiota (GM) has recently been shown to modulate several systemic conditions in human and model systems, most importantly in intestinal disorders. It has also been demonstrated to have significant impacts on patients' susceptibility to colon cancer. The GM can be defined as the dynamic communities of bacteria, viruses, fungi and archaea that inhabit our gut, skin, and most mucosal surfaces. Considering the fact that the human body is exposed to a large number of microorganisms on a daily basis, the constant flux and dynamic interactions between host genetics and the GM can lead to the variability seen in disease manifestation and susceptibility. This leads to a larger question about the relationship of the GM to model systems, and also whether the constant interactions between the taxa affect the development and progression of disease.

Colon cancer is the 3rd leading cause of cancer-related death in the USA. We used embryo rederivation to give isogenic *APC*-gene mutant Pirc rats, a preclinical model of colon cancer distinct complex GMs to understand its effect on disease susceptibility. In this study, we observed significant differences in intestinal tumor multiplicity based on GM profile. Using 16S rRNA sequencing, we characterized the microbial populations of two distinct GM groups and further determined functional differences by liquid chromatography coupled with tandem mass spectrometry (LC-MS/MS) to identify metabolic differences between GM groups. Colonic epithelium and tumors were simultaneously profiled via RNASeq transcriptome analysis. Metabolomics analysis allowed detection of differential metabolites between GM groups and potential bacterial-modulated biomarkers of tumor susceptibility. Simultaneously, bacterial relative abundances showed taxa correlating with suppression of both tumor growth and

phenotype penetrance as early as 1 month of age. To determine the role of individual bacteria Pirc rats were treated with 3 different bacteria associated with reduced or increased adenoma burden namely, *Desulfovibrio vulgaris* Hildenborough, *Prevotella copri*, and *Fusobacterium nucleatum*. The work outlined here addresses adenoma development in Pirc rats to identify the potential relationship between these taxa and the endogenous, complex GM through multiple approaches. The research presented in this dissertation may potentially help unravel the molecular mechanisms contributing to disease susceptibility, and could identify therapeutic targets and biomarkers for early non-invasive detection and treatment of colon cancer.

CHAPTER I
UNDERSTANDING THE ROLE OF THE MICROBIOME IN
COLON CANCER

1. Overview

Mammalian models such as the mouse and the rat have been invaluable in revealing the fundamental biology behind human diseases and conditions, but until recently the impact of the microbiome on disease phenotypes was often overlooked. The unparalleled advantage of mammalian models has been the ability to highly control both the host genetics and the experimental environmental conditions (1). Even under stringent conditions there is still a large amount of phenotypic variation that is attributed to stochastic deviation, often limiting the translatability and reproducibility of many mammalian models to human disease traits. In 2014, the NIH (National Institute of Health) outlined a policy to enhance reproducibility in biomedical research in response to reports suggesting that research using animal models needed to be more stringent and reproducible (2, 3). Franklin and Ericsson outlined several sources and challenges affecting said reproducibility. The most provocative of these is the animal gut microbiota (GM) that can vary across colonies depending on rodent husbandry and sources from which the animals are obtained. Similarly, several studies speculated that the GM may play a significant role in affecting reproducibility of studies involving mammalian models (1, 4-7).

While it has been known for decades that murine pathogens could have a large impact on disease phenotypes, the highly tested and controlled commensal GM was often dismissed as a weak modifier of genetic phenotypes. The first high impact studies that began to implicate the role of the GM were in classic mouse models that had been extensively studied, and only through rethinking the role of the environment was the GM revealed to be a large, controlling factor of the genetic disease phenotypes. In a study

using the non-obese diabetic (NOD) mouse model of type-1 diabetes (T1D), Markle *et al.* found that genetic and environmental factors affected disease susceptibility (8). A significant feature of this study was the lack of disease in male mice, whereas the females developed T1D under specific-pathogen free conditions. It was posited that the differential susceptibility was due to the GM. Transfer of cecal contents, i.e. the GM from male NOD mice to females, protected against development of diabetes in the females. Despite the controlled genetics, they found that the GM had a key role to play in disease etiology. There have been extensive advancements in identifying host pathogens which were largely performed in standard outbred or highly used inbred mouse or rat strains or stocks from a single or limited vendors. Recent studies, however have established that the source of the mouse strain could be a contributing aspect to the nature of factors affecting the GM such as the immune response (9), including differentiation of Th17 cells in mouse models typically used to study intestinal immunity, tolerance and inflammatory bowel disease (IBD) susceptibility (10), potentially suggesting a role for the gut microbiota.

While the GM may differ within an inbred strain due to its source or vendor, host genetics have also been shown to shape the structure of the gut microbiota (5). Petnicki-Ocwieja *et al.* reported in a model for Crohn's disease, that the GM composition of *Nod2*-deficient mice was significantly different from that of their heterozygous littermates. It was also reported that MYD88-deficient mice showed an increased abundance of segmented filamentous bacteria and increased dysbiosis compared to WT (wildtype) animals (11). Several human and mouse studies have established that host genetics have a lasting effect on the GM, which are in some cases heritable, where

identified taxa were a direct readout of host genetics (12-16). Additionally, it was demonstrated that the IL-10 gene knockout in mice leads to substantial shifts in the taxonomic profile of the GM (9), compared to wildtype mice. This in turn was found to affect arsenic metabolism and biotransformation in the knockout mice (17). Ericsson *et al.* also found that host genetics contributed to the differences in operational taxonomic units (OTUs) that were observed between A/J01aHsd, A/J and C57BL/6 mice (5). Despite the complexity of these studies, there are several features regarding the role of host genetics and the microbiome that are yet to be studied. Single and multiple gene knockouts, and use of mammalian model systems have been the mainstay of studies focused on assaying the role of host genetics in disease susceptibility. Herein, it may be suggested that the complexity and context of disease susceptibility can be modulated by the GM in addition to environmental (18-22) and other classical factors such as host genetics, i.e. somatic mutations including base substitutions, indels, rearrangements and copy number variations aside from epigenetics (23, 24). It is also conceivable that several gene-perturbation studies modelled in mice previously, that seemingly failed and were potentially unreported could have been a consequence of the source of the mice, or due to differences in the GM. Anecdotally, it is often heard but underreported that a phenotype is lost when a colony is rederived from one institution to another suggesting the role of the environment, specifically changes of the GM in a model (1).

2. Colon cancer: genetics and models

A disease that is at the center of the Venn diagram encompassing genetics, animal models and the gut microbiota is colorectal cancer (CRC). CRC with an estimated 97,220

new cases in 2018 alone is the third most common cancer according to the American Cancer Society (Key Statistics for Colorectal Cancer; <https://www.cancer.org/cancer/colon-rectal-cancer>). Patients develop adenomas predominantly in the colon, and while the exact etiology is unknown, the risk factors include environmental, genetic, immunological and life-style components (25). Genetic predisposition, contributes to about 30% of the overall incidence, while the remaining cases are sporadic occurrences (26).

Colon cancer susceptibility is a multifactorial process thought to be primarily affected by genetic predisposition, environmental, immune and lifestyle-associated factors. Known colon cancer predisposing genetic conditions such as familial adenomatous polyposis (FAP), hereditary non polyposis colorectal cancer (HNPCC) or Lynch syndrome, the hamartomatous polyposis syndrome, *MYH*-associated polyposis (MAP) and hyperplastic polyposis, only explain a small fraction of heritability of CRC, with ~40% of the families with a positive family history being unaffected by known CRC syndromes (27, 28). The previous decade of cancer research has focused on host genetic susceptibility and the mutations that drive these disorders. To this end, several genes known for their increased penetrance, especially among familial cases include the gatekeeper adenomatous polyposis coli (APC) gene (29), mismatch repair gene mutations (30) and also the TGF- β (transforming growth factor-beta) gene (31). With the advent of deep sequencing technologies it has been shown that cancers have far more mutations than previously thought, averaging anywhere from 33 to 66 mutated genes contributing to the development of colon cancer (23, 24, 32) that can be perturbed via diet, lifestyle or other factors. Simultaneously, genetic modifiers of the CRC phenotype have been

reported by several groups (33-36), including the group IIA secretory phospholipase A2 gene (*Pla2g2a*) (37). Despite several studies pointing towards the necessary role of the host genome and its subsequent mutations in the development of this disease, the exact mechanisms by which these events are triggered remains elusive to a large extent.

To understand the potential mechanisms through which these mutations might be manifested in the host, many groups have performed genome-wide association studies (GWAS) (38-44) and transcriptome sequencing of the normal and tumor epithelial tissues from colon cancer patients. These studies have identified nearly 37 loci linked with CRC risk that have at least one single nucleotide polymorphism or SNP (45). On the other hand, Peng *et al.* analyzed over 4000 samples coupled with 548 normal tissues from 21 different cancer types acquired through The Cancer Genome Atlas (TCGA). The TCGA is a collection of all the genomes and transcriptomes of tissues from patients with several types of cancers, along with corresponding normal tissues from healthy age-matched patients. Peng *et al.* found that a 14-gene signature identified through their analysis was sufficient to precisely differentiate between tumor and normal samples in non-TCGA cancers such as lung, breast, liver, thyroid, esophagus and colon (46). Meanwhile recent studies have focused on determining the differential RNASeq analysis comparing Apc-defective and Apc-restored colon cancer cell lines such as SW80 (47) or by contrasting primary colorectal carcinomas and liver metastases (48). Meanwhile, Adler *et al.* utilized an integrative approach to appreciating the similarities between mouse and human colon tumors, identifying *PRPF6*, a component of the spliceosome that is both differentially expressed and demonstrated a gain in copy number (49). Though these studies are highly informative, they are limited by the nature of the sample, i.e. cell lines, or the timing of

sample collection (post-onset of disease), albeit showing no observable phenotype. Others have also recently proposed the idea of interpreting single-cell SNP analyses based on RNASeq data (50) or the use of whole-exome sequencing along with RNASeq in routine clinical practices for CRC (51). To understand the altered gene expression profiles in normal appearing mucosa APC mutant mice, Son *et al.* used differential gene expression (DEG) analysis in 6-week old *Apc^{+/-Min}* mice comparing it to that of wildtype animals. 130 genes were found to be differentially expressed between these groups via RNASeq analysis (52). These approaches however, also suffer from the same disadvantages of sample collection laid out previously. While the importance of such studies is undeniable, concrete research determining the role of host genetics and the transcriptome prior to onset of disease and how it shapes disease susceptibility is yet to be established.

3. Gut microbiome and colon cancer susceptibility

A recent report by Brodziak *et al.* suggested that the expression of certain modifier genes was modulated by the gut microbiota (53) while others have described genotoxic compounds observed in fecal water serving as biomarkers for tumor incidence (54-58). Despite reports of such complex associations, interaction between the GM and adenoma development, however is largely under-characterized though bacteria found in the gastrointestinal (GI) tract are thought to be responsible for CRC etiology (59-64). The vast majority of these recent studies suffer from the lack of longitudinal data and are retrospective associations. In 2000, Homann *et al.* while studying the role of alcohol on colorectal cancer suggested that alcohol administration to rats led to folate deficiency in

the colonic mucosa, likely due to the high levels of acetaldehyde *microbially* produced from ethanol (65). Half a decade later the human gut microbiome was discussed as having potential implications not only for development of novel therapeutic interventions but also for personalized health care regimens (66-68).

The largest of gut microbiota communities exists in the colon, harboring nearly 10^{14} bacterial cells including families and phyla such as *Lachnospiraceae*, *Firmicutes* and *Bacteroidetes*. These taxa are thought to encompass the majority of the OTUs found in the gastrointestinal tract, especially in the context of those found in CRC patients. These numbers vary depending on various factors, and are less prevalent in the small intestine increasing in abundance from duodenum to ileum, ranging from a single \log_{10} to multiple logs of bacterial copies. Other bacterial families found in the gastrointestinal (GI) tract include *Actinomycetaceae*, *Enterobacteriaceae*, *Lactobacillaceae*, and *Streptococcaceae* among others (69). Epidemiological studies have demonstrated that alterations in the gut microbiota especially the colon have been associated with the presence or absence of human colonic neoplasia. Weir *et al.* showed through stool 16S rRNA gene profiling using samples collected from healthy patients versus those with CRC, that butyrate-producing genera were under-represented in the latter. They also found that *Akkermansia muciniphila* was 4-fold higher in CRC patients (70). Sears and Garrett also highlighted the role of dysbiotic colonic microbiota and its capacity to induce CRC development (71). In light of microbial dysbiosis and the complex GM being implicated in the prognosis of CRC several studies have identified bacteria as etiological factors of the disease (67, 69, 71-73). However, there is still a significant lack of knowledge about how tumorigenesis alters the complex GM and if this modulation is subsequently affected by

host genetics regardless of predisposing mutations. Retrospective studies in human CRC have shown several bacterial operational taxonomic units (OTUs) as being either abundant or less prevalent when compared to controls without disease (62, 70, 71). Often studies performed on tissues post-tumor development lead to disparate results where *Prevotellaceae* or *Prevotella* was found to be enriched in normal mucosa or healthy patients' stool (70, 72), while other groups suggest its enrichment in tumors (73-75). Most of these findings are based on samples obtained after adenoma development therefore raising the question whether the bacteria are inducing the disease or if the presence of tumors enriches their growth.

Addressing this issue, several groups in recent times have tested the role of bacteria such as *Streptococcus gallolyticus*, *Fusobacterium nucleatum*, and *Bacteroides fragilis* in the *Apc^{+Min}* (Apc-Min) mouse model of colon cancer. *Bacteroides fragilis*, a human colonic commensal was shown to induce persistent colitis in wildtype C57BL/6 mice, followed by their capacity to promote colonic tumorigenesis in the Apc-Min model (76, 77). Wu *et al.* demonstrated that the enterotoxigenic *B. fragilis* (ETBF) caused colitis and induced colonic tumors in this model. To enhance the colonization of ETBF, the authors however, treated the mice with a cocktail of clindamycin and streptomycin prior to bacterial administration (76). Although a standard approach for most bacterial-administration experiments, the use of antibiotics potentially simplifies the endogenous GM, creating a pseudo-nearly-germ-free environment. With a toxigenic bacterium such as ETBF or genotoxic species like *Helicobacter pylori* (78), it is likely that such an effect would be observed due to the massive relative abundance of an individual species of bacteria. However, in studies trying to understand the role of commensal, non-toxicogenic

bacteria, the lack of endogenous GM may be a confounding factor, establishing an unnatural system of testing.

To better understand the effect of the complex endogenous GM on colon cancer, Zackular *et al.* demonstrated that transferring the microbiome of AOM/DSS-treated (Azoxy methane/dextran sodium sulfate) tumor-bearing mice to germ-free recipients led to an increased CRC burden. This established and demonstrated the potential of the GM to enhance disease susceptibility (64). To further the role of specific bacteria in the development of colon cancer, Kostic *et al.* showed that treating Apc-Min mice daily for several months with *F. nucleatum* potentiates colonic tumorigenesis in a model with a primarily small intestinal tumor phenotype. Additionally, they also showed that *F. nucleatum*-treated mice demonstrated a pro-inflammatory expression profile, suggesting an immune microenvironment contributing to CRC development (79). The same group previously showed *Fusobacterium* sequences were found via quantitative PCR (polymerase chain reaction) and 16S rDNA analysis to be enriched in carcinomas compared to adjacent normal tissue (60). Subsequently, it was identified that a host polysaccharide, Gal-Gal-NAc (galactose-*N*-acetyl-galactosamine) is recognized by the fusobacterial lectin, Fap2, leading to the binding of *F. nucleatum* species to the Gal-Gal-NAc-expressing CRC cells including those established in mice (80). *Fusobacterium nucleatum* and its potentiating role in CRC, thus has been well-established through these studies, however, it must be noted that testing bacterial adherence in cell-lines or ectopically implanted tumors should be treated with caution when addressing physiologically-relevant assessment of the role of bacteria in humans. Similarly, the phenotype of CRC observed in the Apc-Min model is primarily that of adenomas in the

small intestine, unless treated with AOM/DSS or toxigenic compounds or bacteria. In the study by Kostic *et al.* 6-week old, Apc-Min mice were treated with *F. nucleatum* every day for a period of 8 weeks (79). Although relevant controls were established for this study, tumor initiation in this model was shown to occur soon after birth, as early as 1-2-weeks of age (81, 82). More importantly, gavaging mice for 8 weeks on a daily-basis and then assessing the presence of bacteria at sacrifice in colonic tissues potentially biases the study towards finding *F. nucleatum* in tissues analyzed. While the colonization of *F. nucleatum* in the colon cannot be challenged based on these studies, the role of the bacteria as a driver or merely a passenger, potentially colonizing tumors after disease onset needs to be addressed further. Amitay *et al.* examined the prevalence of *Fusobacterium* in fecal samples collected from over 500 patients across various CRC stages, determined through colonoscopy (83). This analysis included 113 patients with advanced adenomas and 231 without any neoplasms (controls). Although the abundance of *Fusobacterium* was found to be associated strongly with carcinoma presence in 46 patients, it was not associated with that of the advanced adenomas. More importantly, it was determined that *Fusobacterium* was associated positively with advanced cancer stages, suggesting that *Fusobacterium spp.* may be passengers taking advantage of favorable conditions, rather than being causal factors (83). It is, however plausible that *F. nucleatum* though being a passenger can be used as a diagnostic tool for the detection of advanced stages of CRC.

F. nucleatum has been associated across several studies and models with colorectal tumors. Since the establishment of the role of this periodontal pathogenic bacterium in colon cancer, other co-segregating bacteria from the oral community such as

Prevotella, *Peptostreptococcus* and *Porphyromonas spp.* affecting colonic tumors have been brought to light (84-86). The prevalence of *S. gallolyticus* subsp. *gallolyticus*, a biofilm-forming bacterium has also previously been linked with increased CRC (87). In a recent study examining normal colonic tissue and adjacent tumors, biofilm-positive samples showed increased presence of tumors (88, 89). Dejea *et al.* demonstrated that bacterial communities exist on colonic tumors, possibly contributing to enhanced cell proliferation in CRC patients. According to the same study, the risk of developing CRC was 5-fold higher in individuals with certain biofilms, where the metabolites due to the presence of biofilms were also shown to alter host tissue microenvironment. Levels of N^1 , N^{12} -diacetylspermine and other polyamines were significantly higher in biofilm-positive samples compared with biofilm-negative cancers (90, 91).

The role of several OTUs either individually, as a biofilm, or as a community has been implicated in CRC disease severity (64, 70, 92-94), including a novel OTU known as *Providencia* identified to be enriched in the colorectal tumor microenvironment (95). However, these studies do not take into account the reverse association, i.e. how CRC progression affects the composition of the complex GM. The idea of CRC passengers is also prevalent suggesting that tumors serve as a platform for the enrichment of taxa such as *Coriobacteria*, *Veillonella*, *Faecalibacterium*, *Rothia*, *Paracoccus*, *Prevotella*, *Parabacteroides*, and *Acinetobacter* (96). Other studies have similarly shown that the tumor microenvironment also serves as an ideal niche for commensal bacteria (97, 98).

4. Microbiota-induced inflammation/immune responses in CRC

In 1890, Dr. William Coley became interested in the disappearance of malignant tumors he observed in acute streptococcal infection patients (99). This initial report fueled the study of cancer immunology and how immune cells respond to tumorigenesis, either as promoters in some cases, or as inhibitors in others. The antitumor response of the immune system is continually regulated by the host. This is established in three ways, i.e. elimination, equilibrium, and escape. Thus, the immune system can promote cancer cell growth and survival, and simultaneously suppress tumors (100). Several cells of the immune system are capable of immune-surveillance, thereby helping decrease cancer rates through inhibition of tumorigenesis and maintaining regular cellular homeostasis. Some of these immune effector cells include macrophages, dendritic cells (DCs), natural killer (NK), natural killer T (NKT) cells, B and T lymphocytes (101). While it is commonly thought that the infiltration of these cells into adenomas and thereby their direct contact with the aberrantly proliferating cells is associated with destruction of the tumor mass, reduction of tumor burden and improved prognosis, a report by Man *et al.* suggests that infiltration may promote tumor progression, invasion and metastasis (102).

Microbial population analyses along with GWAS studies have linked colon cancer with an aberrant immune response to intestinal microbiota. GM profiling methodologies and recent studies have shown that gut-microbiome associated changes in inflammation have a direct effect on tumorigenesis (64-66). Inflammation via innate and adaptive immune responses directed towards shifts in microbiota can have a significant effect on tumor initiation and progression. Chronic inflammation potentially creates an environment that promotes tumor development through immune cells which can produce chemokines and cytokines upon activation, influencing neoplasticity, invasion, metastasis

and angiogenesis (103). Transcriptional factors such as NF- κ B and STAT3 (signal transducer and activator of transcription) also promote tumorigenesis driven by inflammation, potentially through apoptotic suppression and an increase in cell turnover. Cancerous cell-derived soluble compounds may additionally impair antitumoral immune responses, further stimulating tumor growth and survival (104). As outlined here, most studies involving microbiota and disease phenotype portray or characterize the associative relationships of certain bacterial species with increased incidence of disease. While the mucosal immune system is tolerant of certain bacteria and dietary antigens, cross-communication between commensals and the host immune system can lead to a robust response against pathogenic bacteria and also host-derived inflammatory conditions. Henceforth, we present a few examples of bacterial modulators of immune responses. *Clostridium saccharogumia* was found to induce colonic CD4⁺ T regulatory cells (Tregs) and also created a microenvironment that was rich in transforming growth factor, TGF β (105). These results also demonstrated that conventional mice had greater resistance to colitis as compared to those reared in a specific-pathogen free (SPF) setting. Studies by Scher *et al.* established the association between *Prevotella copri* and the development of rheumatoid arthritis (RA) including a study that increased disease in *P. copri*-treated mice (106). Though a definitive link cannot be made to increased abundance of *P. copri* and RA, since pro-inflammatory cytokines such as Tumor Necrosis Factor alpha (TNF α), IL-1, IL-6, GM-CSF, and chemokines such as IL-8 were found to be abundant in RA patients, it can be conceived that *P. copri* may exacerbate the production of these immune-modulatory compounds (107). Signaling through MYD88, sometimes required for production of NF- κ B mediated inflammatory cytokines, occurs

through several pathogen recognition receptors (PRR) like Toll-like receptor (TLR) which identify pathogen-associated molecular patterns (PAMPs) (108). Some of these PAMPs include lipopolysaccharide or LPS, nucleic acids – bacterial and viral DNA or RNA, bacterial peptides like flagellin, peptidoglycans, lipoteichoic acids, lipoproteins and fungal glucans (109, 110). A commensal bacterium often used as a probiotic, *Lactobacillus acidophilus* was found to induce high-levels of IFN β in dendritic cells through the MYD88 pathway. It was found that IFN β was induced by circumventing the TLR- pathway through phagosomal uptake thereby opening new frontiers of microbial induction of innate immunity (111). A recent review by Slingerland *et al.* focuses and captures the accumulating evidence for the role of the GM in inflammatory diseases. There are several indications to suggest that the GM can induce either a pro- or anti-inflammatory milieu within the host leading to diseases including inflammatory bowel diseases (IBD), Atherosclerosis, Atopic Dermatitis, Psoriasis, Asthma, Fibromyalgia, Guillain-Barré syndrome, and Multiple Sclerosis (112).

For the GM to contribute to or initiate inflammation-mediated tumorigenesis in the colon, several models have been proposed that focus on how IBD acts as a precursor to CRC, where the mucosal barrier potentially comes into contact with microbial antigens and metabolites (113). Grivennikov *et al.* showed that IL-23, produced by tumor-penetrating myeloid cells, promotes tumorigenesis through an upregulation of IL-17, IL-6 and IL-22 in a mouse model of CRC that develop distal colonic tumors (114). Other groups have similarly shown that *Escherichia coli*, a commensal found in the gastrointestinal tract can up-regulate IL-17C cytokine levels in the *Apc^{Min}* mouse model, increasing tumor burden through the recruitment of tumor-potentiating lymphocytes and

suppression of apoptosis post-induction of Bcl-2 and Bcl-xl (115). Dennis *et al.* generated APC^{Δ468} mice to assess the role of T cell-derived IL-10 in colon cancer. They reported that microbes accumulate within colonic polyps, eliciting a local inflammatory response, thus driving an increase in colonic polyposis, whereas IL-10 from T cells and Tregs ameliorated this increase in CRC (116). Similarly, when Apc-Min mice deficient in IL-10 production were conventionalized with bacteria from SPF mice, it lead to increased tumor multiplicity in the model. Gnotobiotic studies following up on this phenomenon showed that *F. nucleatum* isolates lacking the FadA and Fap2 adhesins did not induce inflammation, whereas the *pks+* *E. coli* promoted a toxin-dependent carcinogenesis potentially driven through inflammation (117). Kostic *et al.* demonstrated that colonization of Apc-Min mice with *F. nucleatum* recruits tumor-infiltrating myeloid cells (79), while Ye *et al.* showed that *F. nucleatum* subspecies *animalis* increased IL-17A and TNFα expression, along with CCL20 chemokine expression (118). The latter study also found that *F. nucleatum* subsp. *animalis* stimulated activation and migration of monocytes/macrophages. Similarly, previously well-characterized bacteria such as *Helicobacter spp.* are known to have a significant role in the development of CRC. *Helicobacter hepaticus* infections result in colitis, CRC and also in extra-intestinal diseases across several strains of mice. *Rag2*^{-/-} mice inoculated with *H. hepaticus* were shown to have increased inflammation and subsequent cancer development, simultaneously causing inhibition of DNA repair gene expression in the colon (119, 120).

5. Methods to unravel the complexity of the GM: Altered Schaedler Flora and Complex Microbiota Targeted Rederivation (CMTR)

Most gut microbiota-related studies, in the context of identifying bacterial drivers of colon cancer, tend to lean towards using germ-free (GF) or mono-associated animals. While this approach may be necessary for gleaning insights into the mechanisms of how particular species contribute or modulate the disease, the naturally occurring gut microbiota and its role in the process is ignored (6). It must be noted that in humans, and also in mammalian model systems, large communities of bacteria co-exist, synergistically with the host and with each other. Kostic *et al.* along with others recently noted that the mouse gut microbiota is very similar to that of humans (92), sharing up to eighty bacterial genera within the GM profiles (121, 122). These complex mixtures of bacteria utilize metabolites from each other creating a community metabolite profile that may be more relevant than an individual bacterial metabolite.

While the GF or mono-associated mice approach is necessary the role of the endogenous, complex GM cannot be ignored. An alternative approach to this reductionist methodology is the potential use of animal models with an Altered Schaedler Flora (ASF) GM (123). Developed by R.P. Orcutt in 1978 with eight bacteria within the gastrointestinal tract, the ASF model community has since been used to investigate interactions within members of the GM. Considering their well-characterized microbiome, the ASF taxa allow for studying both homeostatic and disease-related contributions of the bacteria (123). More importantly, with the general acceptance of microbiota-mediated and microbiome-targeted therapies (66), such GM models may be necessary to understand bacterial interactions and to develop therapeutics for human health. However, the maintenance of such a model may be highly expensive limiting the scope and feasibility of long-term studies.

On the other hand, Hart *et al.* recently showed that mouse models could be established with differing complex gut microbiota, via a technique called Complex Microbiota Targeted Rederivation, or CMTR (124). They found that both B6 and C3H IL-10 knockout mice had significantly different disease severities, which was altered exclusively by the GM composition. Their report proposed the use of CMTR as an alternate means to study the role of the microbiome, while establishing the resident, complex GM as a prime factor of disease. These developments in GM modelling including the ASF and CMTR methodologies will be crucial to understanding not only the role of specific bacteria, but that of a known or well-established consortium of bacteria in colon cancer susceptibility in the future.

6. Pirc rat model of colon cancer and differential susceptibility due to GM

Thus far, we have highlighted the varied roles of the gut microbiota in affecting colonic tumorigenesis. In order to model human colonic cancer phenotype, we use a rat model of familial adenomatous polyposis (FAP). The disease in this preclinical model occurs due to mutations in the β -catenin binding domain of the gatekeeper tumor suppressor gene, *adenomatous polyposis coli* (*APC*). *APC* mutations are not only seen in FAP, but also play a rate-limiting role in sporadic CRC (125-127). The *Apc*^{+/*Pirc*} rats develop colonic adenomas compared to mouse models of *APC* which have a small-intestinal phenotype and also show a sex-bias with increased tumor multiplicity observed in males compared to female rats (128). The size of the rat also allows for monitoring adenoma development longitudinally using endoscopy. Using this Pirc (Polyposis in Rat Colon) rat model, we previously demonstrated that the indigenous complex GM has a

significant effect on tumor multiplicity (129). To address how the naturally occurring GM affects CRC susceptibility, we utilized the CMTR technique with the Pirc rat model of FAP (127, 128, 130). By transferring genetically identical Pirc embryos into three different GM backgrounds (124), we demonstrated that the indigenous complex gut microbiota has a significant effect on tumor multiplicity. Upon examination of tumor multiplicity we found that one group harboring the microbiome obtained through the LEW/SsNHsd surrogate dam (GM:Lewis) had a significantly lower tumor burden. The GM:Lewis group also had two rats that did not develop any colonic tumors, revealing that a previously completely penetrant phenotype could become incompletely penetrant purely by altering the GM (131). Based on the results obtained by sequencing the fecal samples of the Pirc rats at 1 month and 4 months, we found several OTUs that were differentially enriched as early as 4 weeks of age, leading to their potential use as biomarkers of disease onset or potential probiotics. This evidence suggests that it may be useful to concentrate on the characterization of the complex, endogenous commensal microbes which contribute to CRC development in conjunction with other OTUs in the community.

7. Biofilms and colon cancer etiology

Recent evidence in the colon cancer field has suggested the pro-tumorigenic capacity of biofilms (132, 133). Some studies have suggested biofilms, in general, may be causative factors, altering the metabolome of the host (134, 135). Meanwhile, others have reported the presence of toxigenic biofilm-forming bacteria such as *Bacteroides fragilis* as initiating factors for disease susceptibility (136). Therefore, it is prudent that

further studies elucidating the role of the GM in colon cancer must take into account virulence or other disease-potentiating factors of the entire community including biofilms in a given system. While the original definition of a biofilm refers to an irreversible association of microbial cells with a surface, enclosed in a polysaccharide matrix (137), it does not specify if the cells are monoclonal or could include polymicrobial populations. In the context of the complex GM, especially in a highly diverse environment such as the colon, biofilms could potentially be comprised of multiple bacterial species.

The role of biofilms in colon cancer etiology was first described by Macfarlane *et al.* in 1997 (138). The prevalence of *S. gallolyticus* subsp. *gallolyticus*, a biofilm-forming bacterium has also previously been linked with increased CRC (87). In a study examining normal colonic tissue and adjacent tumors, biofilm-positive samples showed increased presence of tumors (88, 89). Dejea *et al.* demonstrated that bacterial communities exist on colonic tumors, possibly contributing to enhanced cell proliferation in CRC patients. According to the same study, the risk of developing CRC was 5-fold higher in individuals with biofilms, where the metabolites due to the presence of biofilms were also shown to alter host tissue microenvironment. Levels of N¹, N¹²-diacetylspermine and other polyamines were significantly higher in biofilm-positive samples compared with biofilm-negative cancers (90, 91). Considering the complex and dynamic nature of the gut microbiota, especially in the colon, it may be necessary going forward to understand the role and contribution of individual bacteria to biofilm-formation and to host disease phenotype.

8. Beyond bacterial profiling and associations

The presence or absence and the association of bacterial taxa has been furnished in various reports addressing the role of the microbiota in colon cancer patients (64-66). These associative studies serve the critical purpose of potentially identifying susceptible patients from those that are more resistant or have a delayed-onset of adenomas. More importantly, profiling studies of the GM composition and structure only provide nominal details, but do not yield any insight into the function of the bacteria and the complex GM. With this in view, the missing link between the gut microbiota and the host has been recently established through the metabolome. Studies have shown that bacteria in the GI tract influence the host metabolic pathways (139, 140), including levels of host metabolites. Metabolomics, therefore is becoming an essential process for understanding the function of microbial communities within the gut. This technique offers insights into the real-time changes in small molecules including lipids, neurotransmitters, short-chain fatty acids (SCFA) and amino acids.

Studies have found that bacterial presence in the GI tract affects not only the composition, but also the relative abundance of metabolites (141-143). Interestingly, it is challenging to determine the origin of bacterial or host metabolites. However, it is known that certain bacteria are capable of modifying host metabolites which are commonly found in the host. For examples, oleic acid can be oxidized by *Propionibacterium acnes*. It is thought that the breakdown products of this oxidation process are prevalent in sebaceous sites (143). Similarly, another study found increased levels of branch-chain amino acids (BCAAs) and a subsequent increase in *P. copri* and *Bacteroides vulgatus*. These bacteria were reported to increase levels of circulating BCAAs in serum samples, when mice were fed a high-fat diet (144). Using metagenomics sequencing approaches,

others have similarly shown that bacterial species including *Bilophila wadsworthia* and *A. muciniphila* are associated with metabolic markers for high-risk populations of obesity (145). Understanding the interplay between the host gut microbiota and the metabolome may pave the way for precision medicine treatments taking into consideration the varied GM communities and their potential effect of disease susceptibility.

9. Concluding remarks

Considering the dynamic nature of the gut microbiota, stringent studies addressing the role of host genetics and transcriptome in the context of a complex microbiota community are needed. While the information provided in this chapter is limited to an introduction of the subject, there is a wealth of evidence regarding metabolites produced by the GM which can affect tumor progression and susceptibility through both genetic and epigenetic mechanisms (146). When mono-associated or germ-free studies are deliberated, ASF models and CMTR may provide an interesting prospect for analyzing the role of the complex GM architecture to investigate the mechanisms by which specific bacteria affect CRC. Though the idea of co-culturing or testing communities of bacteria for their effect on colon cancer has been pursued (65), the process is still not widely used. It may also be beneficial for future studies to incorporate complex GM communities into their studies, also taking into consideration biofilms and metabolite exchange among syngeneic communities (147). Other challenges that require addressing include identification of mechanistic links between the metabolic activities of the GM, especially SCFAs and bile acids. This has to be considered in light of the complex GM because it is known that bacterial products could serve as the substrate for

other taxa to flourish or produce molecules such as butyrate which could alter the etiology of the disease through DNA repair mechanisms (148). Another aspect of the disease that we did not delve into is the diet, and how it affects not only CRC progression but also the GM. Identifying and establishing methodologies to stably maintain a GM profile in the host is beneficial, including the investigation into how diet affects the establishment of a stable GM. Above all, the nature of the gut microbiome and the possibility of manipulating certain bacteria should not be disregarded as a potential source of therapeutics against intestinal and other systemic disorders. The continuous advancement in techniques, including deep sequencing, metabolomics, transcriptomics, and proteomics can have a significant impact on understanding the interactions of the multi-faceted etiology of colon cancer. Overall the gut microbiota, whether simple, SPF, complex, or wild is proving to be a jack of all trades or rather of all conditions, diseases and therapeutics.

CHAPTER II

**EARLY TREATMENT WITH *FUSOBACTERIUM NUCLEATUM* SUBSP.
POLYMORPHUM OR *PREVOTELLA COPRI* DECREASES TUMOR BURDEN IN
THE PIRC RAT MODEL OF HUMAN FAMILIAL ADENOMATOUS
POLYPOSIS**

(Susheel Bhanu Busi, Sarah Hansen, and James Amos-Landgraf)

1. Overview

Colorectal cancer is the second leading cause of cancer death (149). The Pirc rat model of colon cancer carries a mutation in the *APC* (Adenomatous Polyposis in Coli) gene leading to colonic adenomas, similar to those seen in familial adenomatous polyposis (FAP) patients (127, 130, 131, 150). Commensal bacteria have been reported through numerous studies involving the *Apc^{+Min}* mice and from human patient samples to be capable of colonizing the gastrointestinal (GI) tract and having a quantifiable impact on disease phenotype (64, 151-154). However, the mouse model of FAP predominantly develops small intestinal tumors, unlike the colonic phenotype observed Pirc rat and the human samples are collected after disease onset.

Most importantly, a recent study demonstrated that the microbiome of the rat resembles more closely that of humans, than the GI microbiome of the mouse (155). *Fusobacterium nucleatum* (*F. nucleatum*) is a Gram-negative, facultative anaerobe found ubiquitously in the human mouth (156), where it is implicated in periodontal diseases and generally considered an oral pathogen (157). Recent studies involving the role of *F. nucleatum* in the development and progression of colorectal cancers suggest a critical role for the bacterium mostly through inflammatory mechanisms (61, 158-160). Aside from the small intestinal phenotype with few colonic tumors observed in the *Apc^{+Min}* model, these studies involved a daily gavage for up to 8 weeks with *F. nucleatum* to establish long term GI colonization.

Simultaneously, around the same time as the reports of *F. nucleatum*'s role in colon cancer were suggested, other studies including our own showed that *Prevotellaceae* and/or *Prevotella* spp. were abundant in healthy colorectal cancer (CRC) patients and

models (64, 70, 131, 161). Contradictory to these reports, some studies found that *Prevotella* was responsible for an increase in dysbiotic colitis, associated with an enhanced susceptibility to arthritis (106), hypertension (162), and was also found to be enriched in a group of cancer patients (163).

In order to explore the potential of *F. nucleatum* to enhance colonic adenomas and determine its longitudinal colonization potential, and to address the disparity with respect to the role of *Prevotella* spp. in colon cancer, we treated the Pirc rat model of colon cancer with two doses of *F. nucleatum* subsp. *polymorphum* or *P. copri* prior to weaning. A pre-weaning time point was established to allow the complex GM to stabilize with the introduced taxa, while it is also thought that adenomas may be initiated as early as 2 weeks of age (164, 165). Though not having colonized the rat gut at 1 week post-weaning, we found that the early treatment of rats with either *Fn. polymorphum* or *P. copri*, led to a decreased adenoma multiplicity at sacrifice irrespective of sex. The number of tumors varied significantly between the treated and control groups at 4 months, surprisingly showing an increased tumor burden in the control, phosphate buffered saline (PBS)-treated rats, compared to those treated with either bacterium.

2. Methods

2.1. Experimental design

Male and female F344-*Apc*^{+/am1137} Pirc rats were used in the experiments to ensure increased significant differences due to the enhanced tumor potentiation of *Fn. polymorphum* or *P. copri* between the treated and control groups. In order to achieve a power of 0.8, and assuming alpha-error of 0.05, 6-8 animals were used per sex per

treatment group. The experimental design is laid out for bacterial treatment and subsequent analyses in Fig.1 and Fig.3.

2.2. Animal husbandry and housing

Pirc rats were generated by crossing male, F344/Ntac-*Apc*^{+/am1137} Pirc rats with wildtype female rats obtained commercially from Envigo Laboratories (Indianapolis, IN), i.e. F344/NHsd. All animals were group housed, prior to time of breeding on ventilated racks (Thoren, Hazleton, PA) in micro-isolator cages. Cages were furnished with corn cob bedding and were fed irradiated 5058 PicoLab Mouse Diet 20 (LabDiet, St. Louis, MO). Rats had *ad libitum* access to water purified by sulfuric acid (pH 2.5-2.8) treatment followed by autoclaving. Prior to breeding, fecal samples were collected from both the breeders using aseptic methods. Female rats were added to the male cage for mating, and after allowing for one day of mating, to establish timed pregnancies, females were moved to new cages and individually housed thereafter.

All procedures were performed according to the guidelines regulated by the Guide for the Use and Care of Laboratory Animals, the Public Health Service Policy on Humane Care and Use of Laboratory Animals, and the Guidelines for the Welfare of Animals in Experimental Neoplasia, and were approved by the University of Missouri Institutional Animal Care and Use Committee.

2.3. Genotyping and animal identification

Pups were ear-punched prior to weaning at 12 days of age using sterile technique. DNA was extracted using the “HotSHOT” genomic DNA preparation method previously outlined (166). Briefly, ear punches were collected into an alkaline lysis reagent (25 mM

NaOH and 0.2 mM EDTA at a pH 12). The ear clips were heated at 90 °C on a heat block for 1 hour, followed by addition of the neutralization buffer (40 mM Tris-HCl, pH 8) and vortexing for 5 seconds. DNA, thus obtained was used for a high resolution melt (HRM) analysis as described previously (131).

2.4. Fecal sample collection

Fecal samples were collected from the dams, prior to gavaging the pups. At 2 weeks of age, the pups were swabbed prior to gavaging with *Fn. polymorphum* or *P. copri*. Swabbing was performed using a cotton-tipped applicator (sterile, Medline catalog no. MDS202095), by dipping in warm PBS and then stimulating the rectal area of the pup. The tip was then cut-off with a sterile pair of scissors and placed into sterile Eppendorf tube. Fecal samples from adult rats post-weaning, and breeders were collected by placing the animal in a clean, sterile cage without bedding. Fecal samples were collected monthly starting at 3 weeks of age or weaning. Freshly evacuated feces were speared with a sterile toothpick or forceps and placed into a sterile Eppendorf tube. All samples were stored at -80 °C until further processing.

2.5. *Fusobacterium nucleatum* subsp. *polymorphum* culture, administration and qPCR

Fn. polymoprhum was obtained from ATCC (ATCC® 10953, Manassas, VA) as a freeze-dried culture. The bacteria were subsequently revived in TSB (tryptic soy broth) liquid media and plated onto TSBA (tryptic soy agar plates supplemented with 5% sheep blood) (Anaerobe Systems, Pasadena, CA). On days 14 and 15 of age, rats were gavaged orally with 0.3 mL of *Fn. polymorphum* cultures resuspended in anaerobic PBS (pH 7) with $\sim 10^9$ CFUs/mL (colony forming units per milliliter). Bacterial titers were estimated

pre- and post-gavage by performing serial dilutions using TSB liquid media and plated onto TSBA plates. Pre- and post-gavage CFUs were determined by manually counting the bacteria on the plates and also using the Promega Colony Counter app for iOS systems on an iPad (Promega Corporation, Madison, WI), and averaged to obtain final CFU counts. The formula used for estimation of total number of bacteria is $B=N/mD$, where, B is the number of bacteria per mL, N is the number of CFU, D is the dilution factor and m is the volume plated, i.e. 100 μ L.

Total extracted fecal DNA was used to determine the number of *Fn. polymorphum* copies in each sample using qPCR (quantitative polymerase chain reaction) based on methods previously established (59). 10 ng of DNA was used for determining the relative abundance of *Fn. polymorphum* based on the Eubacterial 16S copy numbers. *Fn. polymorphum* has 5 copies of the 16S genes which was taken into account when normalizing to the Eubacterial 16S copy numbers. Each sample reaction was setup in quadruplicates. To obtain a standard curve, and to use as a positive control, *Fn. polymorphum* DNA extracted using the fecal DNA extraction protocol, from the stock culture (*Fn. polymorphum*, ATCC® 10953) was used.

2.6. *Prevotella copri* culture, administration and qPCR

Prevotella copri (DSM-18205) was obtained as a freeze-dried culture from the Leibniz Institute DSMZ-German Collection of Microorganisms and Cell Cultures, Braunschweig, Germany. The bacteria were revived using Brain Heart Infusion (BHI, Cat.No.237400, BD Difco, Fisher Scientific, Hampton, NH) and plated onto Columbia Blood agar plates supplemented with 5% defibrinated sheep blood (c. AS-895, Anaerobe Systems, Pasadena, CA). On days 14 and 15 of age, rats were gavaged orally with 0.3 mL

of cultures with $\sim 10^9$ CFUs/mL. Pre- and post-gavage CFUs were determined as described previously, and averaged to obtain final CFU counts. Based on methods described earlier established, qPCR was used to determine *P. copri* copy number from total extracted fecal DNA using the following primer-probe set designed specifically for bacteria: Forward (5'-3'): CCGGACTCCTGCCCCCTGCAA, Reverse (5'-3'): GTTGCGCCAGGCACTGCGAT, Probe (5'-3'): ATTCGGGACGGCAAGCTATACCAA.

Stock culture of *P. copri* was extracted using the same DNA extraction method and used as a positive control, simultaneously establishing a standard curve. The relative abundance in each sample was normalized to that of Eubacterial 16S copy numbers specific to the sample using pan-Eubacterial primers (122). Each sample reaction was setup in quadruplicates.

2.7. Fecal DNA extraction, 16S library preparation and sequencing

Fecal samples were pared down to 65 mg using a sterile blade and then extracted using methods described previously (5). Amplification of the V4 hypervariable region of the 16S rDNA was performed at the University of Missouri DNA core facility (Columbia, MO) also, as previously described (5).

2.8. Colonoscopy

Colonoscopies, described previously (167) were performed monthly on all rats, starting at 4 weeks of age, i.e. one week post-treatment with *Fn. polymorphum* or *P. copri* until necropsy. Tumor images from the colonoscopy were used to determine average size

of the colonic tumors using ImageJ, a free-to-use software distributed through the National Institute of Health (NIH, Bethesda, MD) (168)

2.9. Tumor counts and measurements

All animals were humanely euthanized with CO₂ (carbon di-oxide) administration and necropsied at 16 weeks of age. The small intestine and colon from the rats were placed on to bibulous paper and then splayed opened longitudinally by cutting through the section. Tissues were then fixed overnight in 10% formalin, and were replaced with 70% ethanol for long term storage until adenoma counting was performed. Tumor sizes were measured using the Leica Application Suite 4.2, after capturing post-fixed images as previously described (131).

2.10. Statistical analyses and figures

All statistical analyses and graphing for figures (except Fig.1) were prepared through GraphPad Prism version 7 for Windows (GraphPad Software, La Jolla, CA). *P*-values were set to identify significance at a value less than 0.05, unless otherwise indicated.

3. Results

3.1 Early administration of *Fusobacterium nucleatum* subsp. *polymorphum* or *Prevotella copri* alleviates early tumor multiplicity in the Pirc rat

Pirc rats were divided into control or treated animals to determine the effect of *Fn. polymorphum* or *P. copri* in a rat model of human colon cancer. Control animals were gavaged with anaerobic PBS, while the treated group received either *Fn. polymorphum* or

P. copri cultures (Supplementary Figure 1). All groups received two gastric gavages on days 14, and 15 of age with 300 μ l of either PBS or bacterial cultures resuspended in PBS with $\sim 10^9$ colony forming units (CFU) per mL. We found that at 1 week post-treatment and at 4 months of age, we did not detect significant colonization by either bacterium (Supplementary Fig.1B and 1C). Both the control and the treated rats were sacrificed at 4 months of age. After necropsy, colonic adenoma multiplicity was determined and found to be significantly different between the control and *Fn. polymorphum* –treated rats, and also between the control and *P. copri* –treated Pirc rats (Fig.1), irrespective of sex. These results suggest that early treatment of colon cancer susceptible Pirc rats with *Fn. polymorphum* or *P. copri* alleviates tumor multiplicity.

3.2 Average adenoma burden is not modulated by early bacterial treatment

At each colonoscopy time point, i.e. 1, 2 and 3 months of age, gross images of the colonic lesions were captured as described in the Methods section. ImageJ was used to establish a scale for each image using a ruler next to the colonic tissue, as an internal control to normalize distance of the camera from the colonic tissue (168). Average adenoma burden was calculated from each image, by carefully selecting the tumor section, and averaging out the total adenoma area, by number of adenomas observed as previously described in (131). No differences were observed in the average tumor area via colonoscopy at any of the time points. Similarly, at sacrifice, the colonic tumors were sized as previously described (131). Treatment with *Fn. polymorphum* (Fig.2A) or *P. copri* (Fig.2B) did not affect the average tumor sizes compared to the control, PBS-treated rats. Interestingly, in conjunction with the tumor multiplicity results, this suggests that the progression of tumor development is not affected by the treatment. This raises the

possibility that the initiation of tumors is being modulated due to the treatment with either *Fn. polymorphum* or *P. copri*.

3.3. GM population richness and diversity is unaffected by bacterial administration prior to disease onset

We introduced a novel bacterial species to the endogenous complex GM populations via treatment of Pirc rats with *Fn. polymorphum*. Immediately after treatment, i.e. 1 week post-treatment, we found that the estimated species richness (Chao1) in the bacteria-treated animals was increased significantly compared to the control, PBS-treated animals while the overall diversity did not vary (Fig.3A). The elevated increase in estimated richness and diversity index (Shannon) were at similar levels by 2 months of age (Fig.3B).

3.4. *P. copri* treatment did not affect the richness and diversity of the endogenous gut microbiota immediately after treatment

We used a similar approach, where Pirc rats were treated with *P. copri*. We found that at 1 week post-treatment, the Chao1 values in the bacteria-treated animals were similar to the control, PBS-treated animals (Fig.3A). Likewise, the richness and diversity of the GM in the *P. copri*-treated Pirc rats was unaltered due to treatment.

3.5. *Fn. polymorphum* treatment modulates the predicted microbiota metabolic capacity

We used 16S rDNA sequencing to characterize the endogenous gut microbiota in the colon using fecal samples collected from the treated rats at weaning, i.e. 1 week post-treatment. We found that treatment with *Fn. polymorphum* induced a significant shift in the overall GM community profile of the Pirc rats (Fig.4A, 4B and Supplementary

Fig.2A). More importantly, we determined the predicted metabolic and functional capacity of the bacteria using PICRUSt (phylogenetic investigation of communities by reconstruction of unobserved states) analysis. We found increased metallic ion transport systems in the control animals while spermidine-putrescine transport was predicted to be elevated in the animals treated with the bacteria (Fig.4C). Simultaneously, we found several OTUs (operational taxonomic units) with a fold-change of greater than 2, elevated in either group (Fig.4D).

3.6. GM structure maintains differences post-treatment at 2 months of age

At 2 months of age, the GM profile was characterized as described earlier. We found that the *Firmicutes:Bacteroidetes* ratio was significantly decreased in the *Fn. polymorphum* group (Fig.5A and Supplementary Fig.2B). We also noticed a significant shift in the GM profile observed between the two groups (Fig.5B and 5C).

Staphylococcus, *Mucispirillum*, *Alphaproteobacteria*, *Gemella* and order *RF32* were increased in the control animals (Fig.5E). On the other hand, *Fn. polymorphum*-treated animals showed an increased fold-change of *Bifidobacterium*, *Desulfovibrio*, *Dorea*, *Turicibacter* and other OTUs. We simultaneously found that the predicted functional capacity of the GM profile showed elevated pathways such as heme and methionine biosynthesis, spermidine-putrescine transport and succinate dehydrogenase in the Pirc rats treated with the bacteria. Meanwhile, the control rats showed elevated energy metabolism pathways: glycolysis, sugar transport and the pentose phosphate metabolic activity in the colon (Fig.5D).

3.7. GM profile and function modulated by *P. copri* treatment regardless of colonization

We assessed the gut microbiota (GM) profile using 16S rDNA sequencing and found that the composition and profile of *P. copri*-treated rats differed significantly at one week post-treatment (Fig.6A) and two months of age (Fig.6B). One week after treatment we found significant increases in taxa such as *Candidatus Arthromitus*, *Turicibacter*, *Alphaproteobacteria* and *Bacillaceae* in the control rats, whereas the treated rats showed elevated levels of *Lactobacillus*, *Prevotellaceae 1*, *Pediococcus* and *Anaeroplasma* (Fig.6C). We found increased *Anaeroplasma*, *Prevotellaceae 1*, *Alistipes* and *Butyricimonas* in the *P. copri*-treated rats at 2 months of age, while *Lachnospira*, *Enterobacteriaceae*, *Peptostreptococcaceae 1* and *Bacilli* were elevated in the control animals (Fig.6D). We used predicted metabolic functional modelling of the 16S rDNA sequencing data (169) to understand the role of the bacterial populations in control and *P. copri*-treated rats. We found that pathways involved in pyruvate reduction via ferredoxin oxidoreductases were elevated in the latter, i.e. *P. copri* group both at one week post-treatment and at 2 months of age (Fig.6E and 6F) with increased histidine biosynthesis and gluconeogenesis in the control rats alone at one week post-treatment (Supplementary Figure 3).

4. Discussion

Fusobacterium nucleatum (Fn) has been associated with the prevalence and incidence of colon cancer by several groups (59, 159, 170-174). On the other hand, *P. copri* reports suggest its elevated abundance in the healthy controls (70, 131), while

others suggest its association with elevated inflammatory bowel disease and colon cancer (175, 176). A large proportion of these studies used retrospective approaches where the abundance of the bacteria was determined from tumor tissues, after development of disease and compared to their matched samples from the normal epithelium. Due to this observation, some evidence has pointed to the role of *F. nucleatum* as a passenger of the disease and not a driver of colon cancer (83) while that of *P. copri* is poorly understood. Studies attempting to elucidate the mechanisms of *F. nucleatum* have employed regimens including daily bacterial supplementation (59). However, this approach may be flawed where the increased abundance of the bacterium at sacrifice could be due to the continuous treatment.

To determine if *F. nucleatum* enhances colon cancer susceptibility, we used the Pirc rat model of human colon cancer which recapitulates the phenotype observed in patients with a loss of function mutation in the *Apc* gene observed in both spontaneous tumors and familial cases (130, 150). Patients with colorectal cancer have been reported to have at least four different subtypes of *F. nucleatum* (177, 178). One of the types, *Fn. polymorphum* was detected in a quantitative profile of cancer-associated bacteria (179) and also found to be enriched in oral squamous cell carcinoma patients (180). More importantly, the FadA protein required for adhesion of the bacteria (181, 182) was found to be enriched in the *polymorphum* subspecies (183). Therefore, we treated Pirc rats with *Fn. polymorphum* prior to weaning, and visible onset of colonic adenomas. We found that the colonic tumor multiplicity was decreased but the bacterial treatment did not alter the average tumor size. This suggests that the treatment potentially inhibits the initiation of tumors and not the progression of disease once tumors are formed. Most studies treating

animal models with *F. nucleatum* have demonstrated an increase in tumor multiplicity post-treatment, however, this was not observed in our study. It is known that the complex gut microbiota is capable of modulating disease phenotype (131, 184-187) outlining the possibility of the differences in tumor burden observed. The physiology of the *Apc^{+Pirc}* rat model of colon cancer is different from that of the traditionally used mouse model, i.e. *Apc^{+Min}* (29, 127, 128, 188). This may potentially explain the variation in tumor multiplicity after treating with *Fn. polymorphum*. Alternatively, studies till date have identified the bacterium as *F. nucleatum* (59, 159, 189-195), ignoring the possibility of a subspecies. *Fn. polymorphum*, though reported in human cancers, may have differential effects in our model. This needs further validation, where strains and subspecies isolated from human subjects are tested in animal models to confirm their pathogenicity.

To address the mechanisms contributing to adenoma development, we predicted the metabolic functional capacity of the complex GM using PICRUS analysis. We found enrichment in pathways involved in the spermidine-putrescine transport system and succinate dehydrogenase pathways. Proliferation of undifferentiated colonocytes has been associated with increased polyamines such as spermidine (196, 197), which have also been suggested as potential biomarkers for identifying patients with colorectal cancer (198). Simultaneously, succinate has been proposed as a biomarker for identifying colonic tumors by Wishart *et al.* (199, 200). Moreover, decreased succinate dehydrogenase expression has been associated with growth of CRC cells *in vitro* and other carcinomas (201-203). The GM community found in the *Fn. polymorphum* group showed an elevated succinate dehydrogenase pathway possibly eliminating the genotoxic effect of the substrate in this group compared to the control rats. Simultaneously, we

found that despite the lack of colonization, *P. copri*-treated rats showed elevated levels of the predicted metabolic pathway involved in pyruvate ferredoxin oxidoreductase enzyme production. Reports indicate that this enzyme produces butyrate, mediated via utilization of lactate by taxa such as *Clostridia* which was also found to be elevated in the *P. copri*-treated rats (204-206). Meanwhile, taxa such as *Lactobacillus* and *Butyricimonas* increased in the *P. copri* group are also thought to be butyrate-producers, a SCFA that has been reported to prevent tumorigenesis in mice models of colon cancer (207, 208).

In addition to differential pathways being enriched in the control and treated groups, bacteria found to be associated with non-cancer samples or tissues such as *Bifidobacterium* (209), *Pseudomonas* (210), *Adlercreutzia* (211, 212), *Prevotella* (131) and *Desulfovibrio* (213, 214) were elevated in the Pirc rats treated with *Fn. polymorphum*. Similarly, *Desulfovibrio*, *Lactobacillus*, and *Parabacteroides*, that have been associated with stool and tissues samples collected from healthy volunteer CRC patients (213, 215), were detected in the *P. copri*-treated rats. Considering the complexity of the interactions and the differential functional capacity of each of these taxa, further studies are warranted that can tease apart the individual contributions. For example, *Bifidobacterium* and *Ruminococcus* found to be increased in the treatment group are mucin-resident lactate-producers through anaerobic respiration in the GI tract (214, 216). Reports suggest bacteria such as *Desulfovibrio* can utilize lactate for sulfide formation (213), where other data point towards a pro-apoptotic effect of hydrogen sulfide (217). Such complex interactions between the endogenous commensal GM communities may have created an anti-tumorigenic microenvironment in the *Fn. polymorphum* or *P. copri*-treated Pirc rats. On the other hand, although highly implausible it cannot be ruled out

that treatment with the PBS alone may have caused an increase in pro-tumorigenic bacteria, thus explaining the higher tumor burden observed in the control group as compared to the *Fn. polymorphum* treatment.

Another plausible mechanism by which treatment with *Fn. polymorphum* or *P. copri* promotes decreased tumorigenesis could be via induction of the host immune response either through inflammation or tolerance. It has been reported that *F. nucleatum* modulates the tumor-immune microenvironment and initiates inflammation in the gut, also promoting chemoresistance through modulation of autophagy (59, 218-220). Simultaneously, subspecies *animalis* of the same bacterial species has been shown to enhance proinflammatory cytokine expression in tumors (118). This coupled with the possibility that encountering microbial antigens prior to weaning may enhance tolerogenic capacity to opportunistic pathogens (221, 222) may be associated with the reduced tumor phenotype. Similarly, *P. copri*-treatment is associated with the activation of PPAR γ transcriptional activity (223). This is directly linked to the presence of anti-tumorigenic SCFA, butyrate and propionate. *Prevotella* was also found to be involved in the phosphorylation of PPAR γ through ERK1/2. More importantly, some studies have shown that *P. copri* is capable of inducing an inflammatory immune response (106, 224, 225), through the recruitment of CCR5+CCR6+CD8+ T cells and expression of IL-17E, creating an anti-tumorigenic environment in the GI tract (226-228).

We have shown that treatment with *Fn. polymorphum* or *P. copri* induced a shift in the GM community profile, modulating the predicted metabolic capacity of the bacteria, thereby reducing tumor burden in a rat model of human colon cancer. Going forward, additional validation is required for the role of the bacterium and the interactions

within the community. Our study only raises more questions pointing toward the role of the immune system or the potential for bacterial metabolites to have an anti-tumorigenic effect. Whether treatment at an earlier time point affects the phenotype which is unlike that reported in mice models also needs to be addressed in the future. Nonetheless, our approach to treating animals prior to disease onset in a complex GM system highlights the need to consider the synergistic effect of other bacterial taxa as potential modulators of disease along with any bacteria of interest.

5. Ethics Statement

The study reported here was conducted in accordance with the guidelines established by the Guide for the Use and Care of Laboratory Animals and the Public Health Service Policy on Human Care and Use of Laboratory Animals. All studies and protocols (#6732 and #8732) were approved by the University of Missouri Institutional Animal Care and Use Committee.

6. Author Contributions and Acknowledgements

Experiments were designed by SB and JAL. SH helped gavage the animals with the bacterial cultures. The authors wish to acknowledge Nathan Bivens, the MU DNA Core and the MU Metagenomics Core (MUMC) for assistance with 16S rDNA sequencing experiments; Bill Spollen and the MU Informatics Research Core Facility for assistance with software installation for data analysis; Rat Resource and Research Center; MU Office of Animal Resources and their staff for assistance with animal husbandry.

7. Figures

Figure 1. Tumor multiplicity of rats treated with *Fusobacterium nucleatum* subsp. *polymorphum* or *Prevotella copri*

Pirc rats were divided into a control and *Fn. polymorphum*- or *P. copri*- treated groups. Colonic tumor counts at sacrifice in male and female Pirc rats after treatment are shown. *P*-values below 0.05 were considered to be significantly different between groups. Calculated via a One-way ANOVA with a Dunnett's post-hoc analysis comparing to the means to the control group. Error bars in all figures indicate standard error of the mean (\pm SEM).

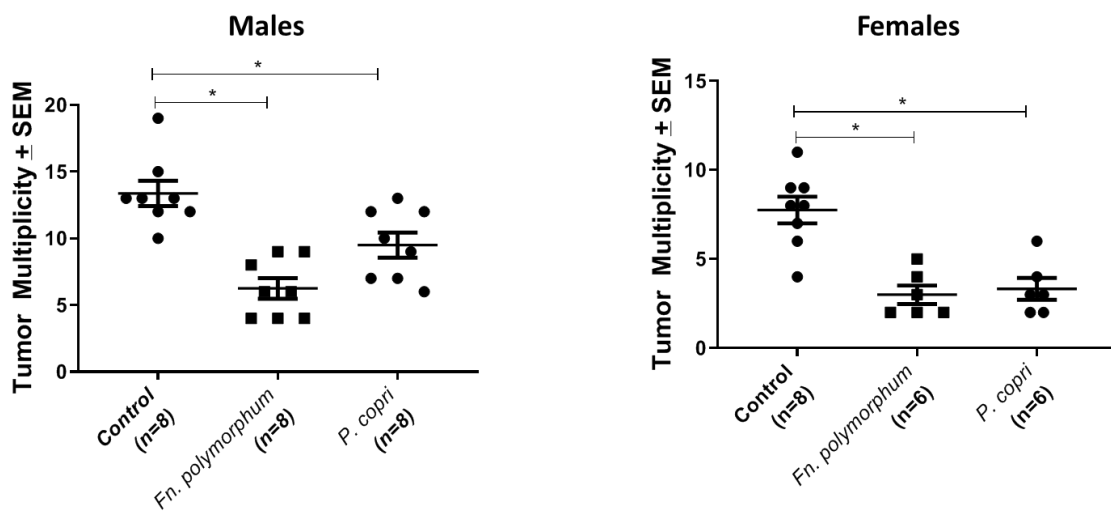
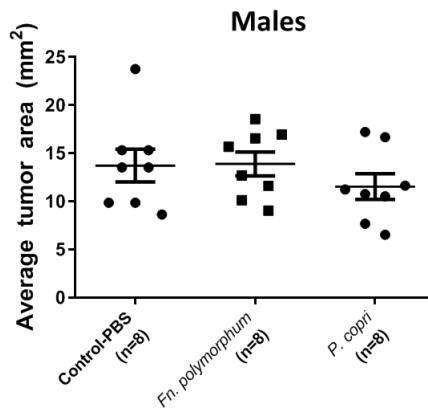


Figure 2. Early *Fn. polymorphum* treatment alleviates tumor multiplicity in the Piric rat

Average tumor area of the colonic tumors at sacrifice in male (A) and female (B) Piric rats after treatment are shown. *P*-values below 0.05 were considered to be significantly different between groups. Calculated via a One-way ANOVA with a Dunnet's post-hoc analysis comparing to the means to the control group. Error bars in all figures indicate standard error of the mean (\pm SEM).

A



B

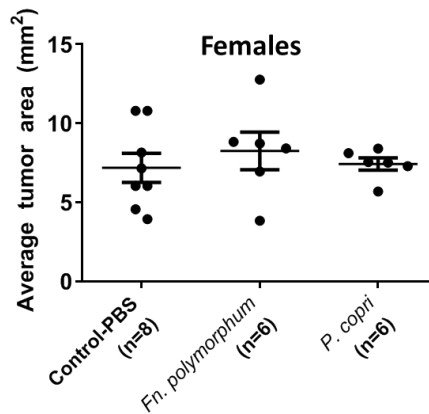
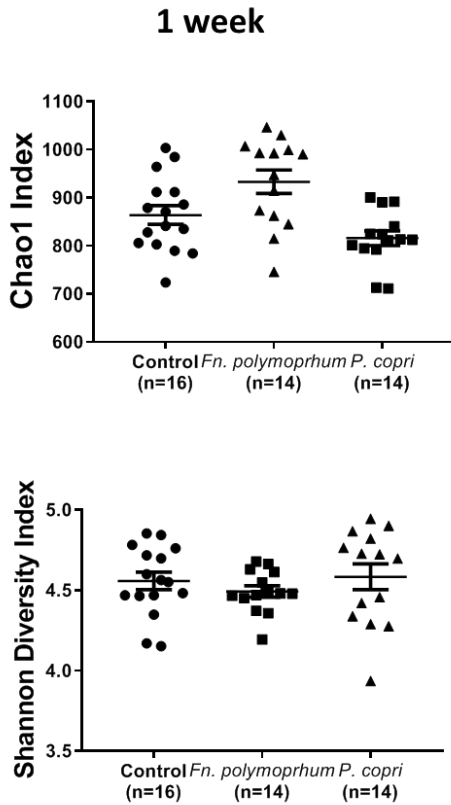


Figure 3. Richness and diversity of the GM population

Chao1 and Shannon Diversity indices were used to estimate the richness and the diversity of the GM population respectively. The data are represented as a dot plot using 16S rDNA sequencing from (A) 1 week post-treatment and at (B) 2 months of age. Error bars in all figures indicate standard error of the mean (\pm SEM).

A



B

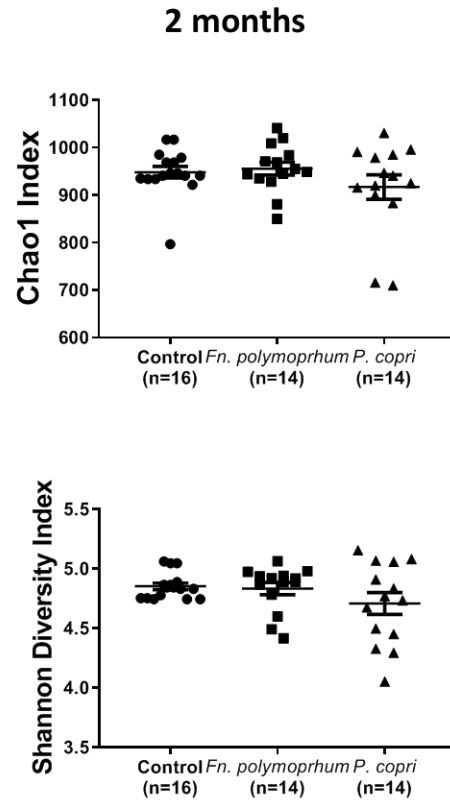
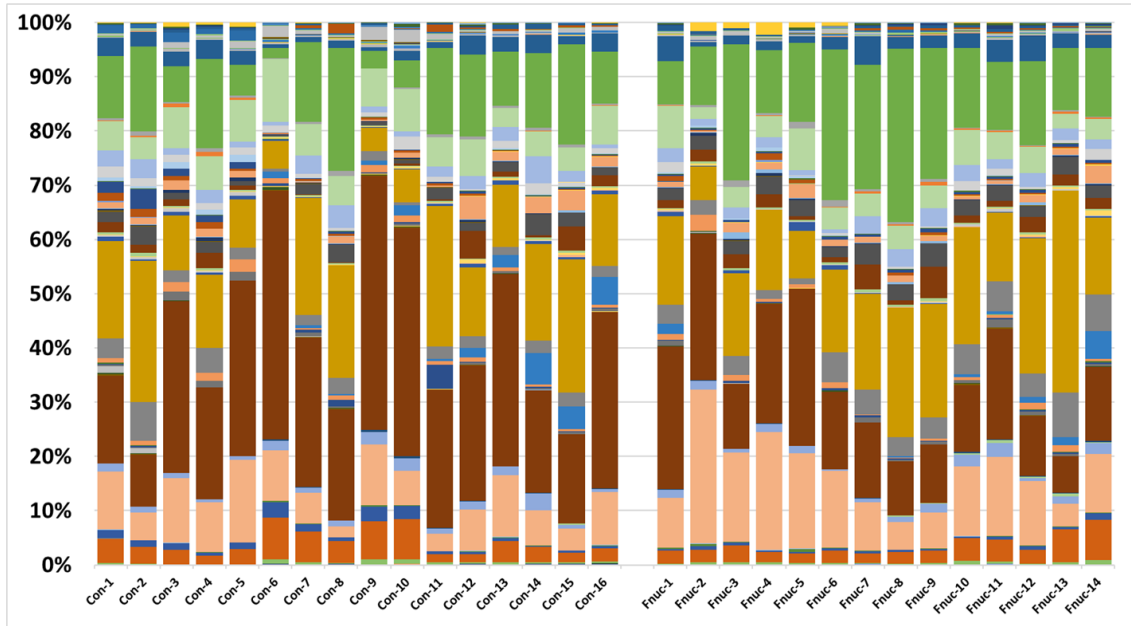


Figure 4. 16S rDNA sequencing analysis of *Fn. polymorphum*-treated rats

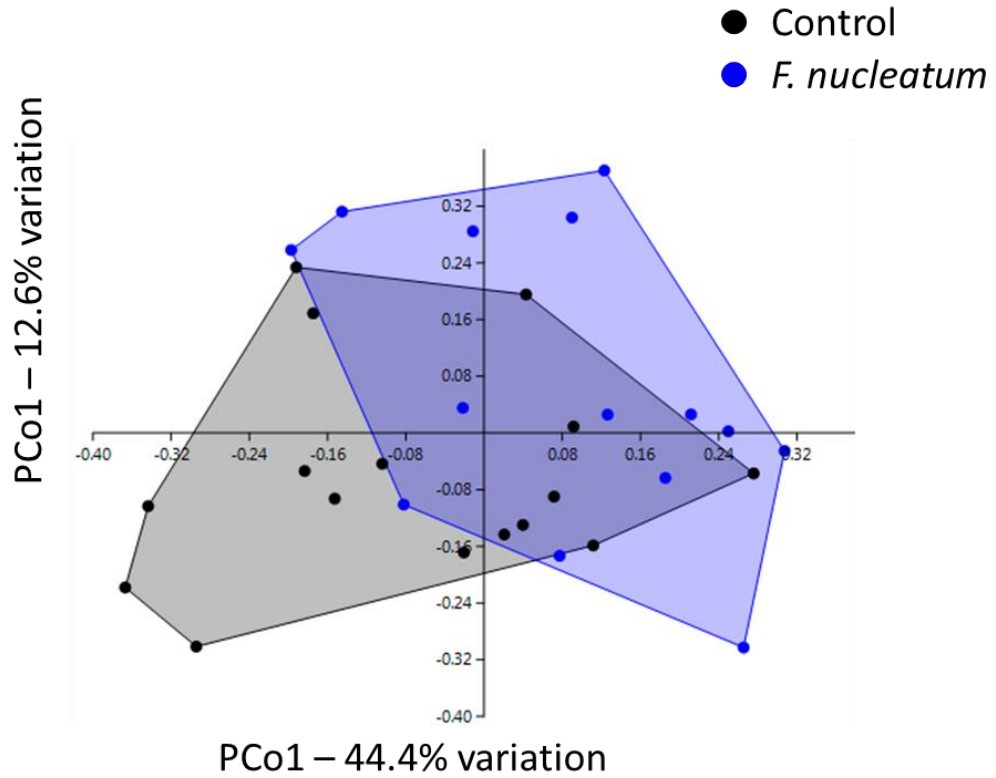
(A) Bar graphs are used to represent the relative abundance of the operational taxonomic units (OTUs) detected at the Genus level in control (n=16) and *Fn. polymorphum* (n=14) treated rats. (B) Principal Coordinate Analysis (PCoA) depicts the overall dissimilarities between the GM profiles of the control and treated rats. Each filled circle; control (black) and *Fn. polymorphum* (blue) represent a single rat. A permutational multivariate analysis (PERMANOVA) using the Bray-Curtis dissimilarity matrix was used to determine significant ($F=4.268$, $P=0.0053$) differences between the groups. P -value was set to less than 0.05. (C) PICRUS1 analysis shows elevated predicted metabolic pathways in the control or *Fn. polymorphum* groups at 1 week post-treatment. (D) Fold-change analysis between the treated and control groups was used to identify taxa with a fold-change greater than 2, contributing to the phenotype. The associated list of bacteria elevated in the control or the *Fn. polymorphum* groups can be found in Table 1.

A

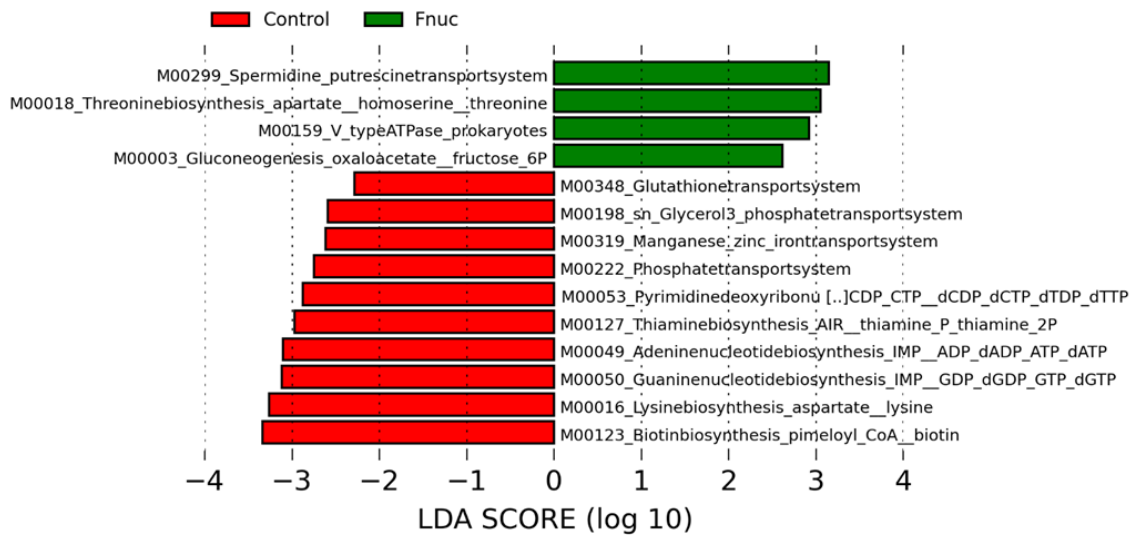


- WPS-2
- Verrucomicrobiaceae
- ML615J-28
- Anaeroplasmata
- Mollicutes
- F16
- Stenotrophomonas
- Psychrobacter
- Aggregatibacter
- Pasteurellaceae
- Chromatiaceae
- Anaerobiospirillum
- Helicobacteraceae
- GMD14H09
- Bilophila
- Kingella
- Sutterella
- Rickettsiales
- Bradyrhizobiaceae
- Alphaproteobacteria
- phylum OD1
- Victivallaceae
- Fusobacterium
- 75-A5
- Holdemania
- Clostridium
- Allobaculum
- Erysipelotrichaceae
- [Mogibacteriaceae]
- Veillonella
- Phascolarctobacterium
- Dialister
- Ruminococcus
- Gemmiger
- Clostridium
- Anaerotruncus
- Ruminococcaceae
- Peptostreptococcaceae1
- RC4-4
- Ruminococcus
- Ruminococcus
- Oribacterium
- Lachnospira
- Defluviitalea
- Clostridium
- Blautia
- Lachnospiraceae1
- Akkermansia
- RFP12
- order RF39
- Acholeplasmatales
- Tenericutes
- Treponema
- Pseudomonas
- Acinetobacter
- Actinobacillus
- Enterobacteriaceae
- Succinivibrio
- Flexispira
- Arcobacter
- Desulfovibrio
- Desulfovibrionaceae
- Comamonadaceae
- order Rickettsiales
- Acetobacter
- order RF32
- Class ABY1
- Victivallis
- Fusobacterium
- Fusobacteriaceae
- Eubacterium
- Coprobacillus
- Bulleidia
- Erysipelotrichaceae1
- SHA-98
- Mogibacteriaceae
- Selenomonas
- Megasphaera
- Subdoligranulum
- Oscillospira
- Faecalibacterium
- Butyrivibrio
- Ruminococcaceae1
- Clostridium
- Peptostreptococcaceae
- Peptococcaceae
- Shuttleworthia
- Roseburia
- Marvinbryantia
- Dorea
- Coprococcus
- Butyrivibrio
- Anaerostipes
- Lachnospiraceae

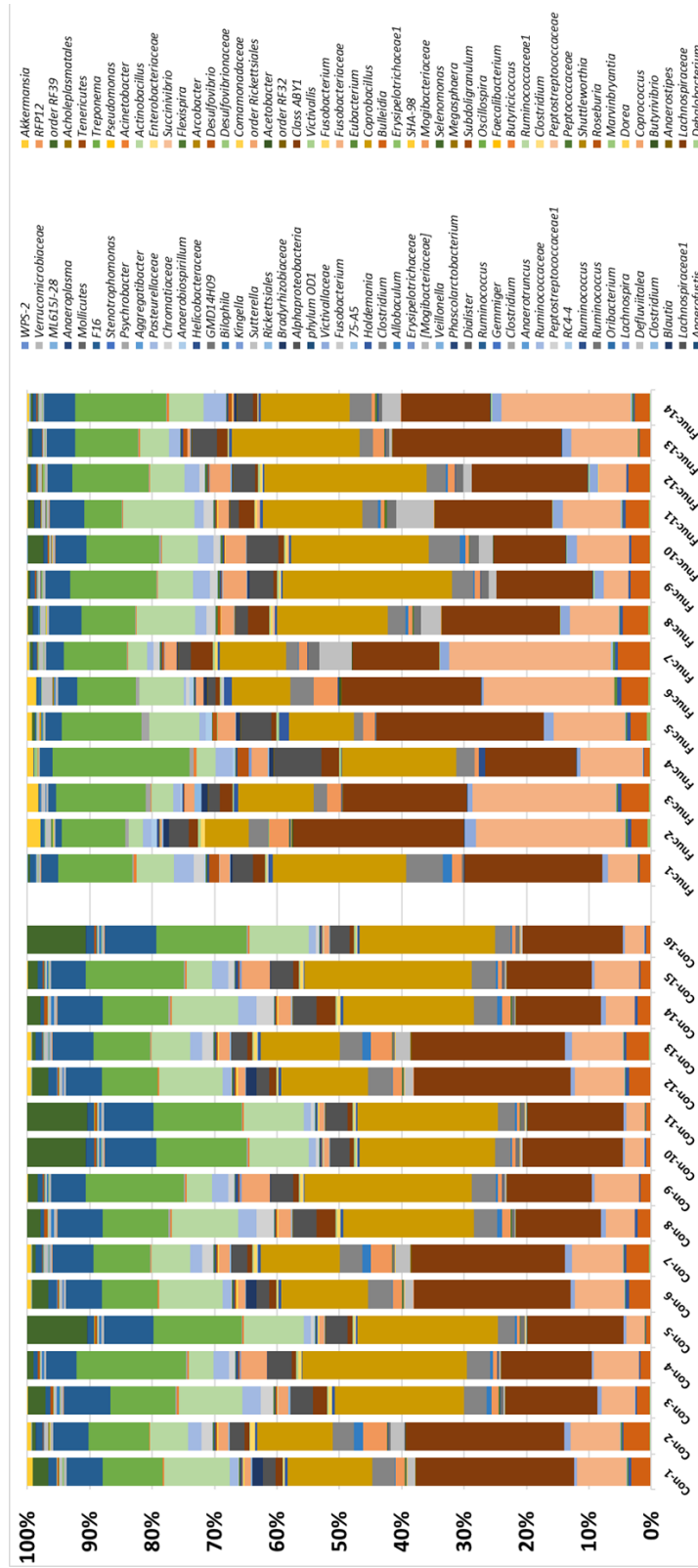
B



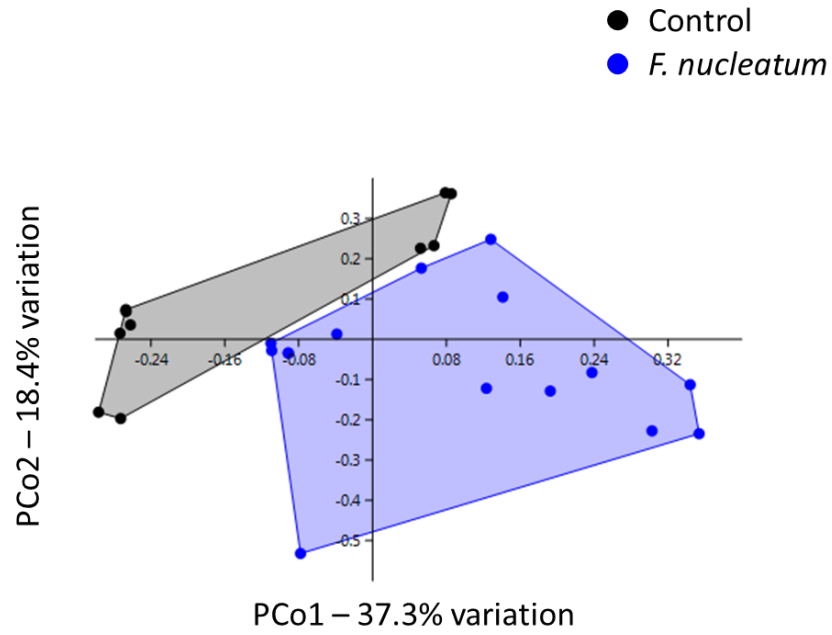
C



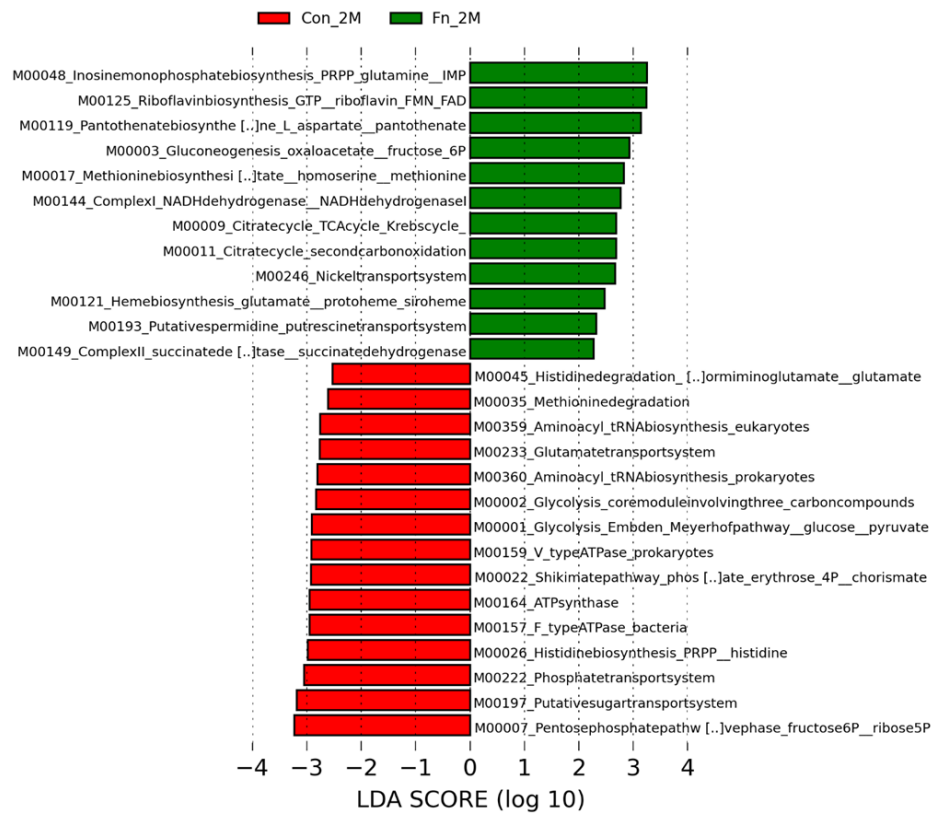
B



C



D



E

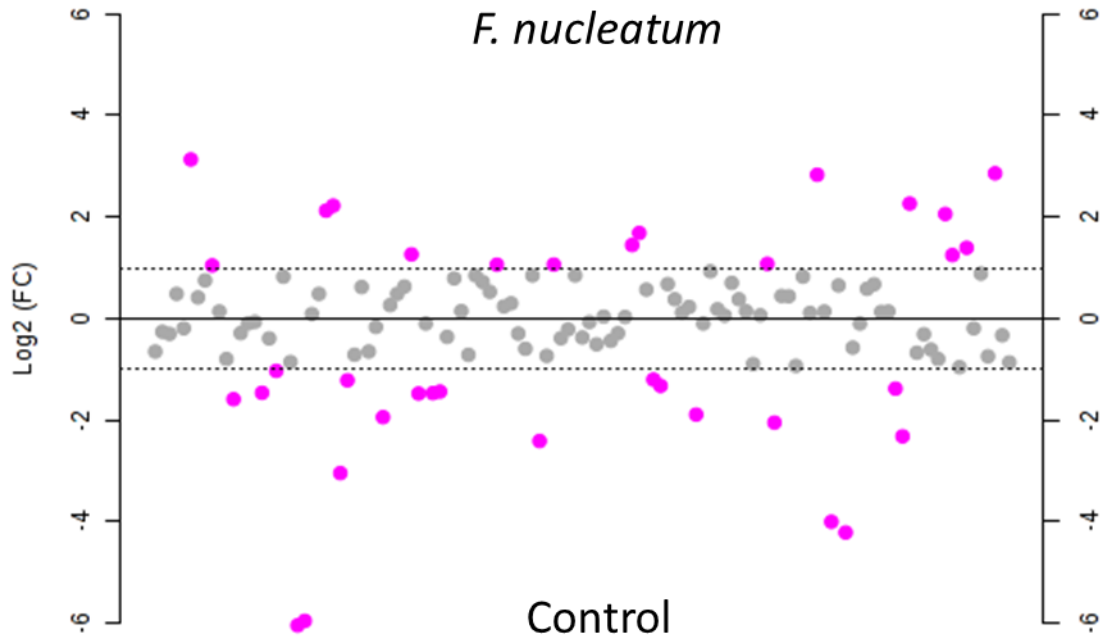
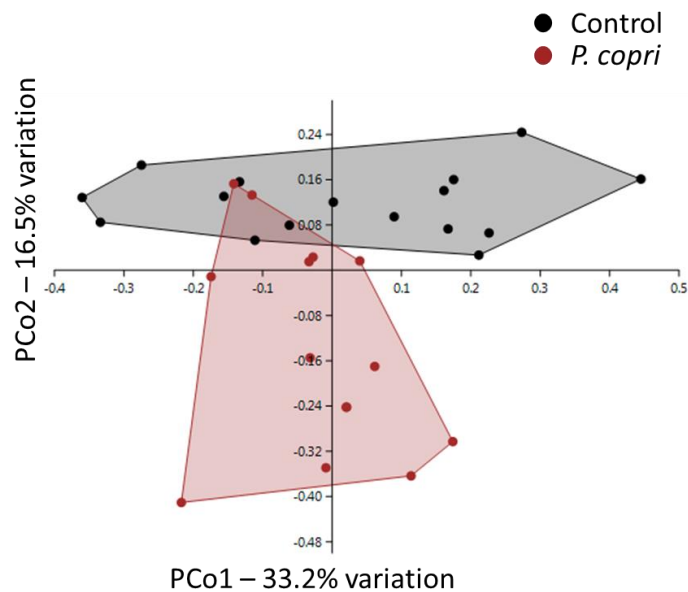


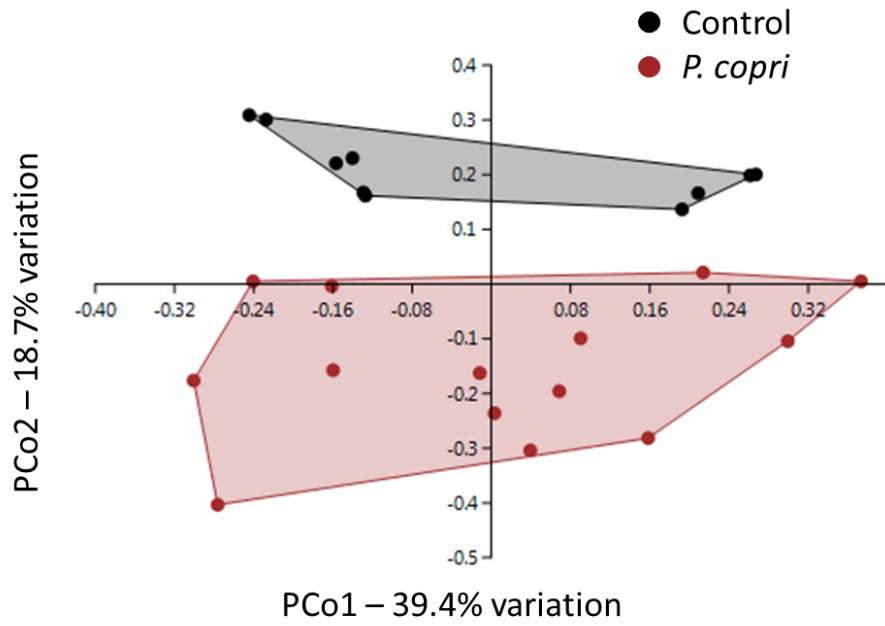
Figure 6. 16S rRNA gene sequencing analysis of control and *P. copri*-treated rats

(A) Principal Coordinate Analysis (PCoA) plot depicting the 16S rDNA gene sequencing dissimilarities between the groups based on the Bray-Curtis distance matrix. A one-way PERMANOVA (permutational multivariate analysis of variance) was used to determine significant differences, with a *P*-value of less than 0.05 set to be significant. Control group: black, filled circles; *P. copri*-treated group: red, filled circles. Each symbol represents the GM community from the fecal sample of a single rat at one week post-treatment ($F=3.592$, $P=0.0033$). (B) PCoA plot of the 16S rRNA dissimilarities at 2 months of age ($F=1.919$, $P=0.0842$). (C) Fold-change analysis depicting the taxa with a fold-change greater than 2 between the control and treated groups at one week post-treatment. Table 3 lists the group in which the taxa are increased. (D) Taxa fold-change analysis at 2 months of age (Table 4). (E) and (F) Predicted functional metabolic capacity generated via PICRUSt at one week post-treatment and 2 months of age respectively.

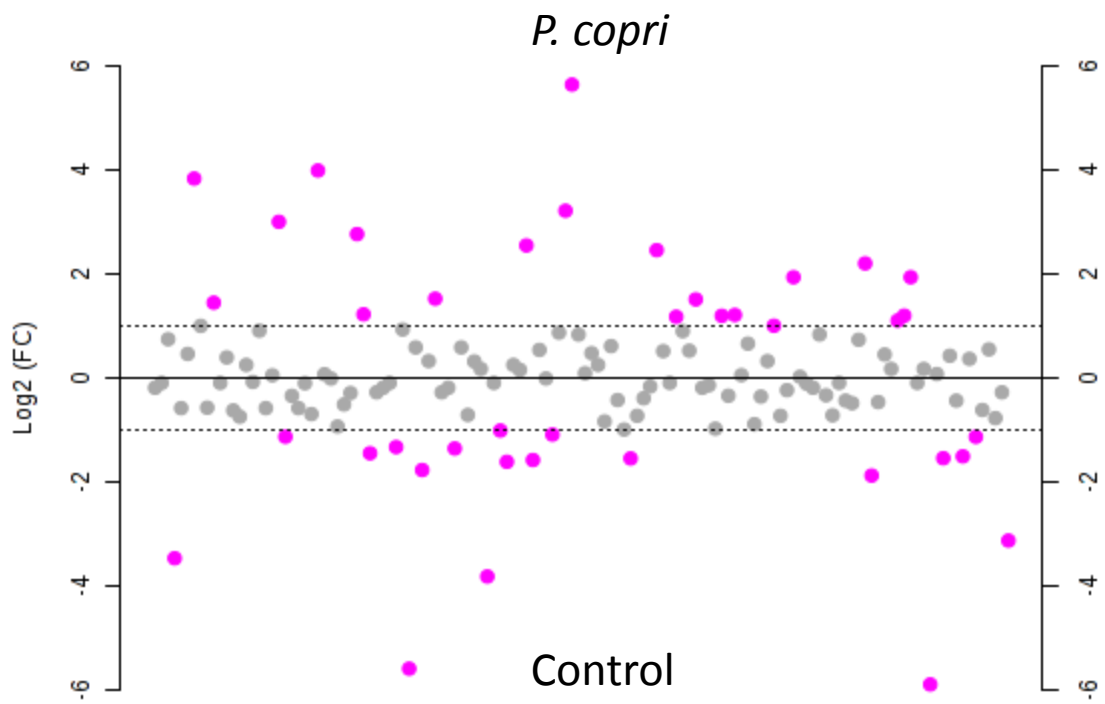
A



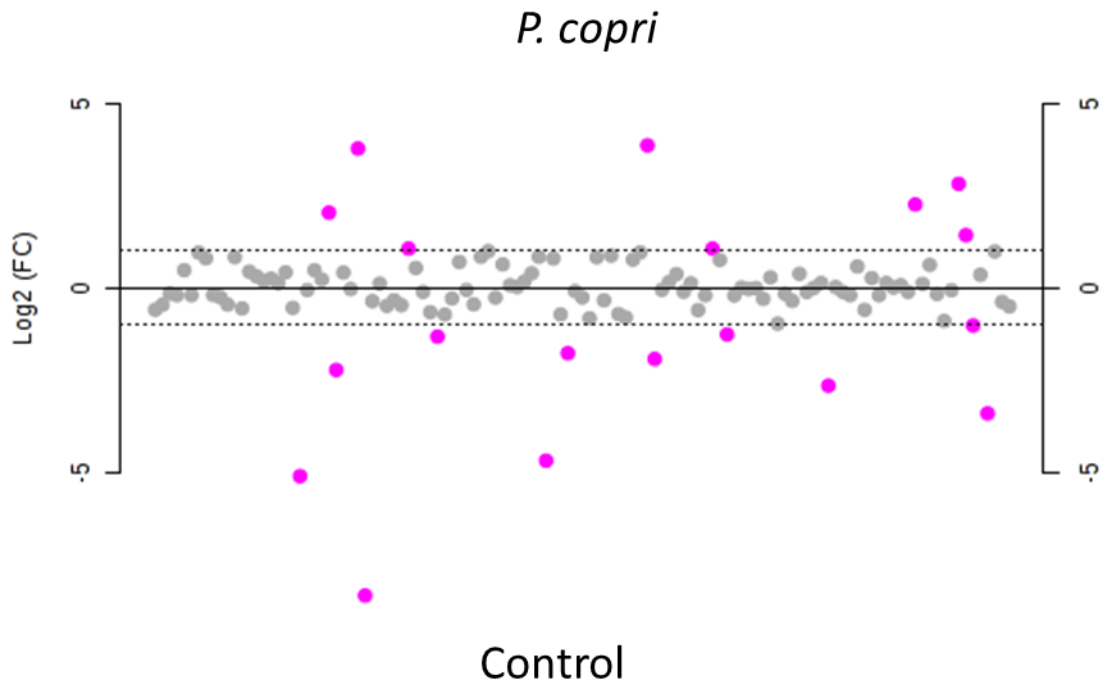
B



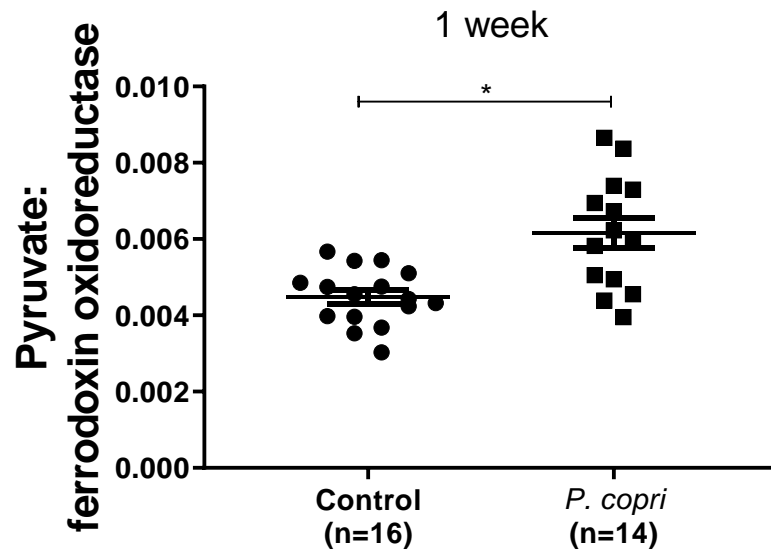
C



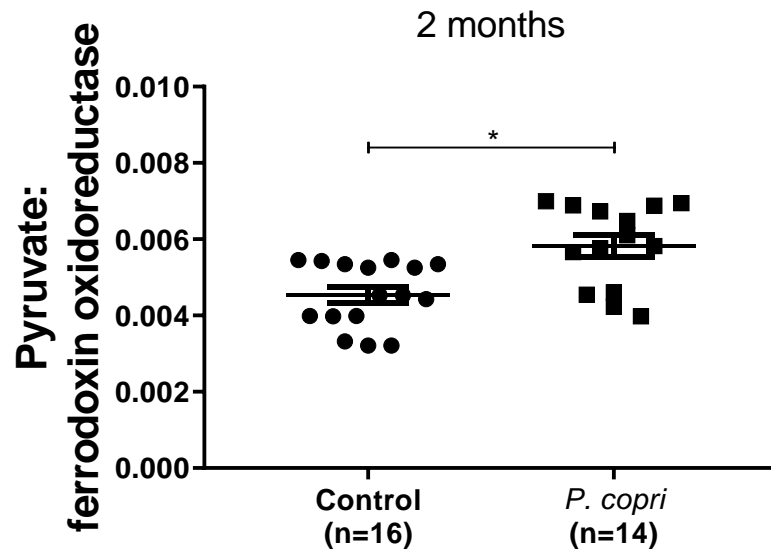
D



E



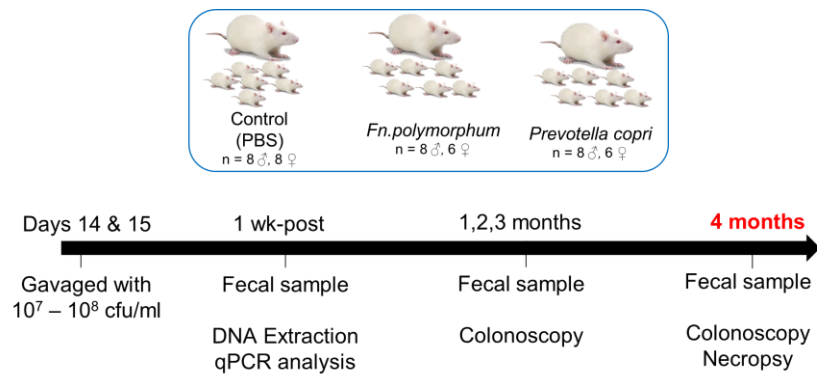
F



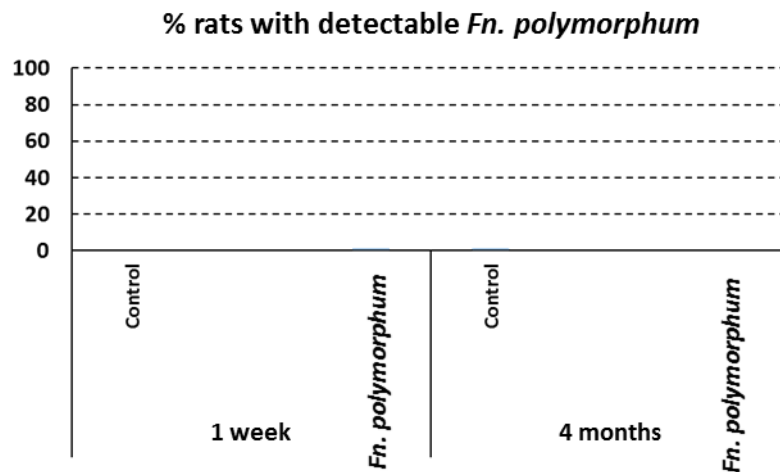
Supplementary figure 1. Pirc rat treatment with *F. nucleatum* subsp. *polymorphum* or *P. copri*

(A) Experimental design: Pirc rats were treated with *F. nucleatum* subsp. *polymorphum* (n=14) or *Prevotella copri* (DSM 18205) (n=14) or anaerobic PBS (n=16). Bacterial colonization was assessed by species-specific qRT-PCR probes at 1 week post-treatment and 4 months of age in the *Fn. polymorphum* (B), and the *P. copri*-treated rats (C).

A

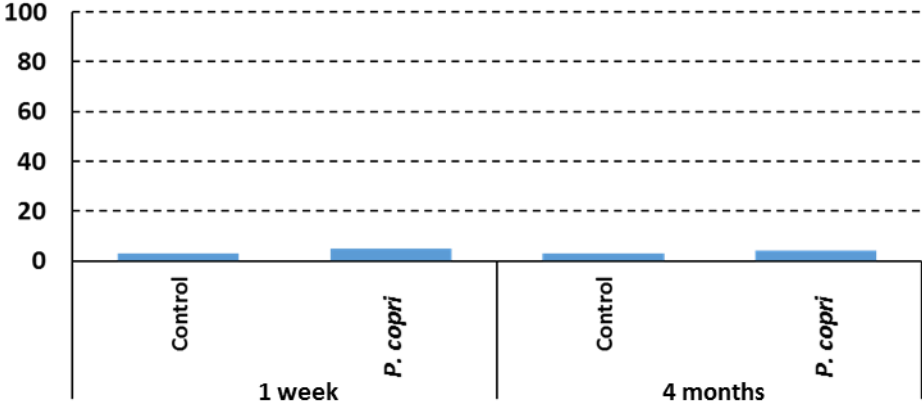


B



C

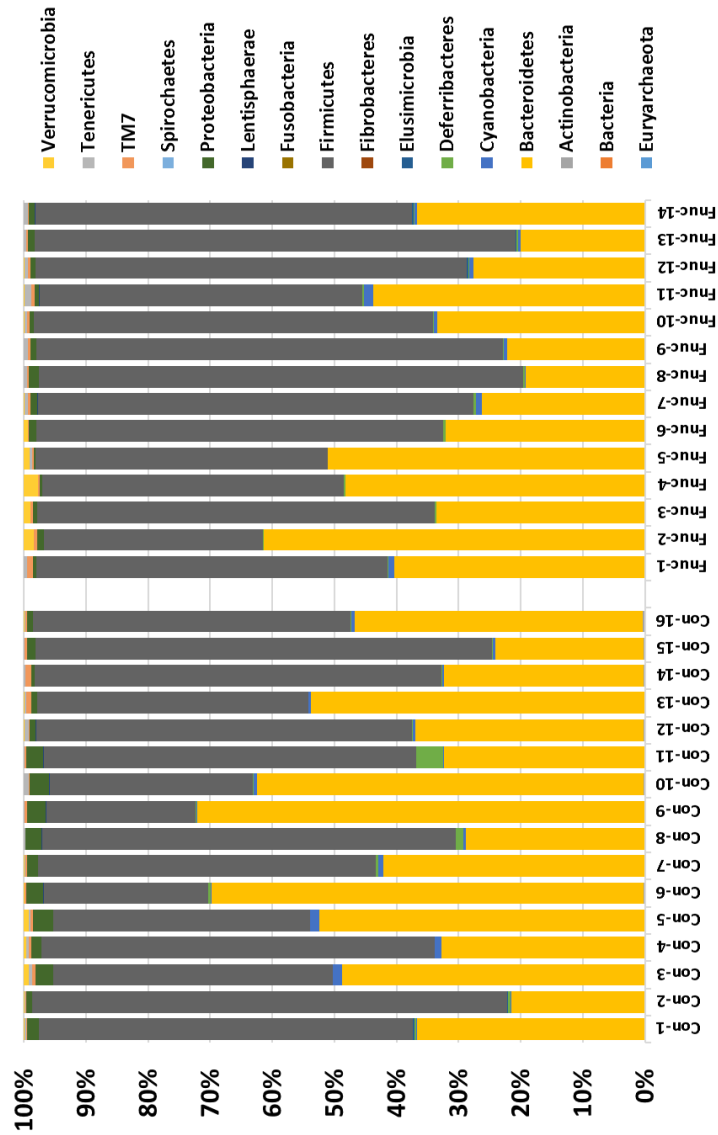
% rats with detectable *P. copri*



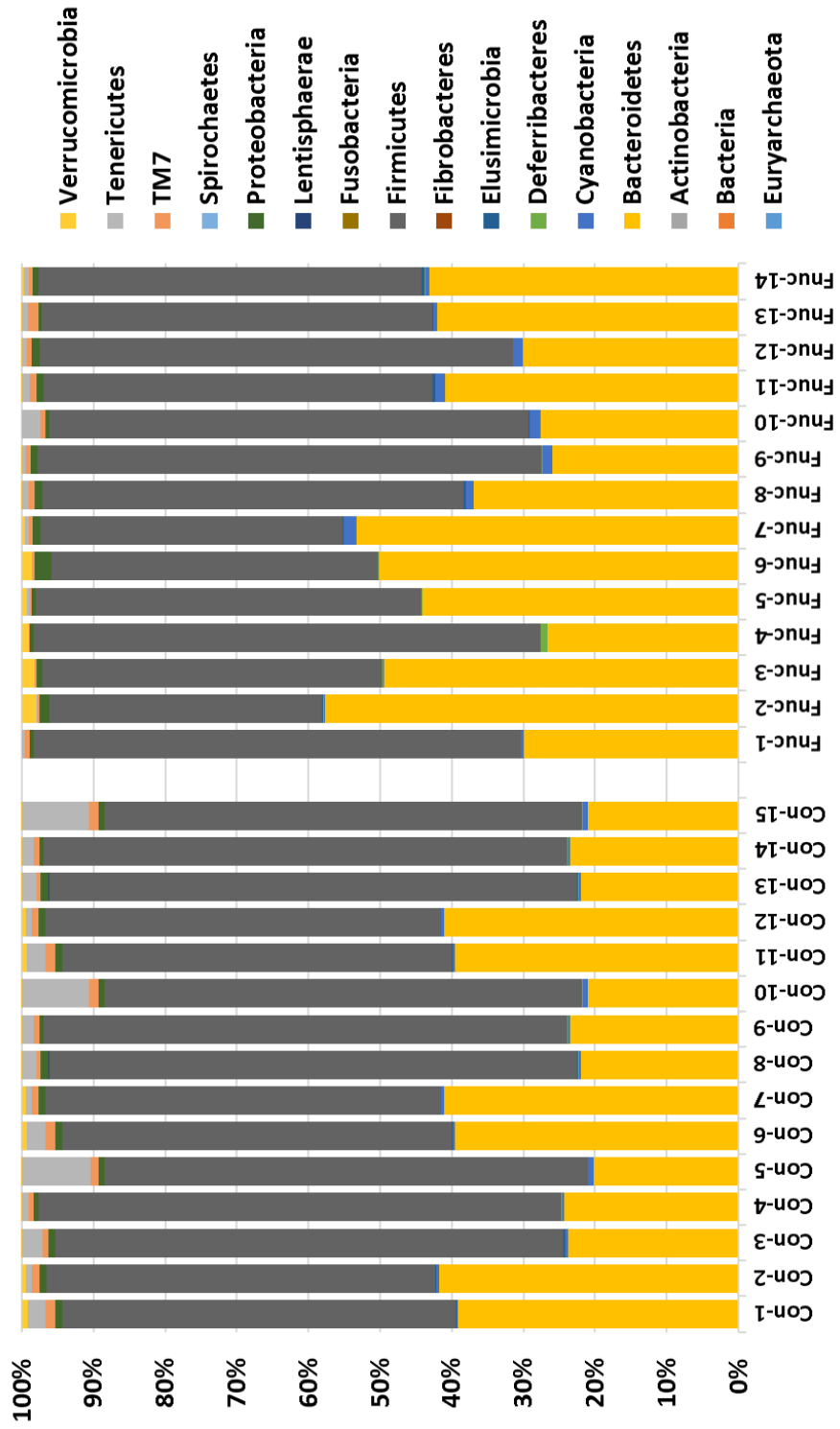
Supplementary figure 2. GM structure at 1 week post-treatment in rats treated with *F. nucleatum* subsp. *polymorphum*

Bar graphs represent the relative abundance of the operational taxonomic units at one week post-treatment (A) and at 2 months of age (B) at the Phyla level. Each bar represents a single rat in the control or *Fn. polymorphum* treated groups.

A

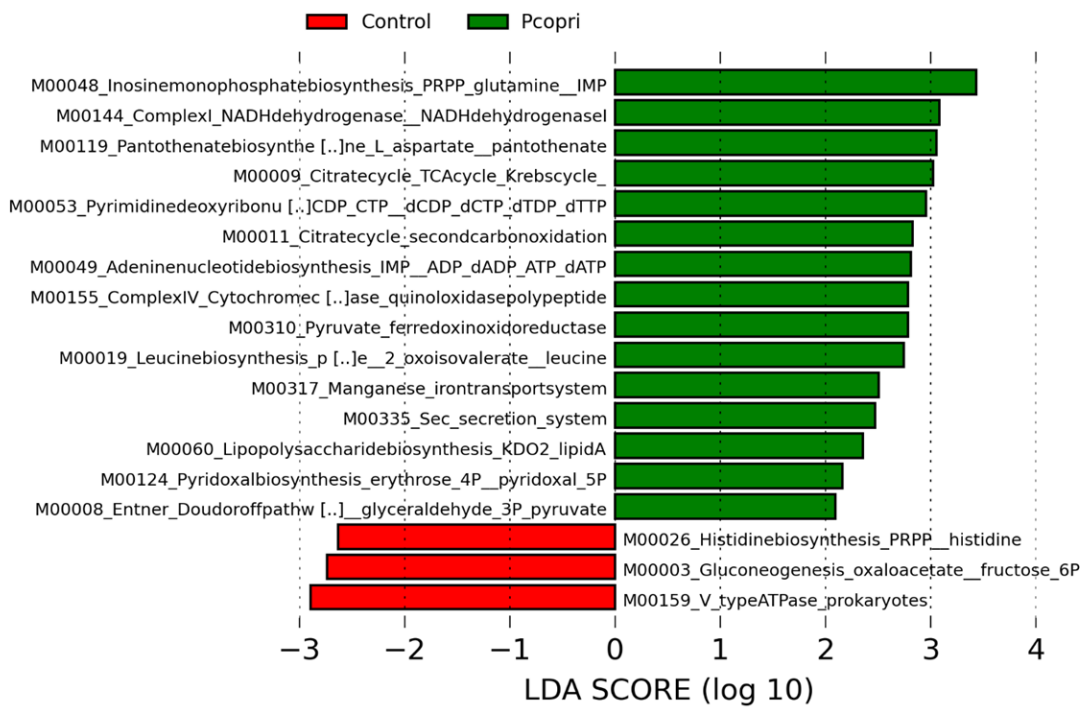


B



Supplementary figure 3. PICRUST analysis of control and *P. copri* rats at 1 week post-treatment

Linear discriminant analysis (LDA) was used to determine the predicted metabolic pathways upregulated in the GM of the control or *P. copri*-treated rats at one week post-treatment. Pathways with a LDA score of 2 or greater are considered as differentially modulated.



8. Tables

Table 1. Operational taxonomic units (OTUs) contributing to phenotype in control and *Fn. polymorphum*-treated rats at one week post-treatment.

OTU	Fold Change	log ₂ (FC)	Increased in
<i>AF12</i>	66.0720185	-6.046	Control
<i>Eubacterium</i>	18.57148163	-4.215	Control
<i>Coprobacillus</i>	16.0475006	-4.0043	Control
<i>02d06</i>	5.329638118	-2.414	Control
order <i>RF32</i>	5	-2.3219	Control
<i>Subdoligranulum</i>	4.142845306	-2.0506	Control
<i>Mucispirillum</i>	3.849559225	-1.9447	Control
<i>RC4-4</i>	3.713606655	-1.8928	Control
<i>Bacteroidia</i>	3.013137279	-1.5913	Control
<i>Staphylococcus</i>	2.785748113	-1.478	Control
<i>Gemella</i>	2.771464996	-1.4706	Control
<i>Prevotellaceae</i>	2.759229623	-1.4642	Control
<i>Facklamia</i>	2.714293469	-1.4406	Control
<i>Alphaproteobacteria</i>	2.60552371	-1.3816	Control
<i>Roseburia</i>	2.509473262	-1.3274	Control
<i>Paraprevotellaceae</i>	2.325581395	-1.2176	Control
<i>Marvinbryantia</i>	2.301601915	-1.2026	Control
<i>Bifidobacterium</i>	8.7667	3.132	<i>Fn. polymorphum</i>
order <i>RF39</i>	7.258	2.8596	<i>Fn. polymorphum</i>
<i>Allobaculum</i>	7.1175	2.8314	<i>Fn. polymorphum</i>
<i>Acetobacter</i>	4.8	2.263	<i>Fn. polymorphum</i>
<i>Barnesiella</i>	4.6667	2.2224	<i>Fn. polymorphum</i>
<i>Barnesiellaceae</i>	4.3601	2.1244	<i>Fn. polymorphum</i>
<i>Desulfovibrio</i>	4.1646	2.0582	<i>Fn. polymorphum</i>
<i>Dorea</i>	3.212	1.6835	<i>Fn. polymorphum</i>
<i>Defluviitalea</i>	2.7255	1.4465	<i>Fn. polymorphum</i>
<i>Pseudomonas</i>	2.625	1.3923	<i>Fn. polymorphum</i>
<i>Bacillaceae</i>	2.4	1.263	<i>Fn. polymorphum</i>
<i>Enterobacteriaceae</i>	2.3765	1.2488	<i>Fn. polymorphum</i>
<i>Ruminococcus 2</i>	2.108	1.0759	<i>Fn. polymorphum</i>
<i>Clostridium</i>	2.0884	1.0624	<i>Fn. polymorphum</i>
<i>Turicibacter</i>	2.0841	1.0594	<i>Fn. polymorphum</i>
<i>Adlercreutzia</i>	2.0636	1.0452	<i>Fn. polymorphum</i>

Table 2. Operational taxonomic units (OTUs) contributing to phenotype in control and *Fn. polymorphum*-treated rats at 2 months of age

OTU	Fold Change	log₂(FC)	Increased in
<i>AF12</i>	66.0720185	-6.046	Control
<i>Eubacterium</i>	18.57148163	-4.215	Control
<i>Coprobacillus</i>	16.0475006	-4.0043	Control
<i>02d06</i>	5.329638118	-2.414	Control
order <i>RF32</i>	5	-2.3219	Control
<i>Subdoligranulum</i>	4.142845306	-2.0506	Control
<i>Mucispirillum</i>	3.849559225	-1.9447	Control
<i>RC4-4</i>	3.713606655	-1.8928	Control
<i>Bacteroidia</i>	3.013137279	-1.5913	Control
<i>Staphylococcus</i>	2.785748113	-1.478	Control
<i>Gemella</i>	2.771464996	-1.4706	Control
<i>Prevotellaceae</i>	2.759229623	-1.4642	Control
<i>Facklamia</i>	2.714293469	-1.4406	Control
<i>Alphaproteobacteria</i>	2.60552371	-1.3816	Control
<i>Roseburia</i>	2.509473262	-1.3274	Control
<i>Paraprevotellaceae</i>	2.325581395	-1.2176	Control
<i>Marvinbryantia</i>	2.301601915	-1.2026	Control
<i>Bifidobacterium</i>	8.7667	3.132	<i>Fn. polymorphum</i>
order <i>RF39</i>	7.258	2.8596	<i>Fn. polymorphum</i>
<i>Allobaculum</i>	7.1175	2.8314	<i>Fn. polymorphum</i>
<i>Acetobacter</i>	4.8	2.263	<i>Fn. polymorphum</i>
<i>Barnesiella</i>	4.6667	2.2224	<i>Fn. polymorphum</i>
<i>Barnesiellaceae</i>	4.3601	2.1244	<i>Fn. polymorphum</i>
<i>Desulfovibrio</i>	4.1646	2.0582	<i>Fn. polymorphum</i>
<i>Dorea</i>	3.212	1.6835	<i>Fn. polymorphum</i>
<i>Defluviitalea</i>	2.7255	1.4465	<i>Fn. polymorphum</i>
<i>Pseudomonas</i>	2.625	1.3923	<i>Fn. polymorphum</i>
<i>Bacillaceae</i>	2.4	1.263	<i>Fn. polymorphum</i>
<i>Enterobacteriaceae</i>	2.3765	1.2488	<i>Fn. polymorphum</i>
<i>Ruminococcus 2</i>	2.108	1.0759	<i>Fn. polymorphum</i>
<i>Clostridium</i>	2.0884	1.0624	<i>Fn. polymorphum</i>
<i>Turicibacter</i>	2.0841	1.0594	<i>Fn. polymorphum</i>
<i>Adlercreutzia</i>	2.0636	1.0452	<i>Fn. polymorphum</i>

Table 3. Operational taxonomic units (OTUs) contributing to phenotype in control and *P. copri*-treated rats at one week post-treatment

OTU	Fold Change	log ₂ (FC)	Increased in
<i>Candidatus Arthromitus</i>	50.203	5.6497	Control
<i>AF12</i>	15.938	3.9944	Control
<i>Odoribacter</i>	6.8125	2.7682	Control
<i>Turicibacter</i>	5.857	2.5502	Control
<i>Lachnospira</i>	5.4976	2.4588	Control
<i>Alphaproteobacteria</i>	4.6071	2.2039	Control
<i>Desulfovibrio</i>	3.8311	1.9378	Control
<i>Erysipelotrichaceae</i>	3.8299	1.9373	Control
<i>Bacillaceae</i>	2.875	1.5236	Control
<i>Adlercreutzia</i>	2.726	1.4468	Control
<i>Bilophila</i>	2.2933	1.1974	Control
<i>Ruminococcaceae</i>	2.2889	1.1947	Control
<i>Lactobacillus</i>	2.023226642	-1.0166	<i>P. copri</i>
<i>Christensenellaceae</i>	2.1360675	-1.095	<i>P. copri</i>
<i>Prevotellaceae 1</i>	2.198092056	-1.1363	<i>P. copri</i>
<i>Anaeroplasma</i>	2.201237095	-1.1383	<i>P. copri</i>
order YS2	2.523340903	-1.3353	<i>P. copri</i>
<i>Staphylococcus</i>	2.571421225	-1.3626	<i>P. copri</i>
<i>Paraprevotella</i>	2.741603838	-1.455	<i>P. copri</i>
<i>Treponema</i>	2.857142857	-1.5146	<i>P. copri</i>
<i>Acinetobacter</i>	2.928600715	-1.5502	<i>P. copri</i>
<i>Clostridium 1</i>	2.937288882	-1.5545	<i>P. copri</i>
<i>Clostridia</i>	3.00003	-1.585	<i>P. copri</i>
<i>Pediococcus</i>	3.071441735	-1.6189	<i>P. copri</i>
<i>Bacilli</i>	3.428532245	-1.7776	<i>P. copri</i>
order RF32	3.691671589	-1.8843	<i>P. copri</i>
<i>Akkermansia</i>	8.797395971	-3.1371	<i>P. copri</i>
<i>Corynebacterium</i>	11.1428062	-3.478	<i>P. copri</i>
<i>Elusimicrobium</i>	48.71157874	-5.6062	<i>P. copri</i>

Table 4. Operational taxonomic units (OTUs) contributing to phenotype in control and *P. copri*-treated rats at 2 months of age

OTU	Fold Change	log ₂ (FC)	Increased in
<i>Candidatus Arthromitus</i>	50.203	5.6497	Control
<i>AF12</i>	15.938	3.9944	Control
<i>Odoribacter</i>	6.8125	2.7682	Control
<i>Turicibacter</i>	5.857	2.5502	Control
<i>Lachnospira</i>	5.4976	2.4588	Control
<i>Alphaproteobacteria</i>	4.6071	2.2039	Control
<i>Desulfovibrio</i>	3.8311	1.9378	Control
<i>Erysipelotrichaceae</i>	3.8299	1.9373	Control
<i>Bacillaceae</i>	2.875	1.5236	Control
<i>Adlercreutzia</i>	2.726	1.4468	Control
<i>Bilophila</i>	2.2933	1.1974	Control
<i>Ruminococcaceae</i>	2.2889	1.1947	Control
<i>Lactobacillus</i>	2.023226642	-1.0166	<i>P. copri</i>
<i>Christensenellaceae</i>	2.1360675	-1.095	<i>P. copri</i>
<i>Prevotellaceae 1</i>	2.198092056	-1.1363	<i>P. copri</i>
<i>Anaeroplasma</i>	2.201237095	-1.1383	<i>P. copri</i>
<i>order YS2</i>	2.523340903	-1.3353	<i>P. copri</i>
<i>Staphylococcus</i>	2.571421225	-1.3626	<i>P. copri</i>
<i>Paraprevotella</i>	2.741603838	-1.455	<i>P. copri</i>
<i>Treponema</i>	2.857142857	-1.5146	<i>P. copri</i>
<i>Acinetobacter</i>	2.928600715	-1.5502	<i>P. copri</i>
<i>Clostridium 1</i>	2.937288882	-1.5545	<i>P. copri</i>
<i>Clostridia</i>	3.00003	-1.585	<i>P. copri</i>
<i>Pediococcus</i>	3.071441735	-1.6189	<i>P. copri</i>
<i>Bacilli</i>	3.428532245	-1.7776	<i>P. copri</i>
<i>order RF32</i>	3.691671589	-1.8843	<i>P. copri</i>
<i>Akkermansia</i>	8.797395971	-3.1371	<i>P. copri</i>
<i>Corynebacterium</i>	11.1428062	-3.478	<i>P. copri</i>
<i>Elusimicrobium</i>	48.71157874	-5.6062	<i>P. copri</i>

CHAPTER III

UTILITY OF THE PIRC RAT MODEL OF HUMAN COLON CANCER TO TEST THE ROLE OF SPECIFIC BACTERIAL TAXA ON INTESTINAL ADENOMA DEVELOPMENT

(Susheel Bhanu Busi, Kara B. De León, Dan R. Montonye, Judy D. Wall, and
James Amos-Landgraf)

1. Overview

Colorectal cancer (CRC) patients predominantly develop adenomas in the colon. While the exact etiology is unknown, the risk factors include genetic predisposition and environmental components (25). Due to the high prevalence of CRC in industrially developed countries, it is thought that environmental stimuli along with a Western style diet comprised of increased consumption of meat, fats and total calories, coupled with longer life expectancies are factors for disease susceptibility (229). Epidemiological studies have suggested that microbial dysbiosis in the gut together with bacterial biofilms are a key factor for disease (88, 231-234). However, the mechanisms behind the role of the complex gut microbiota (GM) and how commensal bacteria contribute to adenomagenesis is largely unknown.

In the human gastrointestinal (GI) tract the complex GM is composed of approximately 10^{14} commensal bacteria, many of which help in breaking down organic and inorganic compounds (235). Recent studies comparing normal epithelial and tumor tissues using culture-independent, 16S ribosomal RNA (rRNA) or shotgun next-generation sequencing (NGS) methods have shown differences in specific bacterial abundances (59, 64, 93, 94, 96, 236-238). Similar to these reports, our previous study assessing the role of the complex GM on colon cancer susceptibility found that *Desulfovibrio* sp. was elevated in the low tumor group, where two rats did not develop any colonic tumors (131). *Desulfovibrio* sp. have been associated with healthy controls in CRC studies and are known to reduce sulfate into hydrogen sulfide, H₂S (64, 96, 131, 239-243). While others have shown that SRBs (sulfate-reducing bacteria) are commonly found in the GI tract (244, 245), Rey *et al.* recently demonstrated that SRB consume

hydrogen (H₂) and short-chain fatty acids such as acetate and lactate, affecting the response of the microbiota to diet (246).

We used a rat model of familial adenomatous polyposis (FAP), i.e. F344/Ntac-*Apc*^{+/*Pirc*} (Pirc) rat to model the human colonic cancer phenotype. The disease in these rats occurs spontaneously due to mutations in the β -catenin binding domain of the gatekeeper tumor suppressor gene, *adenomatous polyposis coli* (*APC*). *APC* mutations are not only seen in FAP patients, but also play a rate-limiting role in sporadic CRC (125-127, 167). The Pirc rats develop colonic adenomas comparable to mouse models of *APC* which have a small-intestinal phenotype and also show a sex-bias with increased tumor multiplicity observed in males compared to females (127). The size of the rat also allows for monitoring adenoma development longitudinally via endoscopy. With the Pirc rat model, we previously demonstrated that the indigenous complex GM has a significant effect on tumor multiplicity (131). We found that rederiving Pirc rats into different GM profiles via CMTR (complex targeted microbiota rederivation) significantly reduced colonic adenoma burden in one of the groups, with a concomitant increase in *Desulfovibrio* sp. (131).

The commensal microbiota and humans are thought to have evolved together (247). A key factor for the commensal, yet fastidious nature of the interaction is their ability to colonize all parts of the body, primarily the colon where up to 10¹⁴ bacteria are thought to co-exist (248). We determined that *Desulfovibrio vulgaris* Hildenborough (DvH), a Gram-negative, sulfate-reducing bacterium typically used for several industrial applications (230) including radionuclide bioremediation of toxic environmental contaminants (249) and wastewater treatment (250), colonized the colon of Pirc rats.

DvH is a known biofilm former, adhering to surfaces using protein filaments (251). We recently reported that *D. vulgaris* Hildenborough wildtype (DvH-MT) and mutant (DvH-MO) strains are biofilm-forming and -deficient respectively, with 12 single nucleotide polymorphisms (SNPs) in the genome differentiating the two strains (256). One of these mutations in DvH-MO is in a type-1 secretion system (T1SS) ABC transporter gene that is required for biofilm formation. We hypothesized that deficiency in the T1SS function, and thereby impaired biofilm formation will lead to reduced colonization and an increased tumor burden in Pirc rats. To test this, we used a fluorescent, T1SS- and biofilm- competent (JWT733) strain and a mutant lacking the type 1 secretion system's ABC transporter protein which caused a deficiency in biofilm formation (JWT716) (252). We simultaneously introduced a dTomato fluorescent marker into JWT733 for longitudinal analysis via endoscopy. We treated Pirc rats with the T1SS competent and deficient strains to determine the effect of colonization on adenoma burden. We found that T1SS competency led to increased colonization in the large intestine, and a significantly reduced adenoma burden in Pirc rats. This is the first report of T1SS competency allowing for bacterial colonization, especially in a model of complex gut microbiota. We also found that the GM communities were modulated by the bacterial treatment, leading to a decrease in sulfide levels detected in the fecal samples in the rats with decreased adenoma burden. More importantly, this study demonstrates the role of type 1 secretion systems in *Desulfovibrio vulgaris* Hildenborough in colonizing the Pirc rat model of human colon cancer and sheds light on previously unexplored *in vivo* effects of hydrogen sulfide on colon cancer.

2. Methods

2.1. Animal husbandry and housing

Pirc rats were generated by crossing male, F344/Ntac-*Apc*^{+/am1137} rats with wildtype female F344 rats obtained commercially from Envigo Laboratories (Indianapolis, IN). Animals were acclimated for a week and housed in groups, prior to set up of breeder pairs on ventilated racks (Thoren, Hazleton, PA) in micro-isolator cages. Cages were furnished with corn cob bedding and were fed irradiated 5058 PicoLab Mouse Diet 20 (LabDiet, St. Louis, MO). Rats had *ad libitum* access to water purified by sulfuric acid (pH 2.5-2.8) treatment followed by autoclaving. Fecal samples were collected for reference from all breeders prior to cohousing using aseptic methods. After allowing for one day of mating, to establish timed pregnancies, females were moved to new cages and individually housed thereafter. All procedures were performed according to the guidelines regulated by the Guide for the Use and Care of Laboratory Animals, the Public Health Service Policy on Humane Care and Use of Laboratory Animals, and the Guidelines for the Welfare of Animals in Experimental Neoplasia, and were approved by the University of Missouri Institutional Animal Care and Use Committee.

2.2. Genotyping and animal identification

Pups were ear-punched prior to weaning at 13 days of age using sterile technique. DNA was extracted with the “HotSHOT” genomic DNA preparation method (166). Briefly, ear punches were collected into an alkaline lysis reagent (25 mM NaOH and 0.2 mM EDTA at a pH 12). The ear clips were heated at 90 °C on a heat block for 30 minutes, followed by addition of the neutralization buffer (40 mM Tris-HCl, pH 8) and

vortexing for 5 seconds. DNA, thus obtained was used for a high resolution melt (HRM) analysis to differentiate wildtype rats from those carrying the *APC* mutation (Pirc) as described previously (131).

2.3. Bacterial strains, media, and growth conditions

All strains and plasmids used in this study are presented in Table 5 and are available upon request. Methods for growth of *Escherichia coli* and DvH cultures and for plasmid generation in *E. coli* were performed as described previously (256). Briefly, *E. coli* cultures were grown at 37°C on LC medium containing either kanamycin (50 µg/mL) or spectinomycin (100 µg/mL) and used for plasmid generation via sequence and ligation-independent cloning (SLIC) (253). The primers used to PCR amplify fragments for the SLIC reaction and to confirm the plasmid via sequencing are shown in Table 1. DvH cultures were grown at 30 °C in an anaerobic growth chamber (approximately 95 % N₂ and 5 % H₂; Coy Laboratory Products, Inc., Grass Lake, MI) in liquid and solidified lactate/sulfate medium supplemented with 1 % (w/v) yeast extract (MOYLS4) (256). Where indicated, G418 (400 µg/mL; Gold Biotechnology, Olivette, MO), spectinomycin (100 µg/mL), or L(+)-arginine hydrochloride (126.5 µg/mL (254); Acros Organics, New Jersey) were added to the DvH cultures. DvH cultures were routinely inoculated onto LC plates containing 40 mM glucose and incubated aerobically at 30 °C for at least two days to ensure there was no aerobic contamination.

DvH-MO is a spontaneously biofilm-deficient strain that contains 12 mutations when compared to wildtype as well as 29 deviations from the deposited sequence (255) that are likely errors in the original genome sequencing (256). One of these mutations, a single nucleotide change in the ABC transporter of the type I secretion system

(DVU1017) is the cause of biofilm deficiency in this strain (256). The culture of DvH-MO used in this study was made by combining three isolated colonies after the culture underwent single colony isolation to remove possible rare variants, including revertants, in the population.

In preparing cultures to be introduced into the rat gastrointestinal tract, 1 mL of a frozen stock stored at -80°C in 10% (v/v) glycerol solution was thawed, inoculated into 10 mL of MOYLS4 medium, and incubated at 30 °C. After approximately 24 h, the culture reached an optical density of 0.8 at 600 nm (late logarithmic phase). The cells were pelleted by centrifugation at 3696 x g for 12 min and the pellet was washed with 10 mL of 1x phosphate buffered saline (PBS) pH 7.3 (257). Centrifugation was repeated and the pellet was resuspended in approximately 10 mL of PBS to yield a final cell concentration of approximately 5×10^8 cells/mL which was confirmed by direct cell count in a Neubauer counting chamber (Clay Adams Co. New York).

2.4. Fluorescent strain (JWT733) construction

To generate a fluorescent DvH lacking antibiotic resistance markers, arginine prototrophy was used as a selectable phenotype. Argininosuccinate lyase (*argH*; DVU1094) is the last gene of an operon encoding three genes putatively involved in arginine biosynthesis. A plasmid, pMO7722, was constructed containing a gene with its native promoter encoding neomycin phosphotransferase II that confers kanamycin resistance. To create a marker exchange deletion of the 3' end of *argH*, a sequence internal to *argH* (165-688 bp) was placed upstream of the antibiotic resistance cassette and a 511-bp sequence from downstream of *argH* was placed downstream of the cassette. This plasmid, pMO7722, was transformed into wildtype DvH via electroporation as

described previously (258). Selection of the marker-exchange deletion mutant in which the 3' end of *argH* (689-1383 bp) was replaced with the kanamycin resistance cassette was selected in solidified MOYLS4 containing G418 and arginine. Resistance to the kanamycin analog G418, sensitivity to spectinomycin, and arginine auxotrophy were confirmed as well as genome structure by Southern blot. One isolate was obtained and designated JWT726 to be used for the introduction of gene(s) of choice by prototrophic selection.

Subsequently, to introduce a fluorescent marker into JWT726 (by the same transformation methods), pMO7743 was constructed to reintroduce the 3' end of *argH* along with the fluorescent marker, *dTomato*. After electroporation, the cells recovered at 30 °C in 1 mL of MOLS4 for 24 h and were then diluted 10-fold with MOLS4 to select for cells capable of synthesizing arginine. After four days, growth was observed and serial dilutions of this culture were embedded into solidified MOYLS4 for single colony isolation. Colonies showing fluorescence under the microscope were selected for phenotypic confirmation of G418 and spectinomycin sensitivity as well as arginine prototrophy. Upon genomic structure confirmation by Southern blot, one isolate was designated JWT733.

2.5. Bacterial treatment and necropsy scheme

F344-*Apc*^{+/am1137} Pirc rats generated were used for all the experiments (Fig.1). On days 14 and 15 of age, male and female Pirc rats were treated with 200 µL of ~10⁸ CFU/mL of either DvH-MT, DvH-MO, JWT733 or JWT716, suspended in anaerobic phosphate buffered saline (PBS, pH 7) via oral gavage. Rats from the control group were simultaneously gavaged with anaerobic PBS to serve as a negative control. At 4 months

of age, animals were sacrificed post-disease onset as described previously (131), with adenoma growth confirmed through colonoscopies every month starting at two months of age (167).

2.6. Fecal collection

Briefly, sterile swabs (ThermoFisher Scientific, Waltham, MA) were used to obtain a pre-treatment fecal sample on day 13 of age from the rats prior to treatment. Fecal samples from adult rats at weaning and post-weaning were collected by placing the animal in a clean, sterile cage without bedding. Fecal samples were thereafter collected at 1 week post-treatment and monthly starting at 1 month of age. Freshly evacuated feces were speared with sterile toothpick or forceps and placed into a sterile Eppendorf tube. All samples were collected into cryovials (ThermoFisher Scientific) and stored at -80 °C until processing for 16S rRNA analysis.

2.7. Fecal DNA extraction, 16S library preparation and sequencing

Fecal samples were pared down to 65 mg using a sterile blade and then extracted using the method described previously (131). Amplification of the V4 hypervariable region of the 16S rDNA was performed at the University of Missouri DNA core facility (Columbia, MO) also, as previously described (131). Briefly, bacterial genomic DNA was used for sequencing of the V4 hypervariable region using universal primers (U515F/806R) flanked by Illumina standard adapter sequences and amplified and pooled for sequencing using the Illumina MiSeq platform. Samples with more than 10,000 reads were used for assembly, binning and annotation with QIIME v1.9 including trimming and chimera removal as described previously (259). Based on 97% nucleotide identity contigs

were assigned to operational taxonomic units (OTUs) via *de novo* OTU clustering. These OTUs were annotated using BLAST (260) against the SILVA database (261, 262).

2.8. PICRUSt, HUMAnN and LEfSe analysis

Using the 16S rRNA amplicon dataset, the Phylogenetic Investigation of Communities by Reconstruction of Unobserved States (PICRUSt) software package (263) was used to predict functional capacity of operational taxonomic units identified in the fecal samples. The HMP Unified Metabolic Analysis Network (HUMAnN) software package (264) was used to predict the metabolic potential of the microbial community present in the various samples between all treatment groups. We then used linear discriminant analysis effect size (LEfSe) to plot differentially variable features with a LDA score greater than 2 logs (\log_{10}) (265).

2.9. Colonoscopy and serum collection

Rats were anaesthetized with isoflurane (3%) and placed on a heating pad to maintain body temperature. Sterile PBS was used to flush and clear colonic contents helping to lubricate and remove any fecal material. Endoscopic video and images were recorded as previously described (167). Colonic tissue samples from the proximal normal epithelium (3 mm³) were collected at two months of age, using a biopsy forceps (FB-230U, Olympus, NJ). For serum collection, 0.5 mL of blood was drawn aseptically via the jugular vein post-colonoscopy and the serum was collected by precipitating the cells at 10,000 x g for 10 minutes. The collected serum was centrifuged again at 16,000 x g for 5 minutes to remove any lysed debris or cells, and then stored in vials at -80 °C until further processing.

2.10. Necropsy, normal epithelium and tumor tissue collection

All animals were humanely euthanized with CO₂ administration and necropsied at sacrifice. The small intestine and colon from the rats were placed on bibulous paper and then splayed opened longitudinally by cutting through the section. Using a sterile scalpel blade (Feather, Tokyo, Japan) normal colonic epithelium tissues were scraped from the top, middle and distal regions of the colon. Tumors in the same locations were collected by resecting half-off from the tumors. All tissues were flash-frozen in liquid nitrogen and stored at -80 °C. Remaining intestinal tissues were then fixed overnight in Carnoy solution (266), which was replaced with 70% ethanol for long term storage until adenoma counting was performed.

2.11. Tumor counts and size measurements

At necropsy/terminal time point i.e. 4 months of age, 0.5-cm sections of the colon were resected as a cylinder prior to splaying open and embedded using a methacrylate resin (Technovit 8100, Electron Microscopy Sciences, Hatfield, PA). The remaining colon sections were cut longitudinally and fixed on bibulous paper using Carnoy solution. Tumor multiplicity was estimated by a double-blind gross counting of colonic tumors using a Leica M165FC microscope (Leica, Buffalo Grove, IL) at 7.3X magnification (127, 131, 128). Briefly, the small intestine and colonic tissues were laid flat in a large petri dish (Sycamore Life Sciences, Houston, TX) and covered with 70% ethanol (ThermoFisher Scientific) to prevent tissue drying. Biologic forceps (Roboz Surgical Instruments, Gaithersburg, MD) were used to gently count polyps observable under the objective. Tissues were kept hydrated throughout the entire process. Tumor sizes were

measured using the Leica Application Suite 4.2, after capturing post-fixed images as previously described (131).

2.12. Methacrylate embedding, sectioning and confocal microscopy

The following protocol was modified from Mark Welch *et al.* (268). Excised tissues, described above were gently coated with 0.5% low melting point agarose (ThermoFisher Scientific), placed into a well in a 24-well cell culture plate (ThermoFisher Scientific). The tissues in agarose were allowed to harden for 2 hours at 4 °C. The samples were then removed from the agarose, and fixed in 2% paraformaldehyde for 12 hours at 4 °C. Samples were washed with 1X PBS, and again coated with 0.5% molten agarose. Excess agarose was trimmed before embedding into Technovit 8100 methacrylate resin using the standard protocol (268). Briefly, samples were dehydrated with acetone for one hour at 4 °C, with repeated changes of acetone, until the solution remains clear. The sample was then covered with the infiltration solution for overnight at 4 °C. Following this, 400 µL of embedding solution was added to the samples in BEEM capsules (Electron Microscopy Services) and allowed to set overnight in an anaerobic chamber since the embedding solution is oxygen-sensitive. The samples were sectioned to 5 µm thickness using a Sorvall JB- Microtome (Dupont Instruments, USA). Confocal microscopy was performed using a SP-8 system (Leica Microsystems) after fluorescent in situ hybridization (FISH) was performed with the below probes. FISH staining was performed as described by Mark Welch *et al.* (268). The probe used for FISH analysis is listed under Table 1.

2.13. Sulfide assay

One fecal pellet from each sample was collected freshly after evacuation into the serum vial and technical triplicates were setup from each rat sample. Fecal samples were dispensed into sealed, anaerobic 5 mL serum vials (Wheaton, Millville, NJ) containing a smaller vial with 1 mL of freshly-prepared 2% wt/vol zinc acetate. Cline's sulfide assay (269) was modified to determine the levels of sulfide dissolved in fecal samples spectrophotometrically at 670 nm utilizing a passive capture technique modified from that described by Ulrich *et al.* (270). Briefly, 0.3 mL of 12 N HCl (hydrochloric acid) was used to drive dissolved sulfides into gaseous form to be captured passively by the zinc acetate solution. Using a calibration curve of standards previously established using sodium sulfide nonahydrate ($\text{Na}_2\text{S}\cdot 9\text{H}_2\text{O}$) in w/v 2% zinc acetate, we determined the concentration of sulfide per sample, and normalized the concentration to the weight of each fecal pellet (271, 272).

2.14. RT-PCR and gene expression analysis

Total RNA was extracted from biopsies of normal colonic tissues using the Allprep DNA/RNA/Protein Mini kit (Qiagen, Germantown, MD) and reverse-transcribed into cDNA with the SuperScript III First-Strand Synthesis System (ThermoFisher Scientific) using the standard described protocol for the kit. Prior to cDNA conversion, the quality of the RNA was assessed using the Experion RNA StdSens analysis kit (Bio-Rad, Hercules, CA). All samples below the RNA Quality Index (RQI) of 7 were excluded from gene expression experiments and analysis. Real-time polymerase chain reaction (RT-PCR) for mRNA expression was used to assay the following bacterial and host genes: *dsr_EUB*, *aps_EUB*, *sat_DvH*, *apsA_DvH*, *CBS*, *CTH*, *TST*, *SQOR*, *HIF1 α* ,

NOX4, *PTGS2* and *CAR1*. *GAPDH* (glyceraldehyde phosphate dehydrogenase) was used as the housekeeping gene for host gene expression (162, 273), while 16S and DNA gyrase B (*gyrB*) were used as bacterial housekeeping genes (274). *MUC2* expression was determined using a PrimeTime® Predesigned qPCR probe (c. Hs.PT.58.46475178.g, Integrated DNA Technologies, Coralville, IA). *GAPDH* was used as the housekeeping gene for the *MUC2* assay. RT-PCR was set up using a SYBR green supermix in quadruplicate reaction per primer-probe set, per sample. The final PCR mixture contained 1 µL each of forward and reverse primers (final concentration of 100 nM), 5 µL of 2X SYBR PCR mix (Applied Biosystems, ThermoFisher Scientific), 2 µL of sterile H₂O and 1 µL of cDNA from each sample at 40 ng. For the *MUC2* assay, iTaq Supermix from Life Technologies (Carlsbad, CA) was substituted for the SYBR supermix. The reaction protocol was carried out with an initial incubation of 10 min at 95 °C followed by 40 cycles of denaturing at 95 °C for 15 s; annealing and elongation at 60 °C for 1 min. The forward and reverse primers used for the genes are shown in Table 1.

2.15. Statistical analyses and figures

All statistical analyses and graphs (except Fig.1) were prepared through GraphPad Prism version 7 for Windows (GraphPad Software, La Jolla, CA). *P*-values were set to identify significance at a value less than 0.05, unless otherwise described or indicated using Analysis of Variance (ANOVA) with a Tukey's post-hoc test to identify differential groups. Correlations were performed using the linear regression module available through GraphPad Prism v7. Correlation of tumor counts with OTUs depicted as a correlogram were performed using the *corrplot* package (275) of R software v.3.1.4 (276), with a Pearson correlation coefficient.

3. Results

3.1. Biofilm-competent *Desulfovibrio vulgaris* Hildenborough (DvH-MT) suppresses adenoma size in Pirc rats

To determine if the colonization potential of a previously identified low tumor group taxon (*Desulfovibrio spp*) affected disease burden, we did a preliminary study where we gavaged male Pirc rats with the wildtype, biofilm-competent (MT) and biofilm-deficient (MO) DvH (Supplementary Fig.1A). We found that at 1 week post-treatment, 100% of the wildtype-treated rats were colonized which was maintained until 4 months of age. In contrast, only 16% of the animals treated had detectable levels of the MO strain after 1 week, and at 4 months of age, and none of the rats showed detectable levels of the MO strain. More importantly, we found that the wildtype strain reduced the average tumor area compared to the mutant MO strain (Supplementary Fig.1B), with the former only having 13% of tumors that were larger than 5 mm² (Supplementary Fig.1C). The mutant strain-treated rats on the other hand had several tumors (~35%) that were bigger than 5 mm² in average area (Supplementary Fig.1B, 1C and Supplementary Fig.2). Overall, we found that the biofilm-competent, wildtype MT strain reduced the average adenoma size in the Pirc rats.

3.2. DvH colonization modulates complex GM architecture

Due to the differential biofilm-forming capacities between the strains, we posited that the gut microbiota (GM) profile/architecture of the two groups would differ from each other post-treatment. Based on 16S rRNA gene sequencing, we found that at one week post-treatment there was a significant shift in overall profiles of the GM (Supplementary Fig.3A and Table 2), which was observed even at 4 months of age

between the wildtype- and mutant-treated groups. The richness and diversity of the groups, assessed by Chao1 and Shannon respectively did not detect any significant differences at these time points (Supplementary Fig.3B). Using a Heatmap analysis, we found several taxa showed significant differences (Two-Way ANOVA, Tukey's post hoc, $P < 0.05$) in the relative abundances between the groups (Supplementary Fig.3C).

3.3. Type 1 secretion system (T1SS) ABC transporter is essential for colonization of Pirc rats

We previously reported that DvH-MO has twelve spontaneous mutations compared to the wildtype (MT) strain. One of these, a single nucleotide change in DVU1017 conferring an alanine to proline change in the ATP-binding domain of the T1SS ATP-binding protein prevents biofilm formation (256). Therefore, we postulated that the ABC transporter gene (ATP-binding protein) of the T1SS, required for biofilm-competency is essential for bacterial colonization in Pirc rats. To test this hypothesis, we used a mutant MT strain with a deletion in the DVU1017 (ABC transporter, ATP-binding protein) gene (JWT716) (256). We also generated a fluorescent, T1SS-competent, MT strain expressing dTomato (JWT733), for detection via colonoscopy (Fig.1A). Attempts to create a fluorescent biofilm-deficient strain were not successful. We treated Pirc rats at days 14 and 15 of age with either JWT733, JWT716 or anaerobic PBS, i.e. the T1SS-competent, T1SS-deficient strains and control treatment respectively (Fig.1B). We used quantitative RT-PCR (real-time polymerase chain reaction) with strain-specific locked nucleic acid (LNA) probes to determine the colonization potential of the two DvH strains. One week after treatment with JWT716, we were not able to detect any bacteria in fecal samples, consistent with the observations in our preliminary study with MO. On the other

hand, we detected JWT733 in 100% and 84% of the fecal samples at 1 week post-treatment and 4 months of age, respectively. Since *Desulfovibrio* belongs to the Proteobacteria phylum, we assessed the levels of Proteobacteria in the fecal samples at 1 week post-treatment. We found this phylum to be elevated in both the treated groups, compared to the control rats (Fig.1C). At 4 months of age levels of Proteobacteria in the fecal (Fig.1D) and normal epithelium biopsy (Fig.1E) samples) however, did not show any significant differences between the groups. At 1 week post-treatment and at 2 months of age, we found variable levels of differential taxa under phylum Proteobacteria (Fig.1C-E). We concurrently used colonoscopy to assess colonization in the colon of the Pirr rats treated with the fluorescent JWT733 strain starting at 2 months of age. We found detectable levels of fluorescence at 2-, 3-, and 4 months of age (Supplementary Fig.4). To determine if the T1SS-, biofilm- competent JWT733 was indeed forming biofilms in the colonic epithelium, we used fluorescent in-situ hybridization (FISH) with a custom probe and found that 40% of all the animals in the JWT733 group had detectable levels of the bacteria in the lumen (Supplementary Fig.5).

3.4. Endogenous complex GM community structure is modified due to DvH treatment

We expected that treatment with the fluorescent, T1SS-competent strain (JWT733) would be similar to the parental, wildtype (MT) strain (Fig.2A and Table 3), modulating the GM due to bacterial colonization. We found additional significant differences in the endogenous GM community structure between the control and the treatment groups in the second round of treatments based on sample type, i.e. fecal or biopsy (Supplementary Fig.6, Table 4). Examination of all the significant OTUs

(ANOVA, $P < 0.05$) contributing to the differences in communities demonstrated different groups of OTUs elevated in the fecal samples compared to the normal epithelium biopsy tissues (Fig.2B). Closer examination of the OTUs contributing to the biopsy (Fig.2C) and fecal (Fig.2D) GM profile differences between the three groups demonstrated varying relative abundances of several OTUs. We noticed that *Ruminoclostridium*, *Lachnoclostridium*, *Tepidimonas*, *Ruminococcus 1*, *Butyrivibrio*, *Roseburia* and *Ruminococcaceae* were elevated in the control rats. In the T1SS-competent, JWT733 rats we found an increase in the abundance of *Allobaculum*, *Dorea*, *Desulfovibrio*, *Bifidobacterium*, *Alistipes*, *Butyricimonas*, *Coprococcus*, *Erysipelotrichaceae*, *Clostridium sensu stricto*, *Ruminococcaceae* UCG-010, *Lachnospiraceae* ND3007, [*Eubacterium*] *nodatum* and *Rikenella*.

3.5. T1SS-competent DvH treatment is associated with decreased adenoma burden

The T1SS-competent (JWT733) treated Pirc rats, irrespective of sex, had significantly reduced adenomas compared to the JWT716 (deficient in protein export by T1SS) and control groups (Fig.3A). The average size of the adenomas was significantly reduced in the JWT733 group compared to the ATP-binding protein-deficient group in the females, while the males showed a slightly decreased average tumor area albeit statistically not significant (Fig.3B). All the tumors in the JWT733 group were smaller than or equal to 10 mm² while the JWT716 and control groups respectively had 35% and 21% of tumors that were larger than 10 mm² in size (Fig.3C). Using quantitative PCR we determined the number of copies of JWT733 from fecal samples at sacrifice and found that the colonic tumor multiplicity was associated with the number of copies of JWT733 in the Pirc rats (Fig.3D). We also performed correlation analysis between the relative

abundance of the OTUs from fecal samples at 1 week post-treatment and 2 months of age and the colonic tumor multiplicity to identify prognostic biomarkers of the disease (Supplementary Fig.7). We found both positive (*Ruminococcaceae*; Fig.3F) and negative (*Lactobacillus* and *Alistipes*; Fig.3E and Fig.3F) correlations among the OTUs.

3.6. Fecal sulfide levels are decreased in JWT733 treatment compared to the control and JWT716 groups

Desulfovibrio sp. is one of the many sulfate-reducing bacteria (SRB) found in the colon (246, 277) that serve as a source of hydrogen sulfide (H₂S) in the GI tract. SRBs including bacteria such as *Escherichia coli*, *Salmonella*, *Clostridia* and *Enterobacter* (278) utilize oxidized sulfur compounds in anaerobic respiration as terminal electron acceptors (279, 280) to produce hydrogen sulfide. Based on this evidence, we tested the level of hydrogen sulfide in the fecal samples. At necropsy (4 months of age), dissolved fecal hydrogen sulfide was not different between groups (Fig.4A). However, at 2 months of age, a time at which adenomas are understood to be developing, we found that the high tumor groups, JWT716 and control rats had significantly elevated hydrogen sulfide in the feces compared to the low tumor, T1SS-competent JWT733 treated group (Fig.4B). We next evaluated the expression of sulfate-reduction genes found in bacteria and the host, in biopsies collected at 2 months of age. Using RT-PCR, we found a decrease in the expression of Eubacterial adenylyl sulfate reductase (*aps*) in the low tumor JWT733 group (Fig.5C). Elevated sulfide levels detected in the assay were simultaneously associated with 2-fold or greater increase of host sulfate-reduction genes: cystathionine beta synthase (*Cbs*) in the JWT716 group, whereas sulfide quinone oxidoreductase (*Sqor*) was increased in the DvH-treated groups (Fig.5D). We found a concomitant increase in

the expression of genes involved in hypoxia and inflammation in the host in the JWT716-treated group (Supplementary Fig.8A). Overall, *Hif1a* and *Ptgs2* gene expression was reduced significantly in the JWT733-treated animals relative to the controls.

Simultaneously, due to the genotoxic nature of the hydrogen sulfide (233), we tested DNA damage and repair genes, where we saw a reduced expression of the *Atm* gene in the JWT733 group compared to the controls and the T1SS-deficient, JWT716 groups (Supplementary Fig.8B). Mucin in the GI tract is also thought to be an efficient source of sulfides (243). Due to the prevalence of mucin-degrading bacteria such as *Ruminococcaceae*, *Lachnospiraceae*, *Prevotellaceae*, *Bacteroides* sp., *Akkermansia muciniphila* and *Bifidobacterium* sp. observed via 16S sequencing (Fig.2), we determined the level of the gene encoding for mucin predominantly in the gut, i.e. *MUC2*. We found that at 2 months of age, *MUC2* expression was considerably reduced in the JWT733 group compared to the high tumor groups (control and JWT716) (Supplementary Fig.8C).

Overall, the data presented here and taken together suggest that the ABC transporter gene in a type 1 secretion system of *D. vulgaris* Hildenborough, is essential for colonization of the colon in Pirc rats. Whether directly or indirectly the T1SS is involved in reduced adenoma burden in this model of early onset colon cancer. We show that treatment with a bacterium in a complex GM setting could lead to significant shifts in the community structure and affect host gene expression during this process. This is also the first report demonstrating increased fecal hydrogen sulfide levels contribute to increased adenomagenesis. This concomitant increase is also associated with increased expression of sulfate-reduction, hypoxia- and inflammation genes. Nonetheless, treatment

with a T1SS-, biofilm- competent *D. vulgaris* Hildenborough strain modulated the host GM, where the bacterium colonized the colon regardless of the complex endogenous GM, modulating adenoma burden.

4. Discussion

Gut microbiota modulates disease susceptibility and severity of colon cancer (131, 159, 281-286). Numerous reports provide evidence to the role of bacterial taxa that could be opportunistic pathogens, while otherwise existing as commensals in the colon of patients (90, 231, 236, 287-291). Studies comparing normal epithelial and tumor tissues using culture-independent methods, have shown differences in specific bacterial taxa abundances (59, 64, 93, 94, 96, 159, 236-238) including *Desulfovibrio spp.* These bacteria have been associated with healthy controls in colorectal cancer (CRC) studies, including our own where we saw an increased abundance of these taxa in the group with fewer adenomas (64, 96, 131). Herein, we report a methodical testing of 16S rDNA gene sequencing data via treatment of a preclinical rodent model of colon cancer with specific bacteria in the context of a complex GM, unlike germ-free or mono-colonized approaches (59, 64, 120, 173, 291-296). This method may also serve as an improved translatable model to identifying biomarkers and therapeutics for human disease. To enhance colonization potential, we used our previously reported biofilm-forming *D. vulgaris* Hildenborough strain (256) to treat Pirc rats. We postulated that the type-1 secretion system (T1SS) required for biofilm-competency in *Desulfovibrio* (or in many bacteria) would be critical for bacterial colonization in a complex GM background. We further

hypothesized that impaired colonization by DvH due to a mutation in the T1SS would lead to an increased adenoma burden in Pirc rats.

We observed that treating Pirc rats with the biofilm-deficient MO strain increased the average adenoma size and caused a shift in the GM architecture due to colonization. Shifts in the GM architecture, evident as early as one week post-treatment and at 2 months of age, suggest that the biofilm-competent strain not only colonized the Pirc rats, but also subsequently modified the GM profile. To narrow down the mutations responsible for the phenotype observed with the MO treatment, we designed a DvH strain with a deletion of the ABC transporter gene of the T1SS. We found that the T1SS-competent, JWT733 strain colonized the Pirc rats despite the presence of the indigenous complex GM. Shepherd *et al.* recently showed that strain engraftment in a complex GM setting could be a function of specific bacterial genes and their corresponding carbohydrate substrate establishing a metabolic niche (297). We report that a T1SS-competent, biofilm-former engrafted within an endogenous, complex community without the need for altering the carbohydrate composition or the diet to avoid GM community changes (298-301). We detected the presence of JWT733 using fluorescent colonoscopy starting at 2 months of age, which was also associated with a decreased adenoma burden (number and average size) irrespective of sex. Although plausible, it is highly unlikely that the presence of dTomato in JWT733 and the lack thereof in JWT716 contributed to decreased adenomagenesis since fluorescence is typically used for all cell-labelling studies (302-305). More importantly, we found that the phenotype observed with the fluorescent, JWT733 was also similar to that observed when treated with the wildtype, MT strain without the fluorescent marker.

Biofilms are a required and critical first-step for bacterial colonization in the marine, steel and corrosion industries (137, 306, 307). It is likely that the proteins exported by the T1SS for biofilm-formation in the wildtype and the JWT733 strains enabled the bacteria to colonize the Pirc rat colon, thereby creating a protective environment locally, i.e. at the mucosa. It is evident from the fecal and mucosal biopsy samples at 2 months of age that the community profiles of the GM between the control, JWT716 and the JWT733-treated groups are significantly different. In the JWT733 rats, the abundance of taxa associated with healthy tissues such as *Allobaculum*, *Desulfovibrio*, *Clostridium sensu stricto*, *Rikenella*, *Bifidobacterium*, *Butyrivibrio*, *Bilophila*, *Coprococcus*, *Lactobacillus*, *Micrococcus*, some *Lachnospiraceae* taxa and *Butyricimonas* is suggestive of a mucosal-associated community that may be protective. OTUs such as *Micrococcus* (163), *Bifidobacterium* (308), *Coprococcus* (309), *Butyrivibrio* and *Allobaculum* (310) have previously been reported to be associated with either healthy stool or tissue samples from CRC patients.

On the other hand, 16S rDNA gene sequencing revealed that the GM communities of the fecal samples are significantly different from those observed in the biopsies. The fecal community of the T1SS-competent included bacteria such as *Alistipes*, *Bacteroides*, *Faecalibacterium*, *Butyricimonas*, *Desulfovibrio* and *Parabacteroides*. Butyrate-producers such as *Faecalibacterium* and *Butyricimonas* had increased relative abundance in the JWT733 group. Studies suggest that these bacteria prevent tumorigenesis in mice models of colon cancer (207, 208). On the other hand bacteria such as *Alistipes* and *Bacteroides* have been associated with increased tumor burden or with carcinoma samples (311). The enrichment of these bacteria in the low

tumor JWT733 rats may be a reflection of their passenger status, i.e. increasing due to tumorigenesis-mediated dysbiosis, similar to the report by Sun *et al.* in a mouse model of CRC (312). At one week of age and at 2 months, both the JWT716 and control groups shared OTUs that were significantly different from the JWT733 group and that which are associated with increased CRC. *Roseburia*, *Lachnospiraceae*, *Ruminococcaceae* and *Prevotellaceae* have been consistently linked with CRC across many studies including those by Schloss *et al.* and Dejea *et al.* (74, 312, 313).

Alternatively, type 1 secretion systems (T1SSs), necessary for polypeptide transport across the bacterial outer membrane, secrete a wide range of proteins including adhesins, cyclases, metalloprotease-phosphatases, hydrolases, and hemolysins. (314-317). The T1SS ABC transporter in DvH is proposed to export two proteins (256, 315). The DVU1012 gene, an integral part of the type 1 secretion system, is known as the hemolysin-type calcium binding repeat protein and shown to have a von Willebrand factor A domain, thought to be involved in cell attachment in eukaryotic cells (256). This gene also shares similarities with the RTX (repeat-in-toxin) gene recently reported in *E. coli* required for colonization of the urinary tract and kidneys (318). One of the functions of the RTX family of genes is the production of alpha-hemolysin, reported in several Gram-negative bacteria including *E. coli* to be capable of causing urinary tract infections and host tissue damage (318-320). Some reports have suggested that hemolysins promote tumorigenesis (321), while others propose that bacterial hemolysins could be protective against colon cancer (322, 323). This disparity in the role of the hemolysins is a potential factor affecting the mechanism of reduced burden in the T1SS-competent strain-treated Piric rats and warrants further investigation in future studies.

Sulfate-reducing bacteria (SRB), including *Desulfovibrio spp*, *Eubacterium*, *Citrobacter*, *Flavonifractor*, *Bacteroides*, *Ruminococcaceae*, and *Bilophila* found in the GI tract (244, 245, 324, 325) are known to use sulfates for anaerobic respiration. They release hydrogen sulfide into the lumen (326-329) and consume hydrogen (H₂), short-chain fatty acids such as acetate and lactate, affecting the response of the microbiota to diet (246). Various studies have shown that hydrogen sulfide possesses apoptotic functions, while also reducing oxidative stress (267, 330, 331). Other roles for exogenous H₂S include anti-inflammatory resolution to experimental colitis, decreased gastric ulcers, and gastrointestinal integrity maintenance (147, 332-337). Simultaneously, cell culture and mice model studies have shown hydrogen sulfide based drugs could suppress colon cancer growth (338-340). We found that the dissolved H₂S levels were significantly higher in the T1SS-deficient (JWT716) and control groups at two months of age. Several mechanisms may contribute to this increase in H₂S despite the lack of colonization by DvH due to the ABC transporter deficiency in the control and JWT716 groups. The GM composition of the JWT733 group biopsies suggests that bacteria capable of sulfide generation were associated with the mucosa, while the control and JWT716-treated rats had increased abundance of SRBs in the fecal samples. We found the associated increase of other sulfate-reducers including *Ruminococcus*, *Bilophila*, *Sutterella*, *Fusobacterium*, *Clostridium sensu stricto*, *Peptococcus*, *Prevotella*, *Streptococcus*, *Flavonifractor*, *Eubacterium* and other *Desulfovibrionaceae* in the high tumor (control and JWT716) groups' fecal samples. These bacteria are capable of utilizing cysteine, sulfomucins, taurine, sulfite, sulfated bile acids, estrogen-3-sulfates and phenylsulfates to produce H₂S (243, 341). Increased sulfide could also be due to the

presence of mucin-degraders such as *Akkermansia* sp., *Ruminococcaceae*, *Ruminiclostridium*, *Lachnospiraceae*, *Lachnoclostridium* in the JWT716 and the control rats. The associated increase of *MUC2* expression suggests the mucin-degradation possibly leads to the release of sulfonated compounds required for H₂S production.

Simultaneously, increased production of H₂S by the host to promote proliferation of colon cancer cells and to support cellular bioenergetics could potentially contribute to the increased luminal levels of H₂S (342, 343). Complementary to the principle of increased H₂S leading to an increased tumor burden we found an associated increase in host sulfate reduction genes' expression along with the high fecal sulfide observed in the control and JWT716 groups. H₂S is a gaseous signaling molecule that is important for normal pathophysiology (233). Cysteine, a major source of H₂S in the gut is catalyzed by cystathionine beta-synthase (*Cbs*) leading to H₂S production which can be oxidized by colonocytes through the action of sulfide quinone reductase (*Sqor*) and thiosulfate sulfur transferase (*Tst*) (233, 344, 345). Along with the increase in Pirc rats' sulfate-reduction genes, we found elevated levels of *Hif1α* and *Ptgs2* in the control and JWT716-treated animals. The elevation of these genes suggests a hypoxic environment due to the increased presence of H₂S (346-349). Hypoxic conditions along with *Hif1α* expression modulates *Nox4* expression in most tissues (350-352). However, the mechanism of this pathway in the colon is unknown, requiring validation in future studies. More importantly in the control and JWT716 groups, we saw an increased expression of the *Ptgs2* (*Cox2*: cyclooxygenase-2) gene which is typically involved in GI inflammation and increased susceptibility to colon cancer (353-357). The increase in *Ptgs2* could also be a host response to the hypoxic condition established due to the increased H₂S (358-360).

Consequential to the elevated and potentially genotoxic nature of hydrogen sulfide, we noticed an increase in the expression of DNA damage response genes *Msh2*, *Atm*, and *Mgmt* in the control and JWT716-treated rats (361, 362). This suggests that the H₂S may be causing mutations or inducing double stranded breaks in the proliferating colonocytes potentially leading to an increased DNA damage response. Alternatively, the increased *Hmox1* and *Bcat* expression in the T1SS-competent group emphasizes the probable spatial nature of hydrogen sulfide. Proximity of hydrogen sulfide to the mucosa may be causing increased proliferation of the colonocytes. In rats following spinal cord injury, hydrogen sulfide activates Wnt/ β -catenin signaling (363). H₂S as a function of the colonization potential of the T1SS-competent strain may be playing a dual role of prevention and promotion of colon cancer depending on the spatial organization of the GM in the T1SS-competent and the other two groups respectively. It may also be plausible that the exogenous hydrogen sulfide produced in the JWT733-treated rats within proximity of the mucosal surface may be protective as shown in *in vitro* and *ex vivo* experiments (364). We found decreased levels of fecal H₂S in the T1SS-competent strain-treated rats at 2 months compared to that of controls and the T1SS-deficient group supporting this notion.

Reports have suggested vast differences in the lumen and mucosa-associated microbiota in patients with CRC (74), a theory supported in our study by the differences in the fecal and biopsy 16S rDNA results. The significance of this spatiotemporal arrangement of the complex GM communities within the lumen and that, which is involved with the mucosa, may be of relevance to understanding the etiology of colon cancer going forward and needs further investigation.

Bacterial colonization factors are attributed to the co-evolution of the host and the prokaryotic commensals living inside the mammalian system (365-367). We report that despite the complexity of the indigenous gut microbiota, suitable factors such as the T1SS ABC transporter mediating biofilm formation could enable colonization of the host. Based on our results, we propose the use of complex GM models as a more translatable approach for therapeutic testing especially due to their physiological relevance. However, validations are required before the excitement of the therapeutic prospects of this bacterial strain are considered. It is necessary to confirm the mechanisms tested here in the context of a different complex GM profile and understand how slight variations in the community profile may affect the phenotype. More importantly, recent reports suggest that biofilms in the colon, albeit mediated by specific bacteria predispose patients to colon cancer (88, 90, 289, 368-371). In light of our report suggesting that biofilm-forming DvH alleviates tumor burden, a more systematic and controlled approach is warranted where other T1SS-competent bacteria, including potential biofilm-formers should be tested thoroughly for their effect on CRC development. The authors acknowledge that it is challenging to model microbial interactions especially in a complex GM setting and the inability to distinguish the presence of bacterial JWT733 cells or T1SS cargo proteins as reasons for reduced adenoma is a limitation of our study. However, the potential for biofilm-competency and thereby the capacity for its formation in the gut suggests the possibility of metabolite exchanges among the complex GM community. The identification of bacterial metabolites, whether hydrogen sulfide or others could have a significant impact in establishing therapeutic routines including through modification of dietary agents. Our study emphasizes the complex and

synergistic interactions, including the possibility of the same metabolite having differential effects contingent on the spatial arrangement of the GM, simultaneously affecting the susceptibility and etiology of colon cancer.

5. Ethics Statement

The guidelines established by the Guide for the Use and Care of Laboratory Animals and the Public Health Service Policy on Human Care and Use of Laboratory Animals were strictly followed during this study. The University of Missouri Institutional Animal Care and Use Committee approved all studies and protocols (#6732 and #8732) for this endeavor.

6. Author Contributions and Acknowledgements

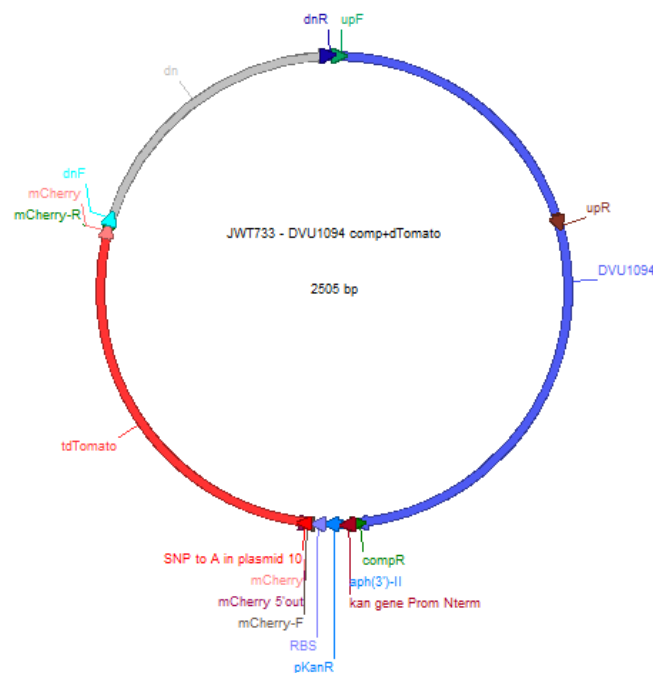
SB, KD, JW and JAL designed the experiments. SB and KD executed the experiments, while DM was instrumental in gavaging the rats. The authors wish to thank Dr. Pamela J.B. Brown and Jeremy J. Daniel at the University of Missouri for kindly providing pSRKKm-tdTomato and Grant M. Zane for the idea of using prototrophy as a selection when introducing genes into the genome; acknowledge Nathan Bivens and the MU DNA Core for assistance with 16S rDNA sequencing; Bill Spollen, Christopher Bottoms and the MU Informatics Research Core Facility for assistance with software installation for data analysis; Rat Resource and Research Center; MU Office of Animal Resources and their staff for assistance with animal husbandry.

7. Figures

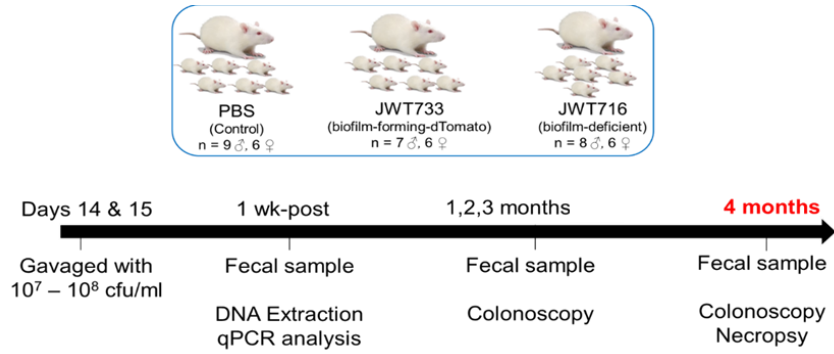
Figure 1. Pirc rat treatment with Type 1 secretion system (T1SS) ABC transporter – competent (JWT733) and –deficient (JWT716) strains of DvH

(A) Schematic for JWT733: Type-1 secretion system (T1SS) –competent strain, indicating the location of the fluorescent dTomato gene. (B) Experimental design: Pirc rats were treated with T1SS-competent (JWT733) or T1SS-deficient (JWT716) strains of DvH. Number of animals used as indicated in figures. Dot plots depict the relative abundance of phylum Proteobacteria in fecal samples at 1 week post-treatment (C), 2 months of age (D), and mucosal biopsies at 2 months of age (E). Error bars indicate standard error of the mean (\pm SEM). Associated bar graphs show the relative abundance of the operational taxonomic units at the Genus level contributing to the Proteobacteria phylum in each sample. AT: ambiguous taxa, ub: uncultured bacterium, uo: uncultured organism and rb: rumen bacterium

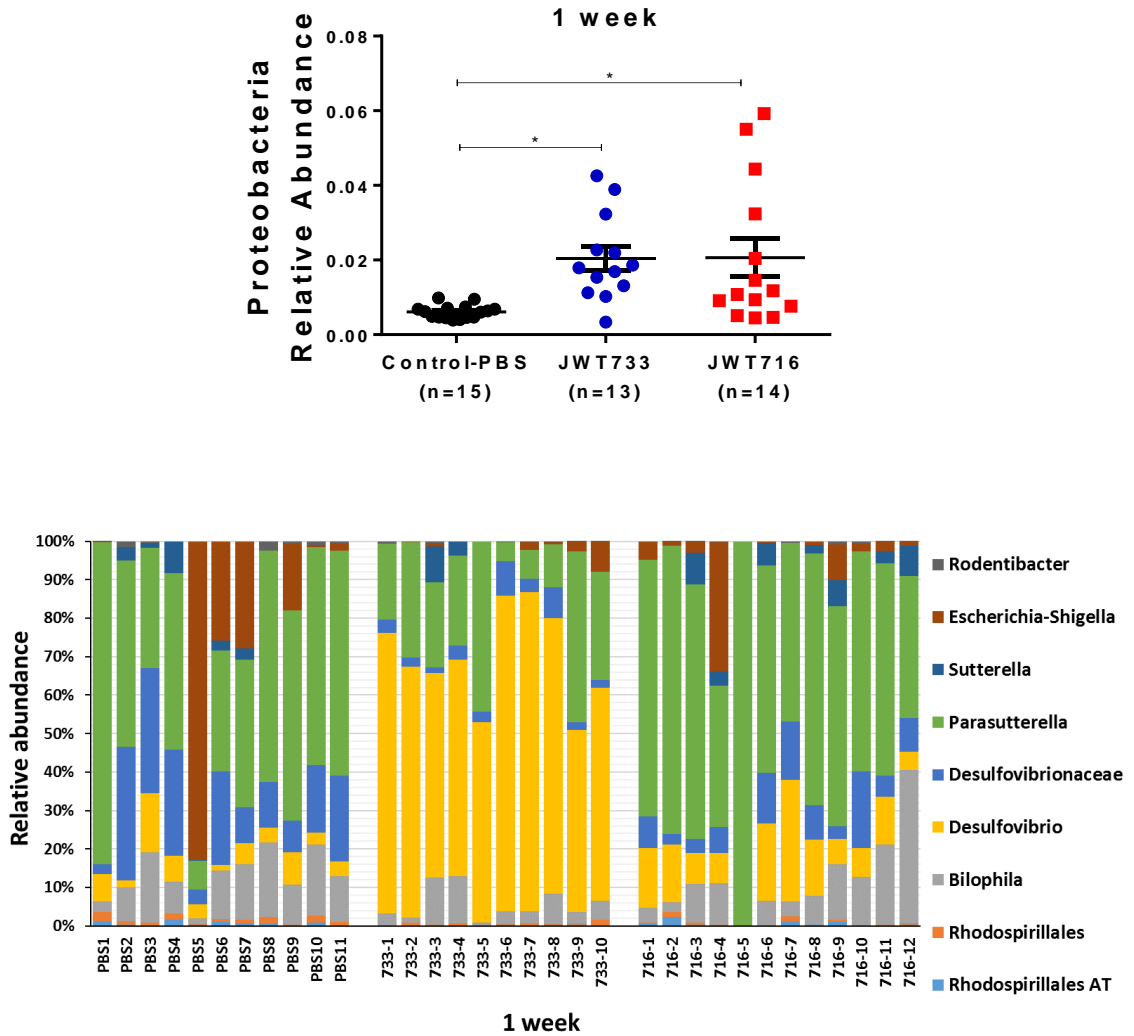
A



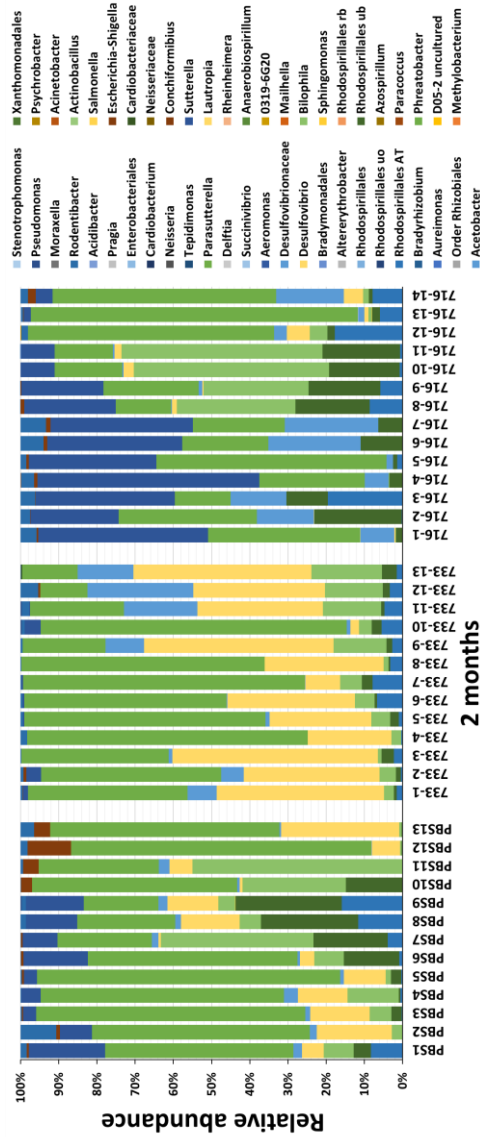
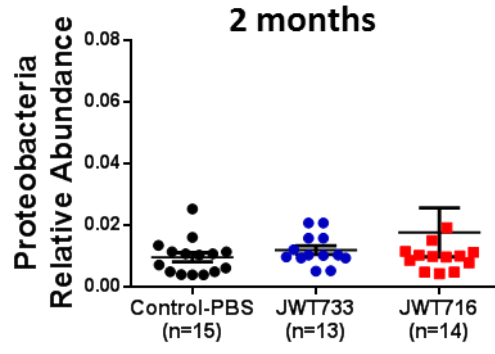
B



C



D



E

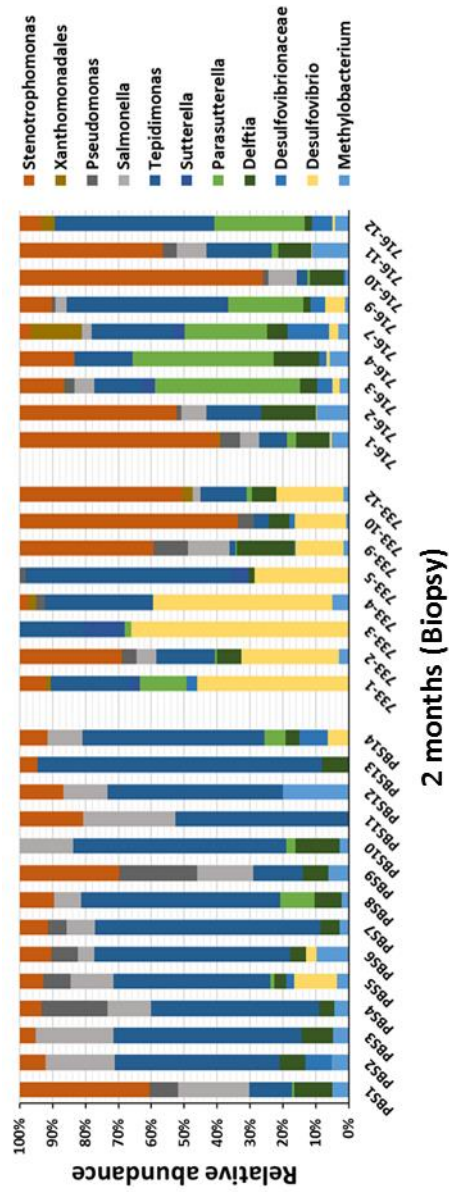
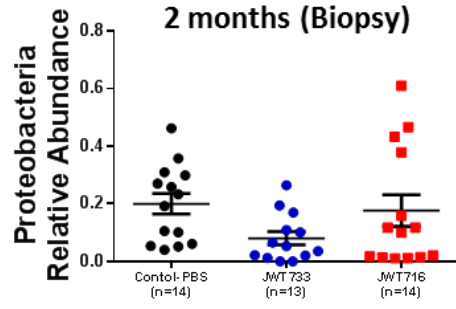
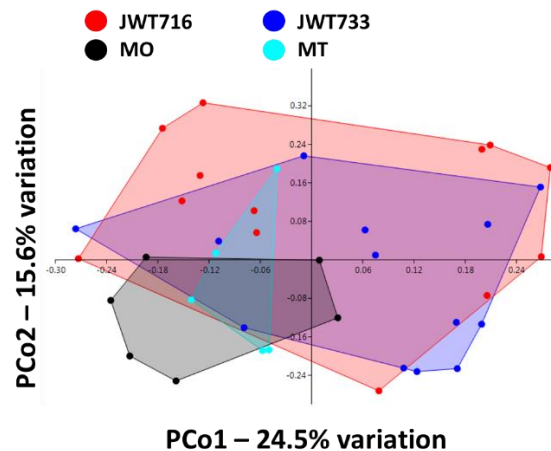


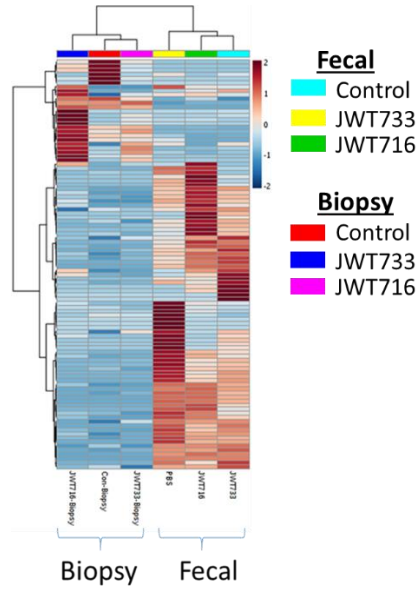
Figure 2. 16S rRNA gene sequencing analysis of control, JWT733 and JWT716 groups

(A) Principal Coordinate Analysis (PCoA) plot depicting the fecal 16S rDNA gene sequencing dissimilarities between the DvH-treated groups based on the Bray-Curtis distance matrix. Post-hoc analysis indicating the differences between individual groups is listed under Table 3. Each symbol represents the GM community from the fecal sample of a single rat at 2 months of age. (B) Heatmap generated from the significantly (ANOVA, $P < 0.05$) differential OTUs between each group of the fecal and biopsy samples, using Ward's clustering algorithm. Range of blue to red color indicates low to high abundance respectively. PBS, $n=15$; JWT733, $n=13$, JWT716, $n=14$, Con-biopsy, $n=15$; JWT733-biopsy, $n=13$ and JWT716-biopsy, $n=14$. (C) Heatmap of the GM profiles obtained from fecal samples collected at 2 months of age via colonoscopy depicting the significantly different OTUs between groups. (D) Heatmap of the GM profiles obtained from biopsy samples collected at 2 months of age depicting the significantly different OTUs between groups.

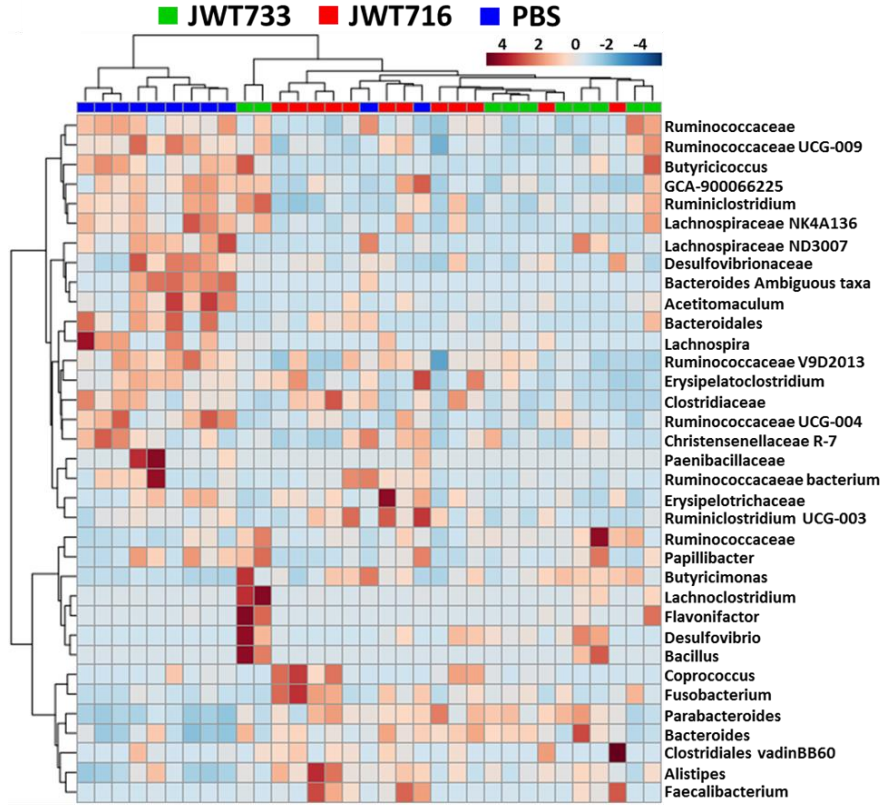
A



B



C



D

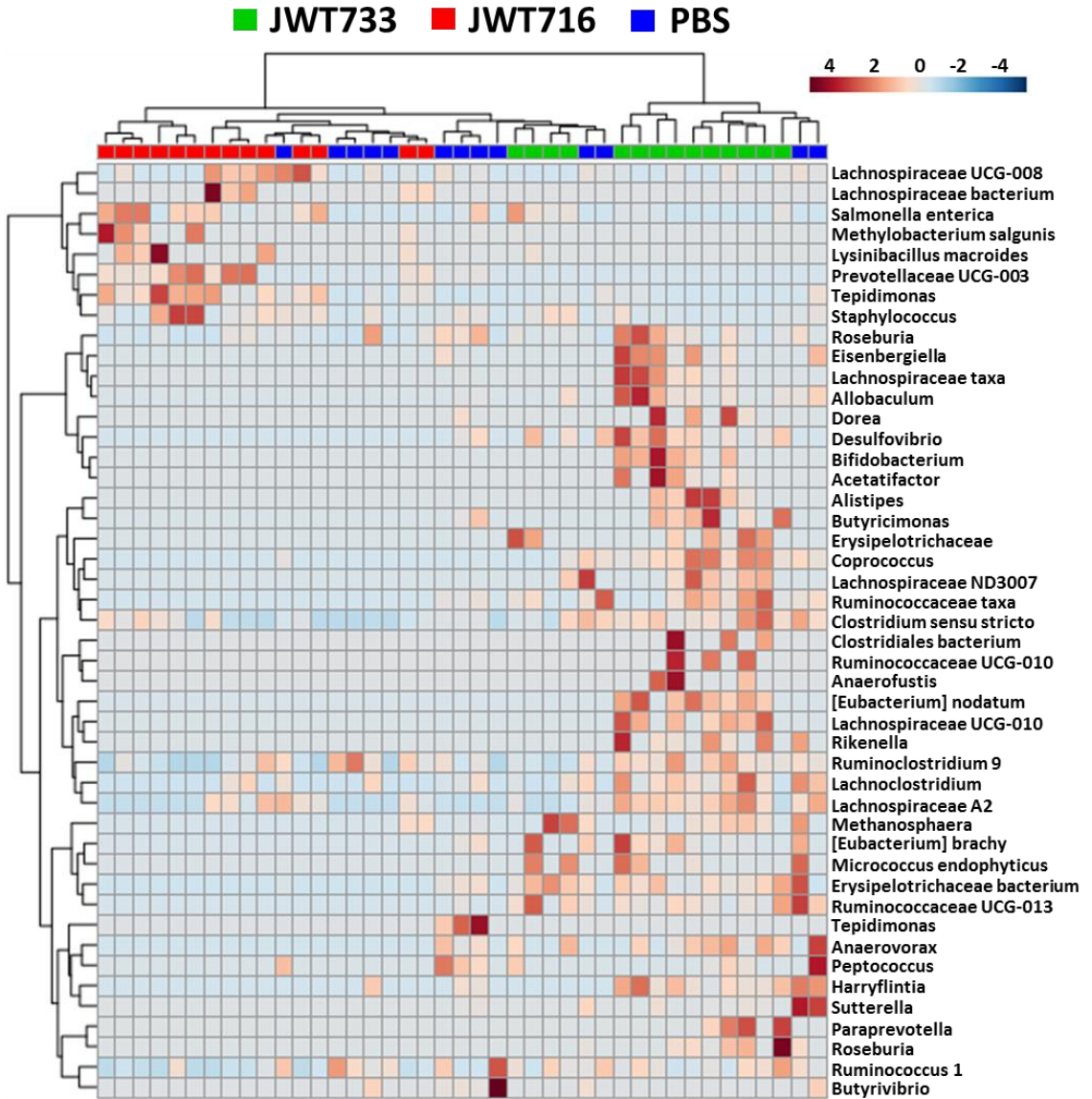
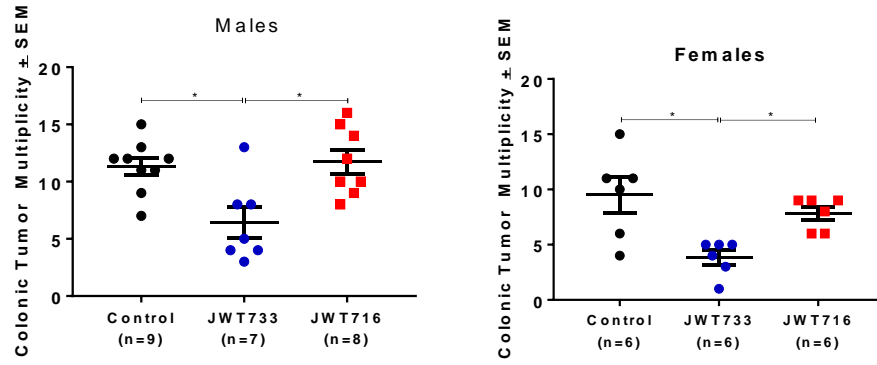


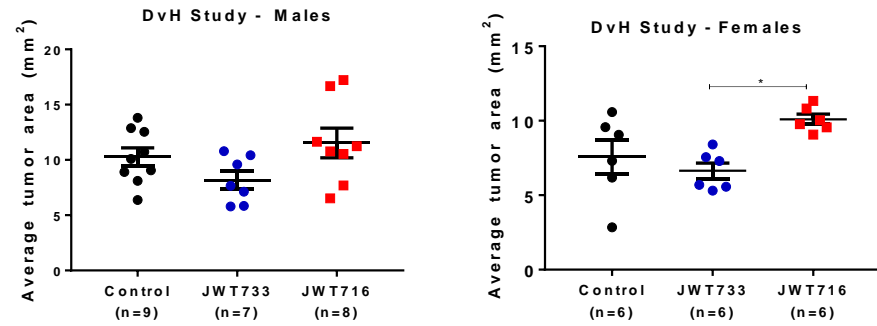
Figure 3. Tumor multiplicity, average tumor burden and OTU-tumor correlations in control and treated Piric rats

(A) Colonic tumor multiplicity in male and female Piric rats at sacrifice, i.e. 4 months of age. (B) Average tumor area observed in male and female Piric rats treated with either anaerobic PBS (control), JWT733 (T1SS-competent) or JWT716 (T1SS-deficient) strains of DvH. For (A) and (B) a One-Way ANOVA with a Tukey's post hoc test was used to determine significance with P -values below 0.05 considered to be significantly different between groups. (C) Tumor sizes observed in the treatment and control groups. Control, $n=15$; JWT733, $n=12$, JWT716, $n=14$. (D) DNA extracted from biopsies collected at 2 months of age tested for detectable bacteria via qRT-PCR with strain-specific probes. JWT733 ($n=13$) and JWT716 ($n=14$) groups. Number of copies of JWT733 in the T1SS-competent (wildtype) treated rats plotted against the colonic tumor multiplicity at 4 months of age. Rats with less than 1000 copies separated from those with greater than 2000. (E) Pearson's correlations ($P<0.05$) between OTUs at one week post-treatment with colonic tumor counts. Representative example of *Lactobacillus* with colonic tumor count along x -axis and relative abundance of the taxa along the y -axis is shown. (F) Correlation of OTUs from 2 month fecal samples is shown with an example of a negative correlation (*Alistipes*) and a positive correlation (*Ruminococcaceae*). Error bars in all figures indicate standard error of the mean (\pm SEM).

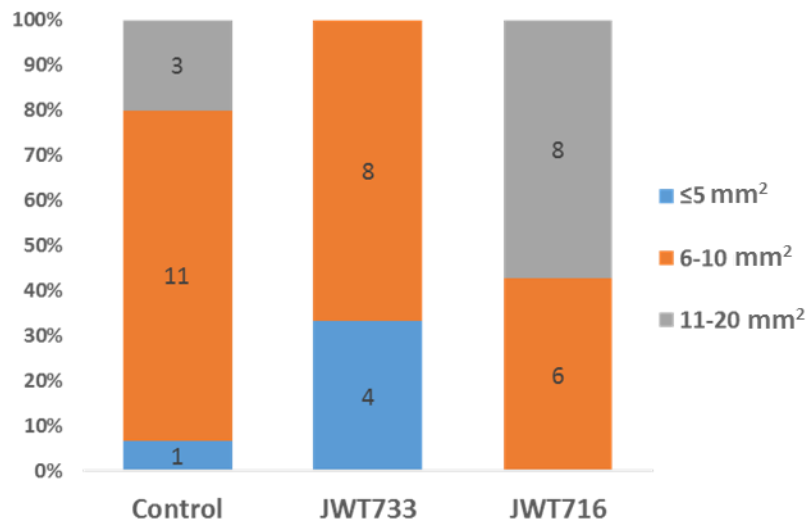
A



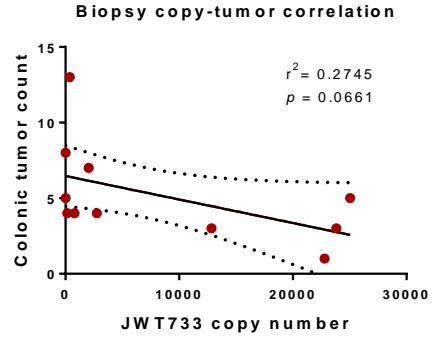
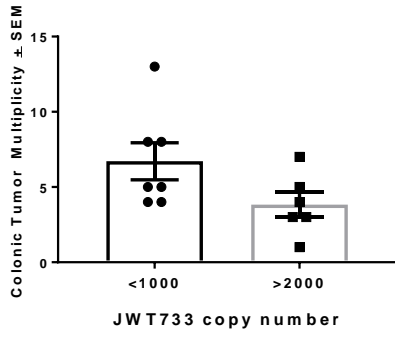
B



C

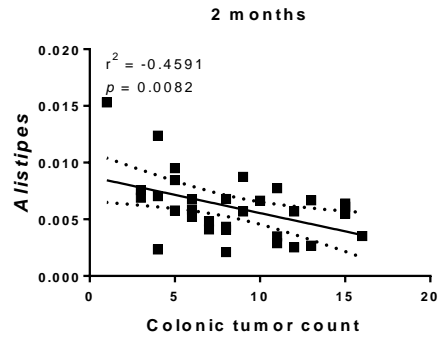
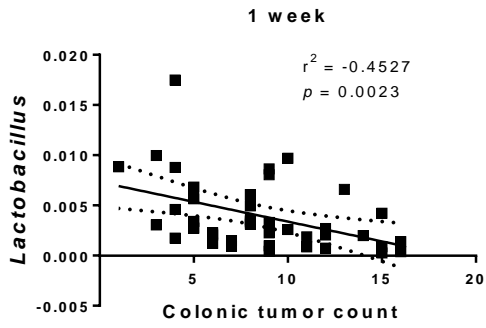


D



E

F



G

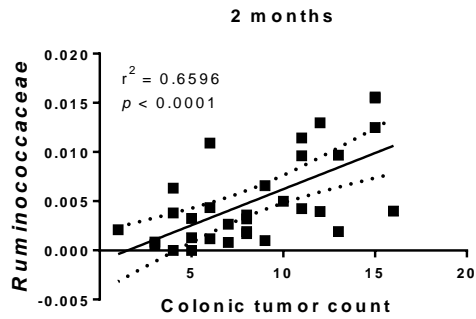
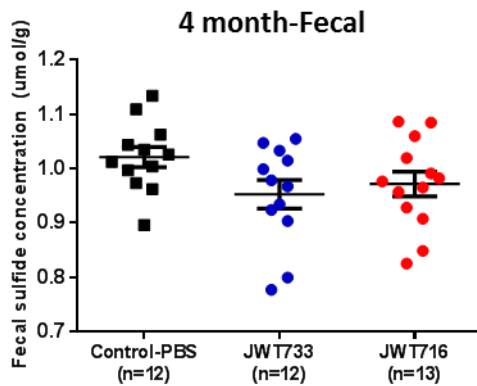


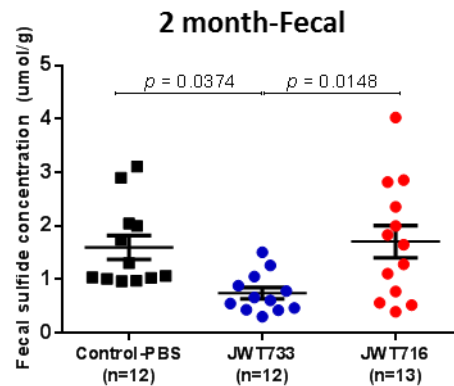
Figure 4. Sulfide assay and qRT-PCR gene expression of rat and bacterial sulfate reduction genes

(A) Fecal sulfide (hydrogen sulfide) concentration measured by Cline assay at 4 months of age in the control and treatment groups. (B) Fecal sulfide concentration measured at 2 months of age. *P*-values below 0.05 were considered to be significantly different between groups. Calculated via a One-Way ANOVA with a Tukey's post hoc test. Relative expression of the bacterial sulfate reduction genes (C), host sulfate reduction genes (D), relative to the PBS-treated control group (n=8) was determined by qRT-PCR. Log fold-change was calculated using the $\Delta\Delta C_q$ values. Red: expression in JWT716 (T1SS-deficient, n=11); Blue: expression in JWT733 (T1SS-competent, n=9) groups. Error bars in all figures indicate standard error of the mean (\pm SEM).

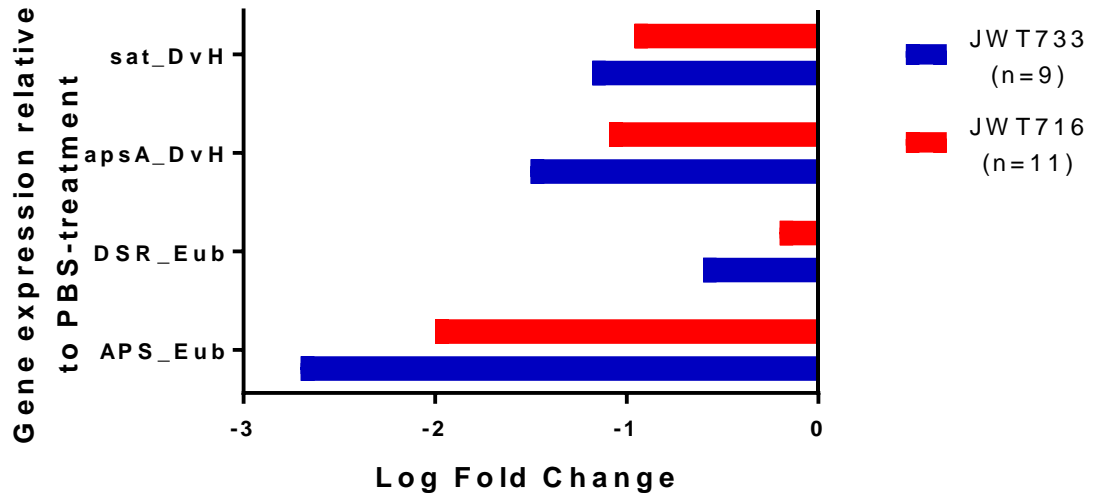
A



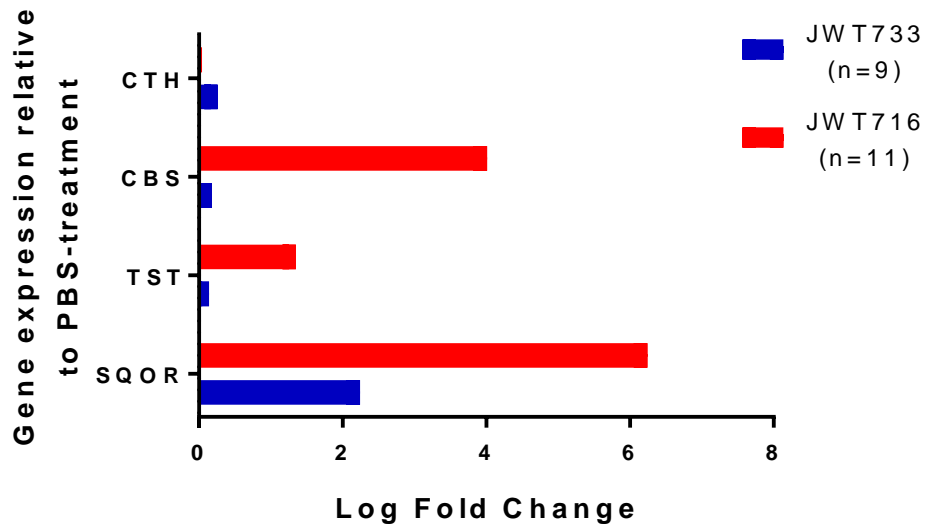
B



C



D



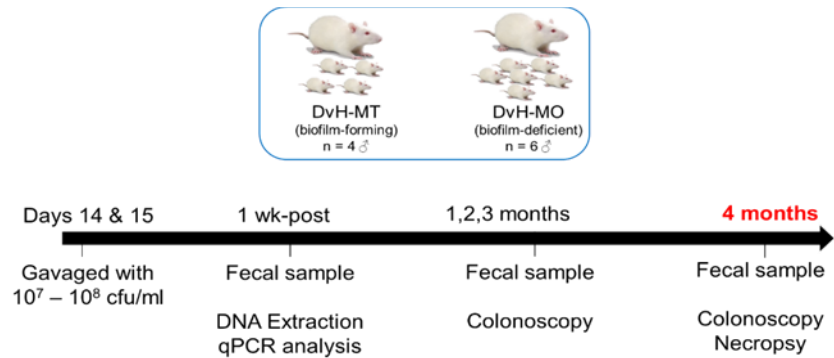
Supplementary figure 1. Treatment of Pirc rats with biofilm -competent and -deficient *Desulfovibrio vulgaris* Hildenborough (DvH)

(A) Experimental design: Pirc rats were treated with biofilm-competent, DvH-MT (n=4) or biofilm-deficient, DvH-MO (n=6) strains of *Desulfovibrio vulgaris* Hildenborough.

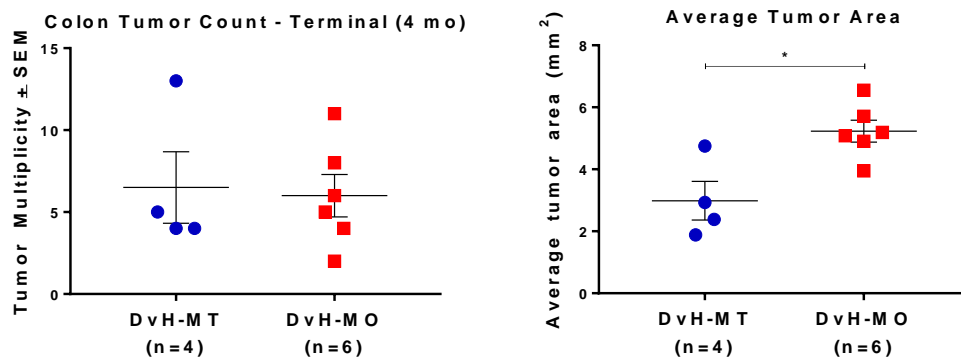
(B) Colonic tumor count and average tumor size at sacrifice. *P*-values below 0.05 were considered to be significantly different between groups. Calculated via a Student's *t*-test.

(C) Bar graph of the differential tumor sizes observed in the DvH-MT and DvH-MO treated Pirc rats at 4 months. Error bars in all figures indicate standard error of the mean (\pm SEM).

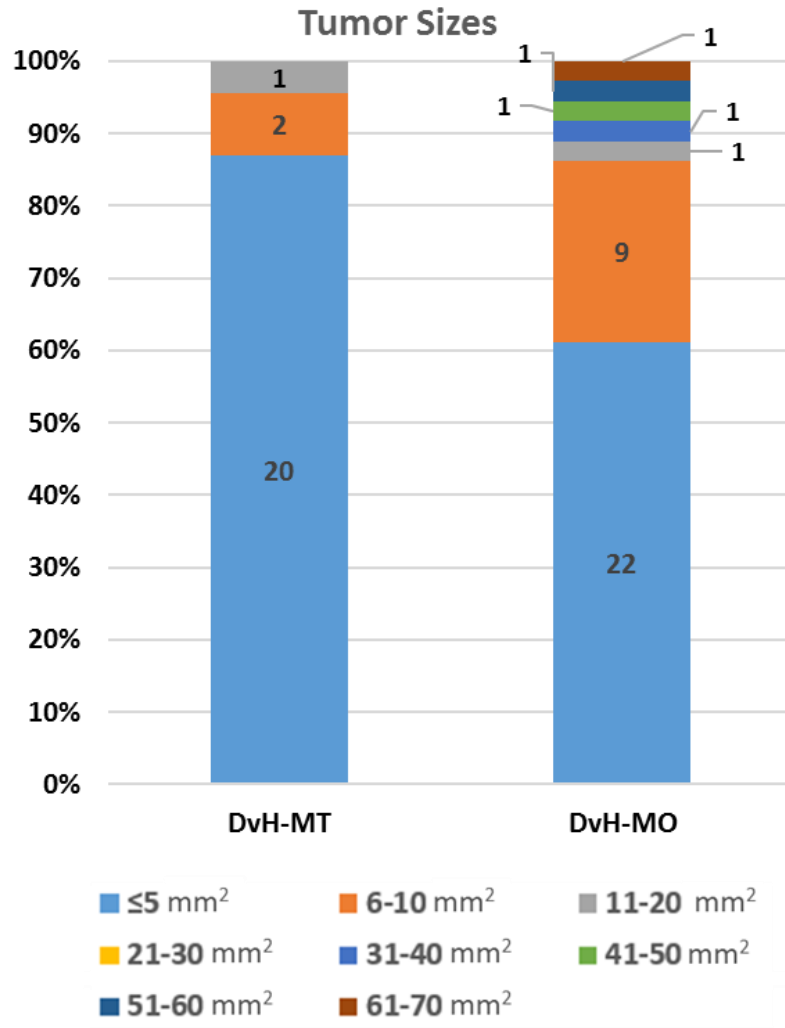
A



B



C



Supplementary figure 2. Adenoma images via colonoscopy in DvH-treated Pirc rats

(A) Representative images of adenomas in DvH-MO-treated rats indicating larger tumor sizes acquired at 4 months of age (sacrifice). Images obtained from 5 different animals.

(B) Images representative of the small lesions observed in the DvH-MT group, obtained from 3 different animals.

A

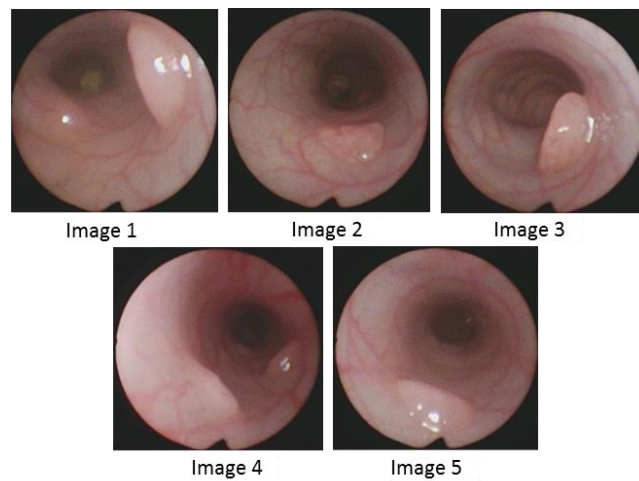


Image.1-5: Representative images of adenomas in the DvH-MO treated rats. Images obtained from 5 different animals

B

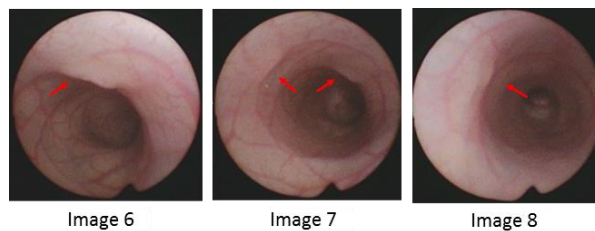
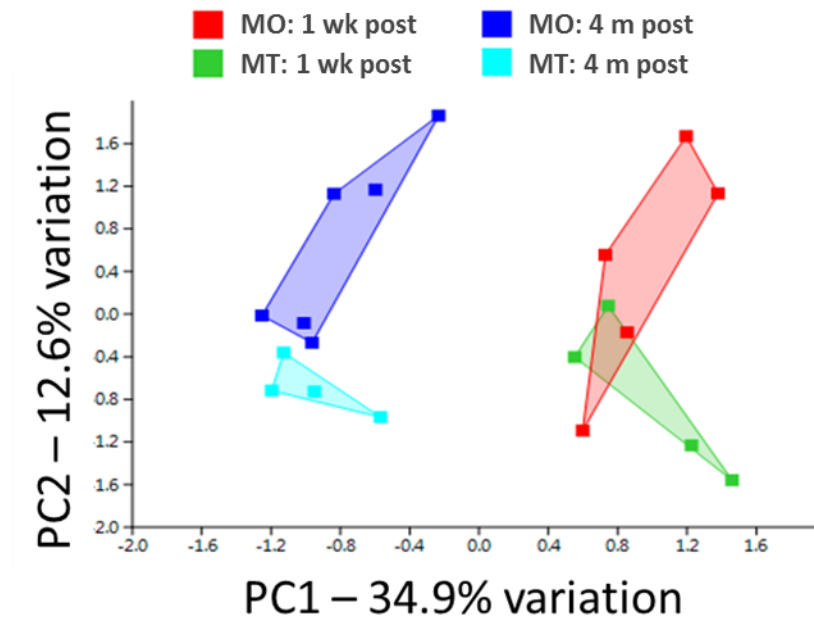


Image.6-8: Representative images of lesions (red arrow) in the DvH-MT-treated rats. Images obtained from 3 different animals

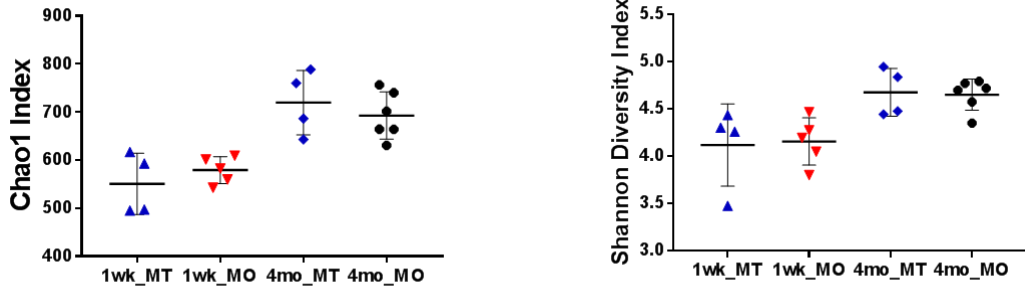
Supplementary figure 3. 16S rRNA gene sequencing analysis of DvH treatment

(A) Principal component analysis (PCA) indicating the differential complex GM profiles observed in the MT (n=4) and MO (n=6) groups at 1 week (green: MT, red: MO) and 4 months (light blue: MT, dark blue: MO) of age. PERMANOVA ($F=4.45$, $P=0.0001$) was used to determine significance differences in GM profiles. A P -value less than 0.05 was considered to be significant. Post-hoc analysis is listed under Table 2. (B) Richness (Chao1) and diversity (Shannon) indices were measured for the same time points. (C) Heatmap analysis using Euclidean distances coupled with Ward's algorithm was performed, identifying the top 55 OTUs (operational taxonomic units). Error bars in all figures indicate standard error of the mean (\pm SEM).

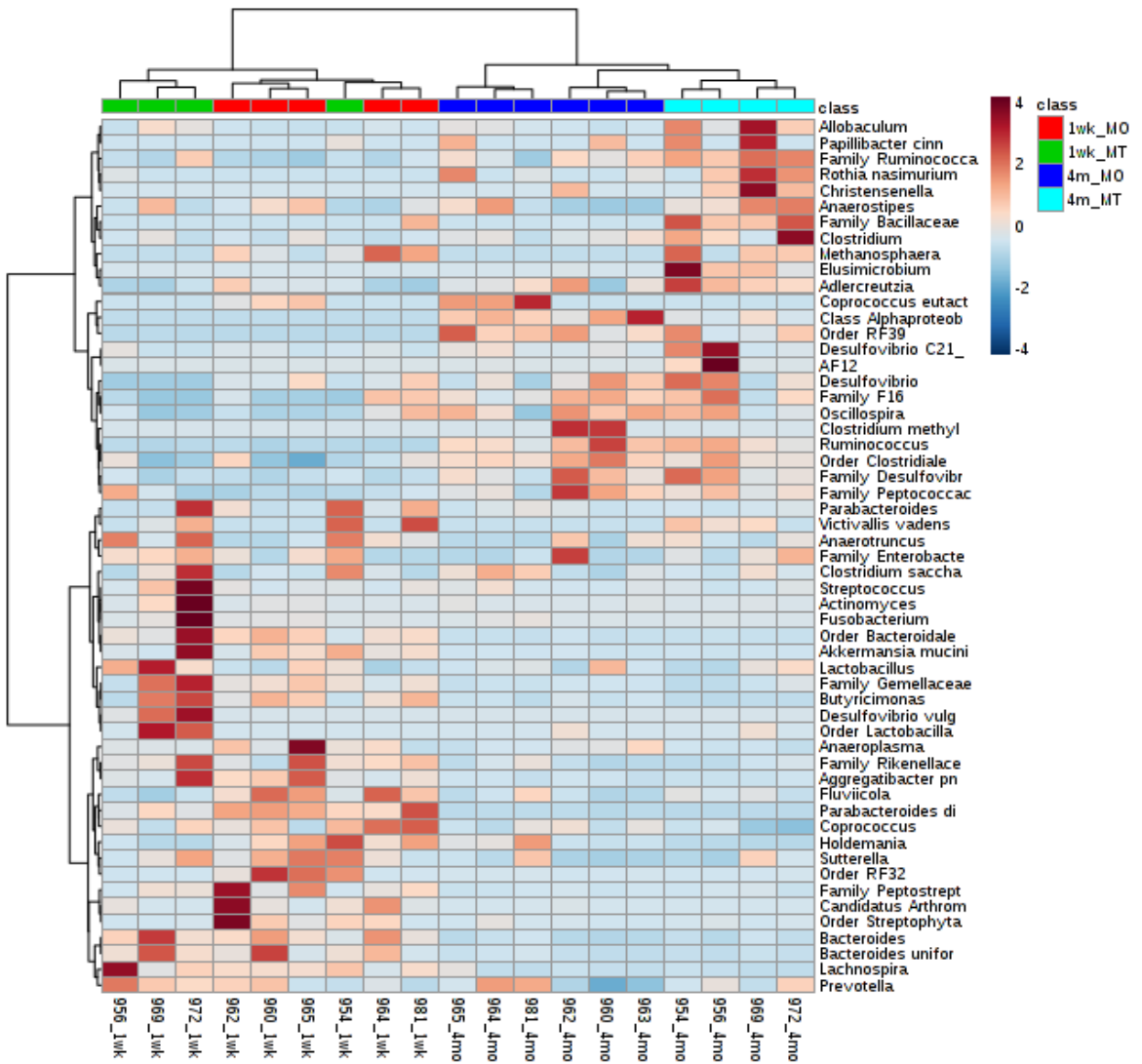
A



B

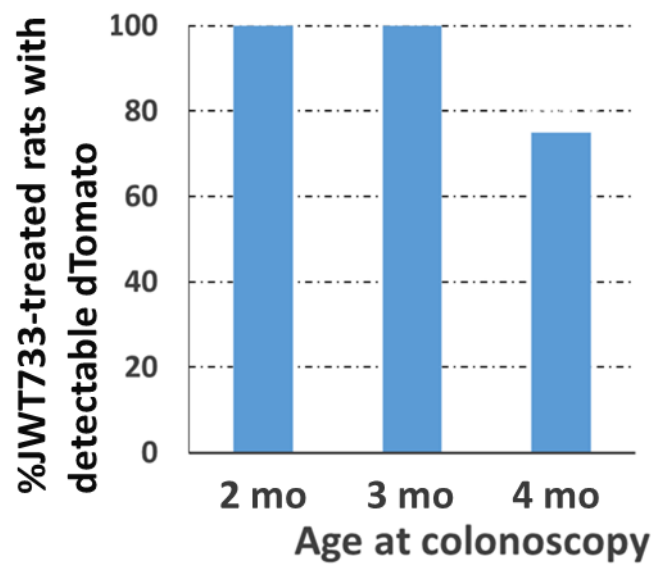
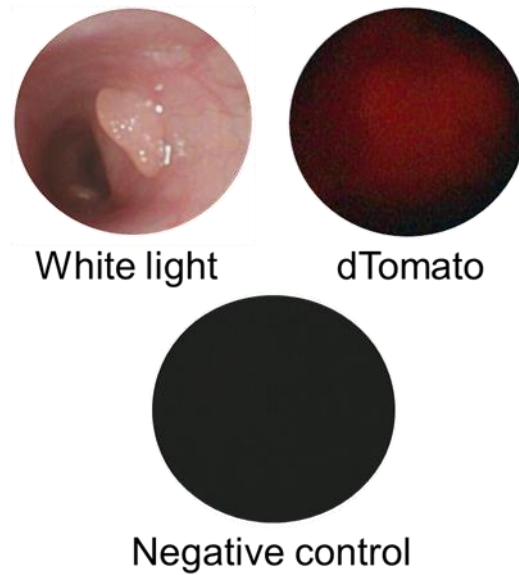


C



Supplementary figure 4. Colonoscopy of fluorescent, T1SS-competent strain-treated rats

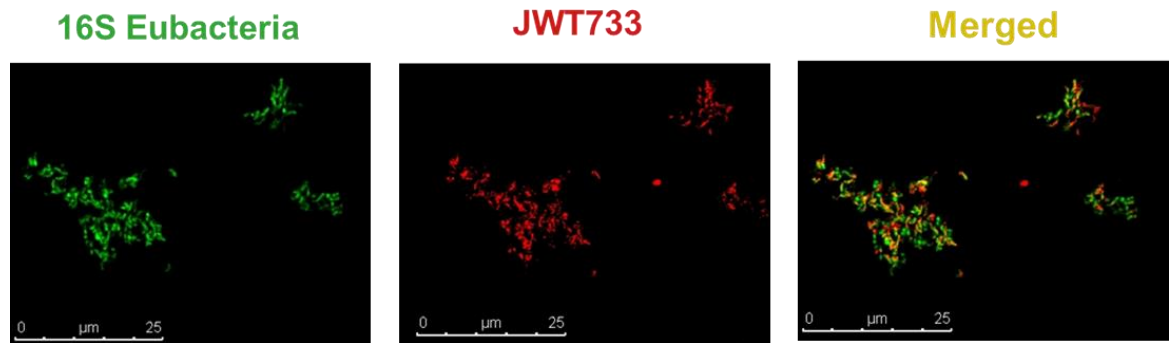
Representative images of colonoscopy with white light, dTomato fluorescence and negative controls to determine percent detection of fluorescent in all rats treated with JWT733.



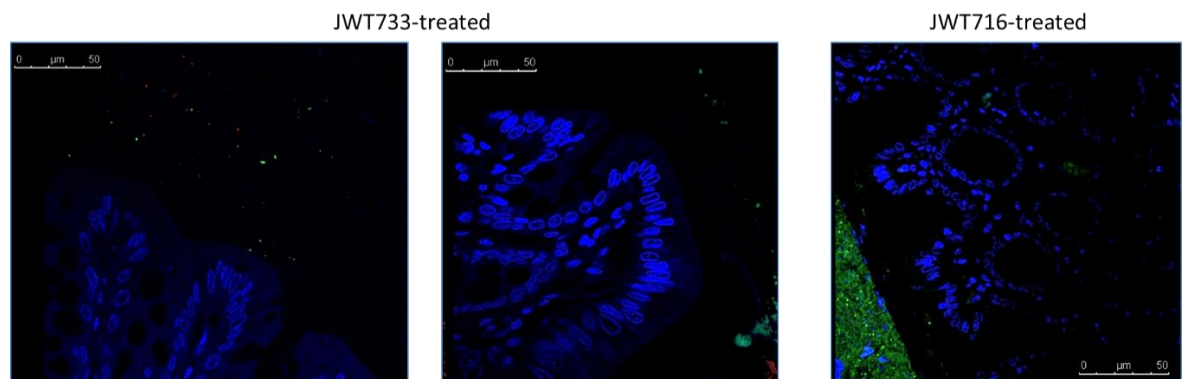
Supplementary figure 5. Fluorescent in-situ hybridization (FISH) and confocal microscopy assessing biofilm formation in vivo in the JWT733 treated rats

(A) Confocal microscopy images to detect fluorescent, T1SS-competent JWT733 strain. Representative images of positive controls for 16S Eubacteria and JWT733. (B) Representative images of the JWT733- and JWT716- treated colonic segments assessed for presence of bacteria. JWT733, n=13 and JWT716, n=12.

A



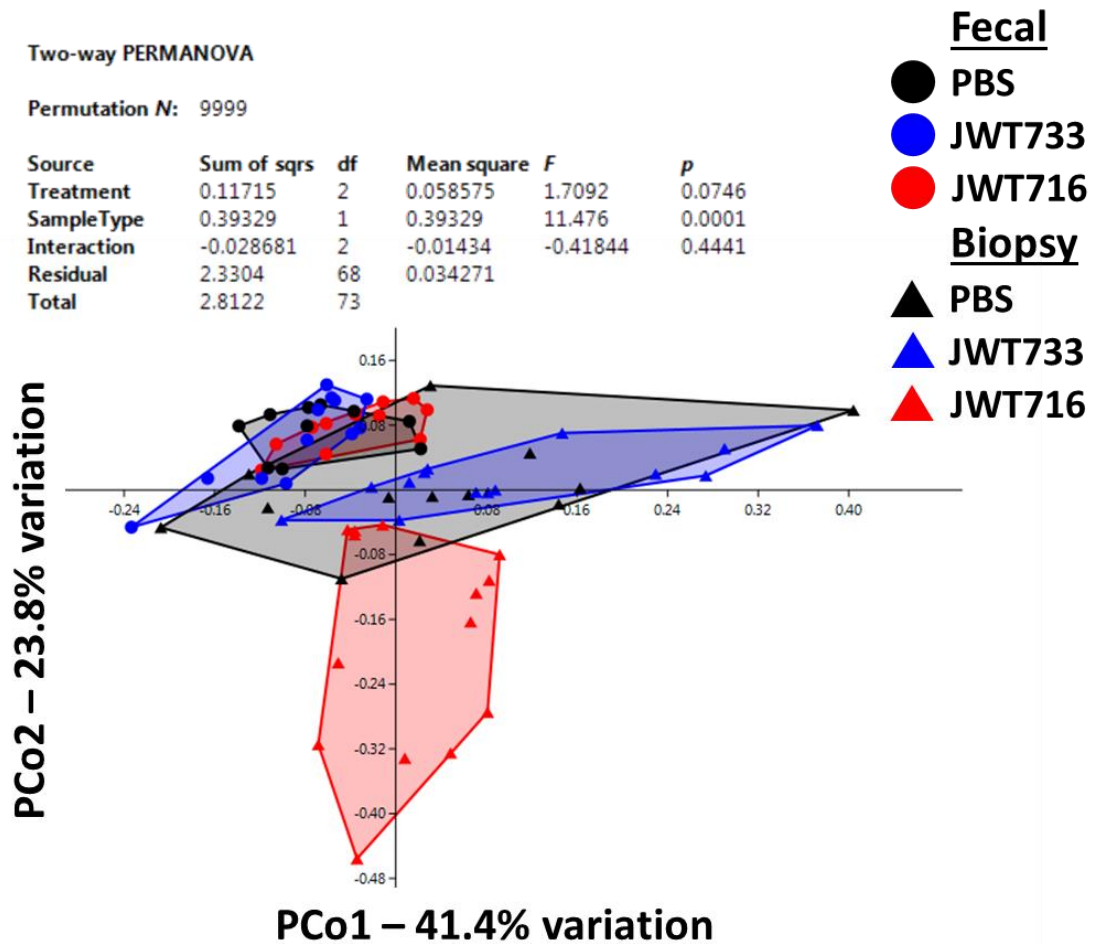
B



16S Eubacteria DAPI JWT733

Supplementary figure 6. 16S rDNA analysis of fecal and biopsy samples from the control, JWT733 and JWT716 groups

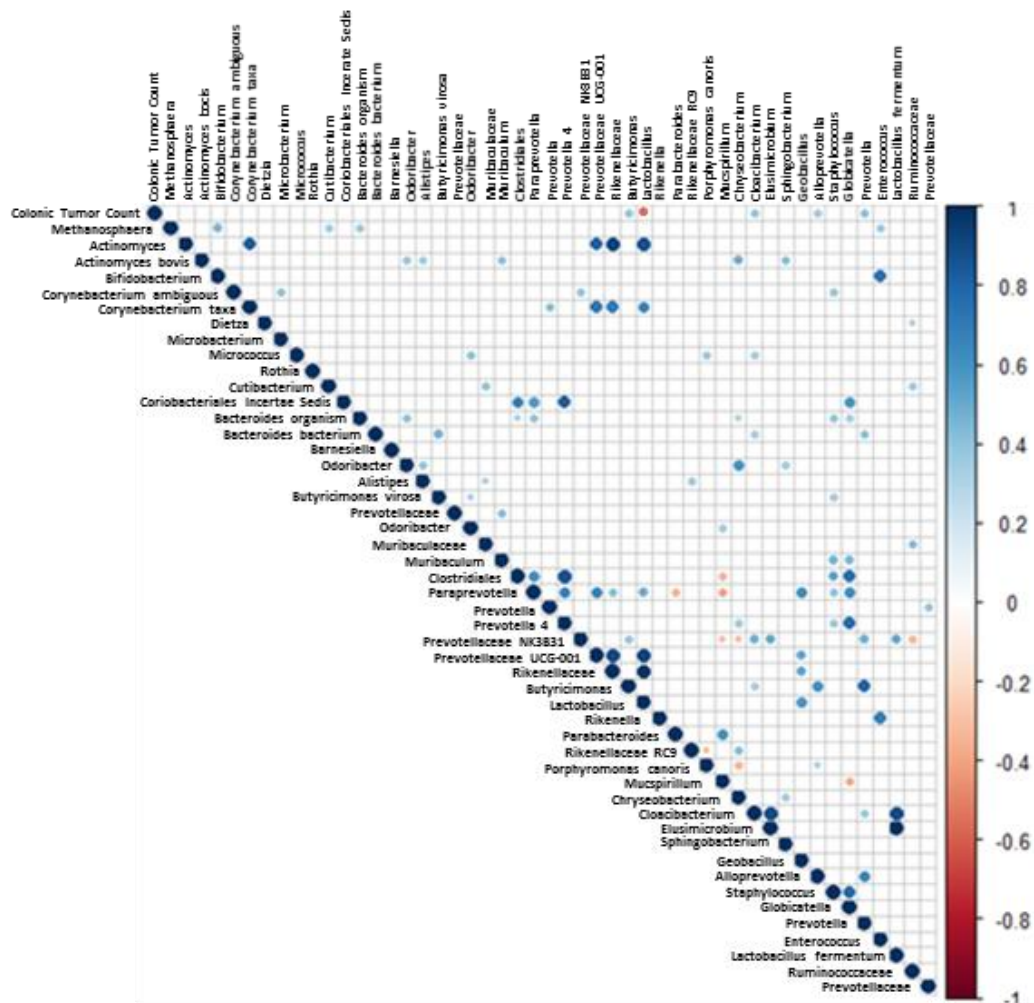
Principal Coordinate Analysis (PCoA) plot depicting the 16S rDNA gene sequencing dissimilarities between the groups at 2 months of age based on the Bray-Curtis distance matrix. Fecal samples are depicted as circles, while biopsy samples are shown as triangles. PBS: black, JWT733: blue and JWT716: green. Post-hoc analysis indicating the differences between individual groups is listed under Table 4. Each symbol represents the GM community from the fecal sample of a single rat at 2 months of age.



Supplementary figure 7. Correlogram analysis of OTUs vs tumor multiplicity at 1 week post-treatment and 2 months of age

(A) Correlogram showing the correlations (Pearson's, $P < 0.05$) between OTUs at one week post-treatment with colonic tumor counts. Color of the dot indicates positive (blue) or negative (red) correlation. Size of the dot represents the mean relative abundance of each OTU. (B) Correlogram of OTUs from 2 month fecal samples and colonic tumor multiplicity is depicted.

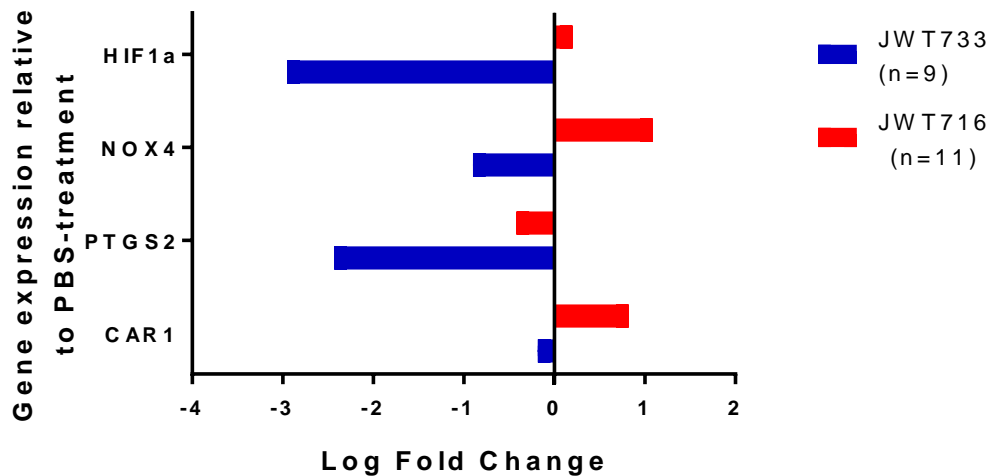
A



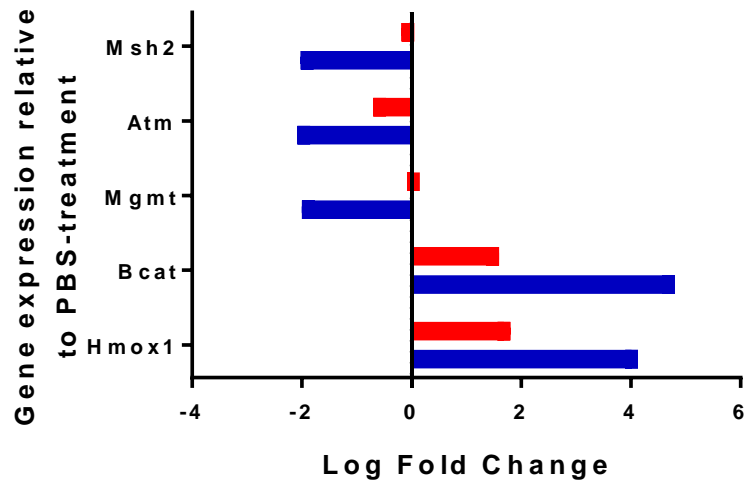
Supplementary figure 8. QRT-PCR analysis of gene expression in control, JWT733 and JWT716 groups

Relative gene expression measured using qRT-PCR with respect to the control (anaerobic-PBS) group determined for inflammation and hypoxia-related (A), and DNA damage response (B) genes in all three groups, i.e. controls (n=8), JWT733 (n=9) and JWT716 groups (n=11). All expression is normalized to *GAPDH* and then to that of the control animals. C) Relative gene expression of *MUC2* in the JWT733 and JWT716 treated animals with respect to the control group.

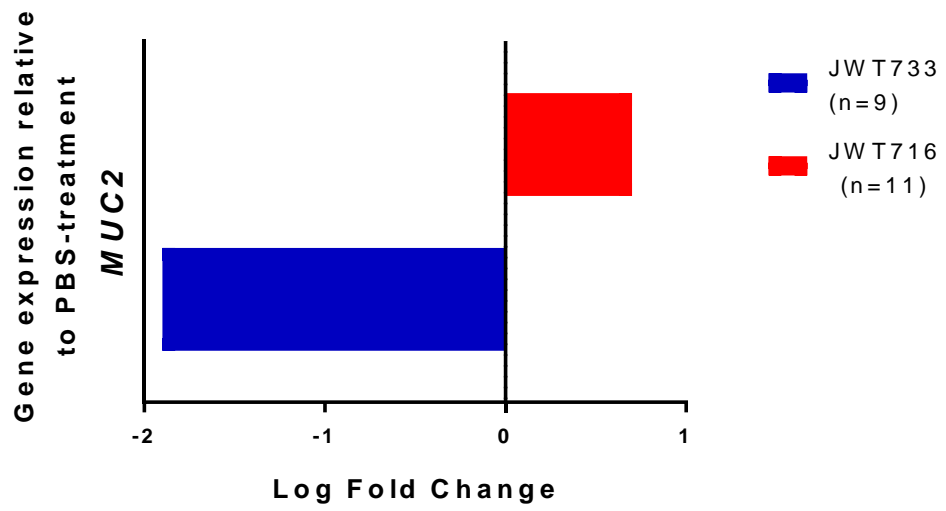
A



B



C



8. Tables

Table 1: Primer and probes used in this study

Primer name	Primer sequence (5'-3') ^A	Purpose of primer ^B
DVU1094-upF	GCCTTTTGCTGGCCTTTTGCTCA CATCGAAGAGGCGGCCATCATC G	amplifying <i>argH</i> at 165 bp, the upstream region for pMO7722 and pMO7743
DVU1094-upR	TCGCCTTCTTGACGAGTTCTTCT GACATCCATGCTGTTGCGGAAG GTG	amplifying <i>argH</i> at 688 bp to generate the upstream region for pMO7722
DVU1094-pKan- comp-R	TTCCCAACCTTACCAGAGGGCG CCCCAGCTGGCAATTCCGGCTA GCGGCCGAGCCAG	amplifying <i>argH</i> to generate the upstream and complement region for pMO7743
DVU1094-dnF	GCGCCCCAGCTGGCAATTCCGG CTGCCCAAGGCTGCACAC	amplifying region downstream of <i>argH</i> to make pMO7722
DVU1094-dnR	CGAGGCATTTCTGTCCTGGCTG GCGTCACCGACCATGACCACC	amplifying 511-bp region downstream of <i>argH</i> to make pMO7722 and pMO7743
DVU1094- tdTomato-comp- dnF	CGGCATGGACGAGCTGTACAA GTAAGTCCCAAGGCTGCACAC	amplifying region downstream of <i>argH</i> to make pMO7743
tdTomato-pKan-F	GGGCGCCCTCTGGTAAGGTTGG GAAGCCCTGCAAGCAGTCCCAG GAGGTACCATATGGTGAGCAA GGGCGAGG	amplifying <i>tdTomato</i> to make pMO7743; overhang contains promotor from <i>Km^r</i> and RBS
tdTomato-pKan-R	TTACTTGTACAGCTCGTCCATG CCG	amplifying <i>tdTomato</i> to make pMO7743
SpecRpUC-F	CCAGCCAGGACAGAAATGCCTC G	amplifying plasmid backbone (Sp ^r -pUC) from pCR8/GW/TOPO
SpecRpUC-R	ATGTGAGCAAAAGGCCAGCAA AAGGC	amplifying plasmid backbone (Sp ^r -pUC) from pCR8/GW/TOPO
Kan gene Prom Nterm	CCGGAATTGCCAGCTGGGGCGC	amplifying <i>Km^r</i> from pCR4-TOPO
KanR	TCAGAAGAAGTTCGTCAAGAAG GCGA	amplifying <i>Km^r</i> from pCR4-TOPO

SpecRpUC-up	CGCCTGGTATCTTTATAGTCCT	sequencing of cloned regions
pMO719-XbaI-dn	TGGGTTTCGTGCCTTCATCCG	sequencing of cloned regions
DVU1094-666F	CACCTTCCGCAACAGCATGGATG	sequencing of cloned regions
DVU1094-815R	GGCAGGAAGATGTAGCCGAATGC	sequencing of cloned regions
RBS_partial-pKanR	ATGGTACCTCCTGGGACTGCTT	sequencing of cloned regions
dTomato-579F	CTACTACGTGGACACCAAGCTGGAC	sequencing of cloned regions
<i>dsr_EUB_F</i>	ACSCACTGGAAGCACG	Expression analysis of eubacterial dissimilatory sulfite reductase gene
<i>dsr_EUB_R</i>	GTGTAGCAGTTACCGCA	
<i>aps_EUB_F</i>	GGGYCTKTCCGCYATCAAYAC	Expression analysis of eubacterial adenosine monophosphate sulfate reductase gene
<i>aps_EUB_R</i>	GCACATGTTCGAGGAAGTCTTC	
<i>sat_DvH_F</i>	CGTTTCCAAGGAAGAAGCAG	Expression analysis of DvH sulfate adenyl transferase gene
<i>sat_DvH_R</i>	GGTCTTCTTCAGCGATGTCC	
<i>apsA_DvH_F</i>	GCTCTTGATACGGGCTTCAG	Expression analysis of DvH adenosine monophosphate sulfate reductase gene
<i>apsA_DvH_R</i>	TCACGAAGCACTTCCACTTG	
<i>CBS_F</i>	GCTGATGGTGTTTGGTGTTG	Expression analysis of rat cystathionine- β -synthase gene
<i>CBS_R</i>	GTGGAAACCAGTCGGTGTCT	
<i>CTH_F</i>	TCCGGATGGAGAAACACTTC	Expression analysis of rat cystathionine- γ -lyase gene
<i>CTH_R</i>	TGAGCATGCTGCAGAGTACC	
<i>TST_F</i>	AGTGCTCAATGGTGGTTTCC	Expression analysis of rat thiosulfate sulfurtransferase gene
<i>TST_R</i>	CCACCAGCTGGAACCTTTTA	
<i>SQOR_F</i>	CTGCAGGACTTCAAGGAAGG	Expression analysis of rat sulfide quinone oxidoreductase gene
<i>SQOR_R</i>	AAATTGTTCCAAGGGCTGTG	
<i>HIF1α_F</i>	TCAAGTCAGCAACGTGGAAG	Expression analysis of rat hypoxia-induced factor-1 α gene
<i>HIF1α_R</i>	TATCGAGGCTGTGTCTGACTG	
<i>NOX4_F</i>	GGATCACAGAAGGTCCTAGC	Expression analysis of rat NADPH oxidase 4 gene
<i>NOX4_R</i>	AGAAGTTCAGGGCGTTCACC	
<i>PTGS2_F</i>	AAAGCCTCGTCCAGATGCTA	

<i>PTGS2_R</i>	ATGGTGGCTGTCTTGGTAGG	Expression analysis of rat prostaglandin-endoperoxide synthase 2 gene
<i>CARI_F</i>	CCCATTACCAATTTTGACC	Expression analysis of rat carbonic anhydrase-1 gene
<i>CARI_R</i>	ACAGAAGACCACGGAGCTGT	
<i>JWT33_FISH</i>	/5Alex647N/GAACTCGTGGCCGTTCATGG/3AlexF647N/	Fluorescent in-situ hybridization (FISH) probe for JWT33
<i>JWT733_F</i>	CCAAGCTGAAGGTGACCAA	Quantification of JWT733 copy number
<i>JWT733_R</i>	ATTACAAGAAGCTGTCCTTCCC	
<i>JWT733_Probe</i>	GTTTCATGTACGGCTCCAAGGCGTA	
<i>JWT716_F</i>	AGATAGCCGCCATGCTG	Quantification of JWT716 copy number
<i>JWT716_R</i>	AAACGCGACAGTGTTC	
<i>JWT716_Probe</i>	GCCCTAGCCATGCCGCTGT	

Note: EUB: eubacteria; DvH: *Desulfovibrio vulgaris* Hildenborough; F: Forward; R:

Reverse

Table 2: Two-Way PERMANOVA post-hoc analysis of GM community profile in fecal and biopsy samples collected at 4 months of age

Bonferroni-corrected <i>P</i> values					
Time point/Group		1 week		4 months	
		MT	MO	MT	MO
1 week	MT	1	0.0158	0.0261	0.005
	MO	0.0158	1	0.0079	0.0022
4 months	MT	0.0261	0.0079	1	0.0147
	MO	0.005	0.0022	0.0147	1

Table 3: One-Way PERMANOVA post-hoc analysis of GM community profile in fecal samples from DvH-treated rats

Bonferroni-corrected <i>P</i> values				
	JWT733	JWT716	MT	MO
JWT733		0.1162	0.1619	0.0109
JWT716	0.1162		0.3188	0.0222
MT	0.1619	0.3188		0.0361
MO	0.0109	0.0222	0.0361	

Table 4: Two-Way PERMANOVA post-hoc analysis of GM community profile in fecal and biopsy samples collected at 4 months of age

Bonferroni-corrected <i>P</i> values						
Samples/ Group	Fecal			Biopsy		
	PBS	JWT733	JWT716	Biopsy- PBS	Biopsy- JWT733	Biopsy- JWT716
PBS		1	0.063	0.0015	0.039	0.0015
JWT733	1		0.071	0.0015	0.0375	0.0015
JWT716	0.063	0.071		0.0015	0.0015	0.0015
Biopsy-PBS	0.0015	0.0015	0.0015		0.1815	0.0015
Biopsy-JWT733	0.039	0.0375	0.0015	0.1815		1
Biopsy-JWT716	0.0015	0.0015	0.0015	0.0015	1	

Table 5: Bacterial strains and plasmids used in the study

Bacterial Strain or Plasmid	Genotype or Relevant Characteristics ^A	Use	Source
<i>Escherichia coli</i>			
α -select (Silver efficiency)	<i>deoR endA1 recA1 relA1 gyrA96 hsdR17</i> (r _K ⁻ m _K ⁺) <i>supE44 thi-1</i> <i>phoA</i> Δ (<i>lacZYA argF</i>)U169 Φ 80 <i>lacZ</i> Δ M15 λ^- F ⁻	Production and replication of plasmids	Bioline
<i>Desulfovibrio vulgaris</i> Hildenborough			
DvH	Wildtype	Biofilm competent	ATCC 29579 ^B
DvH-MO	Contains 12 spontaneous mutations compared to wildtype; one in <i>lapB</i> (G1903C) causes strain to be deficient in biofilm formation	Spontaneously biofilm deficient strain maintained at the University of Missouri	De León <i>et al.</i> (256)
JWT716	DvH Δ <i>lapB</i> ' (1543-2331 bp and G1542T) and Δ <i>upp</i> ; 5-FU ^r , biofilm deficient	Markerless deletion of <i>lapB</i> at 1543 bp from 5' end; introduction of a stop codon at 1542 bp	De León <i>et al.</i> (256)
JWT726	DvH Δ <i>argH</i> ' (689-1383 bp): <i>Km</i> ^r ; <i>Km</i> ^r , arginine auxotroph	Marker exchange deletion of <i>argH</i> at 689 bp from 5' end	This study
JWT733	JWT726 Δ <i>Km</i> ^r :: <i>argH</i> ' (689-1383 bp)-(<i>P</i> _{<i>npr</i>} - <i>RBS-dTomato</i>); fluorescent, <i>Km</i> ^s , arginine prototroph	Complementation of 3' end (689-1383 bp) of <i>argH</i> + <i>dTomato</i> ; markerless fluorescent strain	This study
Plasmids			
pCR8/GW/TOPO	Cloning vector containing <i>Sp</i> ^r and pUC <i>ori</i> cassette; <i>Sp</i> ^r	Source of <i>Sp</i> ^r and pUC <i>ori</i> fragment for plasmid generation in <i>E. coli</i> , non-replicating in DvH	Invitrogen

pCR4-TOPO	Cloning vector containing <i>Km^r</i> ; <i>Km^r</i>	Source of <i>Km^r</i>	Invitrogen
pSRKKm	pBBR1MCS-2 expression vector containing <i>lac</i> promoter and <i>lacI^q</i> , <i>lacZα</i> , and <i>Km^r</i>	Broad host range vector	Khan <i>et al.</i> (372)
pSRKKm-tdTomato	pSRKKm-tdTomato	Source of tdTomato	Gift of P. Brown and J Daniel; Dolla <i>et al.</i> (374)
pMO7722	pCR8/GW/TOPO <i>Sp^r</i> and pUC <i>ori</i> cassette plus <i>argH</i> fragment (165-688 bp) followed by <i>Km^r</i> and DNA region downstream of <i>argH</i> (511-bp); <i>Sp^r</i> and <i>Km^r</i>	Marker-exchange deletion of <i>argH</i> 3' end (689-1383 bp)	This study
pMO7743 ^C	pCR8/GW/TOPO <i>Sp^r</i> and pUC <i>ori</i> cassette plus <i>argH</i> fragment (165-1383 bp) followed by the promoter for <i>Km^r</i> -RBS- <i>dTomato</i> and DNA region downstream of <i>argH</i> (511-bp); <i>Sp^r</i> and fluorescent	Complementation of <i>argH</i> with selection of arginine prototrophy; introduction of fluorescent marker downstream of <i>argH</i> ;	This study

^ADefinitions: *upp*: uracil phosphoribosyltransferase (DVU1025), *lapB*: ABC transporter of a type I secretion system (DVU1017), *argH*: argininosuccinate lyase (DVU1094), RBS: ribosomal binding site 5'- GCAGTCCCAGGAGGTACCAT-3' derived from sequence in Dolla *et al.* 1992 (374), *Km^r*: kanamycin resistance encoded by neomycin phosphotransferase II and containing a mutation of C→A at -34 bp in pMO7722 and pMO7743, *Sp^r*: spectinomycin resistance encoded by *aadA1*

^BAmerican Type Culture Collection, Manassas, VA

^CThe tandem duplication in *tdTomato* was lost during plasmid construction resulting in *dTomato* and containing a mutation of G13A causing an amino acid change of Gly5Ser. Three mutation in *argH* (G1015A, C1118T, and G1241A) resulting in Ala339Thr,

Ala373Val, and Gly414Asp are present in this plasmid but do not affect complementation of arginine prototrophy. Construct was chosen due to apparent increased fluorescence when compared to other *tdTomato* constructs.

^DLeibniz Institute DSMZ-German Collection of Microorganisms and Cell Cultures

CHAPTER IV

**SHIFT FROM A SIMPLIFIED TO COMPLEX GUT MICROBIOTA REDUCES
ADENOMA BURDEN IN A PRECLINICAL RAT MODEL OF COLON CANCER**

(Submitted: Susheel Bhanu Busi, Daniel Davis, Jacob Moskowitz, and

James Amos-Landgraf)

1. Overview

Colorectal cancer (CRC) models, including both mice and rats, have been used to understand the etiology of human diseases for decades (29, 375-378). The ideal model should recapitulate the phenotype observed in humans, but also elucidate contributing factors such as the host microbiota and its relationship to the mechanisms of the disease. Recent evidence suggests that the gut microbiome, i.e. the collection of microorganisms in the large intestine plays an important role in the etiology of the disease (64, 71, 92, 151, 207). Several studies have tried to elucidate the mechanisms by which specific bacteria contribute to disease susceptibility by various methods including the utilization of germ-free (293, 379, 380) or monocolonized animals (381-384), or the use of antibiotics to eliminate endogenous gut microbiota (GM) populations (64, 385). The majority of studies use the *Apc^{+Min}* mouse model that develops the majority of their tumors in the small intestine unlike human disease. Since the GM population has been shown to be different in the small intestine compared to the colon the translatability of these studies may be limited.

The Pirc (F344/NTac-*Apc^{+am1137}*) rat model of human colon cancer demonstrates a more consistent colonic tumor phenotype compared to the *Apc^{+Min}* mice and has been shown to have an altered phenotype with altered gut microbiota (127, 131, 150, 188). To model more closely, the large number of endogenous commensals found in human CRC patients, we previously showed that the endogenous GM could be modulated through complex microbiota targeted rederivation (6, 124). Determining the mechanisms and most importantly the interactions between commensals still poses challenges, considering the multiple permutations and combinations with the taxa found in the model.

In order to tackle the challenge of complexity, we established the Pirc rat on an Altered Schaedler Flora (ASF) gut microbiota (123, 386-388). Instituting Pirc rats on a minimal GM profile could potentially serve as a model for understanding mechanisms and interactions of specific bacteria, in the context of a well-defined, yet complex gut microbiome profile. Using CRASF (Charles-River ASF) rats as surrogates, F1-Pirc rats were established, and at weaning, littermates were transferred from a barrier room to a conventional status room in the animal facility. We hypothesized that transferring the Pirc rats to a conventional room compared to the cleaner, barrier room would increase the colonic tumor burden at sacrifice. Contrary to our hypothesis, we found that the animals maintained in the barrier (clean) room had significantly more colonic adenomas. This is the first time Pirc rats have been established on an Altered Schaedler Flora gut microbiota, but more importantly, suggests an even more central role for the gut microbiota in modulating the colon tumor phenotype of animal models for studying human diseases.

2. Methods

2.1. Animal Care and Use

All procedures were performed according to the guidelines regulated by the Guide for the Use and Care of Laboratory Animals, the Public Health Service Policy on Humane Care and Use of Laboratory Animals, and the Guidelines for the Welfare of Animals in Experimental Neoplasia and were approved by the University of Missouri Institutional Animal Care and Use Committee.

2.2. Charles River Altered Schaedler Flora (CRASF) rats and cross-fostering

7 week old Lewis rats with a limited Altered Schaedler Flora (n = 4 males, and 4 females) were purchased from Charles River Laboratories Inc. Laboratories (Wilmington, MA). The animals were shipped overnight in a sterile double-enclosed isolator cage with sterile bedding and Hydrogel® gel-paks (Portland, ME) to the Discovery Ridge animal facility at University of Missouri. Fecal samples were collected prior to shipping and upon arrival at the facility for 16S rRNA sequencing. Simultaneously, bedding and gel-pak samples that the animals were shipped with were also collected for sequencing. The animals were housed in a barrier room on ventilated racks (Thoren, Hazleton, PA) in micro-isolator cages with autoclaved paper chip bedding, feed and water, and allowed to acclimatize for a week, after which they were setup into breeder pairs. Timed matings for fostering were set up with our F344/NTac *Apc*^{+/am1137} (generation, N=28) conventional rat colony.

Female F344/NTac rats were checked for plugs, and on day 21 post-observation of plugs, a Caesarean was performed. The uterus was tied-off at both ends prior to surgical resection and then transferred in a sterile petridish with betadine solution to the barrier room. In a biosafety hood, the uterus was opened with a pair of sterile scissors and the pups were physically manipulated after removing the amniotic sac and warmed under a heat lamp. Only CRASF breeders with pups on the ground within 36 hours were used as surrogates for fostering the F344/NTac x F344/NTac-*Apc*^{+/am1137} pups. Half the litter and bedding was removed from the CRASF surrogate, and mixed with the to-be fostered pups thoroughly, before placing the F344/NTac x F344/NTac-*Apc*^{+/am1137} fostered pups along

with a few of the CRASF pups with the surrogate mom. At 12 days of age, all pups including the fostered ones were ear-punched for genotyping.

2.3. Genotyping and animal identification

Pups were ear-punched prior to weaning at 12 days of age using sterile technique. DNA was extracted using the “HotSHOT” genomic DNA preparation method previously outlined (166). DNA was used for genotyping using a high resolution melt (HRM) analysis as described previously (131).

2.4. Experimental design, animal husbandry (breeding) and barrier room housing

F1-Pirc rats were generated by crossing one founder male, F344/NTac-*Apc*^{+/am1137} CRASF Pirc rat established via cross-fostering, with wildtype female LEW/Crl ASF rats. The rats were housed on ventilated racks in micro-isolator cages. Cages were furnished with autoclaved paper chip bedding (Shepherd Specialty Paper, Milford, NJ) and were fed irradiated 5053 PicoLab Mouse Diet 20 (LabDiet, St. Louis, MO). Rats had *ad libitum* access to water purified by sulfuric acid (pH 2.5-2.8) treatment followed by autoclaving. Animal handling required complete personal protective equipment (PPE) including face masks, hair nets and TyVek sterile sleeves (Cat.No.17988110, Fisher Scientific, Waltham, MA). Prior to breeding fecal samples were collected from both the breeders using aseptic methods. LEWF344F1-*Apc*^{+/am1137} (F1 generation) ASF pups were generated and genotyped at 12 days of age.

2.5. Conventional room housing

At weaning, F1-Pirc rats were co-housed in the conventional room with F344/NTac animals from the holding colony with an endogenous complex GM when

available, in micro-isolator cages on ventilated racks with nonsterile paper chip bedding. Cage changes for conventional rats were done on open benches. Rats in the conventional room were fed non-irradiated 5008 Lab diet and had *ad libitum* access to acidified (sulfuric acid, pH 2.5-2.8), autoclaved water. The water is acidified after an RO (reverse osmosis) treatment to prevent the growth of most bacteria or fungi.

2.6. Fecal sample collection

Fecal samples were collected from the pups at weaning, and monthly thereafter until sacrifice at 4 months of age. Briefly, fecal samples were collected by placing the animal in a clean, sterile cage without bedding. Freshly evacuated feces were speared with a sterile toothpick or forceps and placed into a sterile Eppendorf tube. All samples were stored at -80 °C until further processing.

2.7. Fecal DNA extraction, 16S library preparation, sequencing and analysis

Fecal samples were pared down to 65 mg using a sterile blade and then extracted using methods described previously (4). Amplification and sequencing of the V4 hypervariable region of the 16S rDNA was performed at the University of Missouri Metagenomics center and DNA core facility (Columbia, MO) and the results annotated using the SILVA 16S database(4). Samples with a read count below 15,000 were removed from the analysis due to insufficient rarefaction. The average read counts for all samples was 57,863. Microbial Community DNA Standards from ZymoBIOMICS™ were used to account for any errors via extraction and sequencing processes. All OTUs with a relative abundance below 0.001% were excluded from analysis. Principal Coordinate analyses were performed in PAST (PAleontological STatistics, version 3.2)

(389). PERMANOVA with default permutations (N=9999) was used to determine significant differences between groups when performing PCoA analyses using the module embedded into PAST3.2. Simultaneously, a scree plot was generated using the chemometrics.R script under the *metaboanalyst* package to identify which principal coordinates to plot for the figures. Heatmaps were generated using the plotHeatMap function from the same package along with the hclust function from the *stat* package. For the Heatmaps, Euclidean distance was used as the similarity measure, while Ward's clustering algorithm accounting for average linkage was used to create the dendrogram. Correlation analyses testing the relationship of OTUs' relative abundance with tumor burden was assessed using the *corrgram* package in R (version 3.4.1), assessing the top 50 OTUs based on the individual relative abundance. PICRUSt, HUMAnN and LEfSE analysis was performed after re-annotating (closed-reference) the 16S rDNA gene sequences against the Greengenes (May, 2013) database as described previously (259).

2.8. Anaerobic culturing of the lab diet feed and DNA extraction

3 samples of 0.5 g of feed from the barrier and conventional rooms were introduced anaerobically into an autoclaved serum vial, closed with a sterile rubber stopper and an aluminum crimp seal. Oxygen was purged from vials and 5 mL of sterile brain heart infusion (BD Difco, ThermoFisher Scientific, USA) media was added using a syringe. The inoculum and media was then incubated anaerobically overnight at 37 °C in a 5% CO₂ incubator. After incubation, the contents of the vial were used for DNA extraction using previously established methods including manual DNA precipitation and the DNeasy kit (Qiagen, Germantown, MD) (131, 261).

2.9. Tumor counts

All animals were humanely euthanized with CO₂ administration and necropsied at 16 weeks (4 months) of age. The small intestine and colon from the rats were placed on to bibulous paper and then splayed opened longitudinally. Tissues were then fixed overnight in Carnoys fixative (30%, 10% glacial acetic acid and 60% absolute ethanol), and were replaced with 70% ethanol for long term storage until adenoma counting was performed.

2.10. Statistical analyses and figures

Statistical analyses and graphing for figures (except Fig.1) were prepared through GraphPad Prism version 7 for Windows (GraphPad Software, La Jolla, CA). *P*-values were set to identify significance at a value less than 0.05, unless otherwise indicated.

3. Results

3.1. Nominal taxa incursion in the Charles River Altered Schaedler Flora (CRASF)

In order to establish F344/NTac-*Apc*^{+/*am1137*} rats onto a CRASF GM, we first had to ensure that the simplified GM profile could be maintained in our facility. We housed four female and four male LEW/CrI ASF (CRASF) rats in a barrier room setting with individually ventilated racks in micro-isolator cages. Fecal samples collected prior to arrival at the facility and upon housing for 3 months at the facility, showed minimal addition of species to the GM profile. Over time, the LEW/CrI ASF animals acquired *Lachnospiraceae* UCG-001, *Lachnospiraceae* UCG-006, *Anaerotruncus*, [*Eubacterium*], *Enterococcus* and *Staphylococcus* (Fig.1A). The F344/NTac-*Apc*^{+/*am1137*} rat that was

cross-fostered onto the CRASF surrogates, at 1 month of age, showed a stable GM similar to that of the CRASF rats (Fig.1A). The ZymoBIOMICS mock microbial community standards simultaneously only acquired *Enterobacteriaceae*, potentially via the sample processing or sequencing or the bioinformatics analysis and annotation pipeline. Interestingly, the incursion of six taxa into CRASF rats led to significant differences when visualized using a Principal Coordinate Analysis (PCoA) to understand the similarities between samples pre- and post- arrival, using the Bray-Curtis distance matrix (Fig.1B). The majority of the GM was maintained stably after housing the CRASF animals in a barrier setting for 3 months. To determine if the OTUs were acquired as a means of shipping to our facility, sequencing was performed on the bedding and gel-paks that the animals arrived with and found that four of the OTUs were possibly assimilated through the gel-paks, with *Muribaculaceae* making a significant contribution to the overall GM profile (Fig.1C).

3.2. Simplified gut microbiota increases susceptibility to colonic adenomas

LEWF344F1-*Apc*^{+/am1137} CRASF rats obtained via the breeding set up were used to understand how the complexity of the GM may modulate disease susceptibility to adenomas in the rat model of colon cancer. At weaning, F1-Pirc littermates were separated into two separate rooms of the animal facility; a barrier room, where all cage changes were performed in a biocontainment hood, and a conventional room (Supplementary Fig.1). We found that the animals housed in the conventional setting had significantly fewer colonic adenomas than those housed under barrier conditions (Fig.2A). This differential tumor abundance was found in both male and female F1-Pirc rats. Interestingly, male rats from the conventional room had significantly more small

intestinal tumors compared to the barrier rats, while female rats showed a similar trend (Fig.2B).

3.3. Altered Schaedler Flora alters the colonic adenoma phenotype and the physiology of the gastrointestinal tract

Animals housed in the barrier room post-weaning demonstrated an increase in the number of proximal adenomas compared to conventional CRASF Pirc rats (Fig.3A). Most of these adenomas were 1 mm or smaller in diameter, however the rats with conventional GM did not show a similar phenotype (Fig.3B). Only one of twelve F1-Pirc rats separated at weaning and housed under a conventional settings had adenomas in the proximal colon that was slightly larger than 1 mm (Table 1). We also found that the overall number of small adenomas was significantly higher in the barrier room animals, irrespective of sex (Fig.3C), and the adenomas larger than 1 mm did not show any significant differences between the barrier and conventional rats (Fig.3D).

Furthermore, we sacrificed a cohort of F1-Pirc ASF animals at weaning and found no differences in their cecal size (Fig.3E). However, sacrifice after housing under barrier or conventional settings for 4 months, revealed considerable differences in cecum size. We found that rats maintained in the barrier room had ceca that were nearly 2-fold larger compared to conventionally-housed rats (Fig.3F). These results suggest that the lack of taxa from the conventional GM and/or their interactions with the Altered Schaedler Flora in barrier rats is capable of modifying the physiology and the phenotype of the F1-Pirc rats.

3.4. Conventional housing affects the GM architecture at 4 months of age

Considering the husbandry, handling, cecal and tumor multiplicity differences between the barrier and conventional rooms, we used 16S rRNA gene sequencing to determine the GM architecture in the F1-Pirc rats. At weaning, we found that the GM of rats at the time of separation into barrier and conventional rooms were similar to each other as indicated by bar graph (Fig.4A) and the Principal Coordinate analysis in Fig.4B (using Bray-Curtis distance matrix) and the overall richness determined by the number of OTUs observed in the samples (Fig.4C). They also resembled the GM profile of the parents, except for the conspicuous decrease in the relative abundance of Genus *Mucispirillum* (Fig.4A).

At sacrifice (4 months of age), considerable differences were observed in the overall profile of the Genera in the GM between the barrier and conventionally-housed F1-Pirc rats (Fig.5A). At the Genus level (Supplementary Fig.2A), several taxa including *Parabacteroides*, *ASF356*, *Blautia*, and *Mucispirillum* were elevated in the barrier F1-Pirc rats. In the conventionalized rats there was an observed increase in the relative abundance of over 50 taxa, the top 35 are depicted in Supplementary Fig.2A. The overall GM profile composition differences are visualized using a Principal Coordinate analysis (Fig.5B). The most separation was observed along PCo1, suggesting that the room differences contribute to the majority of the variability in the GM architecture. There were also significant increases in the richness and diversity indices such as Chao1 and Shannon (Fig.5C-E). These results suggest that the contribution of the room differences, such as husbandry, handling, and exposure to conventional animals have a crucial effect on the acquired taxa. *Firmicutes* and *Tenericutes* were increased in the conventionally-

housed rats, whereas *Bacteroidetes* was decreased. This also led to a significant shift in the *Firmicutes*:*Bacteroidetes* ratio between the two groups (Fig.5F).

We found significant correlations between certain taxa from the barrier room (Fig.6A and Supplementary Fig.3A) at weaning with the colonic tumor burden including the small adenomas. In these F1-Pirc rats, decrease in *Erysipelotrichaceae* and the Genus *Parabacteroides* were associated with an increase in the colonic tumor count, whereas order *Peptostreptococcaceae* was found to show a positive correlation with tumor burden. Other taxa such as *Ruminococcaceae* and *Lachnospiraceae* showed similar correlations. Similarly, *Bacteroides*, *Peptococcus*, *Clostridiales*, *Peptococcaceae* and *Candidatus Saccharomonas* showed significantly positive correlations.

Correlation analysis with the colonic tumor burden of the conventionally-raised F1-Pirc animals (Fig.6B and Supplementary Fig.3B) showed that family *Prevotellaceae* at weaning was negatively correlated with tumor burden. *Clostridium family XIII*, *Lachnospiraceae*, *Ruminococcus UCG-006*, *UCG-008*, *UCG-010* and *Clostridiales*, on the other hand were positively correlated with tumor increase, suggesting a causative role for the taxa from these operational taxonomic units. Simultaneously, we found significant negative correlations between *Parabacteroides* and specific OTUs from the barrier room at 4 months of age. These OTUs included *Ruminococcus NK4A136*, *Roseburia*, *Lachnospiraceae*, *Instestimonas* and *Oscillibacter*. Other OTUs including *Parabacteroides* and *Prevotellaceae* had positive and negative correlations respectively with the other commensals such as *ASF356*, *Mucispirillum*, *Lachnospiraceae* and *Ruminococcus UCG* taxa.

We used PICRUSt (Phylogenetic Investigation of Communities by Reconstruction of Unobserved States) and the HMP Unified Metabolic Analysis Network (HUMANN) to understand the functional capacity of bacterial taxa in the fecal samples collected at 4 months of age (Supplementary Fig.2B). We found that the barrier room F1-Pirc rats had a substantial increase in the spermidine-putrescine transport system and the succinate dehydrogenase pathways. Conversely, the predicted functional capacity of the conventional room rats showed increased abundance of pathways related to bacterial cell doubling time including Krebs's cycle, increased amino acid biosynthesis (methionine and leucine), iron transport systems and increased sulfate reduction to hydrogen sulfide.

3.5. Barrier and conventional room diets have distinct GM populations

Targeting the 16S rRNA gene, we sequenced the feed from the barrier and conventional rooms where we found that the GM profile of the feed from the two rooms did not differ significantly (Supplementary Fig.4A). Feed from the barrier and conventional rooms demonstrated similar abundances of order *Streptophyta* and *Zea luxurians*; genetic content likely derived from plant material used in the preparative process for feed (Supplementary Fig.5A). Though the community profile appeared similar, the relative abundances of *Lactobacillus*, *Leuconostoc*, *Sphingomonas* and *Fusobacterium* were significantly increased in the barrier room feed compared to the conventional diet (Supplementary Fig.5C). More importantly, to delineate between residual genetic content after autoclaving and potential taxa that may colonize the rats in the conventional room we cultured the feed from both rooms. Under anaerobic conditions, we cultured the feed overnight at 37 °C using brain heart infusion medium. We observed several taxa in the feed from the conventional room grew abundantly,

whereas the barrier room chow had minimally detectable levels of taxa such as *Clostridium* and *Bacillus* (Supplementary Fig.4B). This was also observed in the rarefaction curves (Supplementary Fig.5B) when sampling the observed species in each of the samples. We found that the cultures with the conventional feed had several species that were identifiable compared to both the uncultured conventional and barrier feed, including the cultured barrier feed. This suggested that bacteria from the feed could potentially have colonized the gastrointestinal (GI) tract of the F1-Pirc rats that were housed under conventional conditions, possibly altering the phenotype. In fact, we found that operational taxonomic units (OTUs) found in the feed such as *RF39*, *Ruminiclostridium*, *Oscillibacter*, and several Genera of the *Muribaculaceae* order were found in the conventionally raised F1-Pirc animals, but were undetectable in the barrier room rats (Supplementary Fig.5A).

4. Discussion

The human colon is host to approximately 10^{14} bacteria alone, aside from viruses and fungi, which together form the gut microbiota. The interaction between the host and the endogenous GM is highly varied and complex which may be a crucial part of disease susceptibility. However, modelling the interactions of the GM in a complex setting is challenging. Therefore, we generated F344/NTac-*Apc*^{+/am1137} (Pirc) rats and fostered them onto a Charles River Altered Schaedler Flora (CRASF) gut microbiota profile. We were able to stably maintain the ASF GM with only the acquisition of a few OTUs such as *Anaerotruncus*, and *Staphylococcus*. More importantly, the F1-Pirc (LEWF344F1-*Apc*^{+/am1137} CRASF) animals generated resembled the CRASF parents at weaning except

Genus *Mucispirillum* which was decreased in the offspring compared to the breeders. This taxa is difficult to culture *in vitro* compared to other ASF taxa, however, it is still not known whether it is inhibited by the presence of other OTUs usually observed in Altered Schaedler Flora colonies (390).

We hypothesized based on the phenotype of colon cancer in germ-free or antibiotic-treated animal models, that the F1-Pirc CRASF rats in the barrier room would have fewer colonic adenomas. Contrary to our hypothesis, animals maintained under barrier conditions had an increased tumor burden, including significantly increased number of smaller adenomas especially in the proximal section of the colon. In the original report of the Pirc rat (188), microadenomas required histopathological confirmation and were recorded as being smaller than 0.5 mm in diameter. However, in our case the differences between the barrier and conventional rooms were grossly apparent. It must be noted though that excluding the smaller adenoma numbers, there was a trend towards increased tumors in the conventional animals as originally hypothesized. This posits for future studies where F1-Pirc rats would be aged longer than 4 months to understand if the observed small adenomas may develop into adenomas larger than 1 mm in diameter. Another observation from our study was the alteration of the colonic tumor phenotype observed in the F1-Pirc rats from the barrier room. Typically, Pirc rats demonstrate a colonic phenotype where the adenomas develop in the middle and distal portion of the colon with few in the proximal regions, as we observed in the F1-Pirc animals from the conventional room. However, F1-Pirc animals from the barrier room had several adenomas in the proximal section of the colon with few or none in the middle and distal regions. Similar to previous reports of germ-free animals, these animals had

enlarged ceca compared to conventional F1-Pirc rats (391-393). Zackular *et al.* showed in an AOM/DSS (azoxymethane/dextran sodium sulfide)-treated mouse model that a decrease in the overall GM population through the administration of antibiotics, led to a significant decrease in tumor burden (64). Another study similarly demonstrated that transferring tumor-associated microbiota into germ-free mice increased the tumor burden of the mice, otherwise significantly reduced when mice were maintained germ-free (151). Based on these reports, our findings of animals maintained in a barrier room having significantly elevated adenomas is intriguing. Although studies have shown that bacteria are needed for a phenotype to be manifested in animals (394-397), our results suggest that a consortium of taxa may influence disease.

The barrier room was maintained with irradiated chow, paper chip bedding, autoclaved water and animals were always handled in a biosafety cabinet. We housed the conventional room rats with non-irradiated feed, non-autoclaved bedding and used animal handling techniques that did not require aseptic methods. We hypothesized that this would alter the existing CRASF microbiota to a more complex GM. We used 16S rRNA sequencing to determine if the GM, known to be modulated by husbandry factors (1, 6, 398-401) was the crucial modulator of the phenotype observed in our study at 3 months after introduction into the conventional facility, we found the conventional rats had acquired OTUs including *Prevotellaceae*, *Ruminococcaceae*, *Muribaculaceae*, *Parasutterella* and *Desulfovibrionaceae*. *Prevotellaceae* and *Desulfovibrionaceae* have been reported to be associated with healthy patients or a decreased tumor burden in colon cancer studies (64, 73, 131, 174, 402-404). On the other hand, *Blautia*, *Enterococcus*, and some *Lachnospiraceae* taxa found in the barrier room F1-Pirc rats have been associated

with an increased tumor susceptibility (70, 86, 296, 371, 381, 405-409). This was equally evident from the correlations where *Peptococcaceae*, *Clostridiales*, and *Lachnospiraceae*, previously reported to be associated with an increased tumor burden were elevated and positively correlated with the tumor burden in the barrier rats (410-413). Correlation analysis also found that certain OTUs introduced into the conventional rats had a negative association with *Parabacteroides*, potentially suggesting that these OTUs inhibit the proliferation or take over the niche occupied by the latter, i.e. competitive interactions (414). In the barrier room rats we also found predicted functional pathways such as succinate dehydrogenase and spermidine-putrescine transport system to be elevated. Host succinate dehydrogenase mutations are very commonly found in colon cancer (200, 201, 415). This raises the possibility of a breakdown of the host dehydrogenases, thereby leading to an increase in the bacterial dehydrogenase expression to counteract the toxic effect of succinate. Alternatively, many rumen bacteria are known to produce succinate (416) which in turn has been identified as a biomarker for colon cancer via mass spectrometry (417). This suggests elevated levels of succinate, reportedly an onco-metabolite (418) could be promoting tumorigenesis in the barrier room rats via inhibition of PHD (prolyl hydroxylase domain-containing) enzymes (419) via activation of hypoxia-induced factor alpha (HIF- α). Succinate quantitation via metabolomics and PHD enzyme activity will however need to be validated in future studies to determine the mechanisms contributing to increased succinate levels. Similarly, polyamines such as spermidine and putrescine have been reported to be biomarkers for colorectal cancer in human patients (198). In 1988, Upp *et al.* analyzed the polyamine levels including spermidine and putrescine in colon cancer patients and found that they may be used to

identify at-risk patients of the disease (420). More recently, it was identified that GI bacteria such as *Bacteroides fragilis* upregulate spermine oxidase which induces production of spermidine, hydrogen peroxide and aldehydes (421, 422), potentially causing DNA damage. Another thought-provoking observation in our study is the presence of OTUs found in the diet that were detected in the barrier and conventional room fecal samples from F1-Pirc rats. Although, the barrier room rats were not over-ridden by the taxa found via 16S sequencing, this was not true for the conventionally raised rats. We found that the conventionally housed F1-Pirc rats had significant amounts of bacterial taxa that were also detected in the diet, and that were anaerobically cultivable. This suggests that the non-irradiated diet, may be one source of the variation, although it is also possible that the rare OTUs picked up are nonviable residual DNA from dead bacteria or spores. More importantly, this source, potentially led to a significant shift in the phenotype, i.e. number of adenomas.

Colorectal cancer (CRC) animal models have been extensively used to study and understand the etiology of the disease including initiation, development and factors affecting susceptibility (150, 165, 375-378, 423-425). Despite the development of the *Apc^{+/am1137}* rat, the *Apc^{+/Min}* mouse model of colon cancer is still largely used for various studies owing to cost and the ease of genetic manipulation techniques. However, the Pirc (*Apc^{+/am1137}*) rat with a colonic phenotype has created a potentially more translatable alternative to the mouse when studying colon cancer. With studies recently reporting evidence of the role of the gut microbiota in diseases susceptibility including colon cancer (64, 92, 131, 151, 207, 293, 379, 380, 383, 384, 426), the importance of reproducibility in disease models is critical. Several reports have identified

Fusobacterium, in particular *Fusobacterium nucleatum*, as a significant modifier of disease burden. These bacteria along with Enterotoxigenic *Bacteroides fragilis* (ETBF) have often been associated with increased tumor burden and/or carcinoma samples in human patients (159, 170-172, 174, 179, 191, 412, 427-429). However, it should be noted that most of these studies do not take into account the constant interactions and synergistic nature of the commensals within the GI tract. GM populations are a constant source of nutrients and metabolites, which are contingent on the action of one bacterium on the by-products of the replicative processes of another. To model and establish a simplified GM profile to study the role of specific bacteria and their interactions with the host and other commensals, we established *Apc*^{+/am1137} rats on a CRASF gut microbiome profile. The observance of increased tumor number in a limited GM microbiome provides a platform for probiotic experimentation. It can also allow for more refined metabolite profiling and longitudinal assessment in changes in metabolic processing. Utilizing a simplified GM profile for understanding the pathophysiology of colon cancer, may provide insights into the interactions between commensals and with the host, including the mechanisms by which specific taxa promote or prevent adenomagenesis.

5. Ethics Approval and Consent to Participate

The protocols and studies used in this research study were approved by the Institutional Animal Care and Use Committees at the University of Missouri. During the study, the guidelines set forth by the Guide for the Use and Care of Laboratory Animals and the Public Health Service Policy on Humane Care and Use of Laboratory Animals were strictly adhered to.

6. Author Contributions and Acknowledgements

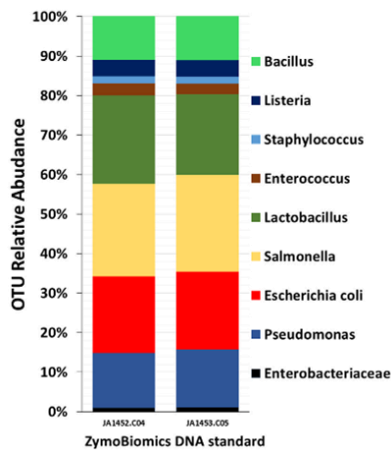
SBB and JAL designed and performed the experiments. DD supplied the data for the different GM profiles from the sequenced feed. JM helped with the necropsy. The authors wish to acknowledge Giedre Turner, Becky Dorfmeier and the MU Metagenomics Center for their assistance with 16S rRNA gene sequencing; Brittany Lister and Office of Animal Resources staff for assistance with animal husbandry; Charles River Laboratories Inc. for assistance making the CRASF animals available and with sample collection prior to shipping. This research was funded by a University of Missouri System Research Board grant. The funders had no role in study design, data collection and analysis, decision to publish, or preparation of the manuscript.

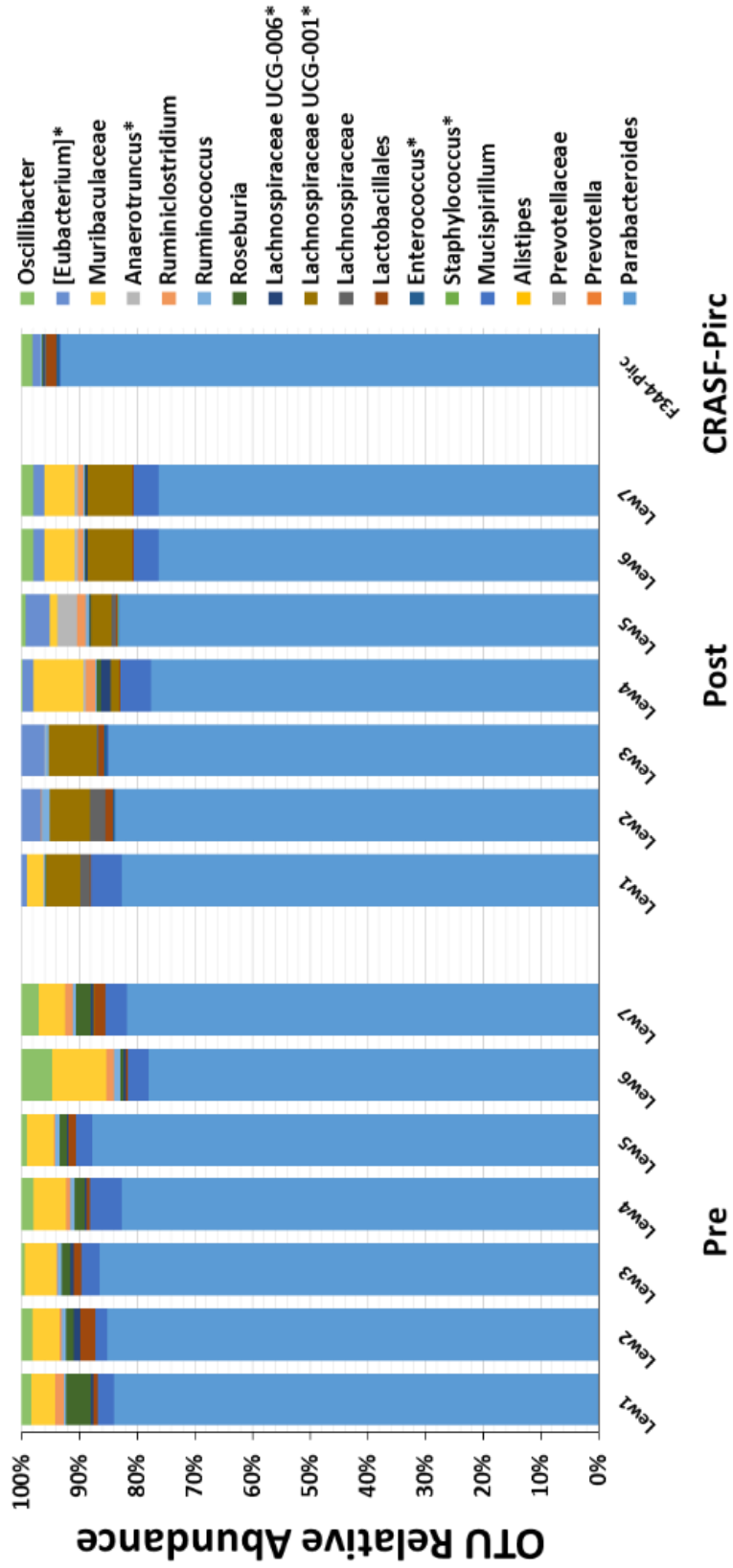
7. Figures

Figure 1. 16S sequencing analysis of fecal microbiota in CRASF rats pre- and post- shipping

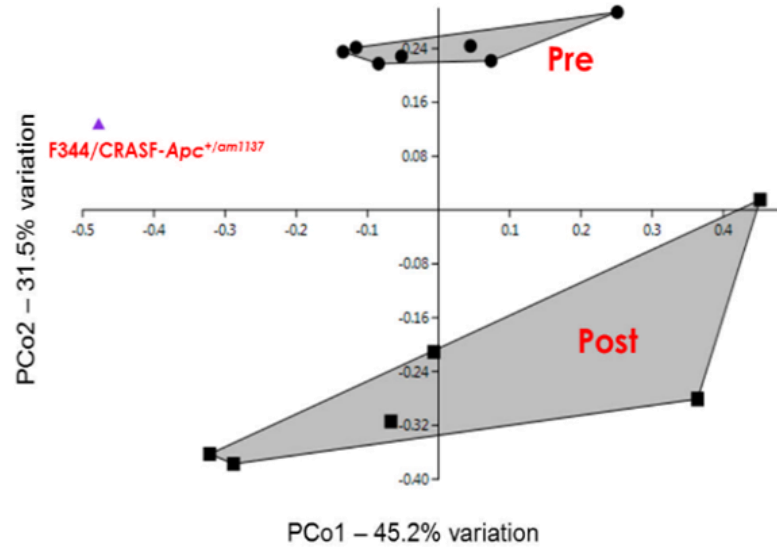
(A) Relative abundance (percentages) of each operational taxonomic unit (OTU) at the Genus level is shown for the ASF rats purchased from Charles River Laboratories, before shipping and 3 months post arrival at the Discovery Ridge animal facility. Also shown is the GM profile of the F344/CRASF-*Apc*^{+/*am1137*} (JA1047.D4) that was fostered onto a CRASF dam. Bar graphs depicting the 16S sequencing data for the ZymoBIOMICS™ microbial community DNA standard is shown on the left that were used as processing and sequencing controls. *OTUs picked up after arrival and housing for 3 months. (B) Principal Coordinate Analysis (PCoA) for the 16S rRNA sequencing data shows that Pre and Post samples (black, filled circles) of the CRASF rats are significantly different (PERMANOVA, $F=6.272$ and $P=0.0001$). The fostered *Apc*^{+/*am1137*} rat is shown as the purple filled triangle. (C) Bar graphs representing each OTU as a single color show the relative abundance of taxa detected in the bedding and the gel-paks via 16S rRNA gene sequencing.

A





B



C

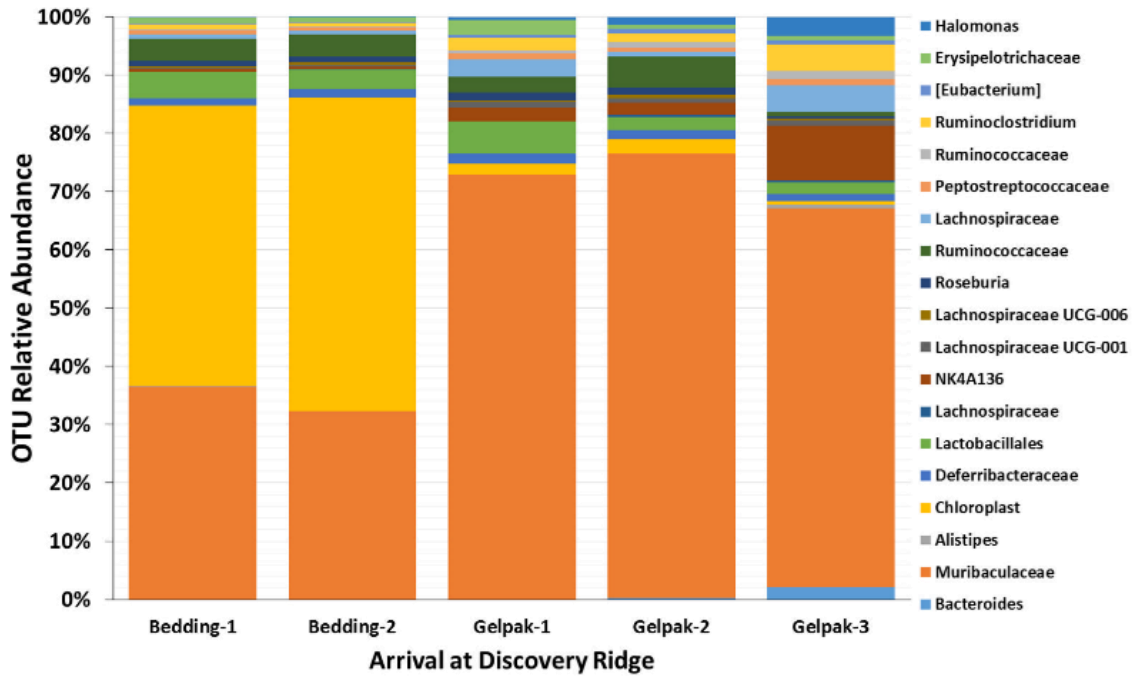
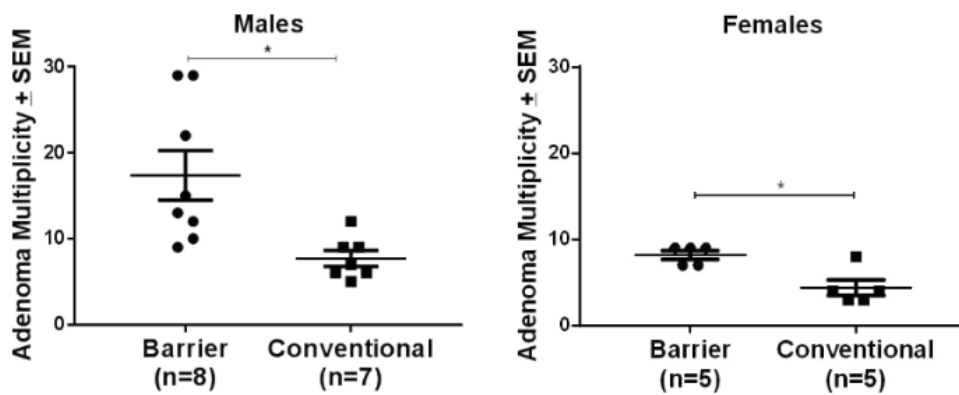


Figure 2. Colonic and small intestinal adenoma multiplicity of barrier and conventional rats at 4 months of age

Colonic (A) and small intestinal (B) adenoma multiplicity for male and female F1-Pirc rats from the barrier and conventional rooms is shown with adenoma counts on the y-axis and the groups on the x-axis. Significance was assessed by a Student's *t*-test, with a *P*-value less than 0.05 was observed. Error bars indicate standard error of the mean (\pm SEM).

A



B

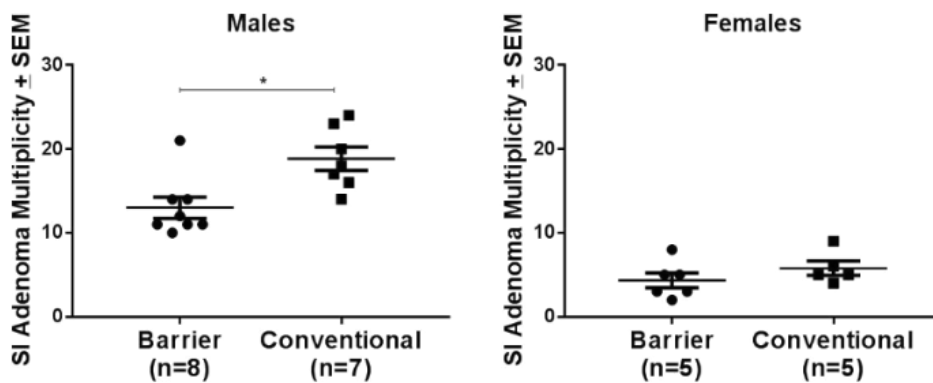
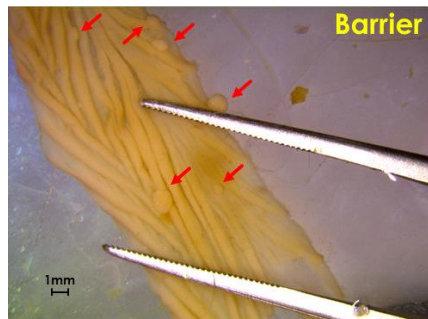


Figure 3. Effect of Altered Schaedler Flora on the colonic adenoma phenotype and the physiology of the gastrointestinal tract

(A) Representative proximal colon section of the (n=13) F1-Pirc rats from the barrier room. Arrows indicate small adenomas, less than 1 mm in diameter. Scale bar = 1mm. Depicted small adenoma sizes: 1 = 0.363mm, 2 = 0.858mm, 3 = 0.875 mm, 4 = 0.993mm, 5 = 0.969mm, and 6 = 0.378mm. (B) Representative proximal colonic region for (n=12) conventionally-housed rats. Images were captured on a Leica M165FC microscope with 1X magnification and a 40X objective. (C) Number of small adenomas determined in males and females respectively in the barrier and conventional rooms. (D) Adenoma multiplicity differences in males and females respectively were determined by excluding the number of small adenomas seen in the F1-Pirc rats. Significance was assessed by a Student's *t*-test, with a *P*-value less than 0.05 was observed as significant. Error bars indicate standard error of the mean (\pm SEM). (E) Representative images of the cecum at weaning, from the barrier and conventional rooms. (F) Barrier and conventional room ceca obtained at sacrifice (representative images), indicating the difference in size between the housing conditions. Images were captured using a Nikon D5200. A ruler is shown for comparison between groups.

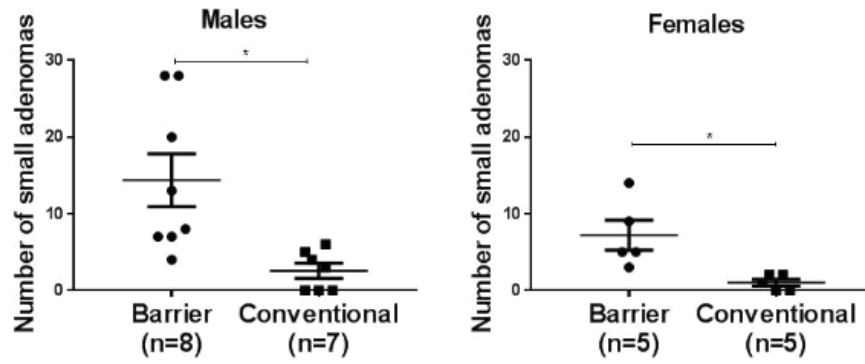
A



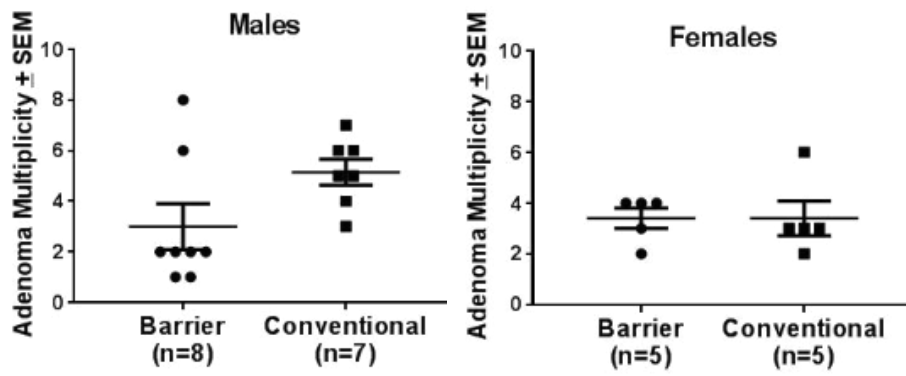
B



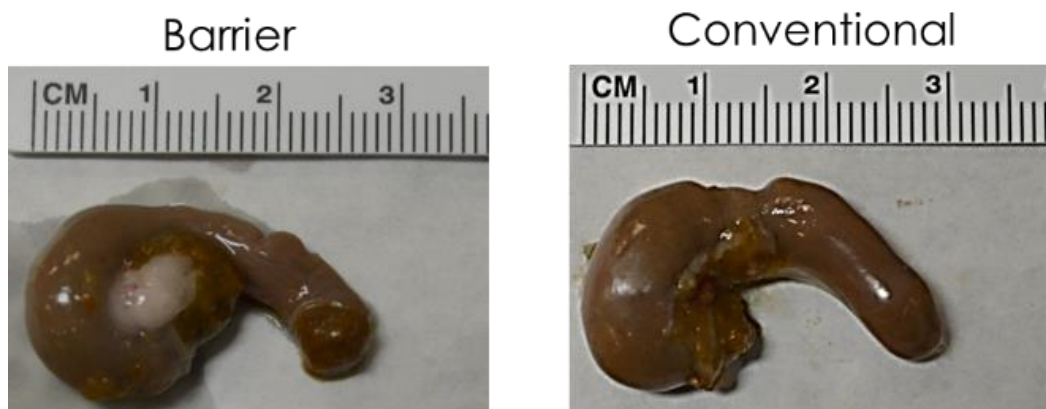
C



D



E



Weaning cecum

F

Barrier



Conventional

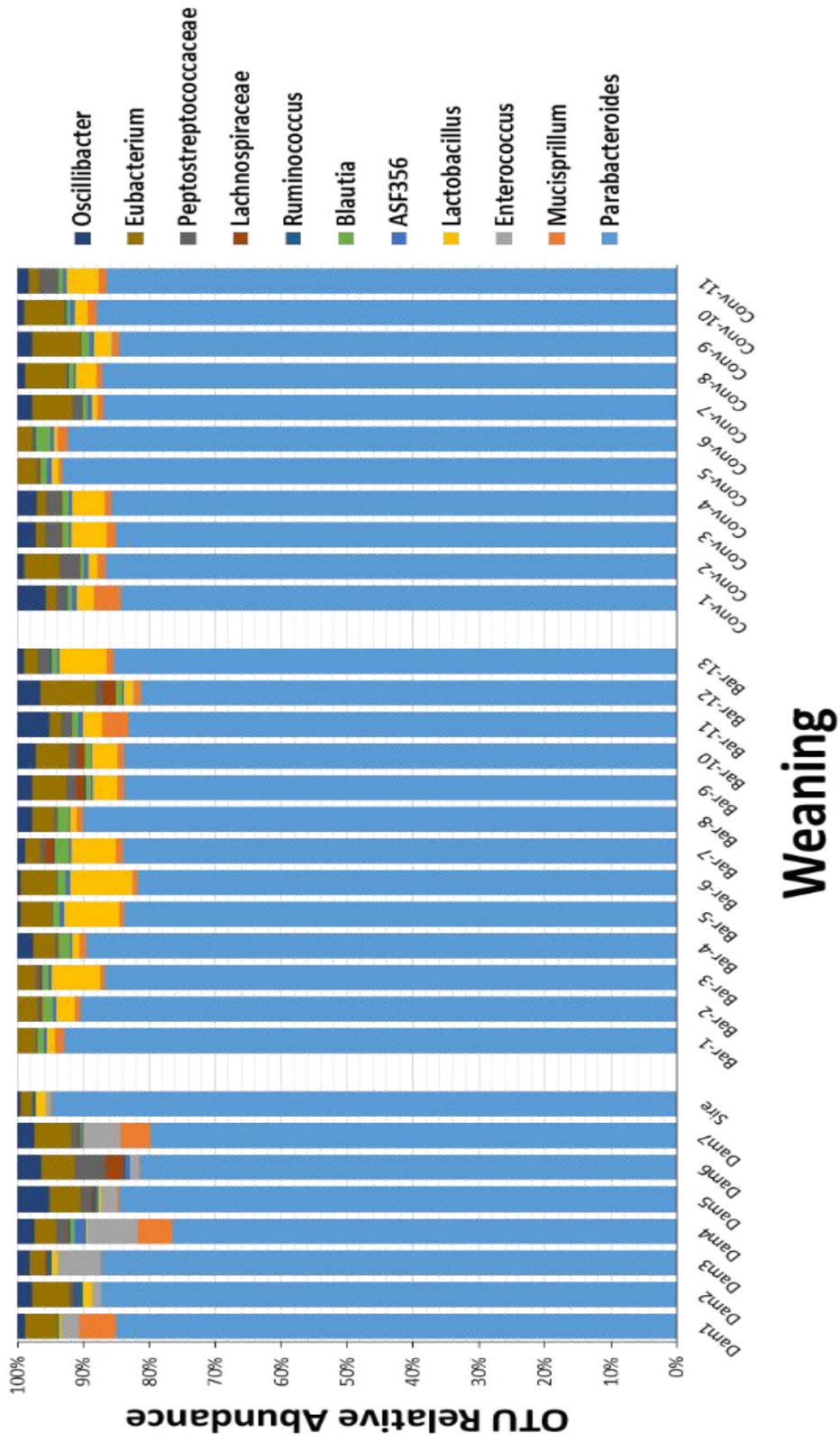


4 month cecum

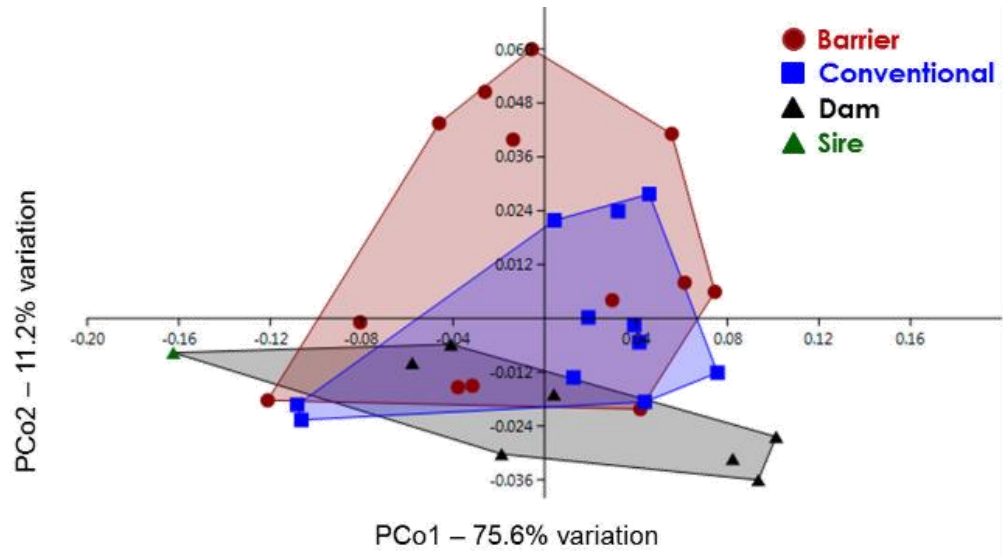
Figure 4. 16S sequencing analysis of fecal microbiota in F1-Pirc rats at weaning

(A) Gut microbiota profiles of the dams and sire along with the barrier and conventionally raised F1-Pirc rats at weaning are displayed as a bar graph depicting the relative abundance of each OTU in percentages. Each color represents a single OTU. (B) Principal Coordinate Analysis using a Bray-Curtis distance matrix depicts the overall similarity or dissimilarity within the groups: barrier (brown, filled circle), conventional (blue, filled square), dams (black, filled triangle), and sire (green, filled triangle). PERMANOVA was used for significance testing; $F=1.112$ and $P=0.3172$. (C) The total number of OTUs observed, i.e. richness of the groups is depicted with the groups along the x -axis and the number of OTUs along the y -axis. No significant differences were found (ANOVA, Tukey's post hoc, $P<0.05$)

A



B



C

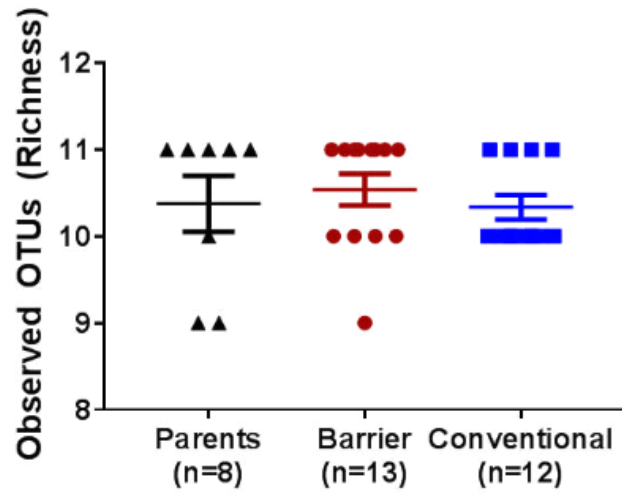
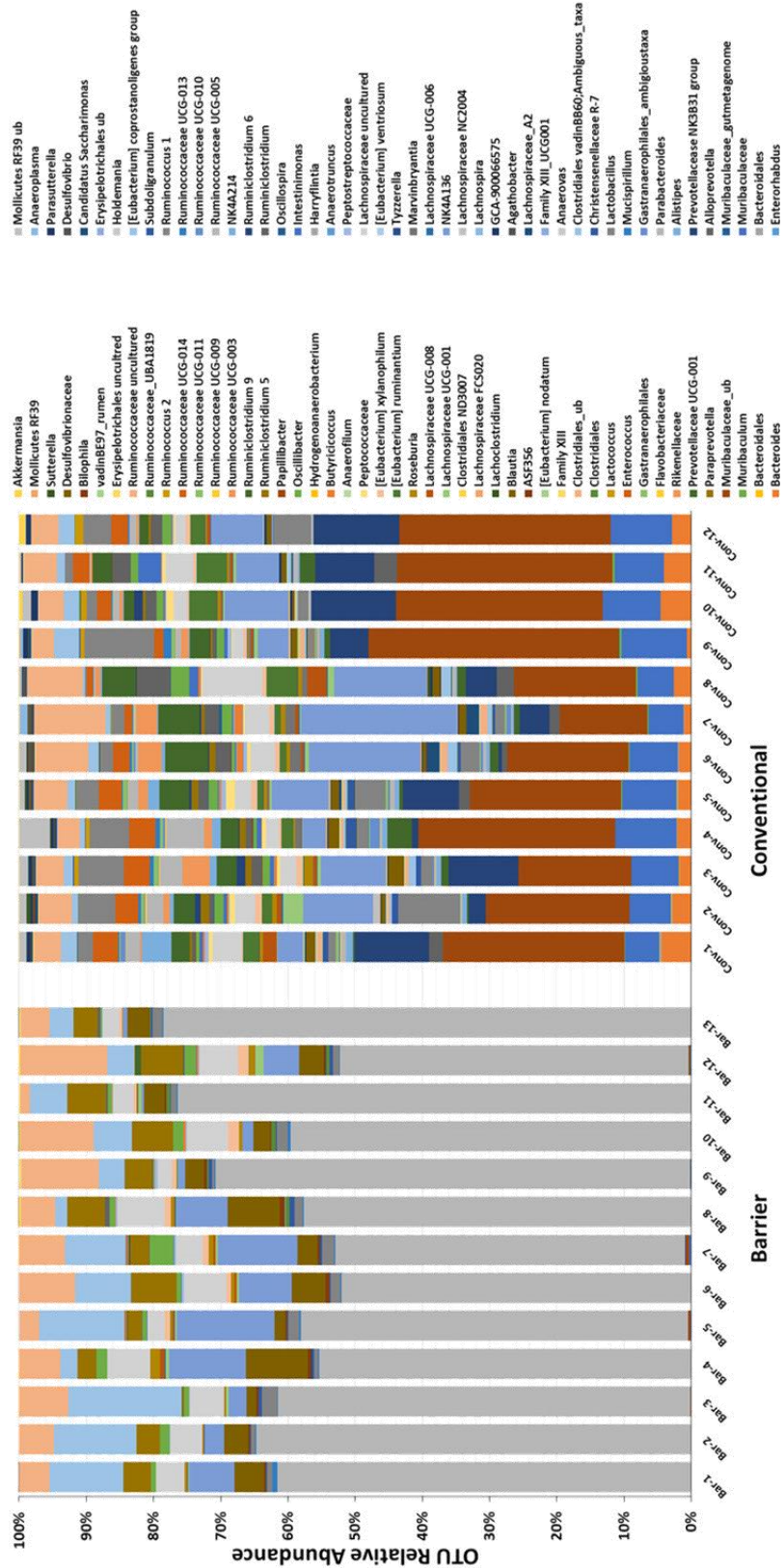


Figure 5. Effect of conventional housing on the GM at 4 months of age

(A) Bar graphs depicting the Phyla and Genera at 4 months of age from the barrier and conventional F1-Pirc rats demonstrate the individual OTUs as a different color. (B) Genus level OTUs were used to visualize the similarities/dissimilarities between each samples and the groups at 4 months of age using a PCoA. PERMANOVA was used to determine significant differences with a P -value less than 0.05. Based on the Genus level data with a cutoff of 0.001% (accounting for sequencing error rates), the richness (C), and diversity indices – Chao1 (D) and Shannon (E) were measured from the raw read counts after normalizing the sequences to 21,639 per sample. (F) The *Firmicutes:Bacteroidetes* ratio of the two housing strategies is depicted. Significance assessed by $P < 0.05$ was determined using a Student's t -test.

A



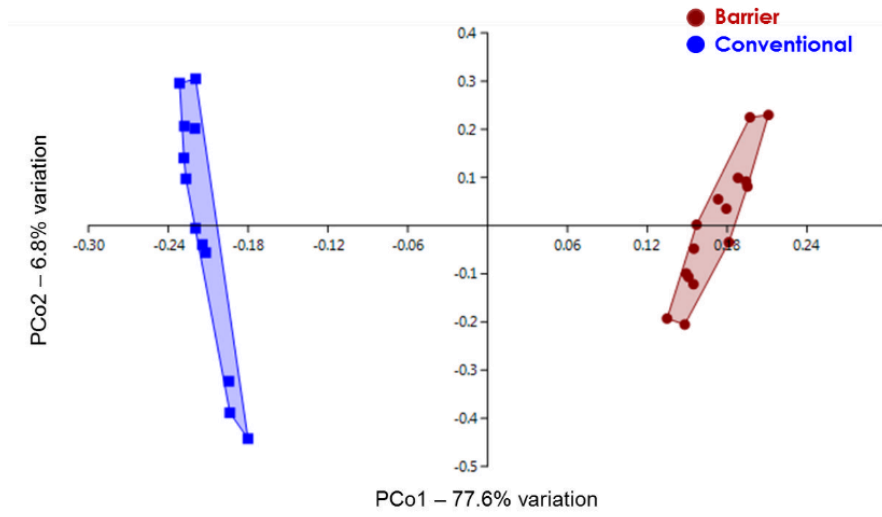
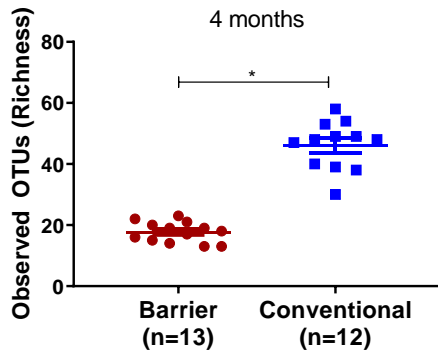
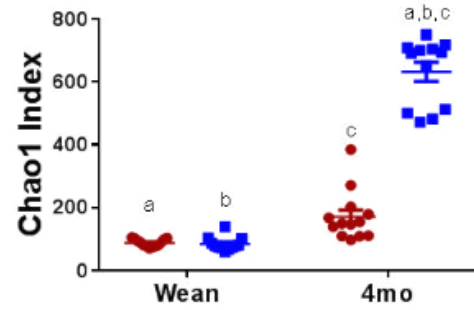
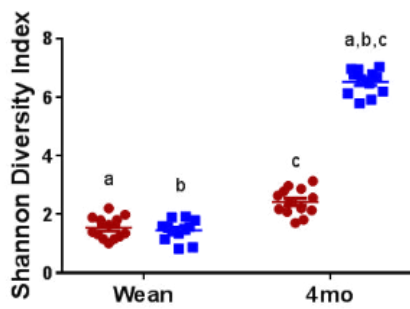
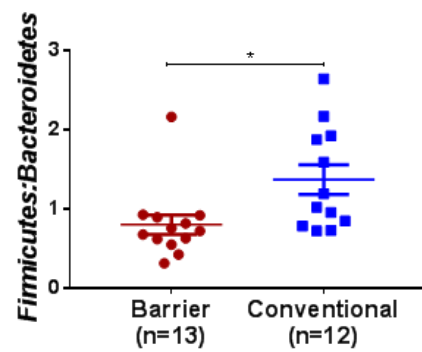
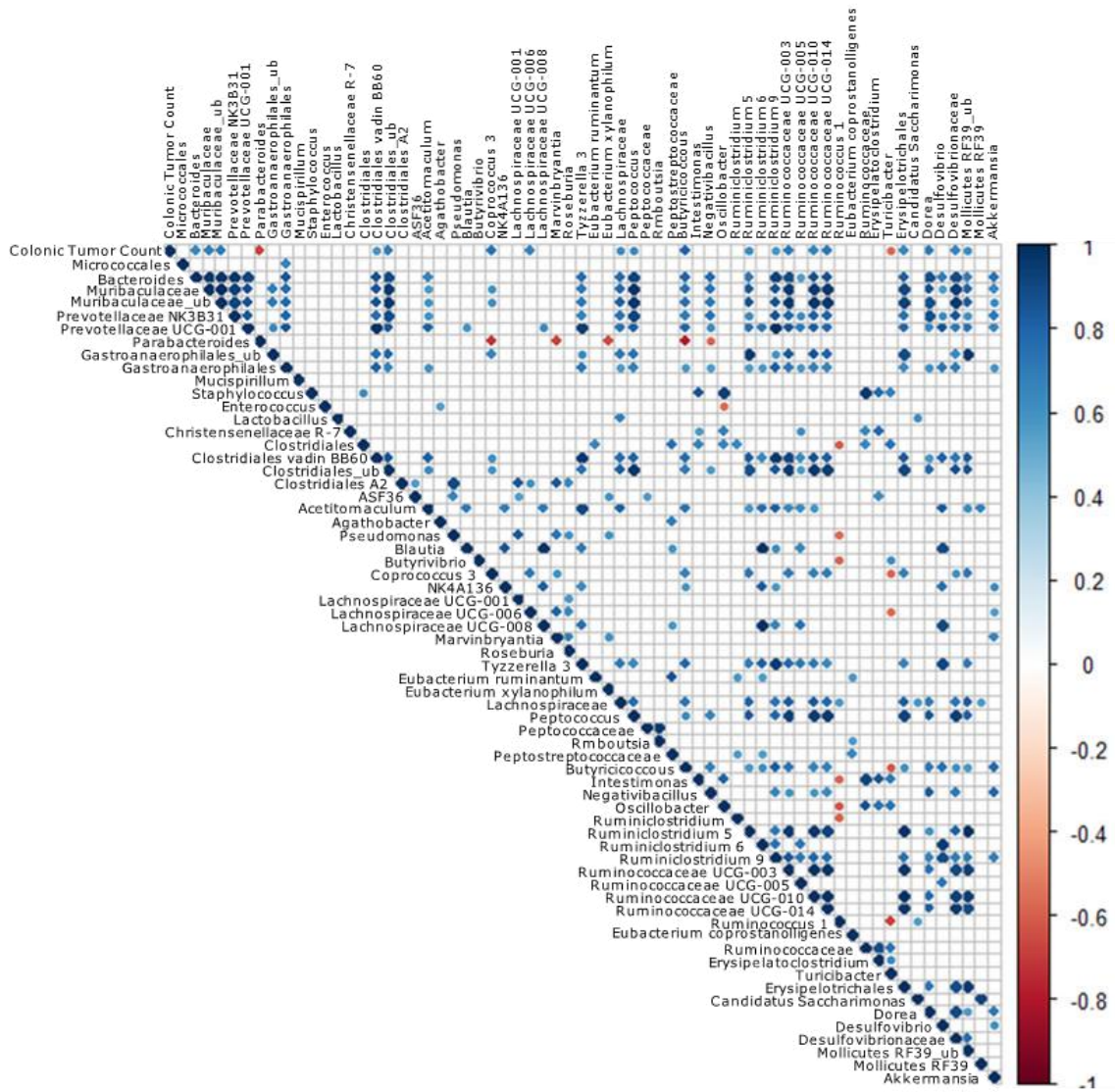
B**C****D****E****F**

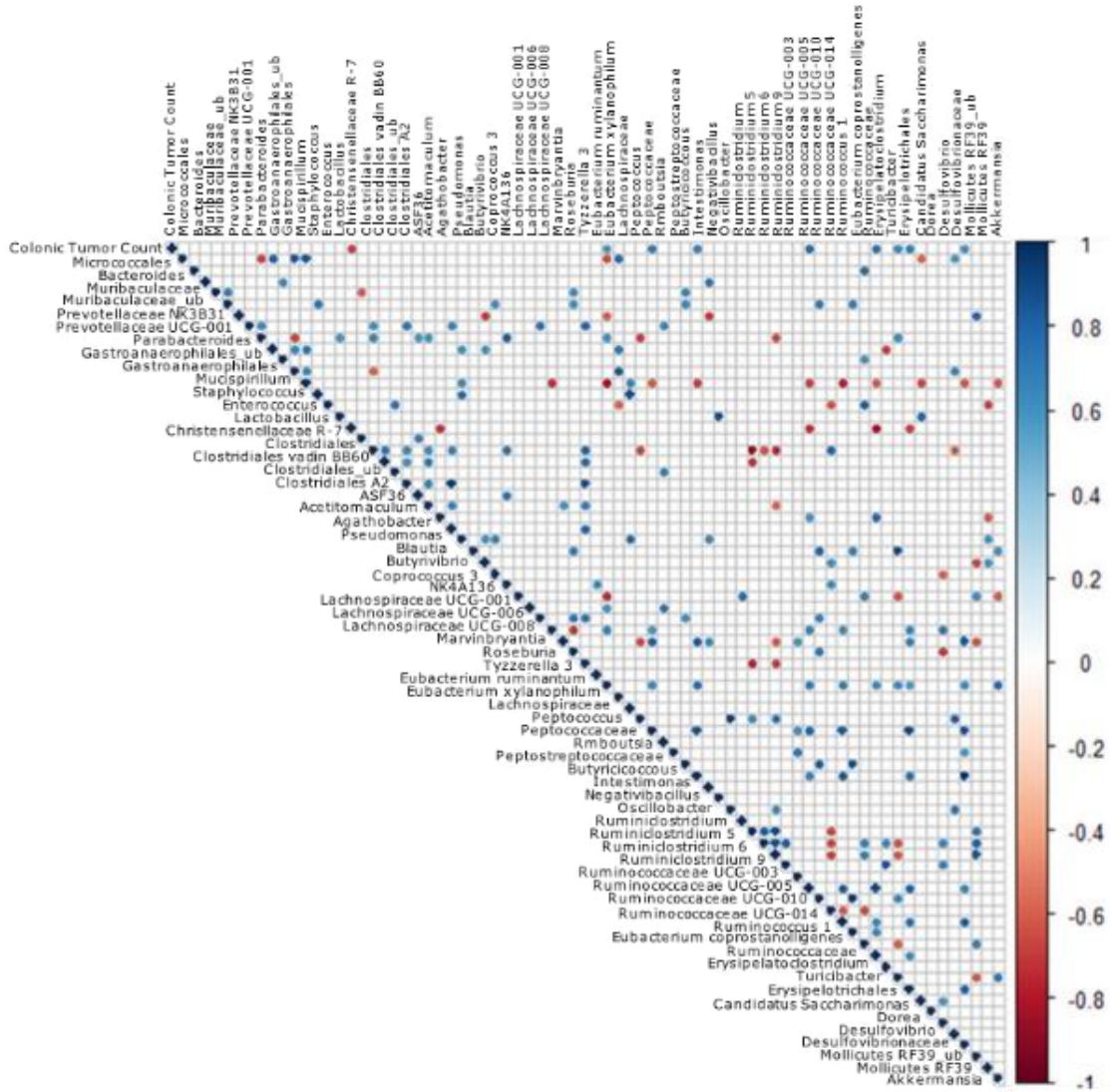
Figure 6. Correlation analysis of OTUs from barrier and conventional rooms with colonic tumor count at 4 months of age

Correlation analyses was performed using the *Corrgram* R package, to determine positive or negative correlations with individual taxa at weaning in the barrier (A) and conventional (B) housing conditions. Correlations with a significant *P*-value of less than 0.05 are depicted by filled circles or diamonds. Empty cells indicate no significant correlations. Positive correlations with $r^2 > 0.75$ are shown as blue diamonds and as blue circles for $r^2 < 0.75$. Negative correlations are shown as red diamonds ($r^2 > 0.75$), and red circles for $r^2 < 0.75$.

A

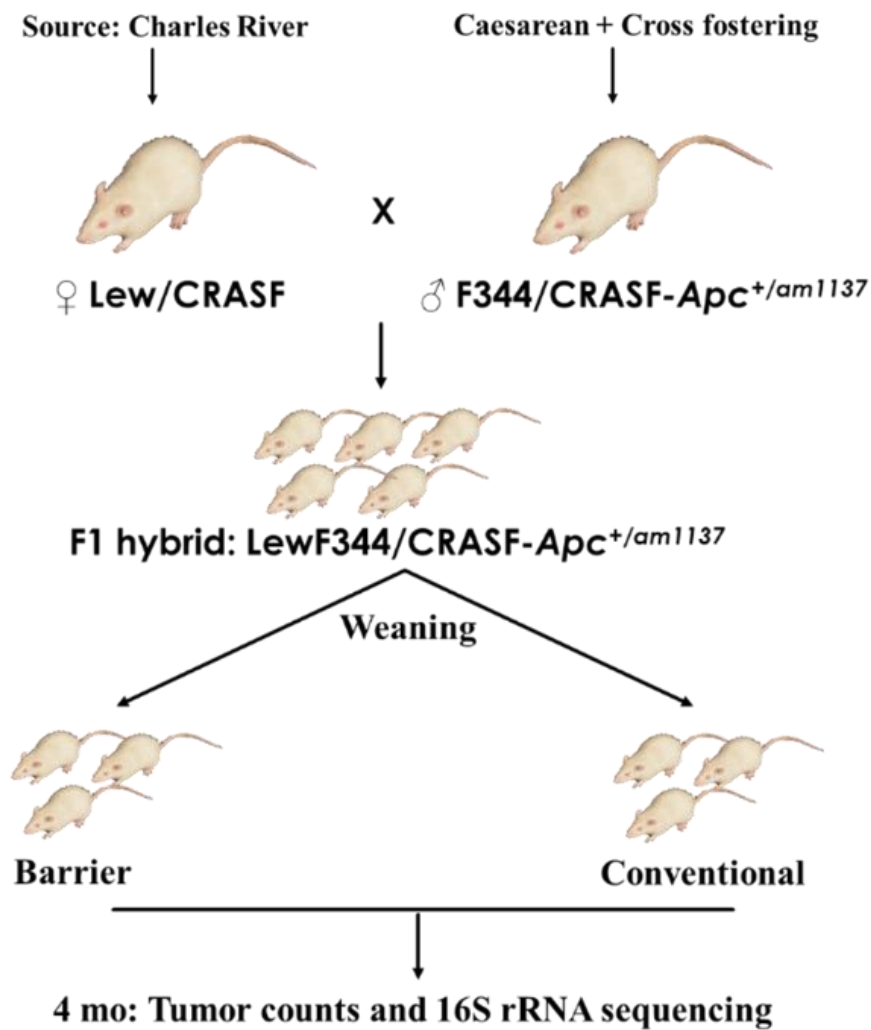


B



Supplementary figure 1. Experimental design

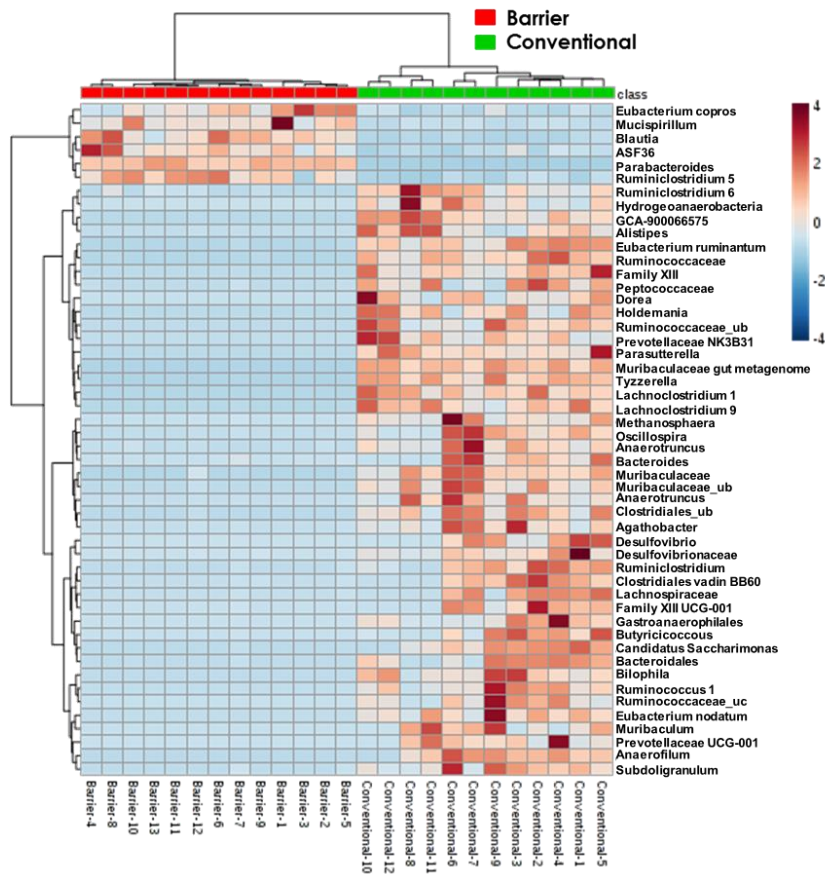
Female LEW/CRASF rats were mated with male F344/CRASF-*Apc*^{+/*am1137*} (Pirc) rats to generate F1-hybrid LEWF344F1-*Apc*^{+/*am1137*} CRASF rats. At weaning, littermates were equally divided and housed either in a barrier room or in a conventional settings. At 4 months of age, colonic tumor counts and 16S rRNA sequencing was used to determine adenoma burden and gut microbiota (GM) profiles.



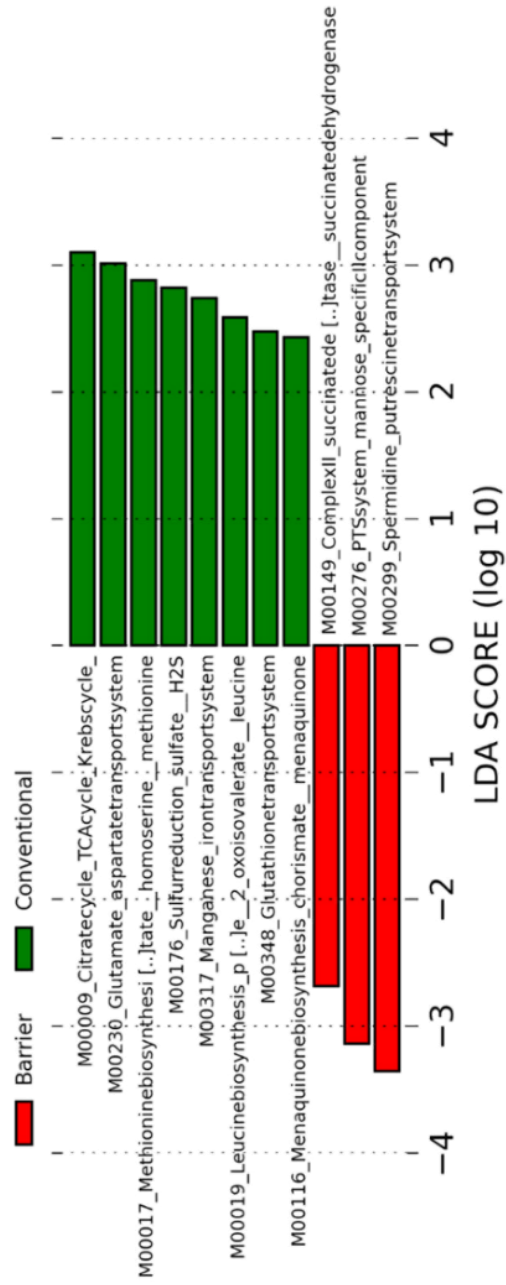
Supplementary figure 2. GM profile and predicted metabolic function of barrier and conventional rats at 4 months of age

(A) Heatmap of the Genera found at 4 months of age, generated using a Euclidean distance measure and Ward's clustering algorithm, depicts the top 50 OTUs that are differential between the groups. Barrier room animals are shown in red on the top bar, while the conventional animals are shown as green. (B) Linear Discriminant Effect Size (LefSe) analysis of the predicted metagenomic pathways obtained via PICRUSt and HUMAnN between the conventional and barrier room animals was performed using fecal DNA on 16S rDNA gene sequencing at 4 months of age.

A



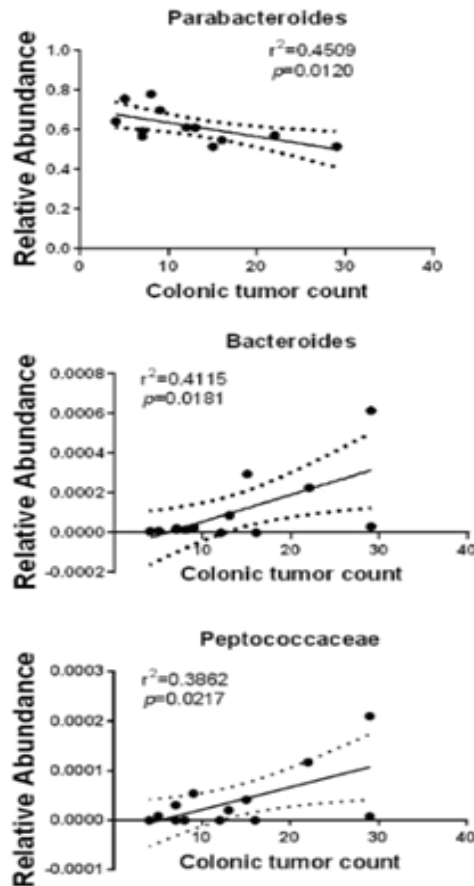
B



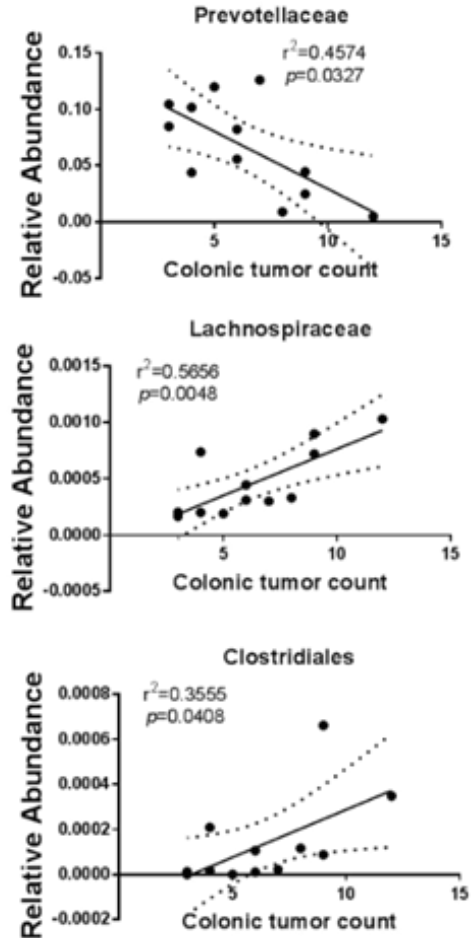
Supplementary figure 3. Correlation analysis of OTUs with colonic tumor count

Representative bacterial taxa relative abundance at 4 months of age correlated positively (*Bacteroides*, *Peptococcaceae*, *Lachnospiraceae* and *Clostridiales*) or negatively (*Parabacteroides* and *Prevotellaceae*) with colonic tumor count in the (A) barrier and (B) conventional F1-Pirc rats. Significance was determined using Pearson's correlation test with a $P < 0.05$ considered to be significant.

A



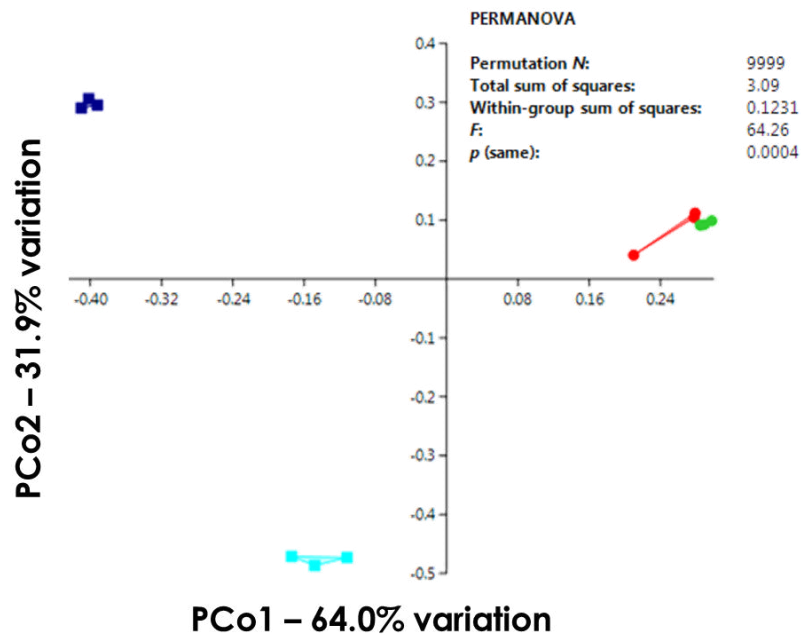
B



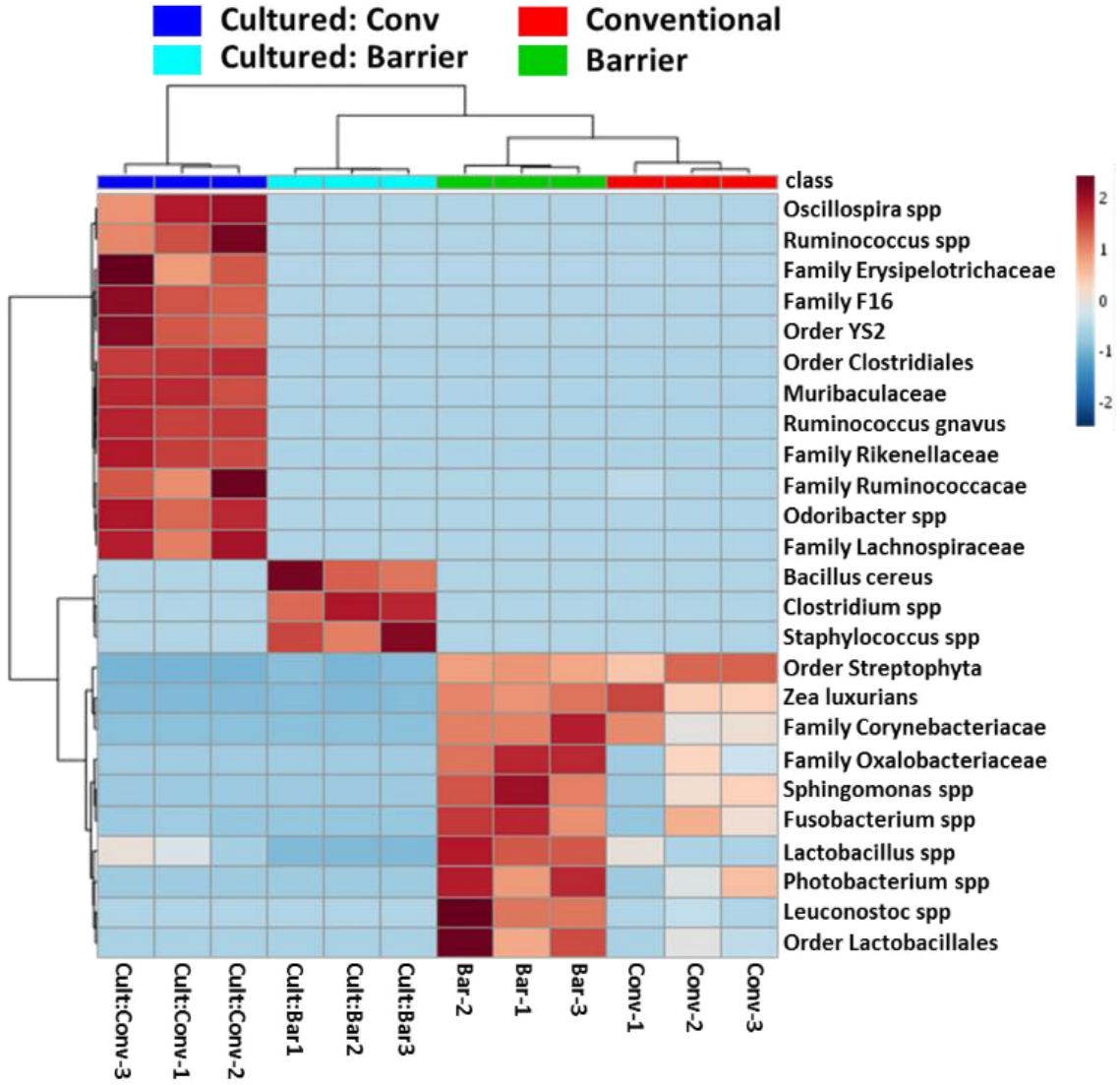
Supplementary figure 4. Bacterial population analysis of barrier and conventional room feed via 16S rDNA sequencing

(A) Principal Coordinate analysis (PCoA) demonstrates the overall GM profile variations along PCo1 and PCo2, between the feed from both the rooms. Each filled circle represents a single sample from the barrier (brown) and conventional (blue) room diet. No significant differences were found despite the separation via a PERMANOVA. (B) Heatmap generated using Euclidean distance and Ward's clustering algorithm was generated to observe the top 25 variable OTUs between the barrier (green) and conventional (red) feed 16S sequencing data. The dendrogram clusters samples based on their similarity with each other, where the individuals OTUs are listed along the y-axis. Relative abundance of the OTUs are plotted in color with increased abundance indicated by the darker red and lower abundance highlighted by the darker blue shading.

A



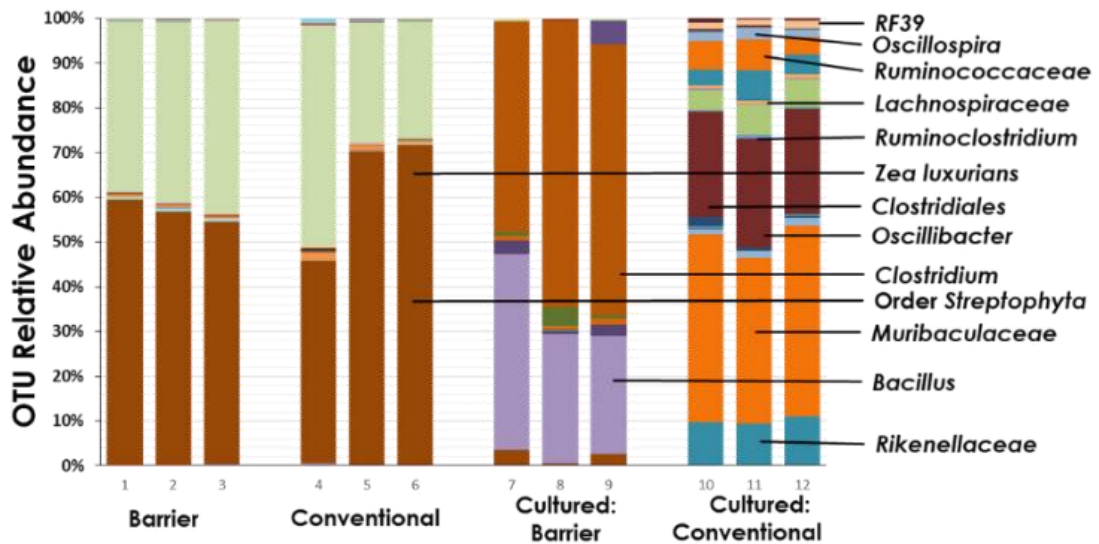
B



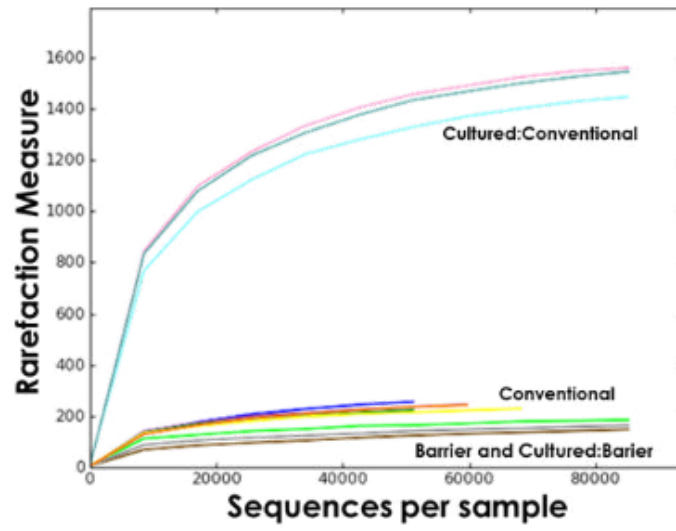
Supplementary figure 5. 16S analysis of cultured feed from barrier and conventional rooms

(A) 16S rRNA sequencing of the V4 hypervariable region from (n=3) diet samples is demonstrated as a stacked bar graph. Each color represents a single operational taxonomic unit (OTU) in the diet in terms of relative abundance along the y-axis. Groups depicted include: barrier diet, conventional diet, cultured barrier diet and cultured conventional diet. (B) Rarefaction curves displaying the depth of sequencing achieved for each sample in the barrier, conventional, and cultured barrier and conventional groups. Total number of observed species (y-axis) is plotted against the number of sequences (x-axis) per sample. (C) Relative abundance of individual bacteria found to be differential between the barrier and conventional feed. Significance was determined by a *P*-value of less than 0.05 using a Student's *t*-test.

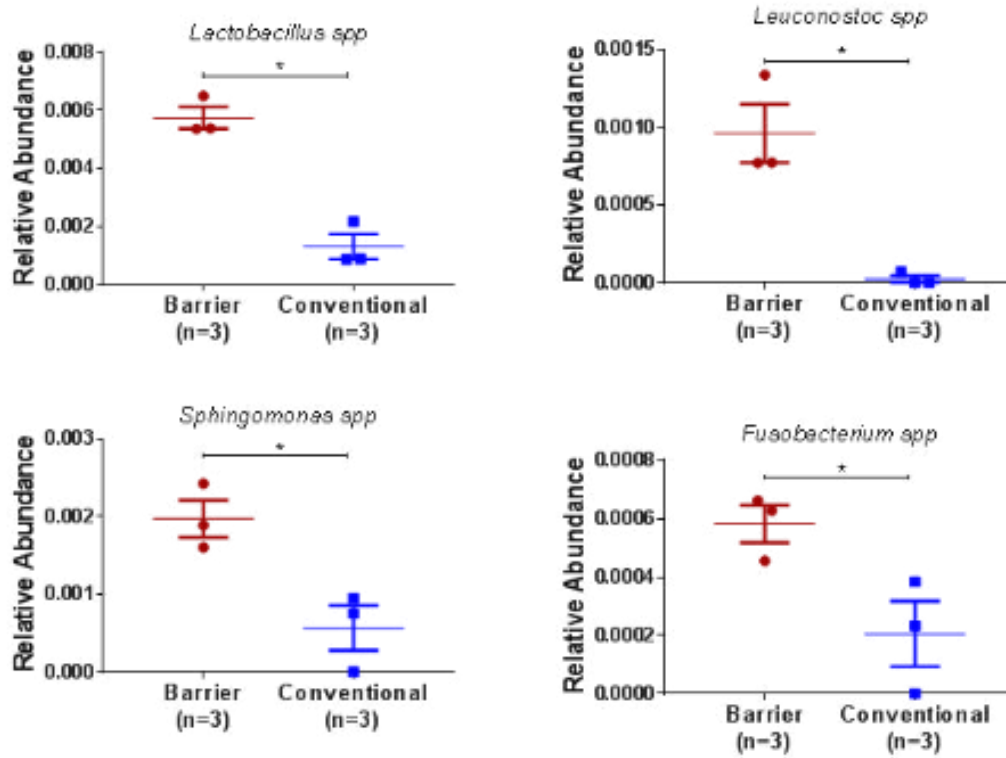
A



B



C



8. Tables

Table 1: Altered Schaedler Flora alters the colonic adenoma phenotype and the physiology of the gastrointestinal tract

Animal #	Sex	Room	SI	Colon (<1mm)	Small adenomas (>1mm)	Proximal small adenomas
1852	F	Barrier	5	3	9	Yes
1853	F	Barrier	3	4	0	No
1882	F	Barrier	3	2	14	Yes
1902	F	Barrier	8	4	5	No
1920	F	Barrier	2	1	5	Yes
1863	M	Barrier	12	6	7	Yes
1883	M	Barrier	11	2	20	Yes
1884	M	Barrier	14	1	28	Yes
1886	M	Barrier	10	1	28	Yes
1908	M	Barrier	21	8	4	No
1926	M	Barrier	11	2	13	Yes
1940	M	Barrier	11	2	8	Yes
1943	M	Barrier	14	2	7	Yes
1860	F	Conventional	9	3	0	No
1879	F	Conventional	6	2	2	No
1880	F	Conventional	5	6	2	No
1922	F	Conventional	4	3	1	No
1934	F	Conventional	5	3	0	No
1865	M	Conventional	23	5	4	Yes
1887	M	Conventional	17	3	3	No
1890	M	Conventional	18	6	6	No
1891	M	Conventional	14	4	5	No
1927	M	Conventional	20	6	0	No
1930	M	Conventional	24	7	0	No
1938	M	Conventional	16	5	0	No

CHAPTER V
INTEGRATED METABOLOME AND TRANSCRIPTOME ANALYSES
PROVIDE NOVEL INSIGHT INTO COLON CANCER MODULATION BY THE
GUT MICROBIOTA

(Susheel Bhanu Busi, Zhentian Lei, Lloyd W. Sumner, and James Amos-Landgraf)

1. Overview

Colorectal cancer is the second leading cause of cancer death and remains difficult to diagnose without invasive or universally available procedures such as colonoscopy (430). Several recent studies in animal models and human patient populations have begun to identify biomarkers that have some diagnostic capability (407, 431-439). Additionally, association studies have shown positive and negative correlations with various bacterial species (440, 441). It is also known in animal models that commensal bacteria in the gastrointestinal (GI) tract have a quantifiable impact on disease phenotype (124, 442, 443). The link between diagnostic biomarkers and the gut microbiota has not been sufficiently investigated and the mechanisms driving phenotypic differences are not well determined. They likely owe, at least in part, to bacterially derived metabolites and corresponding host responses to these metabolites (52, 96, 444-453).

Untargeted metabolomics is a maturing field focused on the large-scale quantitative and qualitative analyses of small molecular weight (<2000) biomolecules. Information from these studies provide unique insight into physiological pathways that have important roles in health and disease (418). Given that microbial species play a critical role in both production and use of host metabolites (140, 454), it is likely that the gut microbiota (GM) has a substantial impact on the overall metabolite composition. Confirming this hypothesis, studies have demonstrated significant differences in metabolites between germ-free mice and their conventionally housed counterparts, emphasizing a microbiota-driven metabolic profile (455). As a result, the role of metabolic mediators as intermediates between the GM and tumorigenesis in both rodent

models and humans has garnered substantial interest. Dazard *et al.* used mass spectrometry to determine that plasma from *Apc^{Min}* mice had a distinct metabolome compared to wildtype (WT) littermates (456). Similarly, gas chromatography-mass spectrometry (GC-MS) was used to identify metabolites within adenomas and adjacent normal tissue that were modulated in *Apc^{Min}* mice (457). Notably, these studies demonstrated that changes can be detected in the metabolome using a rodent model of CRC. However, due to a lack of longitudinal metabolomics data in this model, it is unclear whether these metabolic changes are a consequence of tumor development or are causative of tumor initiation or progression.

We previously showed that naturally occurring GM can modulate colon cancer susceptibility in a preclinical rat model of Familial Adenomatous Polyposis. We rederived isogenic embryos of the F344/NTac-*Apc^{+Pirc}* rat model into different surrogate dams each harboring distinct gut microbiota: GM:F344 and GM:LEW. Through this method we created animals that harbored distinct endogenous complex GMs. *Pirc* rats with the GM:F344 had a higher tumor burden, while GM:LEW rats had a significantly reduced tumor burden, including two animals that had no visible colonic adenomas at 6 months of age (131). The GM and metabolome separately have been shown to affect colon cancer tumorigenesis, however, there are insufficient data demonstrating how the host gene expression is affected. We used a multi-omics approach to evaluate how differences in the microbiome affect the fecal metabolome and host gene expression to understand the mechanisms by which the GM modulates disease susceptibility.

2. Methods

2.1. Animal husbandry and housing

Pirc rats were generated by crossing male, F344/Ntac-*Apc*^{+/*am1137*} Pirc rats with wildtype female rats obtained commercially from Envigo Laboratories (Indianapolis, IN), i.e. F344/NHsd. All animals were group housed, prior to time of breeding on ventilated racks (Thoren, Hazleton, PA) in micro-isolator cages. Cages were furnished with corn cob bedding and were fed irradiated 5058 PicoLab Mouse Diet 20 (LabDiet, St. Louis, MO). Rats had *ad libitum* access to water purified by sulfuric acid (pH 2.5-2.8) treatment followed by autoclaving. Prior to breeding, fecal samples were collected from both the breeders using aseptic methods and banked at -80 °C.

All procedures were performed according to the guidelines regulated by the Guide for the Use and Care of Laboratory Animals, the Public Health Service Policy on Humane Care and Use of Laboratory Animals, the Guidelines for the Welfare of Animals in Experimental Neoplasia, and were approved by the University of Missouri Institutional Animal Care and Use Committee.

2.2. Experimental design

We used previously collected fecal and tissue (normal epithelium or tumor) samples from F344-*Apc*^{+/*am1137*} Pirc rats generated through complex microbiota targeted rederivation (CMTR) as described by Ericsson *et al.* (131). These previously banked samples were used in this study to assess how the GM affects the metabolome and transcriptome (Fig.1). Briefly, fecal samples collected from animals aseptically at 1 month of age and prior to onset of observable colonic tumor phenotype for metabolomics were collected into and immediately snap-frozen with liquid nitrogen and stored at -80 °C

until processing for metabolomics. At 6 months of age, animals were sacrificed post-disease onset, confirmed through colonoscopies as described previously (127). Tumor (T) and adjacent normal epithelium (NE) tissues were collected into cryovials aseptically, flash-frozen and stored at -80 °C.

2.3. Genotyping and animal identification

Pups were ear-punched prior to weaning at 18 days of age using sterile technique. DNA was extracted using the “HotSHOT” genomic DNA preparation method previously outlined (166). Briefly, ear punches were collected into an alkaline lysis reagent (25 mM NaOH and 0.2 mM EDTA at a pH 12). The ear clips were heated at 90 °C on a heat block for 30 minutes, followed by addition of the neutralization buffer (40 mM Tris-HCl, pH 8) and vortexing for 5 seconds. Obtained DNA was used for a high resolution melt (HRM) analysis as described previously (4).

2.4. Serum sample collection

For serum collection, Pirc and WT rats were anaesthetized with isoflurane at 1 month of age. 0.5 mL of blood was drawn aseptically via the jugular vein and the serum was collected by precipitating the cells at 10,000 x g for 10 minutes. The collected serum was centrifuged again at 16,000 x g for 5 minutes to remove any lysed debris or cells, and then stored at -80 °C in glass vials until further processing.

2.5. Ultra-high performance liquid chromatography and mass spectrometry (UHPLC-MS)

Fecal samples were lyophilized at -20 °C using 0.1 millibar of vacuum pressure, following which dried samples (30 mg) were extracted sequentially for both UHPLC-MS and GC-MS. The dried samples were first treated with 1.0 mL of 80% MeOH containing

18 µg/mL umbelliferone, sonicated for 5 minutes and centrifuged for 40 minutes at 3000 x g at 10 °C. 0.5 mL of supernatant was used for UHPLC-MS analysis after a subsequent spin at 5000 x g at 10 °C for 20 minutes and transferring 250 µL of the sample into glass autosampler vials with inserts. For GC-MS analyses of primary polar metabolites, 0.5 mL water was added the remaining extract used above for the UHPLC preparation, sonicated for 5 min, extracted for 30 min, and centrifuged at 3000 g. 0.5 mL of the polar extract was subsequently dried under nitrogen and derivatized using previously established protocols (458). Briefly, N-Methyl-N-(trimethylsilyl) trifluoroacetamide (MSTFA) with 1 % TMCS (2, 2, 2-Trifluoro-N-methyl-N-(trimethylsilyl)-acetamide, Chlorotrimethylsilane) was used to derivatize the polar metabolites, after treatment with methoxyamine-HCl-pyridine. UHPLC-MS analyses were performed on a Bruker maXis Impact quadrupole-time-of-flight mass spectrometer coupled to a Waters ACQUITY UPLC system. Separation was achieved on a Waters C18 column (2.1x 150 mm, BEH C18 column with 1.7-µm particles) using a linear gradient composed of mobile phase A (0.1% formic acid) and B (B: acetonitrile). Gradient conditions: B increased from 5% to 70% over 30 min, then to 95% over 3 min, held at 95% for 3 min, then returned to 5% for re-equilibrium. The flow rate was 0.56 mL/min and the column temperature was 60 °C.

Mass spectrometry was performed in the negative electrospray ionization mode with the nebulization gas pressure at 43.5 psi, dry gas of 12 l/min, dry temperature of 250 °C and a capillary voltage of 4000 V. Mass spectral data were collected from 100 and 1500 m/z and were auto-calibrated using sodium formate after data acquisition.

Metabolites that were significantly different between each group and that contributed to the dendrogram separating low and high tumor animals were selected for

targeted tandem MS (MS/MS) analysis. MS/MS spectral data were collected using the following parameters: MS full scan: 100 to 1500 m/z; 10 counts; active exclusion: 3 spectra, released after 0.15 min; collision energy: dependent on mass, 35 eV at 500 Da, 50 eV at 1000 Da and 70 eV at 2000 Da. Mass spectra were calibrated using sodium formate that was included as a calibration segment towards the end of the gradient separation.

2.6. Metabolomics Data Processing

For UHPLC-MS data, the mass spectral data were first calibrated using sodium formate and converted into netCDF file format for processing using XCMS (ref: <https://www.ncbi.nlm.nih.gov/pubmed/16448051>) that included peak detection, deconvolution, alignment and integration. The signal intensities were then normalized to that of the internal standard umbelliferone (abundance of metabolite/abundance of umbelliferone \times 100%) and used for statistical analysis. MS/MS spectra were searched against our custom spectral library (459) and the Bruker libraries (<https://www.bruker.com/products/mass-spectrometry-and-separations/metabobase-plant-libraries/>), MassBank of North America (MoNA, <http://mona.fiehnlab.ucdavis.edu/>), mzCloud (<https://www.mzcloud.org/>) for confident or putative identifications. Multivariate statistical analysis such as principal component analyses (PCA) and ANOVA was performed using MetaboAnalyst (<http://www.metaboanalyst.ca/>) after pre-treatments of the data, i.e. normalization to sum, log transformation, and auto scaling.

2.7. Fecal DNA extraction, 16S library preparation and sequencing

Fecal samples were pared down to 70 mg using a sterile blade and then extracted using methods described previously (5). Amplification of the V4 hypervariable region of

the 16S rDNA and sequencing was performed at the University of Missouri DNA core facility (Columbia, MO) as previously described (5).

2.8. Normal epithelium and tumor tissue collection

All animals were humanely euthanized with CO₂ (carbon di-oxide) administration and necropsied at sacrifice as described previously (131). The small intestine and colon from the rats were placed on to bibulous paper and then splayed opened longitudinally by cutting through the section. Using a sterile scalpel blade (Feather, Tokyo, Japan) normal colonic epithelium tissues were scraped from the top, middle and distal regions of the colon. Tumors in the same locations were collected by resecting half of the total tissue. All tissues were flash-frozen in liquid nitrogen and stored at -80 °C. Remaining intestinal tissues were then fixed overnight in 10% formalin, which was then replaced with 70% ethanol for long term storage until adenoma counting was performed.

2.9. Tumor counts and measurements

Tumor counts were determined as previously described using a M165FC (Leica, Buffalo Grove, IL) microscope at 0.73X magnification (131, 128). Briefly, the small intestine and colonic tissues were laid flat in a large petri dish (Sycamore Life Sciences, Houston, TX) and covered with 70% ethanol (ThermoFisher Scientific, Waltham, MA) to prevent tissue drying. Biologic forceps (Roboz Surgical Instruments Co., Inc., Gaithersburg, MD) were used to gently count polyps observable under the objective. Tissues were kept hydrated throughout the entire process. Tumor sizes were measured using the Leica Application Suite 4.2, after capturing post-fixed images as previously described (4).

2.10. RNASeq and bioinformatics analysis

Normal epithelium and tumor tissue samples were collected upon necropsy at 180 days of age and were extracted using the Qiagen AllPrep DNA/RNA mini kit (Qiagen, Germantown, MD) after pre-processing using the QIAshredder (Qiagen) columns to extract total RNA (461). The quality of RNA was then assessed using the Experion RNA StdSens analysis kit (Bio-Rad, Hercules, CA). Based on the RNA-quality index (RQI), 18S and 28S peaks in the chromatogram, samples were classified into high (>9), medium (7> or <9) or poor quality (>6). Except for one sample (normal epithelium from rat 044, i.e. 044_N), all other samples were of medium or higher RQI. Total RNA was used for poly-A selection and Illumina TruSeq paired-end library preparation following manufacturer's protocols. 75 bp (base pair) paired-end reads were sequenced on the Illumina MiSeq (462) platform to an average of depth of 50×10^6 reads per sample. All samples were processed at the same time and sequenced on a single lane, to avoid batch effects.

Sequence read alignment was done using TopHat from the Tuxedo protocol as outlined in the original publication (463). To remove adaptors and low-quality reads, Trimmomatic v.0.32 was used with standard settings (464), and then aligned to the Rat genome (Rnor_6.0) (download from: ftp://igenome:G3nom3s4u@ussd-ftp.illumina.com/Rattus_norvegicus/NCBI/RGSC_v3.4/Rattus_norvegicus_NCBI_RGSC_v3.4.tar.gz on May 24th, 2017) using TopHat2 v2.0.12 with default settings. The aligned reads were sorted with SAMtools v1.3, followed by HTseq v0.9.1. Differential gene expression was then estimated using the DESeq2 v1.18.1 in R v3.4 (465). Read count distributions in the normal epithelium and tumor tissues were found to be bimodal, with genes being identified as significant based on an FDR-adjusted *P*-value of < 0.05

and with a fold-change of at least 1.5-fold. Pathway analyses were performed on the top 100 significantly up-regulated genes in either GMs, i.e. GM:F344 or GM:LEW. Pathway over-representation analyses were based on hypergeometric distribution to determine the statistical significance of a particular gene to an over-represented pathway. Topology analysis was also performed using the degree centrality method and the gene-centric Integrated Pathways module of Metaboanalyst v3.0 (466). Enriched pathways based on this analysis were selected using a FDR-adjusted P -value of < 0.05 . A similar analysis was performed for both the NE (normal epithelium) and T (tumor) samples.

2.11. Metabolomics analyses

Mass spectral data from each sample were converted into netCDF formatted files and processed with XCMS to generate lists of mass features and their intensities (467). An average of 499 peaks were found per sample. Peaks appearing in less than a quarter of the samples in each group were ignored. 175 variables were removed for threshold 25 percent, i.e. appearance of peaks in greater than 25% of the samples per group. Variables with missing values were replaced with a small value (0.0000001) for statistical analysis purposes. The data were then normalized to sum, transformed using Log normalization and auto-scaled to ensure maximum-possible binomial distribution. The number of samples, raw peak numbers observed and the final peak list used for each sample processed are described in Table 1.

Statistical analyses were performed based on a threshold of 2, for the fold-change analysis, with values displayed in the log-scale to observe both the up-regulated and downregulated features in a symmetrical way. Principal component analysis (PCA) was performed using the *prcomp* package in R using the *chemometrics.R* script (468). NMDS

(non-metric dimensional scaling) is another method for ordination and was performed using the *vegan* package in R (469). Hierarchical clustering analysis was performed using the Euclidean distance measure using the *Ward* algorithm (to minimize the sum of squares of any two clusters, potentially separating only if large differences exist between groups) and displayed as a dendrogram using the *hclust* function in the *stat* package in R. To determine the metabolites contributing to the separation and rooting of the hierarchical clusters, the samples irrespective of GM were re-classified into those with 'high' or 'low' tumors and a linear discriminant analysis (LDA) was performed using the LefSe module on a high-computing Linux platform (265) with a LDA score of $\log_{10}2$ or greater being significantly differential metabolites between the high and low tumor groups.

2.12. Statistical analyses and figures

All other statistical analyses were performed using Sigmaplot 13.0 (Systat Software, San Jose, CA) and graphing for figures (except Fig.1) was prepared through GraphPad Prism version 7 for Windows (GraphPad Software, La Jolla, CA). *P*-values were set to identify significance at a value less than 0.05, unless otherwise described or indicated. Correlations were performed using the linear regression module available through GraphPad Prism v7.

3. Results

3.1. Metabolite features at 1 month of age predict tumor susceptibility and severity at later developmental stages

Fecal samples collected from rederived Pirr rats harboring distinct GMs were analyzed by UHPLC-MS (Fig.1). An average of 499 peaks were found per sample through this method (Supplementary Table 1). Principal component ordination analysis (PCA) indicated a separation of 33.2% along the first component (PC1) accounting for some variability within each group (Fig. 2A). Non-metric dimensional scaling also showed a similar separation (Fig. 2B) between samples, suggesting that the features identified via UHPLC-MS differentiated the high- (GM:F344) and low-susceptibility (GM:LEW) gut microbiota profiles, with GM:SD occupying the intermediate ordines. Hierarchical clustering was performed using Euclidean distance and Ward's clustering algorithm on the metabolomics dataset to identify the dissimilarity of the samples and groups with respect to each other. The dendrogram demonstrates the separation of the fecal samples, based on colonic tumor burden assessed at terminal 6 months of age (Fig. 2C). Observing that GM:F344 and GM:LEW had the highest and least number of tumors respectively, we further analyzed the differential features contributing to disease susceptibility within these groups (Fig.2D and 3A).

3.2. Metabolomics analyses indicate differential metabolic profiles between GM:F344 and GM:LEW

Using linear discriminant analyses (LDA) we identified the putative metabolites contributing to the high (GM:F344) and low (GM:LEW) tumor groups' separation observed in the dendrogram (Fig.2C and 3B). Some of the putative metabolites identified

in the low tumor group, i.e. GM:LEW, showed up to a 4-fold increase compared to GM:F344, the high tumor group (Fig. 3C). Tandem MS analysis was used to further identify and confirm the nature of the compounds that were differential between the low and high tumor groups. We generated tandem MS spectra for the compounds with the *mz/rt* values of 329.10/9.2 min and 315.12/6.39 min; however, their identities could not be definitively established based on the spectral libraries currently available. We also found significant correlations between individual metabolites at 1 month of age and the colonic tumor numbers (Fig. 3D).

3.3. Bile acid biosynthesis and aspirin-triggered resolvin E biosynthesis pathways are most affected due to putative fecal metabolomics features

Putative identifications for the differential metabolite features listed are based on the METLIN metabolite library available for public access (Table 1). Based on RMD values, four putative metabolites were classified as steroids while the others were classified as polyphenols, carbohydrates, short-chain fatty acids and flavonoids. All putative features identified using UHPLC-MS were subjected to pathway analysis to identify KEGG pathways that were significantly modulated between the two GM profiles. Bile acid biosynthesis (neutral pathway) and aspirin-triggered resolvin E biosynthesis were affected considerably (Fig.4). The pathway analyses also identified potential genes that may affect or be affected by these putative metabolites (Table 2). The putative identities for the metabolites affecting the bile acid and resolvin E biosynthesis pathways include secondary bile acids such as glycocholate, glycochenodeoxycholate and 7 α -hydroxycholest-4-en-3-one (Table 3). We sampled Pirc and WT (wildtype) rats at 1 month of age to validate the bile acid and resolvin E biosynthesis pathways as being risk

factors for eventual development of adenomas, and to determine if these can be observed in serum. We found that the Pirc animals had elevated serum levels of metabolites related to the bile acid pathway (Supplementary Figure 1A).

3.4. Gut microbiota alters gene expression in both the normal epithelium and tumor tissues

RNASeq was performed on NE and T tissues after sacrifice at 6 months of age to determine how the GM may modulate gene expression in isogenic animals. We found that 2173 genes were differentially regulated between GM:F344 and GM:LEW in the normal epithelium tissues (Supplementary Figure 2A). Additionally, 3406 genes were differentially expressed between adenomas from the two GM profiles (Supplementary Figure 2B). Clustering analysis (Fig. 5A) showed that the normal epithelium samples separated from the tumor samples, additionally separating based on GM profile, i.e. GM:F344 and GM:LEW.

3.5. Pathway analyses identify potential mechanisms contributing to high and low colonic tumor susceptibility

Pathway analysis using differentially expressed genes found an enrichment in the fatty acid and the mucin type-*O* glycan biosynthesis pathways, with an increased pathway topology in the high tumor, GM:F344 group (Supplementary Figure 2C). Increased cell cycle, RNA transport, and TCA cycle pathways were also observed in GM:F344. On the other hand, normal epithelium of the Pirc rats with the GM:LEW (low tumor) profile showed an increase in apoptotic pathways along with fat digestion and absorption, and calcium signaling pathways (Supplementary Figure 2D).

We determined the expression differences of the genes contributing to the predicted putative metabolic pathways, i.e. bile acid biosynthesis and aspirin-triggered resolvin E biosynthesis (Fig.4, Table 2 and Supplementary Figure 4). We examined the gene expression involved in the resolvin E biosynthesis pathway and found that *PTGS2* was significantly increased in the normal epithelium tissues of the high tumor group (GM:F344) compared to the GM:LEW group (Fig. 5B). Interestingly, *PTGS2* was highly elevated in tumor tissues of the low tumor (GM:LEW) group at 6 months of age. We also found that *ALOX5* was significantly elevated in the GM:F344 rats with a substantial increase up to 2.5-fold in the GM:F344 tumors compared to the other group (Fig. 5B). Assessing the bile acid biosynthesis genes, we found that *CYP8B1* and *BAAT* were also increased in the tumor tissues of the low tumor (GM:LEW) group compared to Pirc rats in the GM:F344 group (Fig. 5C).

We used the differential putative metabolites and differentially expressed genes in the NE to perform an Integrated Pathway (IP) analysis, taking into account metabolite, host epithelium expression, and microbiota differences. The synergistic IP analysis suggested that colonic tumor susceptibility is associated with primary bile acid biosynthesis, fatty acid elongation and metabolism pathways. We observed increased pathway topology of unsaturated fatty acid biosynthesis corroborating the role of fatty acids in colonic tumor burden (Fig. 6A). To improve the power of our analytical capacity we used canonical correlation analyses to determine the interplay between the OTUs, putative metabolites and the genes identified as differential in the NE. We found that OTUs such as *Prevotella spp*, *Desulfovibrio spp*, *Veillonella parvula* and *Parabacteroides gordonii* are associated with the GM:LEW group in the ordination plot.

Similarly, unannotated genes such as *RGD1304579*, *LOC100363038*, along with *CRABP2*, *JUNB* and *CNDP2* separate along the axes, based on their relationship with either GM:F344 or GM:LEW. While a putative metabolite identified as vigabatrin correlated with GM:LEW, the other metabolites detected clustered with GM:F344 in the analysis (Fig. 6B).

4. Discussion

Colon cancer etiology has been addressed for decades from the perspective of host gene expression and its effect on disease susceptibility. Studies have also addressed the metabolome associated with tumorigenesis separately or in conjunction with the microbiome or the transcriptome. However, these studies have mostly been retrospective, i.e. after disease onset in patients, raising the question of whether the microbiome, metabolome and transcriptome are merely responding to the disease, or causative of tumor development. Here, we present for the first time the integration of three ‘omics’ strategies to understand tumor susceptibility in the Pirc rat model of human colon cancer. Addressing this gap in knowledge we used RNASeq (transcriptome) analyses to determine gene expression in the tumor and adjacent normal colonic epithelium tissues from genetically identical animals harboring two distinct microbiota populations. Multi-omics investigations included Integrated Pathway analysis combining the metabolomics and transcriptomics data, identifying potential biomarkers for disease identification from fecal samples as early as 1 month of age.

Previously, we reported that differential commensal GM altered the susceptibility of isogenic Pirc rats, rederived onto different surrogate dams (131). We now report that

the altered GM profile correlates with differential metabolite features representative of GM:F344 and GM:LEW. Some of the top 10 putative metabolites have identities in the METLIN database, enabling future testing of these compounds and their influence on tumorigenesis. We calculated the relative mass defect (RMD) and found that the putative metabolites belong to one of the following classifications: polyphenol, carbohydrate, flavonoid, steroid and short-chain fatty acids. Two compounds were also putatively identified to be succinic acid and cervonyl carnitine, variations of compounds established by Deng *et al.* as potential biomarkers of colonic adenomatous polyps (470). We surprisingly found that Pirc rats with fewer adenomas (<9, average) differentially clustered from animals with more than 19 adenomas. The metabolite data were prognostic at 1 month of age, substantially prior to the onset of visible adenomas and physiological signs of disease in Pirc rats. Due to the inadequacy of compound libraries in their current state, we could not establish accurate identities of the compounds using tandem MS spectra. Further investigation including advanced methods such as UHPLC-MS-SPE-NMR (nuclear magnetic resonance) could elucidate the identity of these metabolites (471, 472). This information will be used going forward as training datasets for neural network or machine learning algorithms with the objective of establishing a pre-tumorigenesis dataset to identify at-risk populations based on metabolite features (473, 474).

Increased bile acid exposure in the gastrointestinal tract is a known factor for GI cancers and was proposed as a pro-carcinogenic phenomenon as early as 1939 (475-477). Secondary bile acids such as lithocholic acid and deoxycholic acid have been shown to be significantly increased in serum from patients with colonic adenomas (478, 479).

Secondary bile acids could act as tumor promoters by causing the release of arachidonic acid, which in turn induces prostaglandin and reactive oxygen species-mediated DNA damage and inhibition of repair mechanisms (480, 481). In accordance to these reports, we found that the bile acid biosynthesis pathway was elevated in the high tumor group. The resolvin E biosynthesis pathway was also upregulated in the GM:F344 group and leads to production of resolvins, which are known to induce resolution, anti-inflammatory, and anti-carcinogenic pathways (482, 483). However, the dose of resolvins is an essential factor in the mechanism of action. Reports indicate that that low-dose aspirins or resolvins can have beneficial effects (484), whereas an increased dose could lead to a risk of upper GI bleeding (485, 486). This warrants future investigations, in a controlled manner, targeting the metabolites contributing to this pathway in the context of a high disease susceptibility GM. It is noteworthy that the large clinical aspirin trials have not looked at differences in the microbiome as a controllable or confounding factor (487, 488).

Gene expression data available for the Pirc rat model have been limited to studies looking at expression in the role of cytotoxic insult or the expression profile of canonical cancer-related genes in the normal mucosa (489-491). We demonstrated here for the first time that congenic Pirc rats show differential gene expression depending on the GM they harbor. We found that *PTGS2* was significantly elevated in the normal epithelium in the GM:F344 group suggesting that the gut microbiota likely has a role in the differential expression of this gene. *PTGS2* is an integral gene in the cyclooxygenase-2 (*COX2*) mechanism and has been associated with increased colonic tumor burden in several reports (127, 353, 492, 493). Similarly, increased *ALOX5* expression is associated with

increased proliferation and invasion of colonic tumors (494-496). Interestingly, the *COX2* mechanism is suggested in our study based on metabolic pathways obtained from fecal samples collected at 1 month of age. This may need further evaluation in the future, by assessing levels of prostaglandins along with determining the expression levels of *PTGS2*.

Conversely, *BAAT* and *CYP8B1* genes associated with bile acid biosynthesis and lipid metabolism were significantly increased in tumors from GM:LEW. Several reports show that increased *CYP8B1* expression is associated with a poor disease outcome (497-500). However, it is plausible that these oxysterol metabolism genes (497), known to be involved in bile acid transport (501) may be upregulated to control accumulation of bile acids within the colon (502).

Pathway analyses are an insightful, hypothesis-generating method for identifying potential mechanisms that may be involved in the course of colon cancer development. The low adenoma susceptible microbiota in GM:LEW rats had elevated apoptotic, fat digestion pathways and calcium signaling pathways compared to GM:F344. Calcium has been shown to act as a regulator of gene transcription, cell proliferation and migration (506, 510). Several studies have shown that intracellular calcium is altered in tumors (503, 504). GM:LEW with an elevated calcium pathway is an interesting phenomenon, considering that calcium in conjunction with vitamin D has been shown to be correlated with increased adenomas (505), whereas a previous study showed that calcium supplementation with vitamin D had no effect on CRC incidence (506). Our data and other reports (507-510) support the correlation of elevated calcium signaling pathways in the low tumor group. However, this requires further validation, especially the

examination of GM profiles following vitamin D treatment in future studies to resolve the discontinuity.

Using an Integrated Pathway (IP) analysis we found primary bile acid biosynthesis and fatty acid elongation and metabolism as the principal contributors to the variability in disease susceptibility observed in GM:F344 or GM:LEW based on the differential genes in the NE. We found that whether at 1 month or 6 months of age, the predicted metabolic profiles based on 16S rDNA sequencing using PICRUSt were not significantly different between GM:F344 and GM:LEW. This suggests that the IP-derived pathways are the effect of the putatively identified metabolite features and the transcriptome expression between these groups. We simultaneously used sparse canonical correlation analysis to integrate the microbiome, metabolome and the transcriptome to identify potential features associated with disease phenotype and susceptibility. Considering the lack of correlation between metabolomics and transcriptome pathways, this approach was crucial to increase our confidence of prognostic feature detection as the metabolite identifications have not yet been proved through more advanced methods such as NMR. Based on this approach we found that the relative abundance of OTUs (*Prevotella*, *Desulfovibrio*, and *Parabacteroides spp*) (161, 215, 451, 511, 512), previously reported to be associated with reduced colon cancer (131), associated with the low tumor susceptibility (GM:LEW) group.

We found that the microbiome, metabolome and transcriptome play a large role in the etiology of colon cancer, with the GM influencing the other two components enormously. Assimilating these omics strategies has led to the discovery of several targets in all three systems that in the future could be used for screening, and potentially

therapeutics interventions. Our data and approach could enhance precision medicine both in a diagnostic and prognostic manner in the future. More importantly, we demonstrated that the complex GM is an important factor that needs to be defined or controlled for in all studies examining drug or therapeutic interventions because of the altered metabolic profile and the host response.

5. Ethics Statement

Protocols (#6732 and #8732) and the experimental study was approved by the IACUC (Institutional Animal Care and Use Committee) of the University of Missouri. The study outlined here was conducted in accordance with the guidelines established by the Guide for the Use and Care of Laboratory Animals and the Public Health Service Policy on Human Care and Use of Laboratory Animals.

6. Author Contributions and Acknowledgements

SB and JAL designed the experiments. SB performed the extractions and the data analysis. ZL and LWS were instrumental in the metabolomics data generation. The authors wish to acknowledge Miriam Hankins, Marina McCoy, Rebecca Schehr, Aaron Ericsson and Elizabeth Bryda for assistance with fecal collection; Nathan Bivens and the MU DNA Core for assistance with 16S rDNA and RNASeq experiments; Bill Spollen and the MU Informatics Research Core Facility for assistance with software installation for data analysis; Rat Resource and Research Center; MU Office of Animal Resources and their staff for assistance with animal husbandry.

7. Figures

Figure 1. Experimental design

Pirc embryos were rederived into separate dams, F344/NHsd, SD/Crl and Lewis/SsNHsd harboring different GMs, i.e. GM:F344, GM:SD and GM:LEW. Fecal samples were collected at 1 month of age from all animals (n = 4-5/group). At 6 months of age, normal epithelium (NE) and tumor (T) tissues were collected upon necropsy. CMTR: complex microbiota targeted rederivation.

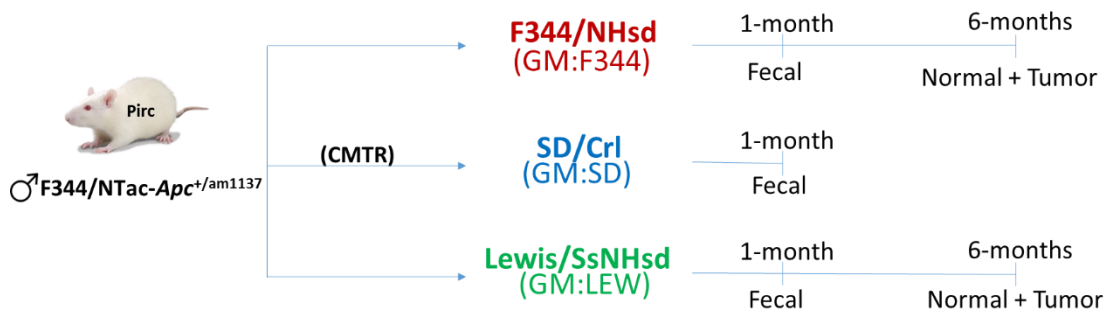
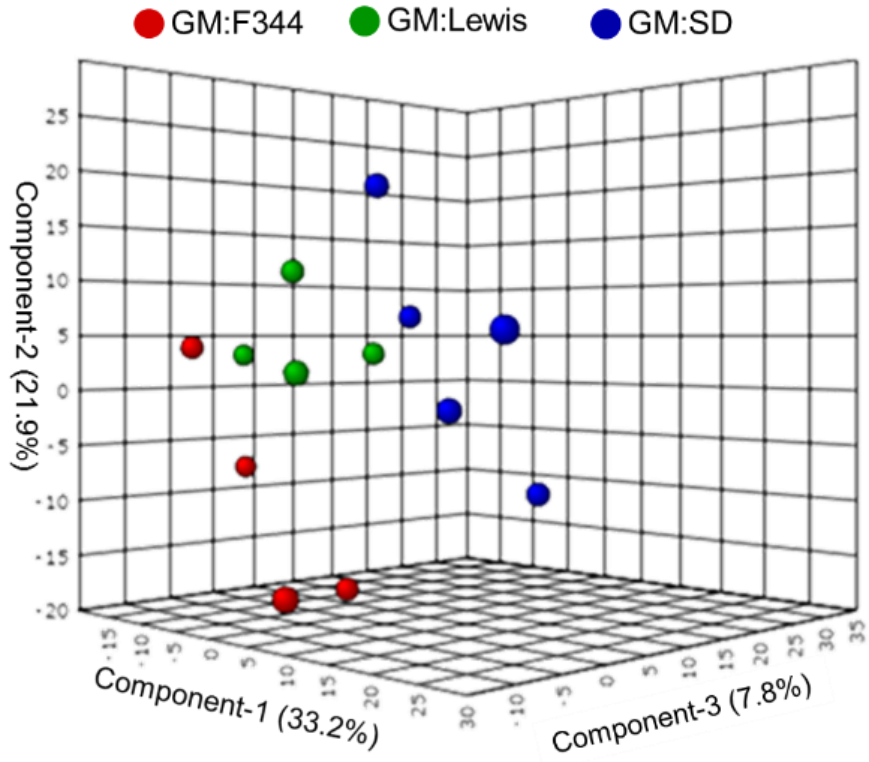


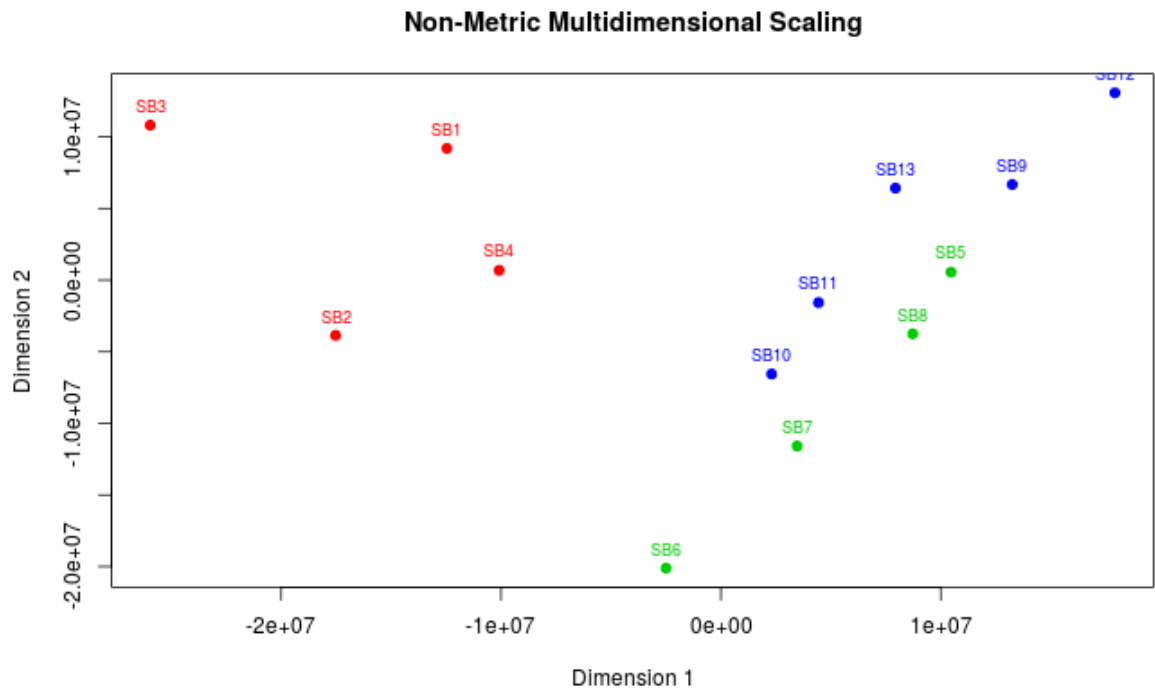
Figure 2. Metabolite features at 1 month of age predict tumor susceptibility and severity

(A) 3D scores plot from a principal component analysis (PCA) depicting the three groups, *viz.* GM:F344 (red), GM:SD (blue) and GM:LEW (green) demonstrates that the samples cluster independent of either group. (B) Non-metric multidimensional scaling (NMDS) is an unsupervised method to understand the ordination of the samples with respect to each other. Both the PCA and NMDS indicate that the groups separate from each other based on metabolite features detected via UHPLC-MS. (C) dendrogram analysis was performed on the putative metabolite features using the Euclidean distance of measurement, and the Ward's clustering algorithm. The major root of the tree separated 2 samples from the remaining 6, irrespective of either GM profile. Retrospectively, it was established that the clustering analysis was based on the colonic tumor multiplicity, indicated by the numbers adjacent to the dendrogram. The two clusters separated based on animals with an average of 9 tumors or those with greater than 19 colonic tumors on average. (D) Metabolite features that were significantly different between the high and low tumor groups were used to generate a Heatmap illustrated with the samples along the *x*-axis and the metabolite features along the *y*-axis. Hierarchical clustering was performed based on samples and indicates that the GM:F344 samples cluster separately from the GM:LEW group. The fold-change is represented by intensity with red being an increased fold-change while blue refers to a decrease.

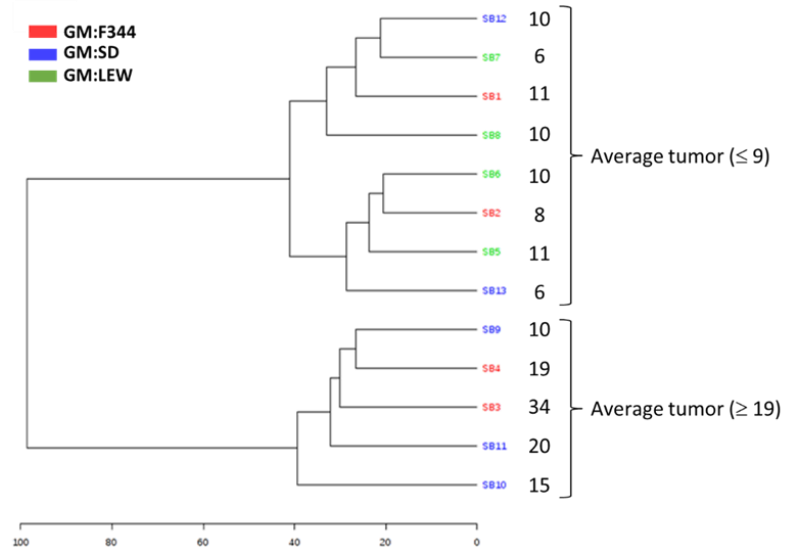
A



B



C



D

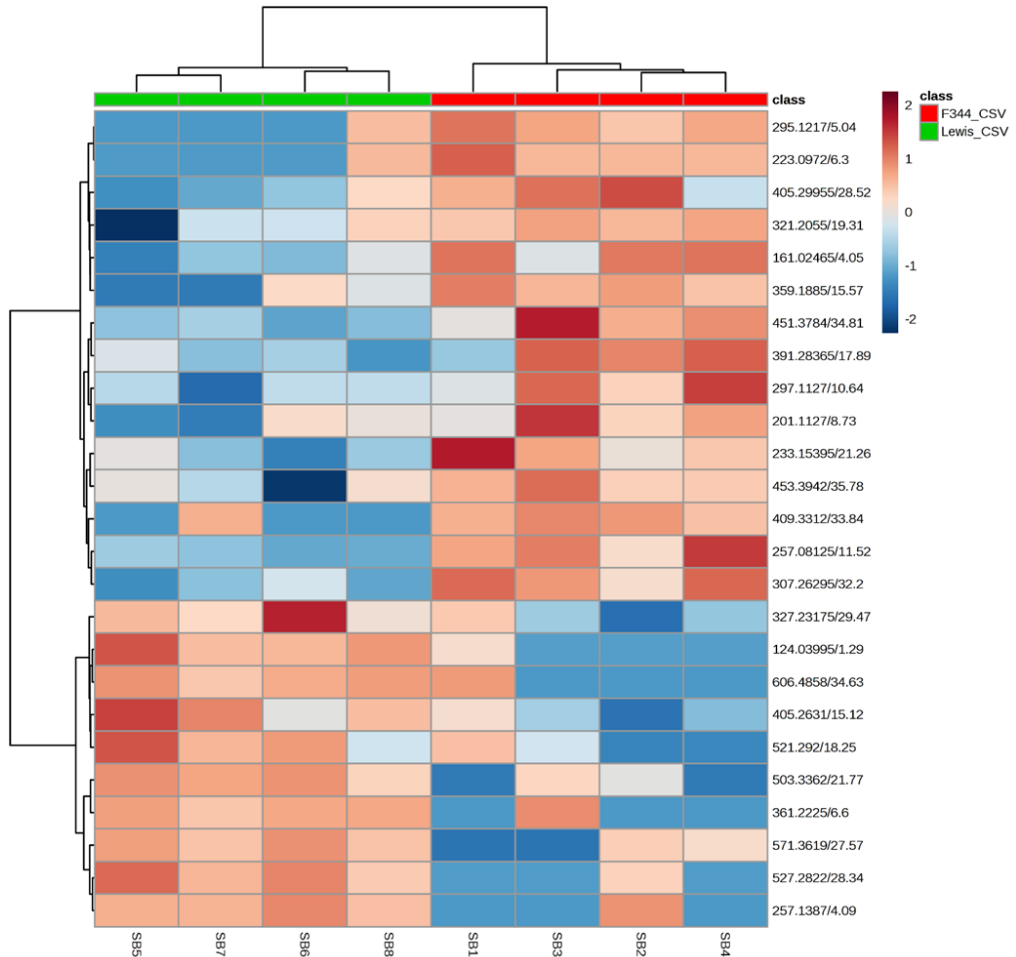
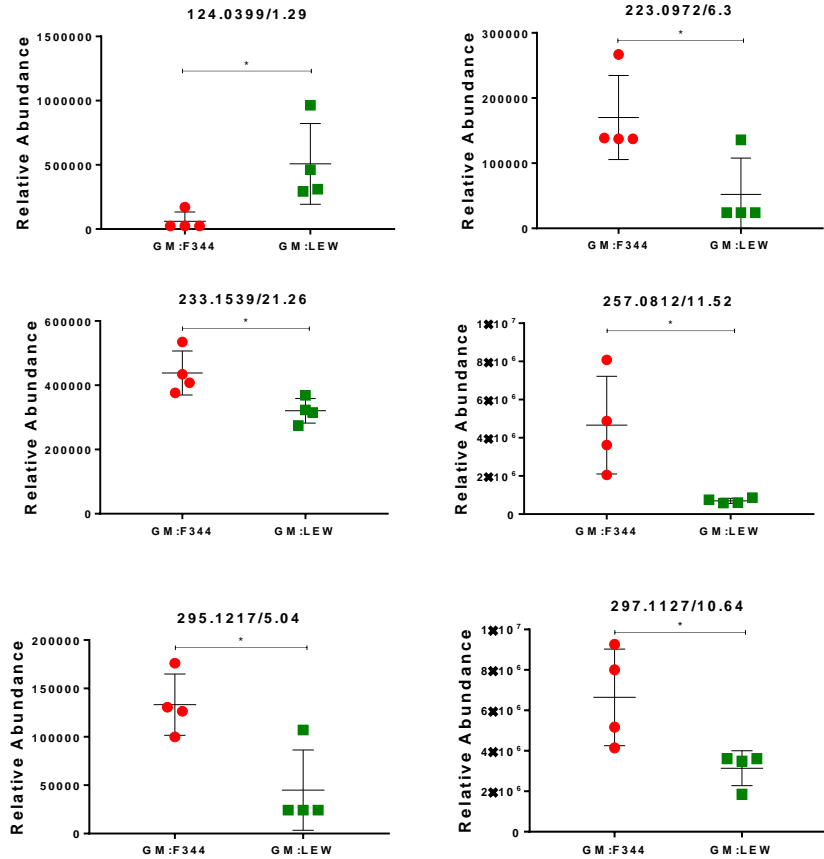
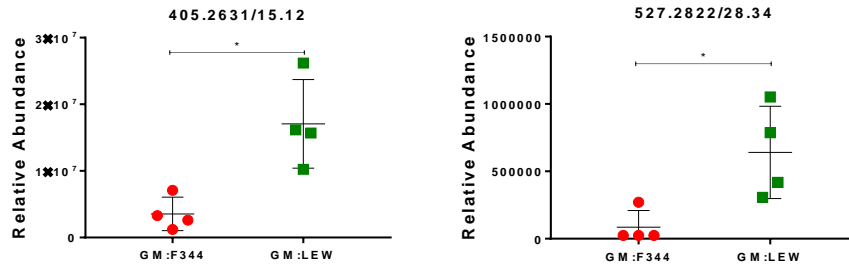


Figure 3. Metabolomics analyses indicate differential features between GM:F344 and GM:LEW

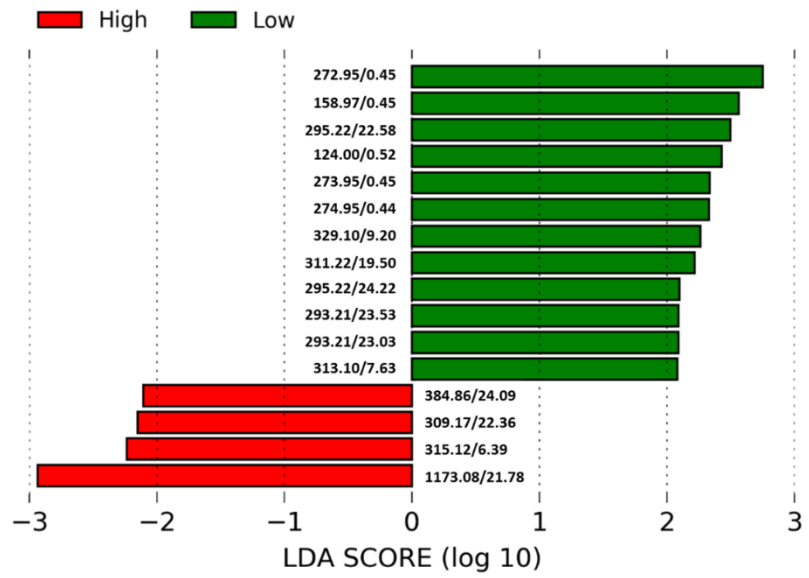
(A) The relative abundance of the top eight metabolites differentially modulated between GM:F344 (red dots) and GM:LEW (green squares) are depicted. (B) Linear Discriminant Analysis (LDA) and fold-change analysis (C) was used to identify the metabolites driving the dendrogram tree separation (A) and differential modulation in high and low tumor groups. (D) Correlation analysis was performed using Pearson’s method to determine positively and negatively correlating metabolites that are associated with increased or decreased tumor multiplicity.

A

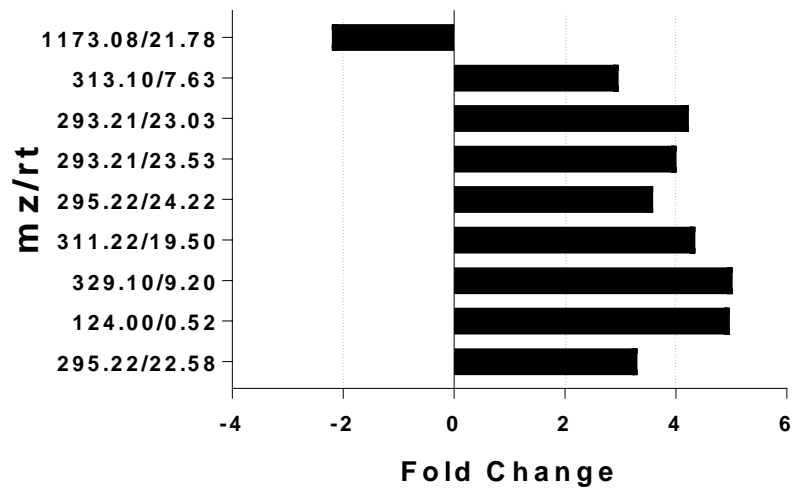




B



C



D

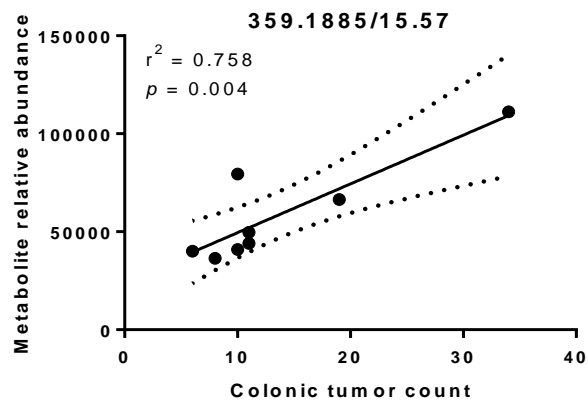
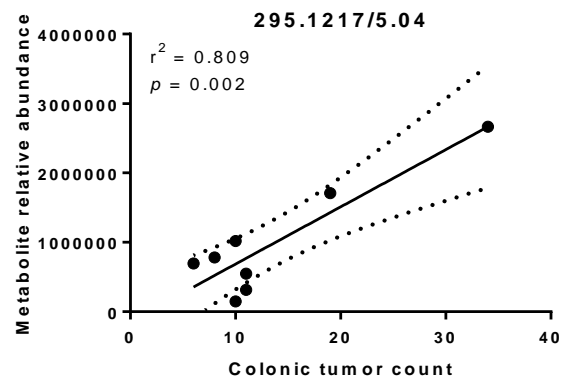
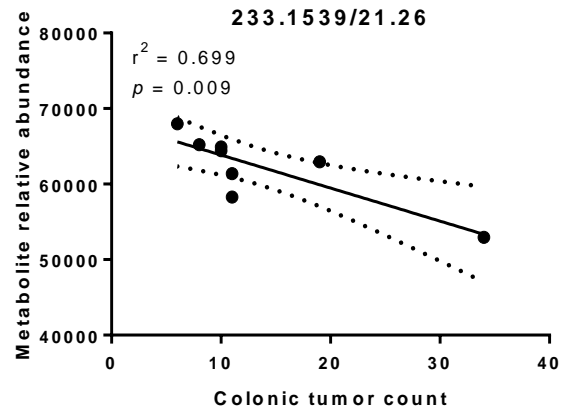


Figure 4. Bile acid biosynthesis and aspirin-triggered resolvin E biosynthesis pathways are most affected by metabolite features

Systems biology analyses, taking into account the differential putatively identified metabolites was performed using the XCMS software. The results showed that bile acid biosynthesis (neutral pathway) and the aspirin-triggered resolvin E biosynthesis were significantly different ($P < 0.01$, Student's t -test) between GM:F344 and GM:LEW. The P -value is indicated along the y-axis.

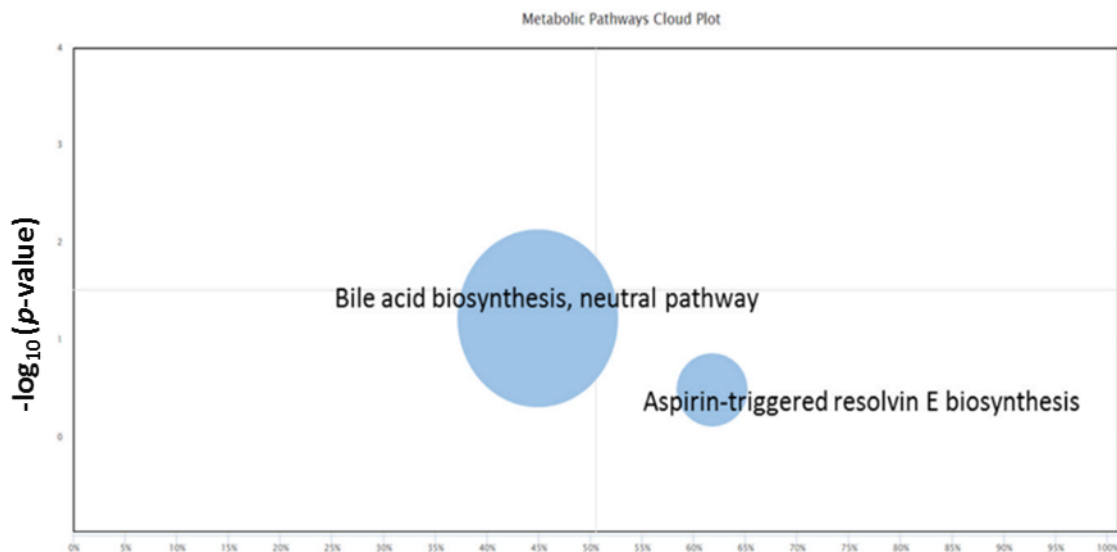
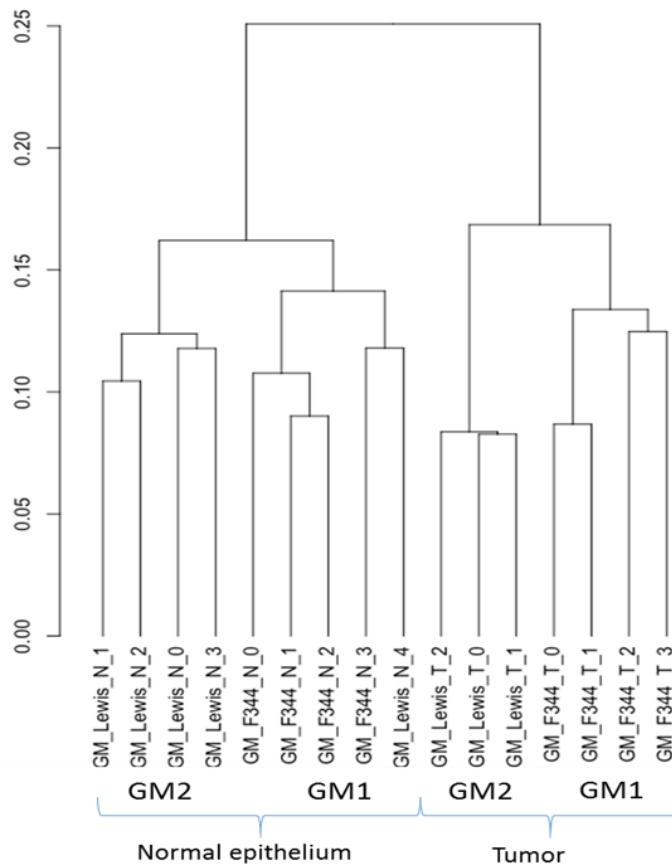


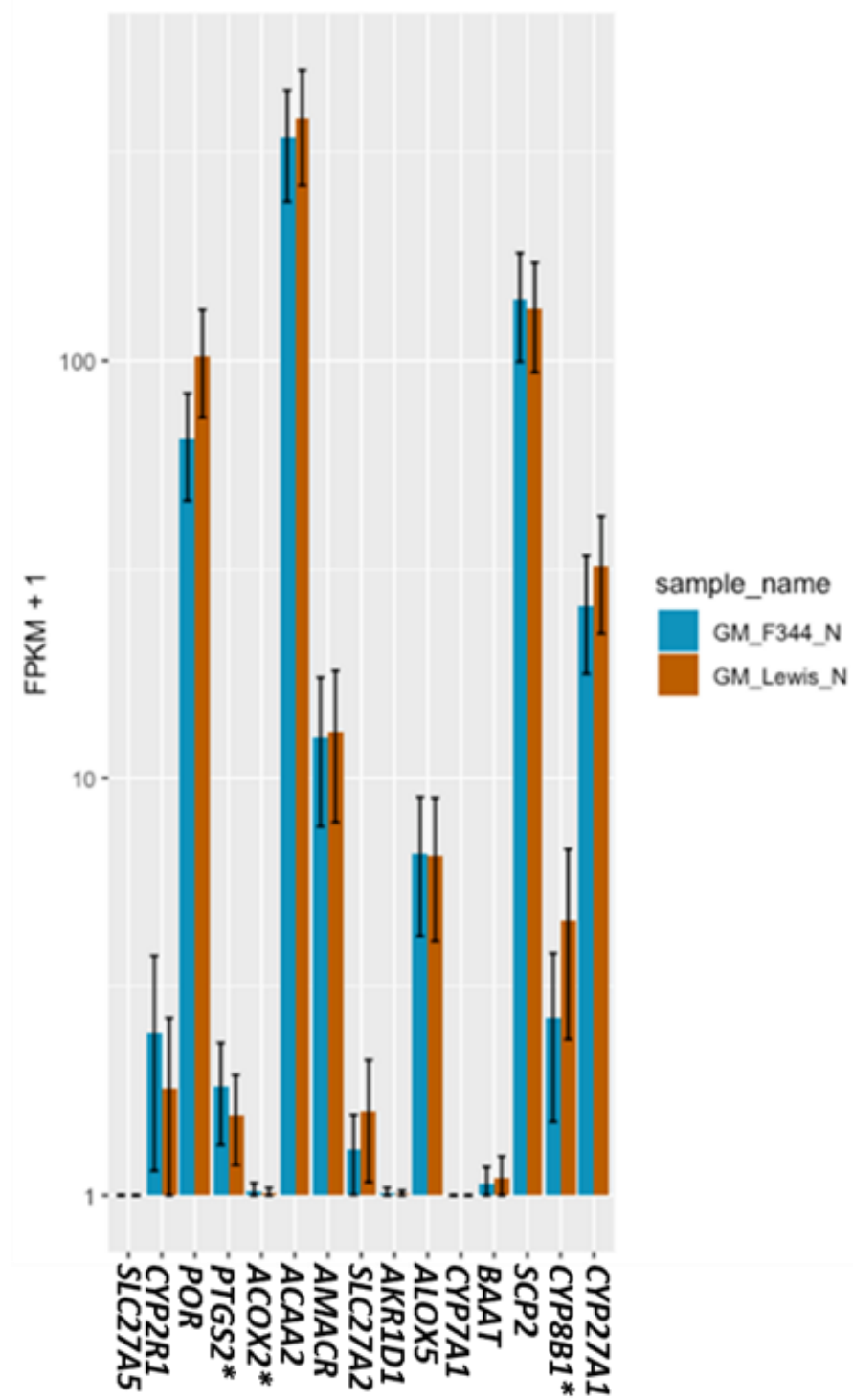
Figure 5. GM modulates differential gene expression in the normal epithelium and tumor tissues

Ordination and hierarchical clustering (A) analyses were used to determine the relationship of the samples to each other and the groups with respect to the other. The y-axis represents the distance measure for similarity between the individual samples. Bar plots (GM:F344 – blue, GM:LEW – brown with standard deviation) depicting the relative expression of the genes involved in the pathways affected by the putative metabolites were assessed in the normal epithelium (B) and tumor (C) samples. FPKM: Fragments Per Kilobase of transcript per Million mapped reads. All the analyses were performed using the cummeRbund package in R.

A



B



C

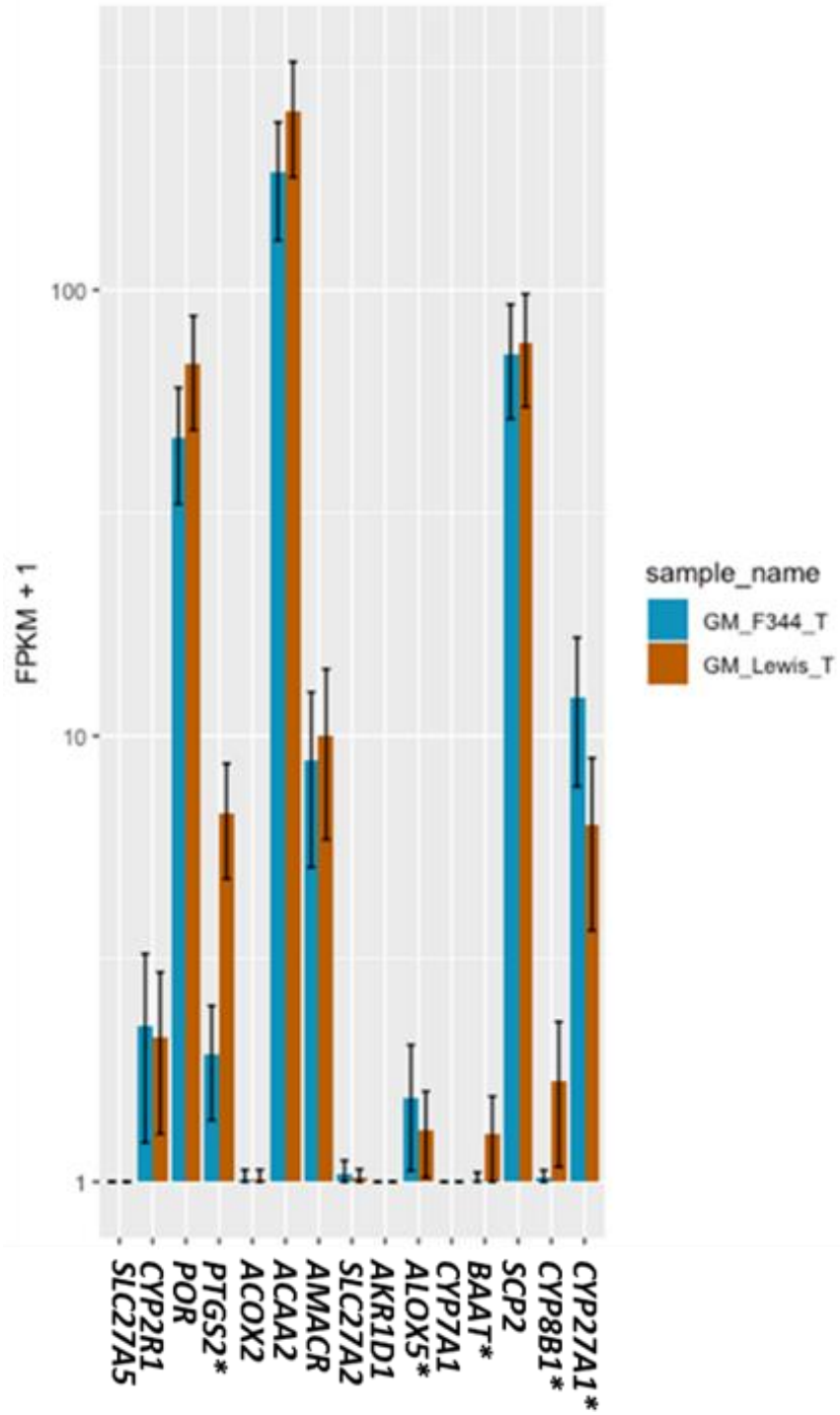
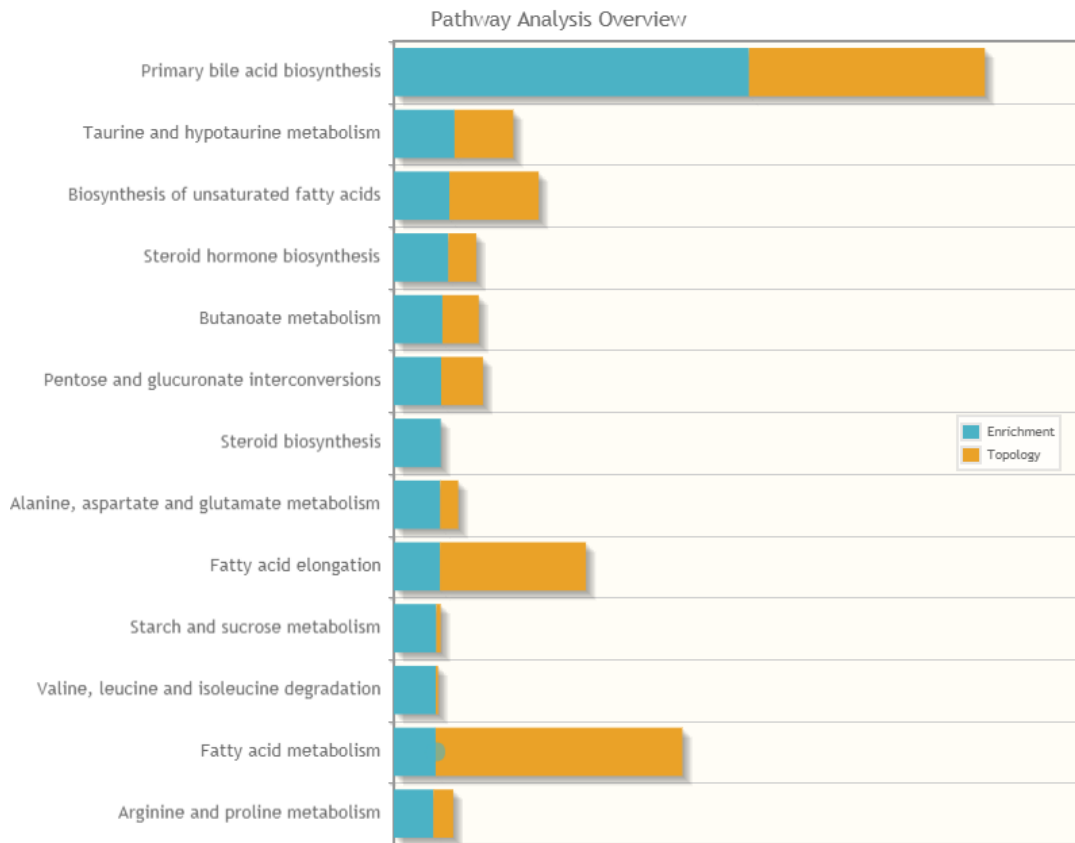


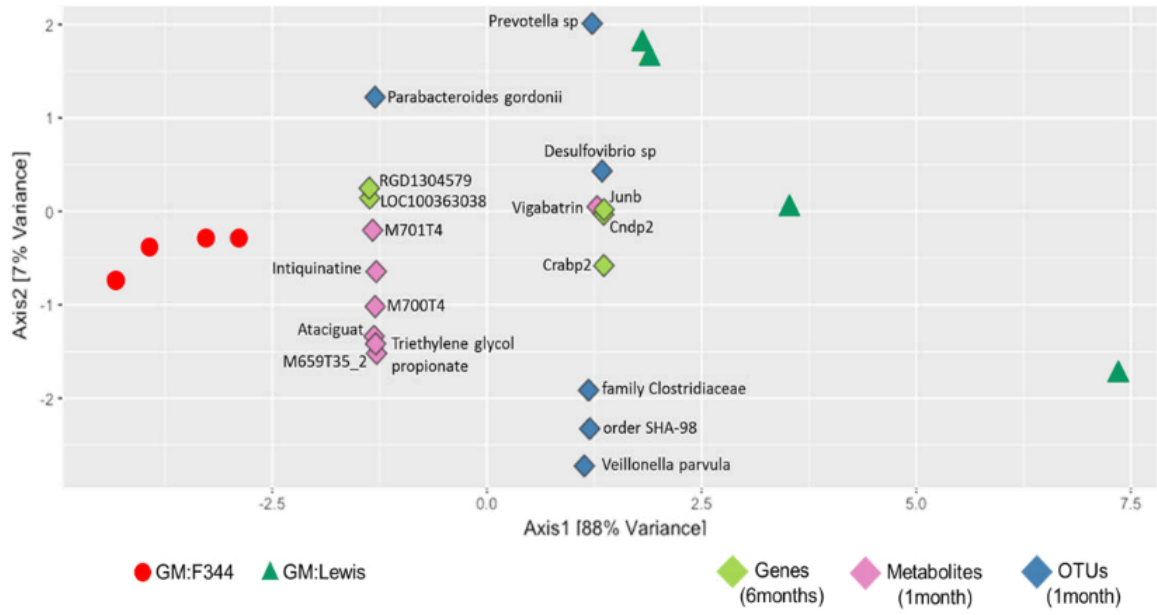
Figure 6. Pathway and correlation analyses identify potential mechanisms, differential factors contributing to low, and high tumor susceptibility

(A) Integrated Pathway analyses depicts pathways enriched and their topology, contributing to the variability in tumor phenotype observed as an effect of the genes and metabolites. (B) Sparse canonical correlation analysis incorporating the genes, metabolites and OTUs contributing to disease susceptibility in GM:F344 (red dots) and GM:LEW (dark green triangles) were analyzed in R, using the structSSI CRAN package. Metabolites, genes and OTUs are shown as diamonds in purple, light green and blue. Axis-1 demonstrated an 88% separation between GM:F344 and GM:LEW.

A

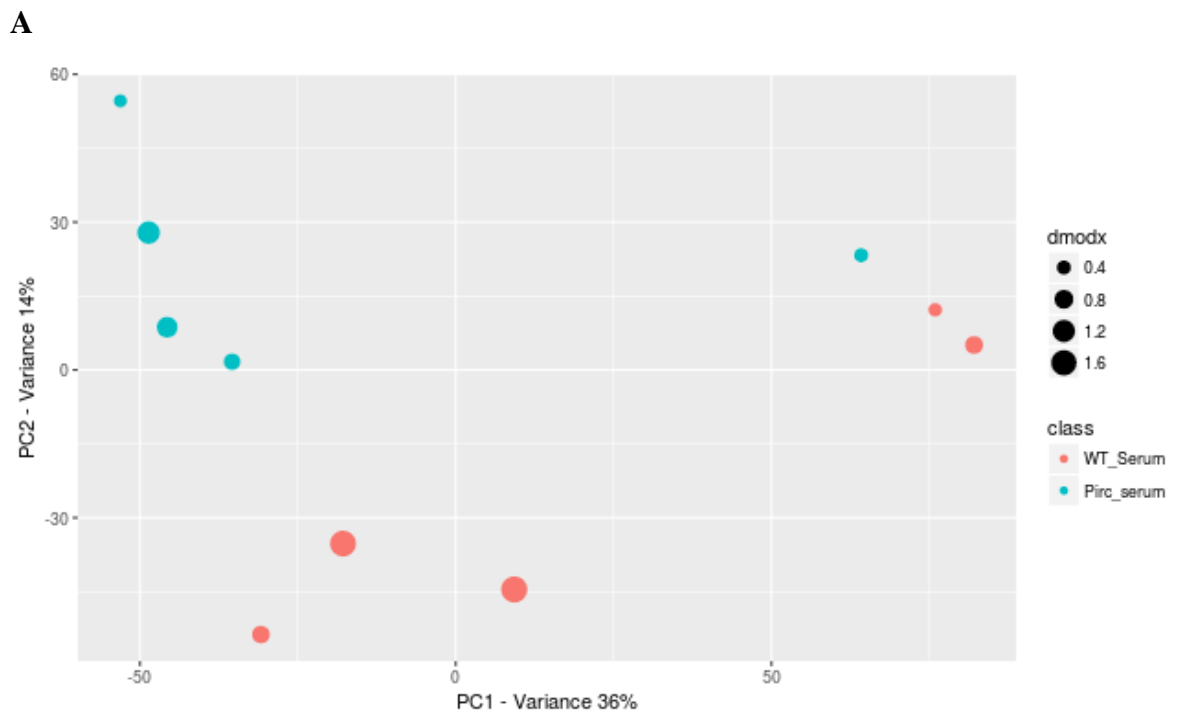


B

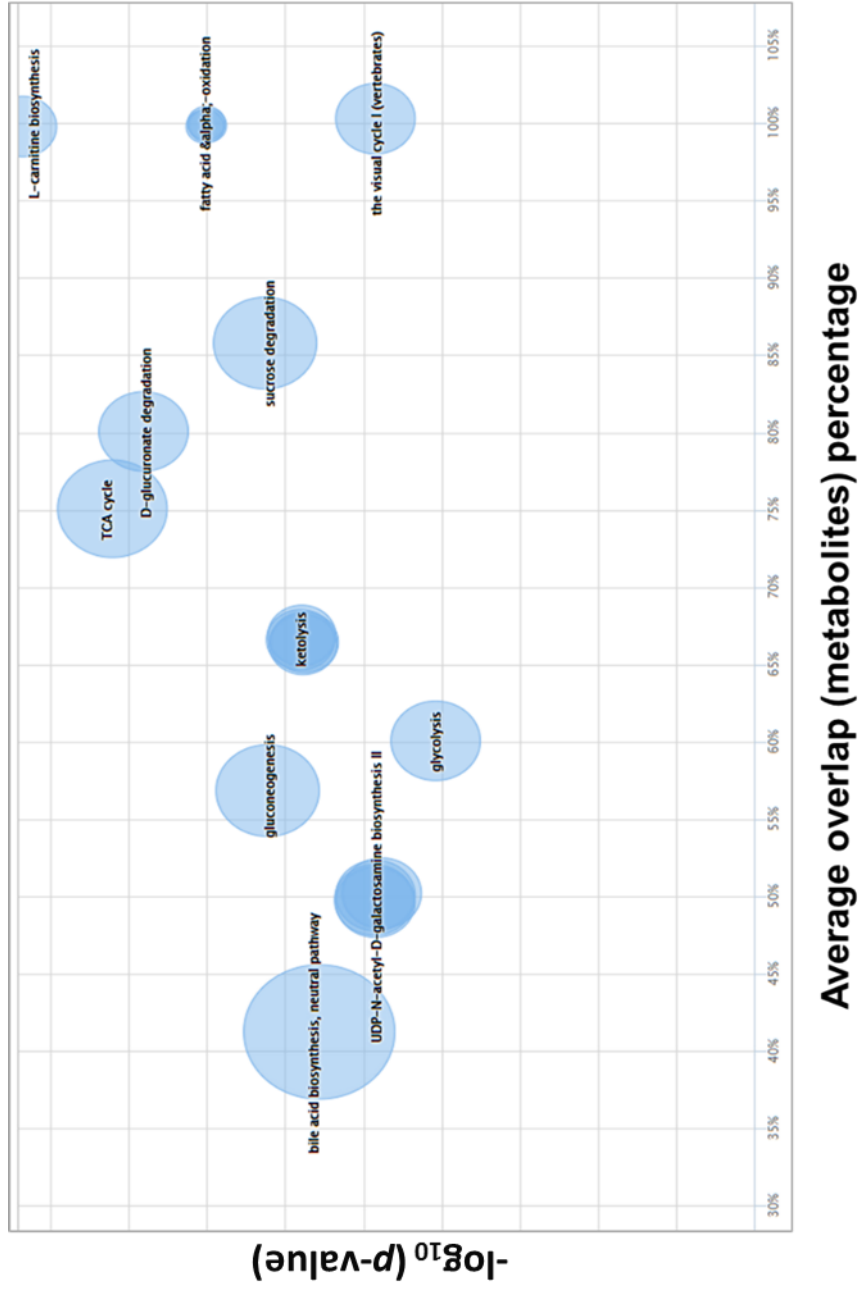


Supplementary figure 1. Serum metabolomics profiles and pathway analyses in Pirc and WT rats

Serum samples collected from Pirc and WT rats at 1 month of age used for LC-MS analysis indicated differential metabolomics profiles (A) including the regulation of bile acid biosynthesis, L-carnitine biosynthesis and fatty acid alpha-oxidation as potential pathways (B), contributing to phenotypic differences.



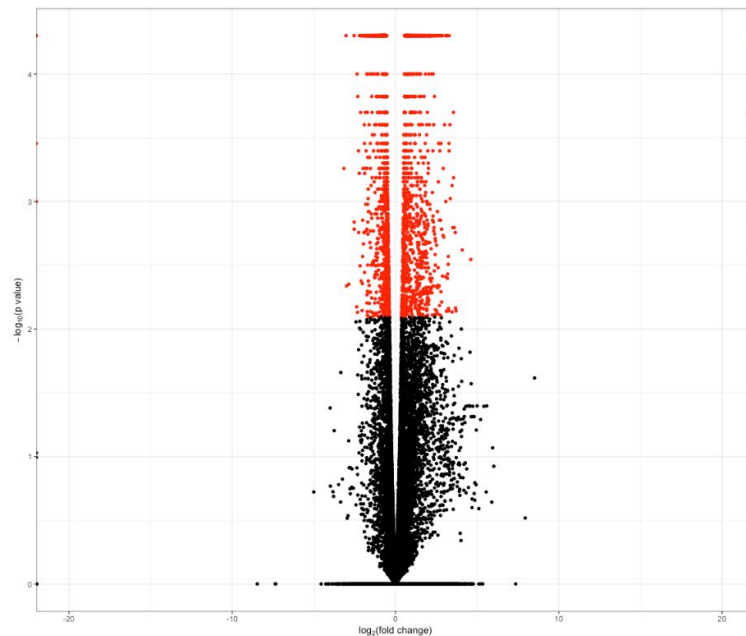
B



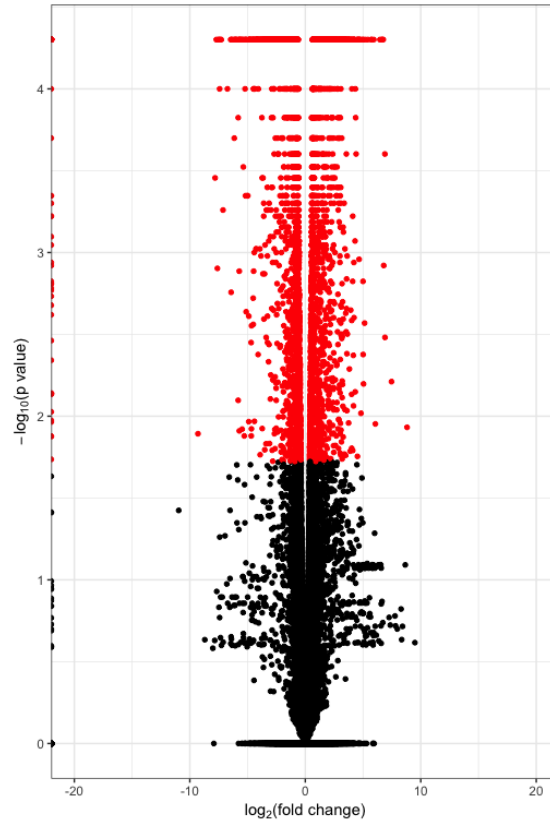
Supplementary figure 2. Differentially expressed genes (DEGs) and pathways altered due to GM in the normal epithelium and tumor tissues

Volcano plot analysis was performed on the differential gene expression in both the normal epithelium (A) and the tumor (B) samples from GM:F344 and GM:LEW. Fold-change and *P*-values are established along the *x*- and *y*- axes. All genes with a fold-change of at least 2, and FDR-corrected *P*-value were used for further analysis. Pathway analyses based on the gene expression in the normal tissues in the GM:F344 (C) and GM:LEW (D) groups was used to identify potential pathways and mechanisms contributing to the low and high tumor susceptibility. Enriched pathways are indicated in blue, while the topology, i.e. the importance of the pathway to the overall phenotype observed is shown in yellow. Integrated Pathway (IP) analysis incorporating the differentially expressed genes and the putative metabolites, significantly different between GM:F344 and GM:LEW, was performed.

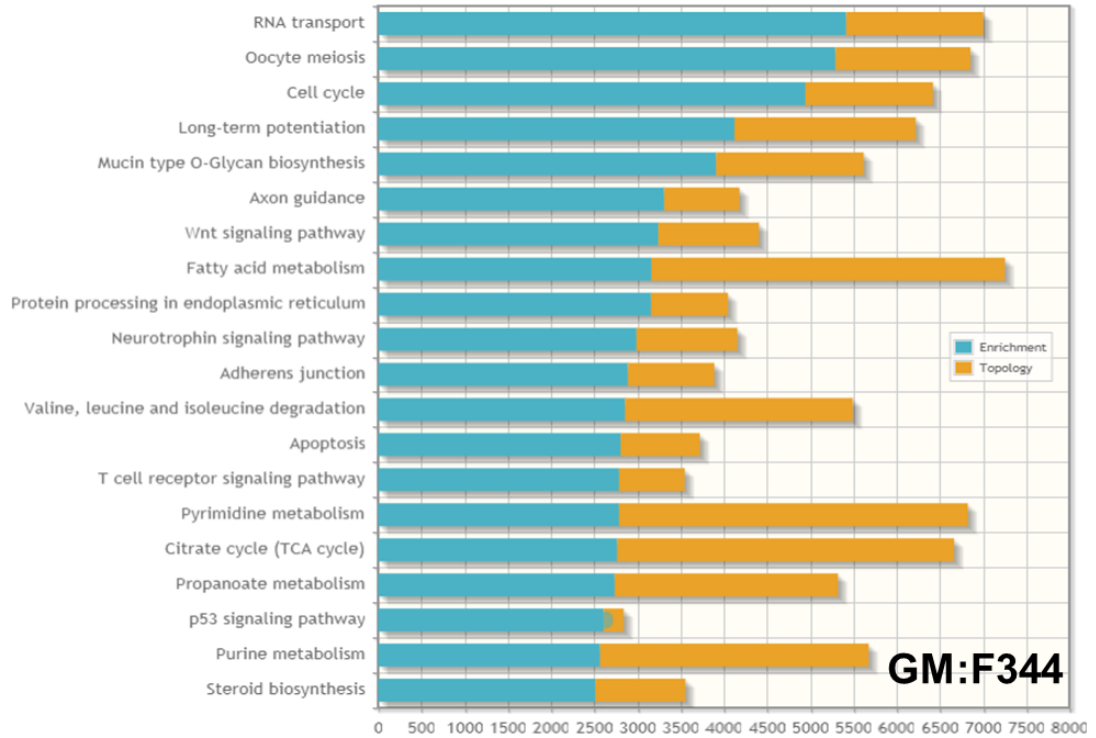
A



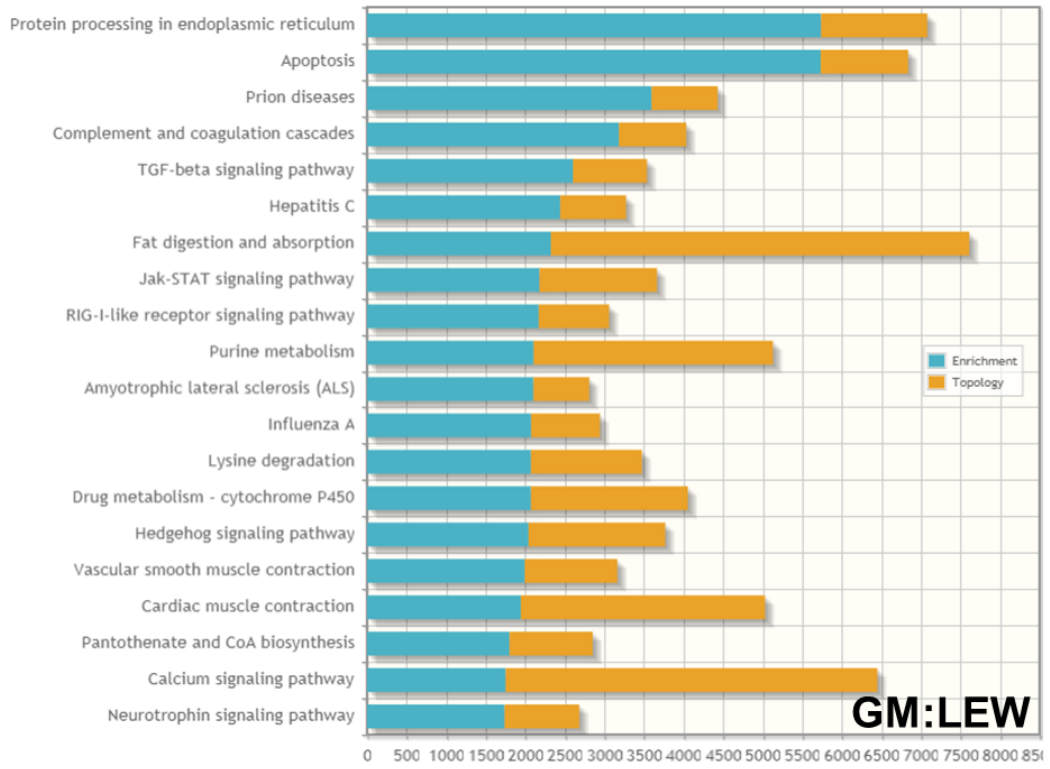
B



C

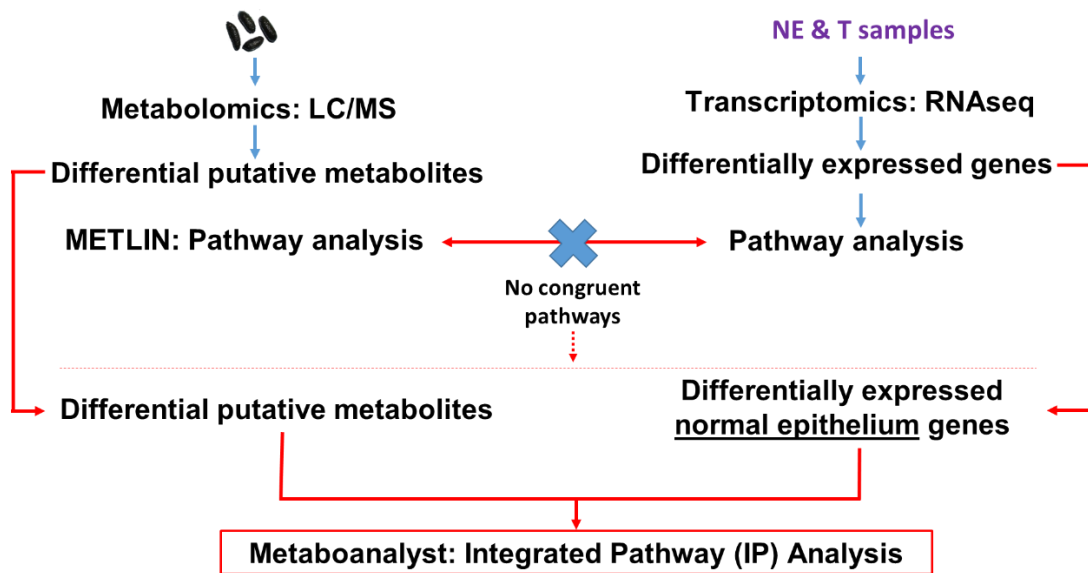


D



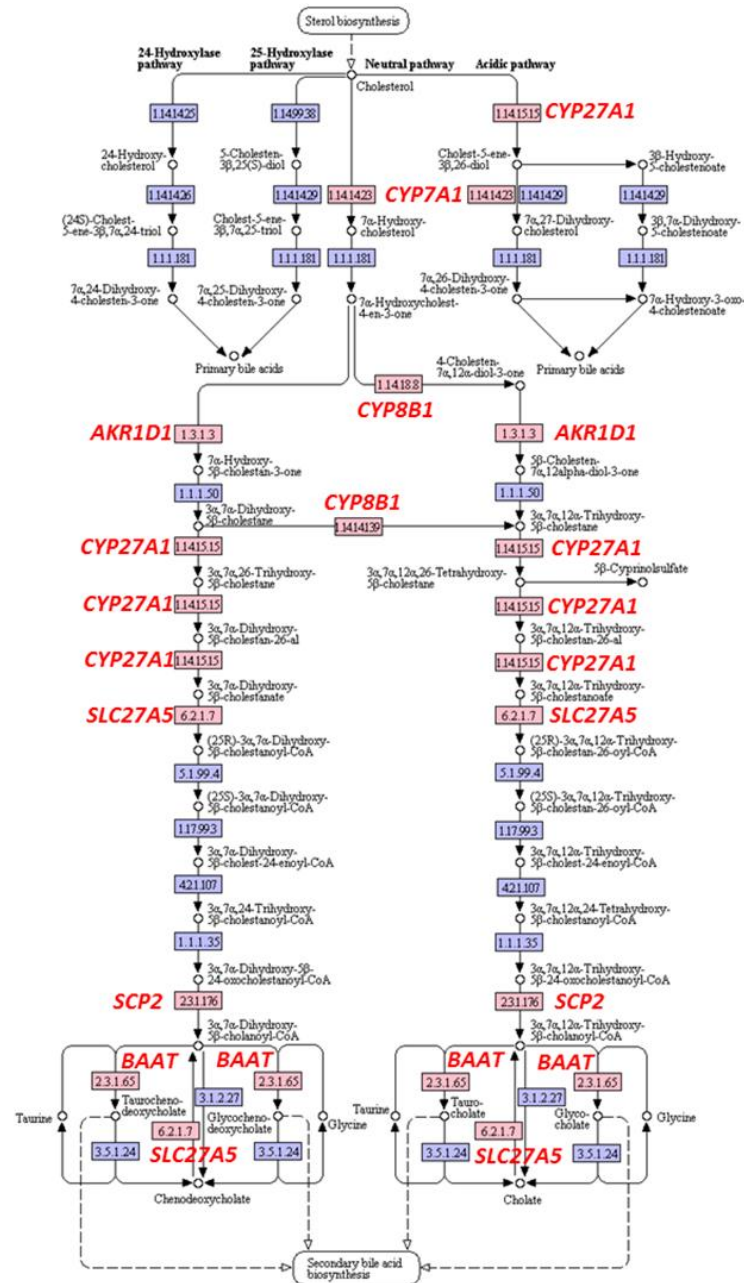
Supplementary figure 3: Analysis flowchart

Metabolomics and gene expression results were used to generate host pathways associated with changes in the gut microbiota (GM). The two analyses did not share pathways of interest. To address the incongruence, the differential putative fecal metabolites and normal epithelium genes were used to generate an Integrated Pathway analysis.



Supplementary figure 4: Bile acid biosynthesis pathway

Genes identified via metabolomics and RNASeq analysis, contributing to the bile acid pathway analyses are identified by highlighting corresponding locations in the KEGG pathway. The pathway was built using the KEGG pathway mapper tool from www.genome.jp/KEGG



00120 8/16/18
(c) Kanehisa Laboratories

8. Tables

Table 1: Compound class, RMD and putative identification of metabolites features in the METLIN databases

LC-MS analysis between groups identified several putative metabolites that are listed in the table as mass-charge to retention time ratios. Chemical formulas generated through the Bruker software, along with the calculated relative mass defect and compound classes are also identified. This is additionally supplemented with the putative identification based on the METLIN library.

Mass-charge/ retention time (mz/rt)	Chemical formula	Relative mass defect (RMD)	Compound class	Putative Identification (METLIN ID)
124.03995/1.29	C ₆ H ₉ O ₃	322.0737	Polyphenol	NA
223.0972/6.3	C ₇ H ₃ N ₂ O ₇	435.6845	Carbohydrate	NA
233.15395/21.26	C ₁₅ H ₂₂ O ₂	660.2933	Steroid	90173
257.08125/11.52	C ₁₇ H ₈ NO ₂	316.0479	Polyphenol	NA
295.1217/5.04	C ₁₈ H ₁₇ NO ₃	412.3723	Carbohydrate	95663
297.1127/10.64	C ₁₈ H ₁₈ O ₄	379.3173	Flavonoid	52682
359.1885/15.57	C ₂₄ H ₂₅ NO ₂	524.7941	Steroid/SCFA*	675713
405.2631/15.12	C ₂₄ H ₃₆ O ₅	649.2079	Steroid	84737
527.2822/28.34	C ₁₃ N ₁₃ O ₁₂	535.1973	Steroid/SCFA*	NA

*SCFA – short-chain fatty acid; NA – not applicable

Table 2: Normal epithelium genes involved in the bile acid biosynthesis and aspirin-triggered resolving E biosynthesis pathways

The genes listed in the table are part of the putative metabolite pathways differentially regulated between the high and low tumor GM groups. The predicted enzyme activity is listed adjacent to gene names.

Pathway	Genes	Enzyme activity	FDR-adjusted P-value	Group increased in
Bile acid biosynthesis, neutral pathway	<i>HSD3B7</i>	3 β -hydroxysteroid dehydrogenase type 7	0.861931	NA
	<i>ACAA2</i>	3-ketoacyl-CoA thiolase, mitochondrial	0.321851	NA
	<i>AKR1D1</i>	3-oxo-5- β -steroid 4-dehydrogenase	0.837208	NA
	<i>CYP8B1</i>	7- α -hydroxycholest-4-en-3-one 12- α -hydroxylase	0.00627491	GM:LEW
	<i>AMACR</i>	α -methylacyl-CoA racemase	0.78729	NA
	<i>BAAT</i>	bile acid-CoA: amino acid N-acyltransferase	0.0206231	GM:LEW
	<i>SLC27A5</i>	bile acyl-CoA synthetase	0.395957	NA
	<i>SCP2</i>	chenodeoxycholoyl-CoA synthase	0.85358	NA
	<i>CYP7A1</i>	cholesterol 7 α -monooxygenase	0.0779986	NA
	<i>POR</i>	cholesterol 7 α -monooxygenase	0.093983	NA
	<i>ACOX2</i>	peroxisomal acyl-coenzyme A oxidase	0.0756656	NA
	<i>CYP27A1</i>	sterol 26-hydroxylase	0.0999591	NA
	<i>SLC27A2</i>	very long-chain acyl-CoA synthetase	1	NA
<i>CYP2R1</i>	Vitamin D 25-hydroxylase	0.853166	NA	
Aspirin-triggered resolving E biosynthesis	<i>PTGS2</i>	18R-hydro(peroxy)-EPE synthase	0.000469693	GM:F344
	<i>ALOX5</i>	5S hydroperoxy HEPE synthase	0.000469693	GM:F344

Table 3: Putative metabolites contributing to bile acid and aspirin-triggered resolving E biosynthesis

The table lists the putative metabolites involved in the bile acid biosynthesis and aspirin-triggered resolvin E pathways. The METLIN and KEGG identification numbers are also listed for testing in the future.

Pathway	Putative metabolites	METLIN ID	KEGG ID
Bile acid biosynthesis, neutral pathway	(25R)-3 α ,7 α ,12 α -trihydroxy-5 β -cholestan-26-oate	NA	NULL
	glycocholate	202	C01921
	glycochenodeoxycholate	203	C01921
	Adenosine monophosphate (AMP)	34478	C056466
	(25R)-5 β -cholestane-3 α ,7 α ,12 α ,26-tetraol	43029	C00020
	7 α ,12 α -dihydroxy-5 β -cholestan-3-one	43117	C05446
	7 α ,12 α -dihydroxycholest-4-en-3-one	43118	C05453
	7 α -hydroxycholest-4-en-3-one	43126	C17339
	(25R)-3 α ,7 α -dihydroxy-5 β -cholestan-26-al	57924	C05455
	(25R)-3 α ,7 α ,12 α -trihydroxy-5 β -cholestan-26-al	57926	C01301
	(25R)-3 α ,7 α -dihydroxy-5- β -cholestanate	63323	C04554
Aspirin-triggered resolving E biosynthesis	resolvin E1	NA	C18171
	18R-hydroxy-eicosapentaenoate	NA	NULL
	5S hydro(peroxy),18R-hydroxy-eicosapentaenoate	NA	NULL
	(5Z,8Z,11Z,14Z,17Z)-icosapentaenoate	6423	C06428
	resolvin E2	36355	C18173

Supplementary Table 1: Summary of data processing results

The raw peaks obtained via XCMS for each individual samples analyzed through LC-MS is shown with an average peak abundance in the samples being 497. The number of missing or zero peaks for each sample along with the number of peaks processed for analysis based on the cutoff established in the Methods sections are listed. The raw data for the metabolomics analyses is hosted through the Metabolomics Workbench on the NIH Metabolomics Data Repository under the DataTrack ID #1539 for public access.

Samples	Peaks (raw)	Missing/Zero	Peaks (processed)
SB1	536	126	246
SB2	423	167	246
SB3	528	148	246
SB4	498	149	246
SB5	500	129	246
SB6	537	100	246
SB7	491	129	246
SB8	478	169	246
SB9	486	151	246
SB10	512	127	246
SB11	493	159	246
SB12	501	148	246
SB13	479	155	246

CHAPTER VI
CONCLUSIONS AND FUTURE DIRECTIONS

1. Conclusive highlights

Colon cancer remains the third leading cause of cancer death despite decades of research and animal models that have been around for over 25 years. Nearly 1 in 24 individuals will be diagnosed by this disease in their lifetime. Association of the gut microbiota (GM) within the gastrointestinal (GI) are equally staggering. Therefore, the avenues for understanding colon cancer etiology are numerous whether one chooses to assess the effect of toxins, diet, age, sex, predisposing conditions such as inflammatory bowel disease or Crohn's, and (or) genetics. However, the model in which one tests these factors plays a significant role in the translatability of the results. We chose the Pirc rat, a robust and translatable model of human colon cancer that predominantly develops adenomas in the colon. A significant advantage of this model is the development of adenomas due to a mutation in the *APC* gene, allowing us to identify mechanisms prior to onset of late-stage cancer. More importantly, the Pirc rat also harbors a complex GM profile similar to those found in humans. This ideology is the rationale for the studies described throughout this body of research, focusing on unravelling the role of the endogenous, complex GM on colon cancer susceptibility. Specifically, our work addresses the effect of particular bacteria (*chapter 2*) and the role of a sulfate-reducing, biofilm-forming bacterium (*chapter 3*) on disease phenotype. Considering the complex nature of the GM, we proceed to simplify the gut microbiota in *chapter 4*, to not only understand the role of individual bacteria but also to develop an alternate GM model of colon cancer. Along with the GM profiling data, it must be necessary to acknowledge the importance of additional omics strategies, which in conjunction with the former may

increase the strength of the associations identified between the GM and colon cancer development. We address this approach in *chapter 5*.

In *chapter 2* we treated Pirc rats with two bacteria: *Fusobacterium nucleatum* subsp. *polymorphum* and *Prevotella copri*. Though the bacteria did not colonize the GI tract, we found that treatment was sufficient to alter the endogenous GM structure and population. More interestingly, *F. nucleatum* is associated with an increased susceptibility to colonic tumors in the literature and in samples collected from healthy and patient volunteers. We found that treating with this bacterium at an early stage of development alleviated the adenoma burden in the colon. Similarly, treatment with *P. copri*, reportedly associated with healthy patients, alleviated tumor burden and altered the endogenous GM profile. In each of these treatments we found similar operational taxonomic units (OTUs) that correlated with the severity of disease. Our findings demonstrate that reports of pro-tumorigenic associations in the literature need to be carefully evaluated and considered when designing studies, especially with respect to the complex GM. It is plausible that the community population within the GM may be a significant driver of the tumor microenvironment. However, this hypothesis may only apply when treating with other commensals and may not explain the etiology of pathogenic bacteria.

Chapter 3 describes the role of a sulfate-reducing bacterium, *Desulfovibrio vulgaris* Hildenborough (DvH) on disease susceptibility in Pirc rats. We and others have reported the association of *Desulfovibrio* spp. with a lower tumor incidence in the colon. To test this, we generated biofilm –forming and –deficient strains of this bacterium, by creating a single nucleotide polymorphism (SNP) in the DVU1017 gene of a type-1

secretion system (T1SS). We found that the T1SS-competent, biofilm-forming strain colonized the Pirc rat colon even up to 3 months post-treatment. On the other hand, the lack of biofilm-formation due to the mutation in the T1SS affected the colonization potential of the strain. Contrary to what was observed in *chapter 2*, we found that DvH engrafted within the host despite the endogenous, complex GM. This engraftment led to a decreased adenoma burden in the colon of rats treated with the T1SS-competent, biofilm-forming strain. Based on 16S marker gene profiling, we found that the relative abundance of certain OTUs increased along with DvH colonization, while others decreased. This information may prove to be useful in future studies focused on understanding the interaction of various species within the complex GM. We also found that the increase in adenoma burden in the T1SS-deficient strain-treated rats is associated with a concomitant increase in the fecal hydrogen sulfide levels. This further pointed towards the possibility of an increase in genotoxicity, based on elevated levels of genes involved in DNA repair mechanisms. Since several reports in the literature suggest a tumor-promoting role for hydrogen sulfide in colon cancer patients, this model may offer several unique opportunities to investigate the role of this compound and other sulfate-reducing bacteria.

The complexity of the interactions between the thousands of bacteria within the endogenous GM is quite challenging to tease apart. Therefore, in *chapter 4*, we established the Pirc rat on a comparatively simplified gut microbiota profile. Utilizing the availability of Charles River Altered Schaedler Flora (CRASF) rats, we cross-fostered the Pirc rat, establishing a colony of F1-Pirc rats with an Altered Schaedler Flora GM profile. We found that we could reconstitute the complex GM in CRASF-Pirc by moving them from the barrier room to a conventional setting at our animal facility. Even more

interestingly, we noticed that simplified GM altered the colonic adenoma phenotype in Pirc rats. CRASF-Pirc rats housed under barrier conditions also had a significantly higher number of colonic adenomas compared to those housed in the conventional room. Expectedly, the conventional housing altered the composition and structure of the GM in the F1 CRASF-Pirc rats. These findings are contrary to reports in the literature which suggest that a simplified GM reduces colonic tumor burden in animal models. However, establishing the Pirc rats on a CRASF, simplified GM profile with only 10 OTUs allows for future studies evaluating the effect of a single bacterium or a consortia of bacteria on colon cancer susceptibility.

In *chapter 5*, we investigated the role of the complex GM on the metabolome and host transcriptome. We generated metabolome profiles from fecal samples at 1 month of age, prior to any observable disease. We found that these profiles could potentially predict tumor susceptibility in Pirc rats at later developmental stages. We additionally found significantly different metabolites and profiles based on the GM profile of the Pirc rats, differentiating high adenoma animals from those with a low number of colonic adenomas. Simultaneously, we observed that the host transcriptome was also significantly altered based on the GM profile of the rats. We found that the number and type of genes expressed in the colonic normal epithelium varied significantly between the groups depending on their gut microbiota composition and profile. Through an Integrated Pathway analysis we found that the bile acid biosynthesis pathway was significantly elevated in the high tumor Pirc rats. Our data not only illustrate the utility of the Pirc rat for multi-omics studies, but outline the possibility of certain host pathways being regulated by the GM via the metabolome and the host transcriptome.

2. Future directions

Through our research, we have provided compelling evidence unravelling some aspects of the role of the endogenous, complex GM. However, our work has provided few answers and raised further questions. The bacteria used to treat Pirc rats in *chapters 2 and 3*, including *P. copri* and *Fn. polymorphum* are known to be biofilm-formers. This raises the question of the role of biofilm-formation in colonization. Why did DvH, a biofilm-former colonize more efficiently when compared to *P. copri* or *Fn. polymorphum*?

Future studies may need to assess the status and characteristics of the T1SS in *P. copri* and *Fn. polymorphum* compared to DvH. This may provide clues as to whether the T1SS system is indeed responsible for colonization through the export of its putative protein, hypothesized to be a hemolysin. Alternatively, it is plausible that the predicted hemolysin may be eliminating some of the endogenous population, thus creating a niche for the engraftment of *D. vulgaris* Hildenborough. Additional studies could also be designed towards enhancing or deteriorating the hemolytic activity of the protein exported by the type-1 secretion system, to address its role on adenoma development, since hemolysins, especially those produced by *Streptococcus* spp. have been shown to be in anti-cancer therapies.

On a different note, for each of the studies in *chapter 2 and 3*, the Pirc rats were treated with the bacteria (*P. copri*, *Fn. polymorphum* and *D. vulgaris* Hildenborough) as early as 14 days of age. This is also thought to be the period where the immune system is developing in rodent models. In all three cases, treatment of these rats saw a significant decrease in colonic adenoma burden, despite associations of one of these bacteria with

increased colonic cancer in humans. The immune repertoire of the Piric rat in the context of an infection or the introduction of a new species of bacteria is still unknown. While one has to first establish the characteristics of the immune responses in the Piric rat against exogenous bacteria, it may also be prudent to test colonic epithelia and the mesenteric lymph nodes for an increase or decrease of cytokines such as TNF- α , IL-6, TGF- β , IL-1 β and IL-10. It may be plausible that we observed a reduction in the colonic adenomas due to the early treatment time point employed in both studies inducing increased immune-surveillance of the colon. It may be speculated that this immune-surveillance may potentially be contributing to an increase in a pro-inflammatory, anti-tumorigenic immune profile within the GI tract. Another way of assessing the impact of the early treatment time point, would be the treatment of pregnant dams, or treatment after onset of observable disease, i.e. 2 months of age. This will simultaneously help address the developmental mechanisms of the adenoma, i.e. whether the bacterial treatment affects tumor initiation or progression.

Another association between *P. copri*, *Fn. polymorphum*, and *D. vulgaris* Hildenborough is their sulfate-reducing and utilization capacity. Though significantly elevated levels of fecal hydrogen sulfide was not observed within the groups treated with the colonizing DvH strain, there was an elevation of host sulfate-related genes. This raises the possibility that the hydrogen sulfide (H₂S) generated within the colon mediates a scavenging response within the host. H₂S is well-established inducer of inflammation, reportedly based on both *in vitro* and *in vivo* studies. Therefore, the levels of hydrogen sulfide and their subsequent association with any inflammation should be verified going forward through supplementation with compounds such as sodium hydrosulfide. More

importantly, the time at which inflammation is occurring and confirmed will be crucial and essential to determine if a pro-inflammatory event promotes tumors or suppresses it. To address this, one may also have to undertake a cohort study, where a group of treated animals are sacrificed immediately after treatment to determine the immune and inflammation profile of the colon and mesenteric lymph nodes that supply the GI tract. Designing these studies, it is crucial to realize that in our study we found significantly different community populations in the fecal samples when compared to the mucosa-associated (biopsy) GM. This may also reflect the status of the immune response differences that may impact local versus systemic functions, thereby modulating not only the GM but also host responses differentially.

The studies outlined above highlight the role of the complex GM and potential ways to generate further postulates that may be useful in understanding mechanisms by which the GM modulates disease susceptibility. On the other hand, the CRASF-Pirc rats only have 10 operational taxonomic units within the colon that still lead to adenomagenesis in the rats. This model may be used in future studies, to test the efficacy of specific bacteria, for example *P. copri* in reducing adenoma susceptibility. More importantly, such a treatment approach will help shed light on which endogenous OTUs decline in relative abundance and highlight other OTUs that subsequently increase. This may aid in demonstrating the biochemical and metabolic interactions between the OTUs colonizing the CRASF-Pirc rats. Additionally, the limited GM in the CRASF rats, could be used for testing phage therapy approaches, where the introduction of specific bacteria and their corresponding phages may be tested for their capacity to eliminate the target bacteria and possible untargeted effects on the endogenous GM. Similarly, the limited

and simplified GM could also be used to isolate bacteria and establish a new GM profile with or without the bacteria of interest. By understanding the metabolic and growth requirements of the isolated bacteria, synthetically-designed mimics of enzymes such as zinc metalloproteases may be used to disrupt the enzymatic activity of opportunistic pathogens from a commensal population. Likewise, a consortium of bacteria or compounds such as short-chain fatty acids (SCFA) may be added into the existing CRASF GM, potentially enhancing the relative abundance of bacteria capable of utilizing or producing SCFAs in the endogenous population to determine whether certain GM profiles or compounds correlate with the adenoma burden.

It is imperative that many of the potential studies described here should be augmented with metabolomics and (or) proteomics studies to understand the exact mechanisms by which bacteria interact with the host. Most of these interactions are potentially through bacterially-derived compounds, or those modified by the endogenous GM. Therefore, the first and foremost set of experiments need to address the identity of the putative metabolites. Plant metabolites and proteomics are very well-characterized in the realm of small molecules and proteins. However, the identities of metabolites found within mammalian systems still remain largely unknown. Further investigation including advanced methods such as UHPLC-MS-SPE-NMR (ultra-high performance liquid chromatography-mass spectrometry-solid phase extraction-nuclear magnetic resonance) will be needed to determine the identity of metabolites associated with high and low tumor burdens. Additionally, we have to establish that the bile acid metabolites observed in the Pirc rat are similar to those found and reported in human case studies to ensure translatability of the Pirc rat model to human metabolomics studies. This will

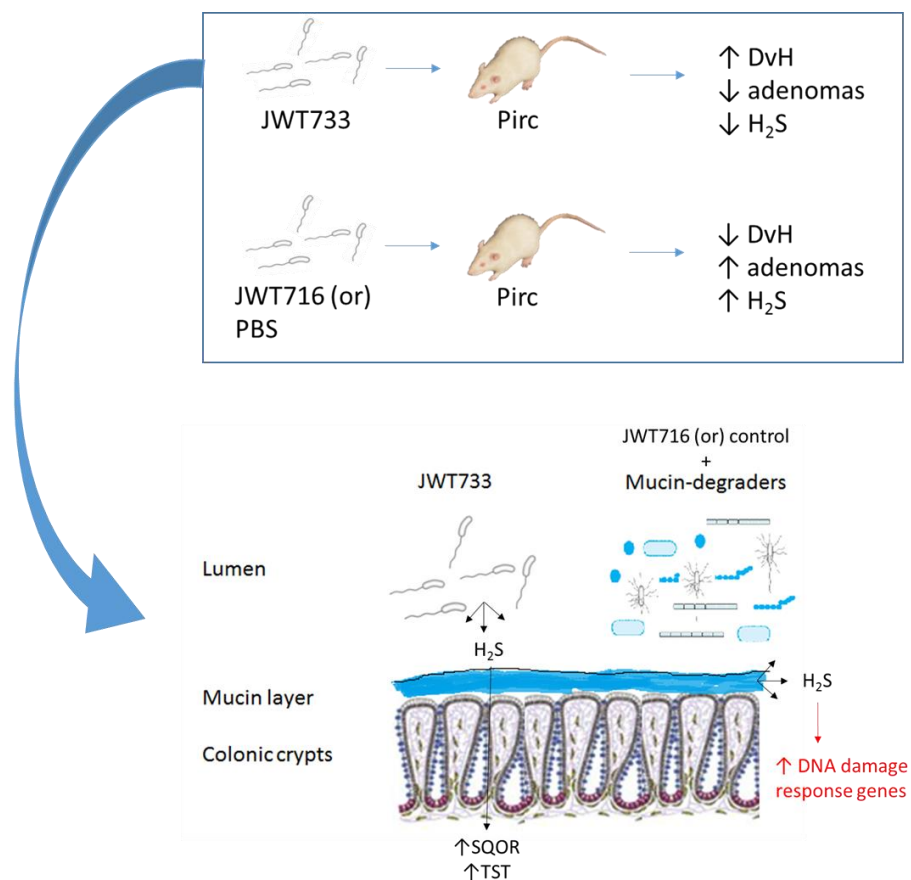
simultaneously corroborate the Pirc rat as a viable and translational model not only for GM studies, but also for testing metabolites and other therapeutic compounds. Recent studies have shown that therapeutic bile acids such as Ursodeoxycholic acid do not affect the gut microbiota, but could reduce adenoma risk in males (513). In light of this, the information generated in our study where the metabolite profiles could predict disease severity at later stages of development should be validated thoroughly using additional datasets that are publicly available. These validations may pave the way for identifying other diagnostic and prognostic compounds for identifying disease and treatment in colon cancer patients. This may also be used for machine learning approaches as training datasets, establishing a pre-tumorigenic dataset to identify at-risk human populations. The transcriptome and Integrated Pathway analyses also need to be further confirmed using animal models including surgical (bile duct ligation) and genetic manipulation techniques. The latter may include the use of mouse models of biliary dysregulation such as the *Abcb4*^{-/-} mice, or the *Cyp7a1*, *Cyp8b1*, *Cyp27a1* knockout mice models. Careful consideration, however, to the genetic background and the GM profile of these mice is essential to ensure consistent and reproducible results as we have shown here that the latter may have a significant impact of the overall metabolome profile. Alternatively, with the advent of gene-editing technologies, future studies may employ these methods to generate corresponding rat models, including a double-knockout in the Pirc rat to test the role of certain bile acid pathways in colon cancer development.

With advancements in technologies and methodologies, the questions and future directions raised here may soon become obsolete. Nonetheless, this work is a critical point of initiation, whereby one may develop *n* number of hypotheses going forward.

While each of the studies reported here have their own conclusions and future directions, collectively they serve the purpose of improving human health and therapeutic options.

While gut microbiota profiling studies are currently a normal state of affairs, future studies in this realm need to be augmented with other omics strategies. Metabolomics, proteomics, metagenomics, and metatranscriptomics are similarly useful methods whose incorporation into the overall analysis raises the power of deduction significantly. These strategies may help improve upon the currently available diagnostic and prognostic procedures, enhancing patient-targeted, and precision medicine methodologies.

3. Graphical abstract: Effect of *Desulfovibrio vulgaris* Hildenborough on adenomas in Piric rats



BIBLIOGRAPHY

1. Franklin CL, Ericsson AC. Microbiota and reproducibility of rodent models. *Lab Animal*. 2017;46(4):114-22. doi: 10.1038/labani.1222. PubMed PMID: PMC5762113.
2. Jilka RL. The road to reproducibility in animal research. *Journal of Bone and Mineral Research: the official journal of the American Society for Bone and Mineral Research*. 2016;31(7):1317-9. doi: 10.1002/jbmr.2881. PubMed PMID: PMC4935620.
3. Kenall A, Edmunds S, Goodman L, Bal L, Flintoft L, Shanahan DR, Shipley T. Better reporting for better research: a checklist for reproducibility. *Genome Biology*. 2015;16(1):141. doi: 10.1186/s13059-015-0710-5. PubMed PMID: PMC4512157.
4. Bleich A, Fox JG. The mammalian microbiome and its importance in laboratory animal research. *ILAR Journal*. 2015;56(2):153-158. doi: 10.1093/ilar/ilv031
5. Ericsson AC, Davis JW, Spollen W, Bivens N, Givan S, Hagan CE, McIntosh M, Franklin CL. Effects of vendor and genetic background on the composition of the fecal microbiota of inbred mice. *PLOS One*. 2015;10(2):e0116704. doi: 10.1371/journal.pone.0116704.
6. Ericsson AC, Franklin CL. Manipulating the gut microbiota: methods and challenges. *ILAR Journal*. 2015;56(2):205-17. doi: 10.1093/ilar/ilv021. PubMed PMID: PMC4554251.
7. Bleich A, Hansen AK. Time to include the gut microbiota in the hygienic standardisation of laboratory rodents. *Comparative Immunology, Microbiology & Infectious Diseases*. 2012;35(2):81-92. Epub 2012/01/20. doi: 10.1016/j.cimid.2011.12.006. PubMed PMID: 22257867.
8. Markle JGM, Frank DN, Mortin-Toth S, Robertson CE, Feazel LM, Rolle-Kampczyk U, von Bergen M, McCoy KD, Macpherson AJ, Danska JS. Sex differences in the gut microbiome drive hormone-dependent regulation of autoimmunity. *Science*. 2013;339(6123):1084.
9. Denning TL, Norris BA, Medina-Contreras O, Manicassamy S, Geem D, Madan R, Karp CL, Pulendran B. Functional specializations of intestinal dendritic cell and macrophage subsets that control Th17 and regulatory T cell responses are dependent on the T cell/APC ratio, source of mouse strain, and regional localization. *Journal of Immunology*. 2011;187(2):733-47. Epub 2011/06/15. doi: 10.4049/jimmunol.1002701. PubMed PMID: 21666057; PMCID: PMC3131424.
10. Ivanov II, de Llanos Frutos R, Manel N, Yoshinaga K, Rifkin DB, Sartor RB, Finlay BB, Littman DR. Specific microbiota direct the differentiation of Th17 cells in the mucosa of the small intestine. *Cell Host & Microbe*. 2008;4(4):337-49. doi: 10.1016/j.chom.2008.09.009. PubMed PMID: PMC2597589.

11. Larsson E, Tremaroli V, Lee YS, Koren O, Nookaew I, Fricker A, Nielsen J, Ley RE, Bäckhed F. Analysis of gut microbial regulation of host gene expression along the length of the gut and regulation of gut microbial ecology through MyD88. *Gut*. 2012;61(8):1124-31.
12. Turnbaugh PJ, Hamady M, Yatsunencko T, Cantarel BL, Duncan A, Ley RE, Sogin ML, Jones WJ, Roe BA, Affourtit JP, Egholm M, Henrissat B, Heath AC, Knight R, Gordon JI. A core gut microbiome in obese and lean twins. *Nature*. 2008;457:480. doi: 10.1038/nature07540 <https://www.nature.com/articles/nature07540#supplementary-information>.
13. Goodrich JK, Waters JL, Poole AC, Sutter JL, Koren O, Blekhman R, Beaumont M, Van Treuren W, Knight R, Bell JT, Spector TD, Clark AG, Ley RE. Human genetics shape the gut microbiome. *Cell*. 2014;159(4):789-99. doi: 10.1016/j.cell.2014.09.053. PubMed PMID: PMC4255478.
14. Goodrich JK, Davenport ER, Beaumont M, Jackson MA, Knight R, Ober C, Spector TD, Bell JT, Clark AG, Ley RE. Genetic determinants of the gut microbiome in UK twins. *Cell Host & Microbe*. 2016;19(5):731-43. doi: <https://doi.org/10.1016/j.chom.2016.04.017>.
15. Xie H, Guo R, Zhong H, Feng Q, Lan Z, Qin B, Ward KJ, Jackson MA, Xia Y, Chen X, Chen B, Xia H, Xu C, Li F, Xu X, Al-Aama JY, Yang H, Wang J, Kristiansen K, Wang J, Steves CJ, Bell JT, Li J, Spector TD, Jia H. Shotgun metagenomics of 250 adult twins reveals genetic and environmental impacts on the gut microbiome. *Cell Systems*. 2016;3(6):572-84.e3. doi: <https://doi.org/10.1016/j.cels.2016.10.004>.
16. Ridaura VK, Faith JJ, Rey FE, Cheng J, Duncan AE, Kau AL, Griffin NW, Lombard V, Henrissat B, Bain JR, Muehlbauer MJ, Ilkayeva O, Semenkovich CF, Funai K, Hayashi DK, Lyle BJ, Martini MC, Ursell LK, Clemente JC, Van Treuren W, Walters WA, Knight R, Newgard CB, Heath AC, Gordon JI. Cultured gut microbiota from twins discordant for obesity modulate adiposity and metabolic phenotypes in mice. *Science*. 2013;341(6150):10.1126/science.1241214. doi: 10.1126/science.1241214. PubMed PMID: PMC3829625.
17. Lu K, Mahbub R, Cable PH, Ru H, Parry NMA, Bodnar WM, Wishnok JS, Styblo M, Swenberg JA, Fox JG, Tannenbaum SR. Gut microbiome phenotypes driven by host genetics affect arsenic metabolism. *Chemical Research in Toxicology*. 2014;27(2):172-4. doi: 10.1021/tx400454z.
18. Parsa N. Environmental factors inducing human cancers. *Iranian Journal of Public Health*. 2012;41(11):1-9. PubMed PMID: PMC3521879.
19. Anand P, Kunnumakara AB, Sundaram C, Harikumar KB, Tharakan ST, Lai OS, Sung B, Aggarwal BB. Cancer is a preventable disease that requires major lifestyle changes. *Pharmaceutical Research*. 2008;25(9):2097-116. doi: 10.1007/s11095-008-9661-9. PubMed PMID: PMC2515569.

20. Sankpal UT, Pius H, Khan M, Shukoor MI, Maliakal P, Lee CM, Abdelrahim M, Connelly SF, Basha R. Environmental factors in causing human cancers: emphasis on tumorigenesis. *Tumour Biology: the journal of the International Society for Oncodevelopmental Biology & Medicine*. 2012;33(5):1265-74. Epub 2012/05/23. doi: 10.1007/s13277-012-0413-4. PubMed PMID: 22614680.
21. Brennan P. Gene–environment interaction and aetiology of cancer: what does it mean and how can we measure it? *Carcinogenesis*. 2002;23(3):381-7. doi: 10.1093/carcin/23.3.381.
22. Migliore L, Coppede F. Genetic and environmental factors in cancer and neurodegenerative diseases. *Mutation Research*. 2002;512(2-3):135-53. Epub 2002/12/05. PubMed PMID: 12464348.
23. Pleasance ED, Cheetham RK, Stephens PJ, McBride DJ, Humphray SJ, Greenman CD, Varela I, Lin M-L, Ordóñez GR, Bignell GR, Ye K, Alipaz J, Bauer MJ, Beare D, Butler A, Carter RJ, Chen L, Cox AJ, Edkins S, Kokko-Gonzales PI, Gormley NA, Grocock RJ, Haudenschild CD, Hims MM, James T, Jia M, Kingsbury Z, Leroy C, Marshall J, Menzies A, Mudie LJ, Ning Z, Royce T, Schulz-Trieglaff OB, Spiridou A, Stebbings LA, Szajkowski L, Teague J, Williamson D, Chin L, Ross MT, Campbell PJ, Bentley DR, Futreal PA, Stratton MR. A comprehensive catalogue of somatic mutations from a human cancer genome. *Nature*. 2010;463(7278):191-6. doi: 10.1038/nature08658. PubMed PMID: PMC3145108.
24. Bignell GR, Greenman CD, Davies H, Butler AP, Edkins S, Andrews JM, Buck G, Chen L, Beare D, Latimer C, Widaa S, Hinton J, Fahey C, Fu B, Swamy S, Dalgliesh GL, Teh BT, Deloukas P, Yang F, Campbell PJ, Futreal PA, Stratton MR. Signatures of mutation and selection in the cancer genome. *Nature*. 2010;463:893. doi: 10.1038/nature08768 <https://www.nature.com/articles/nature08768#supplementary-information>.
25. Mattar MC, Lough D, Pishvaian MJ, Charabaty A. Current management of inflammatory bowel disease and colorectal cancer. *Gastrointestinal Cancer Research: GCR*. 2011;4(2):53-61. PubMed PMID: PMC3109885.
26. Jasperson KW, Tuohy TM, Neklason DW, Burt RW. Hereditary and familial colon cancer. *Gastroenterology*. 2010;138(6):2044-58. Epub 2010/04/28. doi: 10.1053/j.gastro.2010.01.054. PubMed PMID: 20420945; PMCID: PMC3057468.
27. van Wezel T, Middeldorp A, Wijnen JT, Morreau H. A review of the genetic background and tumour profiling in familial colorectal cancer. *Mutagenesis*. 2012;27(2):239-45. doi: 10.1093/mutage/ger071.
28. Rustgi AK. The genetics of hereditary colon cancer. *Genes & Development*. 2007;21(20):2525-38. Epub 2007/10/17. doi: 10.1101/gad.1593107. PubMed PMID: 17938238.

29. Amos-Landgraf JM, Clipson L, Newton MA, Dove WF. The many ways to open the gate to colon cancer. *Cell Cycle*. 2012;11(7):1261-2. Epub 2012/03/17. doi: 10.4161/cc.19888. PubMed PMID: 22421162; PMCID: PMC3350873.
30. Marinus MG. DNA Mismatch Repair. *EcoSal Plus*. 2012;5(1):10.1128/ecosalplus.7.2.5. doi: 10.1128/ecosalplus.7.2.5. PubMed PMID: PMC4231543.
31. de la Chapelle A. Genetic predisposition to colorectal cancer. *Nature Reviews Cancer*. 2004;4(10):769-80. Epub 2004/10/29. doi: 10.1038/nrc1453. PubMed PMID: 15510158.
32. Vogelstein B, Papadopoulos N, Velculescu VE, Zhou S, Diaz LA, Jr., Kinzler KW. Cancer Genome Landscapes. *Science*. 2013;339(6127):1546-58. Epub 2013/03/30. doi: 10.1126/science.1235122. PubMed PMID: 23539594; PMCID: PMC3749880.
33. McCart AE, Vickaryous NK, Silver A. Apc mice: models, modifiers and mutants. *Pathology - Research and Practice*. 2008;204(7):479-90. doi: <https://doi.org/10.1016/j.prp.2008.03.004>.
34. Silverman KA, Koratkar R, Siracusa LD, Buchberg AM. Identification of the modifier of Min 2 (*Mom2*) locus, a new mutation that influences Apc-induced intestinal neoplasia. *Genome Research*. 2002;12(1):88-97. doi: 10.1101/gr.206002. PubMed PMID: PMC155250.
35. Hamilton BA, Yu BD. Modifier genes and the plasticity of genetic networks in mice. *PLOS Genetics*. 2012;8(4):e1002644. doi: 10.1371/journal.pgen.1002644.
36. Halberg RB, Katzung DS, Hoff PD, Moser AR, Cole CE, Lubet RA, Donehower LA, Jacoby RF, Dove WF. Tumorigenesis in the multiple intestinal neoplasia mouse: Redundancy of negative regulators and specificity of modifiers. *Proceedings of the National Academy of Sciences of the United States of America*. 2000;97(7):3461.
37. Cormier RT, Hong KH, Halberg RB, Hawkins TL, Richardson P, Mulherkar R, Dove WF, Lander ES. Secretory phospholipase Pla2g2a confers resistance to intestinal tumorigenesis. *Nature Genetics*. 1997;17:88. doi: 10.1038/ng0997-88.
38. Al-Tassan NA, Whiffin N, Hosking FJ, Palles C, Farrington SM, Dobbins SE, Harris R, Gorman M, Tenesa A, Meyer BF, Wakil SM, Kinnersley B, Campbell H, Martin L, Smith CG, Idziaszczyk S, Barclay E, Maughan TS, Kaplan R, Kerr R, Kerr D, Buchanan DD, Win AK, Hopper J, Jenkins M, Lindor NM, Newcomb PA, Gallinger S, Conti D, Schumacher F, Casey G, Dunlop MG, Tomlinson IP, Cheadle JP, Houlston RS. A new GWAS and meta-analysis with 1000 Genomes imputation identifies novel risk variants for colorectal cancer. *Scientific Reports*. 2015;5:10442. Epub 2015/05/21. doi: 10.1038/srep10442. PubMed PMID: 25990418; PMCID: PMC4438486.
39. Peters U, Jiao S, Schumacher FR, Hutter CM, Aragaki AK, Baron JA, Berndt SI, Bezieau S, Brenner H, Butterbach K, Caan BJ, Campbell PT, Carlson CS, Casey G, Chan

AT, Chang-Claude J, Chanock SJ, Chen LS, Coetzee GA, Coetzee SG, Conti DV, Curtis KR, Duggan D, Edwards T, Fuchs CS, Gallinger S, Giovannucci EL, Gogarten SM, Gruber SB, Haile RW, Harrison TA, Hayes RB, Henderson BE, Hoffmeister M, Hopper JL, Hudson TJ, Hunter DJ, Jackson RD, Jee SH, Jenkins MA, Jia WH, Kolonel LN, Kooperberg C, Kury S, Lacroix AZ, Laurie CC, Laurie CA, Le Marchand L, Lemire M, Levine D, Lindor NM, Liu Y, Ma J, Makar KW, Matsuo K, Newcomb PA, Potter JD, Prentice RL, Qu C, Rohan T, Rosse SA, Schoen RE, Seminara D, Shrubsole M, Shu XO, Slattery ML, Taverna D, Thibodeau SN, Ulrich CM, White E, Xiang Y, Zanke BW, Zeng YX, Zhang B, Zheng W, Hsu L. Identification of genetic susceptibility loci for colorectal tumors in a genome-wide meta-analysis. *Gastroenterology*. 2013;144(4):799-807.e24. Epub 2012/12/26. doi: 10.1053/j.gastro.2012.12.020. PubMed PMID: 23266556; PMCID: PMC3636812.

40. Houlston RS, Cheadle J, Dobbins SE, Tenesa A, Jones AM, Howarth K, Spain SL, Broderick P, Domingo E, Farrington S, Prendergast JG, Pittman AM, Theodoratou E, Smith CG, Olver B, Walther A, Barnetson RA, Churchman M, Jaeger EE, Penegar S, Barclay E, Martin L, Gorman M, Mager R, Johnstone E, Midgley R, Niittymaki I, Tuupanen S, Colley J, Idziaszczyk S, Thomas HJ, Lucassen AM, Evans DG, Maher ER, Maughan T, Dimas A, Dermitzakis E, Cazier JB, Aaltonen LA, Pharoah P, Kerr DJ, Carvajal-Carmona LG, Campbell H, Dunlop MG, Tomlinson IP. Meta-analysis of three genome-wide association studies identifies susceptibility loci for colorectal cancer at 1q41, 3q26.2, 12q13.13 and 20q13.33. *Nature Genetics*. 2010;42(11):973-7. Epub 2010/10/26. doi: 10.1038/ng.670. PubMed PMID: 20972440; PMCID: PMC5098601.

41. Schumacher FR, Schmit SL, Jiao S, Edlund CK, Wang H, Zhang B, Hsu L, Huang SC, Fischer CP, Harju JF, Idos GE, Lejbkowitz F, Manion FJ, McDonnell K, McNeil CE, Melas M, Rennert HS, Shi W, Thomas DC, Van Den Berg DJ, Hutter CM, Aragaki AK, Butterbach K, Caan BJ, Carlson CS, Chanock SJ, Curtis KR, Fuchs CS, Gala M, Giovannucci EL, Gogarten SM, Hayes RB, Henderson B, Hunter DJ, Jackson RD, Kolonel LN, Kooperberg C, Kury S, LaCroix A, Laurie CC, Laurie CA, Lemire M, Levine D, Ma J, Makar KW, Qu C, Taverna D, Ulrich CM, Wu K, Kono S, West DW, Berndt SI, Bezieau S, Brenner H, Campbell PT, Chan AT, Chang-Claude J, Coetzee GA, Conti DV, Duggan D, Figueiredo JC, Fortini BK, Gallinger SJ, Gauderman WJ, Giles G, Green R, Haile R, Harrison TA, Hoffmeister M, Hopper JL, Hudson TJ, Jacobs E, Iwasaki M, Jee SH, Jenkins M, Jia WH, Joshi A, Li L, Lindor NM, Matsuo K, Moreno V, Mukherjee B, Newcomb PA, Potter JD, Raskin L, Rennert G, Rosse S, Severi G, Schoen RE, Seminara D, Shu XO, Slattery ML, Tsugane S, White E, Xiang YB, Zanke BW, Zheng W, Le Marchand L, Casey G, Gruber SB, Peters U. Genome-wide association study of colorectal cancer identifies six new susceptibility loci. *Nature Communications*. 2015;6:7138. Epub 2015/07/08. doi: 10.1038/ncomms8138. PubMed PMID: 26151821; PMCID: PMC4967357.

42. Schmit SL, Schumacher FR, Edlund CK, Conti DV, Raskin L, Lejbkowitz F, Pinchev M, Rennert HS, Jenkins MA, Hopper JL, Buchanan DD, Lindor NM, Le Marchand L, Gallinger S, Haile RW, Newcomb PA, Huang SC, Rennert G, Casey G, Gruber SB. A novel colorectal cancer risk locus at 4q32.2 identified from an international

genome-wide association study. *Carcinogenesis*. 2014;35(11):2512-9. Epub 2014/07/16. doi: 10.1093/carcin/bgu148. PubMed PMID: 25023989; PMCID: PMC4271131.

43. Houlston RS, Webb E, Broderick P, Pittman AM, Di Bernardo MC, Lubbe S, Chandler I, Vijayakrishnan J, Sullivan K, Penegar S, Carvajal-Carmona L, Howarth K, Jaeger E, Spain SL, Walther A, Barclay E, Martin L, Gorman M, Domingo E, Teixeira AS, Kerr D, Cazier JB, Niittymaki I, Tuupanen S, Karhu A, Aaltonen LA, Tomlinson IP, Farrington SM, Tenesa A, Prendergast JG, Barnetson RA, Cetnarskyj R, Porteous ME, Pharoah PD, Koessler T, Hampe J, Buch S, Schafmayer C, Tepel J, Schreiber S, Volzke H, Chang-Claude J, Hoffmeister M, Brenner H, Zanke BW, Montpetit A, Hudson TJ, Gallinger S, Campbell H, Dunlop MG. Meta-analysis of genome-wide association data identifies four new susceptibility loci for colorectal cancer. *Nature Genetics*. 2008;40(12):1426-35. Epub 2008/11/18. doi: 10.1038/ng.262. PubMed PMID: 19011631; PMCID: PMC2836775.

44. Tenesa A, Farrington SM, Prendergast JG, Porteous ME, Walker M, Haq N, Barnetson RA, Theodoratou E, Cetnarskyj R, Cartwright N, Semple C, Clark AJ, Reid FJ, Smith LA, Kavoussanakis K, Koessler T, Pharoah PD, Buch S, Schafmayer C, Tepel J, Schreiber S, Volzke H, Schmidt CO, Hampe J, Chang-Claude J, Hoffmeister M, Brenner H, Wilkening S, Canzian F, Capella G, Moreno V, Deary IJ, Starr JM, Tomlinson IP, Kemp Z, Howarth K, Carvajal-Carmona L, Webb E, Broderick P, Vijayakrishnan J, Houlston RS, Rennert G, Ballinger D, Rozek L, Gruber SB, Matsuda K, Kidokoro T, Nakamura Y, Zanke BW, Greenwood CM, Rangrej J, Kustra R, Montpetit A, Hudson TJ, Gallinger S, Campbell H, Dunlop MG. Genome-wide association scan identifies a colorectal cancer susceptibility locus on 11q23 and replicates risk loci at 8q24 and 18q21. *Nature Genetics*. 2008;40(5):631-7. Epub 2008/04/01. doi: 10.1038/ng.133. PubMed PMID: 18372901; PMCID: PMC2778004.

45. Pashayan N, Duffy SW, Chowdhury S, Dent T, Burton H, Neal DE, Easton DF, Eeles R, Pharoah P. Polygenic susceptibility to prostate and breast cancer: implications for personalised screening. *British Journal of Cancer*. 2011;104(10):1656-63. Epub 2011/04/07. doi: 10.1038/bjc.2011.118. PubMed PMID: 21468051; PMCID: PMC3093360.

46. Peng L, Bian XW, Li DK, Xu C, Wang GM, Xia QY, Xiong Q. Large-scale RNA-Seq transcriptome analysis of 4043 cancers and 548 normal tissue controls across 12 TCGA cancer types. *Scientific Reports*. 2015;5:13413. doi: 10.1038/srep13413 <https://www.nature.com/articles/srep13413#supplementary-information>.

47. King LE, Love CG, Sieber OM, Faux MC, Burgess AW. Differential RNA-seq analysis comparing APC-defective and APC-restored SW480 colorectal cancer cells. *Genomics Data*. 2016;7:293-6. doi: <https://doi.org/10.1016/j.gdata.2016.02.001>.

48. Lee J-R, Kwon CH, Choi Y, Park HJ, Kim HS, Jo H-J, Oh N, Park DY. Transcriptome analysis of paired primary colorectal carcinoma and liver metastases reveals fusion transcripts and similar gene expression profiles in primary carcinoma and

liver metastases. *BMC Cancer*. 2016;16:539. doi: 10.1186/s12885-016-2596-3. PubMed PMID: PMC4962348.

49. Adler AS, McClelland ML, Yee S, Yaylaoglu M, Hussain S, Cosino E, Quinones G, Modrusan Z, Seshagiri S, Torres E, Chopra VS, Haley B, Zhang Z, Blackwood EM, Singh M, Junttila M, Stephan JP, Liu J, Pau G, Fearon ER, Jiang Z, Firestein R. An integrative analysis of colon cancer identifies an essential function for PRPF6 in tumor growth. *Genes & Development*. 2014;28(10):1068-84. Epub 2014/05/03. doi: 10.1101/gad.237206.113. PubMed PMID: 24788092; PMCID: PMC4035536.

50. Chen J, Zhou Q, Wang Y, Ning K. Single-cell SNP analyses and interpretations based on RNA-Seq data for colon cancer research. *Scientific Reports*. 2016;6:34420. doi: 10.1038/srep34420 <https://www.nature.com/articles/srep34420#supplementary-information>.

51. Perkins G, Fabre E, Fallet V, Blons H, Pecuchet N, Gounant V, Gibault L, Michel-Jeljeli E, Antoine M, Roux E, Wislez M, Le Corre D, Leroy K, Lacave R, Taieb J, Cadranet J, Laurent-Puig P. Whole exome sequencing (WES) and RNA sequencing (RNA-seq) in routine clinical practice for colorectal cancer (CRC) and non-small cell lung cancer (NSCLC) patients. *Annals of Oncology*. 2016;27(suppl_6):96P-P. doi: 10.1093/annonc/mdw363.44.

52. Son JS, Khair S, Pettet DW, III, Ouyang N, Tian X, Zhang Y, Zhu W, Mackenzie GG, Robertson CE, Ir D, Frank DN, Rigas B, Li E. Altered Interactions between the Gut Microbiome and Colonic Mucosa Precede Polyposis in *Apc^{+Min}* Mice. *PLOS One*. 2015;10(6):e0127985. doi: 10.1371/journal.pone.0127985.

53. Brodziak F, Meharg C, Blaut M, Loh G. Differences in mucosal gene expression in the colon of two inbred mouse strains after colonization with commensal gut bacteria. *PLOS One*. 2013;8(8):e72317. doi: 10.1371/journal.pone.0072317. PubMed PMID: PMC3739790.

54. Klinder A, Forster A, Caderni G, Femia AP, Pool-Zobel BL. Fecal water genotoxicity is predictive of tumor-preventive activities by inulin-like oligofructoses, probiotics (*Lactobacillus rhamnosus* and *Bifidobacterium lactis*), and their synbiotic combination. *Nutrition & Cancer*. 2004;49(2):144-55. Epub 2004/10/19. doi: 10.1207/s15327914nc4902_5. PubMed PMID: 15489207.

55. Daniela E, Sara S, Marcella M, Giovanni A, Meynier A, Sophie V, Cristina CM. Fecal water genotoxicity in healthy free-living young Italian people. *Food & Chemical Toxicology: an international journal published for the British Industrial Biological Research Association*. 2014;64:104-9. Epub 2013/12/04. doi: 10.1016/j.fct.2013.11.019. PubMed PMID: 24296136.

56. Hebels DG, Sveje KM, de Kok MC, van Herwijnen MH, Kuhnle GG, Engels LG, Vleugels-Simon CB, Mares WG, Pierik M, Masclee AA, Kleinjans JC, de Kok TM. Red meat intake-induced increases in fecal water genotoxicity correlate with pro-carcinogenic gene expression changes in the human colon. *Food & Chemical Toxicology: an*

international journal published for the British Industrial Biological Research Association. 2012;50(2):95-103. Epub 2011/10/25. doi: 10.1016/j.fct.2011.10.038. PubMed PMID: 22019696.

57. Turunen KT, Pletsas V, Georgiadis P, Triantafyllidis JK, Karamanolis D, Kyriacou A. Impact of beta-glucan on the fecal water genotoxicity of polypectomized patients. *Nutrition & Cancer*. 2016;68(4):560-7. Epub 2016/04/05. doi: 10.1080/01635581.2016.1156713. PubMed PMID: 27043932.

58. Windey K, De Preter V, Huys G, Broekaert WF, Delcour JA, Louat T, Herman J, Verbeke K. Wheat bran extract alters colonic fermentation and microbial composition, but does not affect faecal water toxicity: a randomised controlled trial in healthy subjects. *The British Journal of Nutrition*. 2015;113(2):225-38. Epub 2014/12/17. doi: 10.1017/s0007114514003523. PubMed PMID: 25498469.

59. Kostic AD, Chun E, Robertson L, Glickman JN, Gallini CA, Michaud M, Clancy TE, Chung DC, Lochhead P, Hold GL, El-Omar EM, Brenner D, Fuchs CS, Meyerson M, Garrett WS. *Fusobacterium nucleatum* potentiates intestinal tumorigenesis and modulates the tumor-immune microenvironment. *Cell Host & Microbe*. 2013;14(2):207-15. Epub 2013/08/21. doi: 10.1016/j.chom.2013.07.007. PubMed PMID: 23954159; PMCID: PMC3772512.

60. Kostic AD, Gevers D, Pedamallu CS, Michaud M, Duke F, Earl AM, Ojesina AI, Jung J, Bass AJ, Taberero J, Baselga J, Liu C, Shivdasani RA, Ogino S, Birren BW, Huttenhower C, Garrett WS, Meyerson M. Genomic analysis identifies association of *Fusobacterium* with colorectal carcinoma. *Genome Research*. 2012;22(2):292-8. Epub 2011/10/20. doi: 10.1101/gr.126573.111. PubMed PMID: 22009990; PMCID: Pmc3266036.

61. Rubinstein MR, Wang X, Liu W, Hao Y, Cai G, Han YW. *Fusobacterium nucleatum* promotes colorectal carcinogenesis by modulating E-cadherin/ β -catenin signaling via its FadA adhesin. *Cell Host & Microbe*. 2013;14(2):195-206. doi: 10.1016/j.chom.2013.07.012. PubMed PMID: PMC3770529.

62. Sanapareddy N, Legge RM, Jovov B, McCoy A, Burcal L, Araujo-Perez F, Randall TA, Galanko J, Benson A, Sandler RS, Rawls JF, Abdo Z, Fodor AA, Keku TO. Increased rectal microbial richness is associated with the presence of colorectal adenomas in humans. *The ISME Journal*. 2012;6(10):1858-68. Epub 2012/05/25. doi: 10.1038/ismej.2012.43. PubMed PMID: 22622349; PMCID: Pmc3446812.

63. Alam A, Leoni G, Quiros M, Wu H, Desai C, Nishio H, Jones RM, Nusrat A, Neish AS. The microenvironment of injured murine gut elicits a local pro-restitutive microbiota. *Nature Microbiology*. 2016;1(2):15021. doi: 10.1038/nmicrobiol.2015.21.

64. Zackular JP, Baxter NT, Iverson KD, Sadler WD, Petrosino JF, Chen GY, Schloss PD. The gut microbiome modulates colon tumorigenesis. *MBIO*. 2013;4(6):e00692-13. doi: 10.1128/mBio.00692-13. PubMed PMID: PMC3892781.

65. Homann N, Tillonen J, Salaspuro M. Microbially produced acetaldehyde from ethanol may increase the risk of colon cancer via folate deficiency. *International Journal of Cancer*. 2000;86(2):169-73. Epub 2000/03/30. PubMed PMID: 10738242.
66. Kinross JM, von Roon AC, Holmes E, Darzi A, Nicholson JK. The human gut microbiome: Implications for future health care. *Current Gastroenterology Reports*. 2008;10(4):396-403. doi: 10.1007/s11894-008-0075-y.
67. Garrett WS, Lord GM, Punit S, Lugo-Villarino G, Mazmanian Sarkis K, Ito S, Glickman JN, Glimcher LH. Communicable ulcerative colitis induced by T-bet deficiency in the innate immune system. *Cell*. 2007;131(1):33-45. doi: <https://doi.org/10.1016/j.cell.2007.08.017>.
68. Eckburg PB, Bik EM, Bernstein CN, Purdom E, Dethlefsen L, Sargent M, Gill SR, Nelson KE, Relman DA. Diversity of the human intestinal microbial flora. *Science*. 2005;308(5728):1635-8. Epub 2005/04/16. doi: 10.1126/science.1110591. PubMed PMID: 15831718; PMCID: PMC1395357.
69. Sekirov I, Russell SL, Antunes LC, Finlay BB. Gut microbiota in health and disease. *Physiological Reviews*. 2010;90(3):859-904. Epub 2010/07/29. doi: 10.1152/physrev.00045.2009. PubMed PMID: 20664075.
70. Weir TL, Manter DK, Sheflin AM, Barnett BA, Heuberger AL, Ryan EP. Stool microbiome and metabolome differences between colorectal cancer patients and healthy adults. *PLOS One*. 2013;8(8):e70803. Epub 2013/08/14. doi: 10.1371/journal.pone.0070803. PubMed PMID: 23940645; PMCID: PMC3735522.
71. Sears CL, Garrett WS. Microbes, microbiota and colon cancer. *Cell Host & Microbe*. 2014;15(3):317-28. doi: 10.1016/j.chom.2014.02.007. PubMed PMID: PMC4003880.
72. O'Keefe SJD, Li JV, Lahti L, Ou J, Carbonero F, Mohammed K, Posma JM, Kinross J, Wahl E, Ruder E, Vippera K, Naidoo V, Mtshali L, Tims S, Puylaert PGB, DeLany J, Krasinskas A, Benefiel AC, Kaseb HO, Newton K, Nicholson JK, de Vos WM, Gaskins HR, Zoetendal EG. Fat, fiber and cancer risk in African Americans and rural Africans. *Nature Communications*. 2015;6:6342-. doi: 10.1038/ncomms7342. PubMed PMID: PMC4415091.
73. Sobhani I, Tap J, Roudot-Thoraval F, Roperch JP, Letulle S, Langella P, Corthier G, Tran Van Nhieu J, Furet JP. Microbial dysbiosis in colorectal cancer (CRC) patients. *PLOS One*. 2011;6(1):e16393. Epub 2011/02/08. doi: 10.1371/journal.pone.0016393. PubMed PMID: 21297998; PMCID: PMC3029306.
74. Chen W, Liu F, Ling Z, Tong X, Xiang C. Human intestinal lumen and mucosa-associated microbiota in patients with colorectal cancer. *PLOS One*. 2012;7(6):e39743. doi: 10.1371/journal.pone.0039743. PubMed PMID: PMC3386193.

75. Flemer B, Lynch DB, Brown JMR, Jeffery IB, Ryan FJ, Claesson MJ, Riordain M, Shanahan F, Toole PW. Tumour-associated and non-tumour-associated microbiota in colorectal cancer. *Gut*. 2016. Apr;66(4):633-643. doi: 10.1136/gutjnl-2015-309595. Epub 2016 Mar 18.
76. Wu S, Rhee KJ, Albesiano E, Rabizadeh S, Wu X, Yen HR, Huso DL, Brancati FL, Wick E, McAllister F, Housseau F, Pardoll DM, Sears CL. A human colonic commensal promotes colon tumorigenesis via activation of T helper type 17 T cell responses. *Nature Medicine*. 2009;15(9):1016-22. Epub 2009/08/25. doi: 10.1038/nm.2015. PubMed PMID: 19701202; PMCID: PMC3034219.
77. Rhee KJ, Wu S, Wu X, Huso DL, Karim B, Franco AA, Rabizadeh S, Golub JE, Mathews LE, Shin J, Sartor RB, Golenbock D, Hamad AR, Gan CM, Housseau F, Sears CL. Induction of persistent colitis by a human commensal, enterotoxigenic *Bacteroides fragilis*, in wildtype C57BL/6 mice. *Infection & Immunity*. 2009;77(4):1708-18. Epub 2009/02/04. doi: 10.1128/iai.00814-08. PubMed PMID: 19188353; PMCID: PMC2663167.
78. Kountouras J, Kapetanakis N, Polyzos SA, Katsinelos P, Gavalas E, Tzivras D, Zeglinas C, Kountouras C, Vardaka E, Stefanidis E, Kazakos E. Active *Helicobacter pylori* infection is a risk factor for colorectal mucosa: early and advanced colonic neoplasm sequence. *Gut & Liver*. 2017;11(5):733-4. Epub 2017/07/07. doi: 10.5009/gnl16389. PubMed PMID: 28683520; PMCID: PMC5593337.
79. Huan S, Yang Z, Zou D, Dong D, Liu A, Liu W, Huang L. Rapid detection of *nusG* and *fadA* in *Fusobacterium nucleatum* by loop-mediated isothermal amplification. *Journal of Medical Microbiology*. 2016;65(1):760-769. doi: 10.1099/jmm.0.00030.
80. Abed J, Emgård JEM, Zamir G, Faroja M, Almogy G, Grenov A, Sol A, Naor R, Pikarsky E, Atlan KA, Mellul A, Chaushu S, Manson AL, Earl AM, Ou N, Brennan CA, Garrett WS, Bachrach G. Fap2 mediates *Fusobacterium nucleatum* colorectal adenocarcinoma enrichment by binding to tumor-expressed Gal-GalNAc. *Cell Host & Microbe*. 2016;20(2):215-25. doi: 10.1016/j.chom.2016.07.006. PubMed PMID: PMC5465824.
81. Shoemaker AR, Moser AR, Midgley CA, Clipson L, Newton MA, Dove WF. A resistant genetic background leading to incomplete penetrance of intestinal neoplasia and reduced loss of heterozygosity in *Apc^{Min/+}* mice. *Proceedings of the National Academy of Sciences of the United States of America*. 1998;95(18):10826.
82. Haigis KM, Hoff PD, White A, Shoemaker AR, Halberg RB, Dove WF. Tumor regionality in the mouse intestine reflects the mechanism of loss of *APC* function. *Proceedings of the National Academy of Sciences of the United States of America*. 2004;101(26):9769.
83. Amitay EL, Werner S, Vital M, Pieper DH, Hofler D, Gierse IJ, Butt J, Balavarca Y, Cuk K, Brenner H. *Fusobacterium* and colorectal cancer: causal factor or passenger?

Results from a large colorectal cancer screening study. *Carcinogenesis*. 2017;38(8):781-8. Epub 2017/06/06. doi: 10.1093/carcin/bgx053. PubMed PMID: 28582482.

84. Kremer BHA, van Steenberghe TJM. *Peptostreptococcus micros* coaggregates with *Fusobacterium nucleatum* and non-encapsulated *Porphyromonas gingivalis*. *FEMS Microbiology Letters*. 2000;182(1):57-61. doi: 10.1111/j.1574-6968.2000.tb08873.x.

85. Zeller G, Tap J, Voigt AY, Sunagawa S, Kultima JR, Costea PI, Amiot A, Bohm J, Brunetti F, Habermann N, Herczeg R, Koch M, Luciani A, Mende DR, Schneider MA, Schrotz-King P, Tournigand C, Tran Van Nhieu J, Yamada T, Zimmermann J, Benes V, Kloor M, Ulrich CM, von Knebel Doeberitz M, Sobhani I, Bork P. Potential of fecal microbiota for early-stage detection of colorectal cancer. *Molecular Systems Biology*. 2014;10:766. Epub 2014/11/30. doi: 10.15252/msb.20145645. PubMed PMID: 25432777; PMCID: PMC4299606.

86. Baxter NT, Zackular JP, Chen GY, Schloss PD. Structure of the gut microbiome following colonization with human feces determines colonic tumor burden. *Microbiome*. 2014;2:20. Epub 2014/06/27. doi: 10.1186/2049-2618-2-20. PubMed PMID: 24967088; PMCID: PMC4070349.

87. Boleij A, Muytjens CMJ, Bukhari SI, Cayet N, Glaser P, Hermans PWM, Swinkels DW, Bolhuis A, Tjalsma H. Novel clues on the specific association of *Streptococcus gallolyticus* subsp *gallolyticus* with colorectal cancer. *Journal of Infectious Diseases*. 2011;203(8):1101-9. doi: 10.1093/infdis/jiq169.

88. Dejea CM, Wick EC, Hechenbleikner EM, White JR, Mark Welch JL, Rossetti BJ, Peterson SN, Snedrud EC, Borisy GG, Lazarev M, Stein E, Vadivelu J, Roslani AC, Malik AA, Wanyiri JW, Goh KL, Thevambiga I, Fu K, Wan F, Llosa N, Housseau F, Romans K, Wu X, McAllister FM, Wu S, Vogelstein B, Kinzler KW, Pardoll DM, Sears CL. Microbiota organization is a distinct feature of proximal colorectal cancers. *Proceedings of the National Academy of Sciences of the United States of America*. 2014;111(51):18321.

89. Yu YN, Fang JY. Gut microbiota and colorectal cancer. *Gastrointestinal Tumors*. 2015;2(1):26-32.

90. Johnson CH, Dejea CM, Edler D, Hoang LT, Santidrian AF, Felding BH, Ivanisevic J, Cho K, Wick EC, Hechenbleikner EM, Uritboonthai W, Goetz L, Casero RA, Jr., Pardoll DM, White JR, Patti GJ, Sears CL, Siuzdak G. Metabolism links bacterial biofilms and colon carcinogenesis. *Cell Metabolism*. 2015;21(6):891-7. Epub 2015/05/12. doi: 10.1016/j.cmet.2015.04.011. PubMed PMID: 25959674; PMCID: PMC4456201.

91. Villanueva MT. Metabolism: Bacterial biofilms may feed colon cancer. *Nature Reviews Cancer*. 2015;15(6):320-. doi: 10.1038/nrc3970.

92. Kostic AD, Howitt MR, Garrett WS. Exploring host-microbiota interactions in animal models and humans. *Genes & Development*. 2013;27(7):701-18. Epub

2013/04/18. doi: 10.1101/gad.212522.112. PubMed PMID: 23592793; PMCID: PMC3639412.

93. Sears CL. The who, where and how of *Fusobacteria* and colon cancer. 2018;7:e28434. doi:10.7554/eLife.28434. PubMed PMID: 29533185.
94. Sekirov I, Russell SL, Antunes LCM, Finlay BB. Gut microbiota in health and disease. *Physiological Reviews*. 2010;90(3):859-904. doi: 10.1152/physrev.00045.2009.
95. Burns MB, Lynch J, Starr TK, Knights D, Blekhman R. Virulence genes are a signature of the microbiome in the colorectal tumor microenvironment. *Genome Medicine*. 2015;7(1):55. Epub 2015/07/15. doi: 10.1186/s13073-015-0177-8. PubMed PMID: 26170900; PMCID: PMC4499914.
96. Marchesi JR, Dutilh BE, Hall N, Peters WHM, Roelofs R, Boleij A, Tjalsma H. Towards the human colorectal cancer microbiome. *PLOS One*. 2011;6(5):e20447. doi: 10.1371/journal.pone.0020447.
97. Iida N, Dzutsev A, Stewart CA, Smith L, Bouladoux N, Weingarten RA, Molina DA, Salcedo R, Back T, Cramer S, Dai R-M, Kiu H, Cardone M, Naik S, Patri AK, Wang E, Marincola FM, Frank KM, Belkaid Y, Trinchieri G, Goldszmid RS. Commensal bacteria control cancer response to therapy by modulating the tumor microenvironment. *Science*. 2013;342(6161):967.
98. Swartz MA, Iida N, Roberts EW, Sangaletti S, Wong MH, Yull FE, Coussens LM, DeClerck YA. Tumor microenvironment complexity: emerging roles in cancer therapy. *Cancer Research*. 2012;72(10):2473-80. doi: 10.1158/0008-5472.can-12-0122.
99. McCarthy EF. The toxins of William B. Coley and the treatment of bone and soft-tissue sarcomas. *The Iowa Orthopaedic Journal*. 2006;26:154-8. PubMed PMID: PMC1888599.
100. Carvalho MI, Pires I, Prada J, Queiroga FL. A role for T-lymphocytes in human breast cancer and in canine mammary tumors. *BioMed Research International*. 2014;2014:11. doi: 10.1155/2014/130894.
101. Kim R, Emi M, Tanabe K. Cancer immunoediting from immune surveillance to immune escape. *Immunology*. 2007;121(1):1-14. doi: 10.1111/j.1365-2567.2007.02587.x.
102. Man YG, Stojadinovic A, Mason J, Avital I, Bilchik A, Bruecher B, Protic M, Nissan A, Izadjoo M, Zhang X, Jewett A. Tumor-infiltrating immune cells promoting tumor invasion and metastasis: existing theories. *Journal of Cancer*. 2013;4(1):84-95. Epub 2013/02/07. doi: 10.7150/jca.5482. PubMed PMID: 23386907; PMCID: Pmc3564249.

103. Cario E. Microbiota and innate immunity in intestinal inflammation and neoplasia. *Current Opinion in Gastroenterology*. 2013;29(1):85-91. Epub 2012/12/05. doi: 10.1097/MOG.0b013e32835a670e. PubMed PMID: 23207600.
104. Kuraishy A, Karin M, Grivennikov Sergei I. Tumor promotion via injury- and death-induced inflammation. *Immunity*. 2011;35(4):467-77. doi: 10.1016/j.immuni.2011.09.006.
105. Atarashi K, Tanoue T, Shima T, Imaoka A, Kuwahara T, Momose Y, Cheng G, Yamasaki S, Saito T, Ohba Y, Taniguchi T, Takeda K, Hori S, Ivanov II, Umesaki Y, Itoh K, Honda K. Induction of colonic regulatory T cells by indigenous *Clostridium* species. *Science*. 2011;331(6015):337-41. doi: 10.1126/science.1198469.
106. Scher JU, Szczesnak A, Longman RS, Segata N, Ubeda C, Bielski C, Rostron T, Cerundolo V, Pamer EG, Abramson SB, Huttenhower C, Littman DR. Expansion of intestinal *Prevotella copri* correlates with enhanced susceptibility to arthritis. *eLife*. 2013;2:e01202. doi: 10.7554/eLife.01202. PubMed PMID: PMC3816614.
107. Feldmann M, Brennan FM, Maini RN. Role of cytokines in rheumatoid arthritis. *Annual Review of Immunology*. 1996;14:397-440. Epub 1996/01/01. doi: 10.1146/annurev.immunol.14.1.397. PubMed PMID: 8717520.
108. Kawai T, Akira S. The role of pattern-recognition receptors in innate immunity: update on Toll-like receptors. *Nature Immunology*. 2010;11(5):373-84.
109. Nicaise V, Roux M, Zipfel C. Recent advances in PAMP-triggered immunity against bacteria: pattern recognition receptors watch over and raise the alarm. *Plant Physiology*. 2009;150(4):1638-47. Epub 2009/06/30. doi: 10.1104/pp.109.139709. PubMed PMID: 19561123; PMCID: Pmc2719144.
110. Mogensen TH. pathogen recognition and inflammatory signaling in innate immune defenses. *Clinical Microbiology Reviews*. 2009;22(2):240-73. doi: 10.1128/cmr.00046-08.
111. Weiss G, Maaetoft-Udsen K, Stifter SA, Hertzog P, Goriely S, Thomsen AR, Paludan SR, Frøkiær H. MyD88 drives the IFN- β response to *Lactobacillus acidophilus* in dendritic cells through a mechanism involving IRF1, IRF3, and IRF7. *The Journal of Immunology*. 2012;189(6):2860-8. doi: 10.4049/jimmunol.1103491.
112. Slingerland AE, Schwabkey Z, Wiesnoski DH, Jenq RR. clinical evidence for the microbiome in inflammatory diseases. *Frontiers in Immunology*. 2017;8:400. doi: 10.3389/fimmu.2017.00400. PubMed PMID: PMC5388779.
113. Francescone R, Hou V, Grivennikov SI. Microbiome, inflammation, and cancer. *Cancer Journal*. 2014;20(3):181-9. Epub 2014/05/24. doi: 10.1097/ppo.0000000000000048. PubMed PMID: 24855005; PMCID: PMC4112188.

114. Grivennikov SI, Wang K, Mucida D, Stewart CA, Schnabl B, Jauch D, Taniguchi K, Yu GY, Osterreicher CH, Hung KE, Datz C, Feng Y, Fearon ER, Oukka M, Tessarollo L, Coppola V, Yarovsky F, Cheroutre H, Eckmann L, Trinchieri G, Karin M. Adenoma-linked barrier defects and microbial products drive IL-23/IL-17-mediated tumour growth. *Nature*. 2012;491(7423):254-8. Epub 2012/10/05. doi: 10.1038/nature11465. PubMed PMID: 23034650; PMCID: PMC3601659.
115. Song X, Gao H, Lin Y, Yao Y, Zhu S, Wang J, Liu Y, Yao X, Meng G, Shen N, Shi Y, Iwakura Y, Qian Y. Alterations in the microbiota drive interleukin-17C production from intestinal epithelial cells to promote tumorigenesis. *Immunity*. 2014;40(1):140-52. Epub 2014/01/15. doi: 10.1016/j.immuni.2013.11.018. PubMed PMID: 24412611.
116. Dennis KL, Wang Y, Blatner NR, Wang S, Saadalla A, Trudeau E, Roers A, Weaver CT, Lee JJ, Gilbert JA, Chang EB, Khazaie K. Adenomatous polyps are driven by microbe-instigated focal inflammation and are controlled by IL-10-producing T cells. *Cancer Research*. 2013;73(19):5905-13. Epub 2013/08/21. doi: 10.1158/0008-5472.can-13-1511. PubMed PMID: 23955389; PMCID: PMC4322779.
117. Tomkovich S, Yang Y, Winglee K, Gauthier J, Muhlbauer M, Sun X, Mohamadzadeh M, Liu X, Martin P, Wang GP, Oswald E, Fodor AA, Jobin C. Locoregional effects of microbiota in a preclinical model of colon carcinogenesis. *Cancer Research*. 2017;77(10):2620-32. Epub 2017/04/19. doi: 10.1158/0008-5472.can-16-3472. PubMed PMID: 28416491; PMCID: PMC5468752.
118. Ye X, Wang R, Bhattacharya R, Boulbes DR, Fan F, Xia L, Adoni H, Ajami NJ, Wong MC, Smith DP, Petrosino JF, Venable S, Qiao W, Baladandayuthapani V, Maru D, Ellis LM. *Fusobacterium nucleatum* subspecies *animalis* influences proinflammatory cytokine expression and monocyte activation in human colorectal tumors. *Cancer Prevention Research*. 2017;10(7):398-409. Epub 2017/05/10. doi: 10.1158/1940-6207.capr-16-0178. PubMed PMID: 28483840.
119. Chen J, Pitmon E, Wang K. Microbiome, inflammation and colorectal cancer. *Seminars in Immunology*. 2017;32:43-53. doi: <https://doi.org/10.1016/j.smim.2017.09.006>.
120. Chen Y, Peng Y, Yu J, Chen T, Wu Y, Shi L, Li Q, Wu J, Fu X. Invasive *Fusobacterium nucleatum* activates beta-catenin signaling in colorectal cancer via a TLR4/P-PAK1 cascade. *Oncotarget*. 2017;8(19):31802-14. Epub 2017/04/21. doi: 10.18632/oncotarget.15992. PubMed PMID: 28423670; PMCID: PMC5458249.
121. Krych L, Hansen CH, Hansen AK, Van Den Berg FW, Nielsen DS. Quantitatively different, yet qualitatively alike: a meta-analysis of the mouse core gut microbiome with a view towards the human gut microbiome. *PLOS One*. 2013;8(5):e62578.
122. Huws SA, Edwards JE, Kim EJ, Scollan ND. Specificity and sensitivity of eubacterial primers utilized for molecular profiling of bacteria within complex microbial

ecosystems. *Journal of Microbiological Methods*. 2007;70(3): 565-569.
doi:10.1016/j.mimet.2007.06.013. PubMed PMID: 17683816.

123. Wymore Brand M, Wannemuehler MJ, Phillips GJ, Proctor A, Overstreet A-M, Jergens AE, Orcutt RP, Fox JG. The Altered Schaedler Flora: continued applications of a defined murine microbial community. *ILAR Journal*. 2015;56(2):169-78. doi: 10.1093/ilar/ilv012. PubMed PMID: PMC4554250.

124. Hart ML, Ericsson AC, Franklin CL. Differing complex microbiota alter disease severity of the IL10(-/-) mouse model of inflammatory bowel disease. *Frontiers in Microbiology*. 2017;8:792. doi: 10.3389/fmicb.2017.00792. PubMed PMID: PMC5425584.

125. Fodde R. The APC gene in colorectal cancer. *European Journal of Cancer*. 2002;38(7):867-71. Epub 2002/04/30. PubMed PMID: 11978510.

126. Fearnhead NS, Britton MP, Bodmer WF. The ABC of APC. *Human Molecular Genetics*. 2001;10(7):721-33. doi: 10.1093/hmg/10.7.721.

127. Irving AA, Yoshimi K, Hart ML, Parker T, Clipson L, Ford MR, Kuramoto T, Dove WF, Amos-Landgraf JM. The utility of Apc-mutant rats in modeling human colon cancer. *Disease Models & Mechanisms*. 2014;7(11):1215-25. doi: 10.1242/dmm.016980. PubMed PMID: PMC4213726.

128. Amos-Landgraf JM, Heijmans J, Wielenga MC, Dunkin E, Krentz KJ, Clipson L, Ederveen AG, Groothuis PG, Mosselman S, Muncan V, Hommes DW, Shedlovsky A, Dove WF, van den Brink GR. Sex disparity in colonic adenomagenesis involves promotion by male hormones, not protection by female hormones. *Proceedings of the National Academy of Sciences of the United States of America*. 2014;111(46):16514-9. Epub 2014/11/05. doi: 10.1073/pnas.1323064111. PubMed PMID: 25368192; PMCID: PMC4246303.

129. Busi SB, Lei Z, Sumner L, Amos-Landgraf J. Abstract 2400: Complex gut microbiota modulate rat colon adenoma susceptibility, metabolites, and host gene expression. *Cancer Research*. 2018;78(13 Supplement): 2400.

130. Amos-Landgraf JM, Kwong LN, Kendzioriski CM, Reichelderfer M, Torrealba J, Weichert J, Haag JD, Chen K-S, Waller JL, Gould MN, Dove WF. A target-selected Apc-mutant rat kindred enhances the modeling of familial human colon cancer. *Proceedings of the National Academy of Sciences of the United States of America*. 2007;104(10):4036-41. doi: 10.1073/pnas.0611690104. PubMed PMID: PMC1805486.

131. Ericsson AC, Akter S, Hanson MM, Busi SB, Parker TW, Schehr RJ, Hankins MA, Ahner CE, Davis JW, Franklin CL, Amos-Landgraf JM, Bryda EC. Differential susceptibility to colorectal cancer due to naturally occurring gut microbiota. *Oncotarget*. 2015;6(32):33689-704. Epub 2015/09/18. doi: 10.18632/oncotarget.5604. PubMed PMID: 26378041; PMCID: PMC4741795.

132. Li S, Konstantinov SR, Smits R, Peppelenbosch MP. Bacterial biofilms in colorectal cancer initiation and progression. *Trends in Molecular Medicine*. 2017;23(1):18-30. doi: <https://doi.org/10.1016/j.molmed.2016.11.004>.
133. Dickson I. Colorectal cancer: Bacterial biofilms and toxins prompt a perfect storm for colon cancer. *Nature Reviews Gastroenterology & Hepatology*. 2018;15(3):129. Epub 2018/02/24. doi: 10.1038/nrgastro.2018.16. PubMed PMID: 29472633.
134. Johnson Caroline H, Dejea Christine M, Edler D, Hoang Linh T, Santidrian Antonio F, Felding Brunhilde H, Ivanisevic J, Cho K, Wick Elizabeth C, Hechenbleikner Elizabeth M, Uritboonthai W, Goetz L, Casero Robert A, Jr., Pardoll Drew M, White James R, Patti Gary J, Sears Cynthia L, Siuzdak G. Metabolism links bacterial biofilms and colon carcinogenesis. *Cell Metabolism*. 2015;21(6):891-7. doi: 10.1016/j.cmet.2015.04.011.
135. Dejea CM, Fathi P, Craig JM, Boleij A, Taddese R, Geis AL, Wu X, DeStefano Shields CE, Hechenbleikner EM, Huso DL, Anders RA, Giardiello FM, Wick EC, Wang H, Wu S, Pardoll DM, Housseau F, Sears CL. Patients with familial adenomatous polyposis harbor colonic biofilms containing tumorigenic bacteria. *Science*. 2018;359(6375):592.
136. Drewes JL, White JR, Dejea CM, Fathi P, Iyadorai T, Vadivelu J, Roslani AC, Wick EC, Mongodin EF, Loke MF, Thulasi K, Gan HM, Goh KL, Chong HY, Kumar S, Wanyiri JW, Sears CL. High-resolution bacterial 16S rRNA gene profile meta-analysis and biofilm status reveal common colorectal cancer consortia. *NPJ Biofilms & Microbiomes*. 2017;3(1):34. doi: 10.1038/s41522-017-0040-3.
137. Donlan RM. Biofilms: microbial life on surfaces. *Emerging Infectious Diseases*. 2002;8(9):881-90. doi: 10.3201/eid0809.020063. PubMed PMID: PMC2732559.
138. Macfarlane S, McBain AJ, Macfarlane GT. Consequences of biofilm and sessile growth in the large intestine. *Advances in Dental Research*. 1997;11(1):59-68. doi: 10.1177/08959374970110011801.
139. Passalacqua KD, Charbonneau M-E, O'Riordan MXD. Bacterial metabolism shapes the host:pathogen interface. *Microbiology Spectrum*. 2016;4(3):10.1128/microbiolspec.VMBF-0027-2015. doi: 10.1128/microbiolspec.VMBF-0027-2015. PubMed PMID: PMC4922512.
140. Wong ACN, Vanhove AS, Watnick PI. The interplay between intestinal bacteria and host metabolism in health and disease: lessons from *Drosophila melanogaster*. *Disease Models & Mechanisms*. 2016;9(3):271-81. doi: 10.1242/dmm.023408. PubMed PMID: PMC4833331.
141. Theriot CM, Bowman AA, Young VB. Antibiotic-induced alterations of the gut microbiota alter secondary bile acid production and allow for *Clostridium difficile* spore germination and outgrowth in the large intestine. *mSphere*. 2016;1(1). pii: e00045-15. doi: 10.1128/mSphere.00045-15. PubMed PMID: PMCID: PMC4863611

142. Shaffer M, Armstrong AJS, Phelan VV, Reisdorph N, Lozupone CA. Microbiome and metabolome data integration provides insight into health and disease. *Translational Research*. 2017;189:51-64. doi: <https://doi.org/10.1016/j.trsl.2017.07.001>.
143. Antunes LCM, Han J, Ferreira RBR, Lolić P, Borchers CH, Finlay BB. Effect of antibiotic treatment on the intestinal metabolome. *Antimicrobial Agents & Chemotherapy*. 2011;55(4):1494-503. doi: 10.1128/AAC.01664-10.
144. Pedersen HK, Gudmundsdottir V, Nielsen HB, Hyotylainen T, Nielsen T, Jensen BAH, Forslund K, Hildebrand F, Prifti E, Falony G, Le Chatelier E, Levenez F, Doré J, Mattila I, Plichta DR, Pöhö P, Hellgren LI, Arumugam M, Sunagawa S, Vieira-Silva S, Jørgensen T, Holm JB, Trošt K, Consortium M, Kristiansen K, Brix S, Raes J, Wang J, Hansen T, Bork P, Brunak S, Oresic M, Ehrlich SD, Pedersen O. Human gut microbes impact host serum metabolome and insulin sensitivity. *Nature*. 2016;535:376. doi: 10.1038/nature18646 <https://www.nature.com/articles/nature18646#supplementary-information>.
145. Brahe LK, Le Chatelier E, Prifti E, Pons N, Kennedy S, Hansen T, Pedersen O, Astrup A, Ehrlich SD, Larsen LH. Specific gut microbiota features and metabolic markers in postmenopausal women with obesity. *Nutrition & Diabetes*. 2015;5:e159. doi: 10.1038/nutd.2015.9 <https://www.nature.com/articles/nutd20159#supplementary-information>.
146. Paul B, Barnes S, Demark-Wahnefried W, Morrow C, Salvador C, Skibola C, Tollefsbol TO. Influences of diet and the gut microbiome on epigenetic modulation in cancer and other diseases. *Clinical Epigenetics*. 2015;7:112. doi: 10.1186/s13148-015-0144-7. PubMed PMID: PMC4609101.
147. Wang G, Li W, Chen Q, Jiang Y, Lu X, Zhao X. Hydrogen sulfide accelerates wound healing in diabetic rats. *International Journal of Clinical & Experimental Pathology*. 2015;8(5):5097-104. Epub 2015/07/21. PubMed PMID: 26191204; PMCID: Pmc4503076.
148. Belcheva A, Irrazabal T, Robertson SJ, Streutker C, Maughan H, Rubino S, Moriyama EH, Copeland JK, Kumar S, Green B, Geddes K, Pezo RC, Navarre WW, Milosevic M, Wilson BC, Girardin SE, Wolever TM, Edelmann W, Guttman DS, Philpott DJ, Martin A. Gut microbial metabolism drives transformation of MSH2-deficient colon epithelial cells. *Cell*. 2014;158(2):288-99. doi: 10.1016/j.cell.2014.04.051. PubMed PMID: 25036629.
149. Bhandari A, Woodhouse M, Gupta S. Colorectal cancer is a leading cause of cancer incidence and mortality among adults younger than 50 years in the USA: a SEER-based analysis with comparison to other young-onset cancers. *Journal of Investigative Medicine: the official publication of the American Federation for Clinical Research*. 2017;65(2):311-5. doi: 10.1136/jim-2016-000229. PubMed PMID: PMC5564445.
150. Amos-Landgraf JM, Irving AA, Hartman C, Hunter A, Laube B, Chen X, Clipson L, Newton MA, Dove WF. Monoallelic silencing and haploinsufficiency in early murine

intestinal neoplasms. Proceedings of the National Academy of Sciences of the United States of America. 2012;109(6):2060-5. doi: 10.1073/pnas.1120753109. PubMed PMID: PMC3277532.

151. Zackular JP, Baxter NT, Chen GY, Schloss PD. Manipulation of the gut microbiota reveals role in colon tumorigenesis. *mSphere*. 2016;1(1):e00001-15. doi: 10.1128/mSphere.00001-15. PubMed PMID: PMC4863627.

152. Yang I, Eibach D, Kops F, Brenneke B, Woltemate S, Schulze J, Bleich A, Gruber AD, Muthupalani S, Fox JG, Josenhans C, Suerbaum S. Intestinal microbiota composition of Interleukin-10 deficient C57BL/6J mice and susceptibility to *Helicobacter hepaticus*-induced colitis. *PLOS One*. 2013;8(8):e70783. doi: 10.1371/journal.pone.0070783. PubMed PMID: PMC3739778.

153. Contreras AV, Cocom-Chan B, Hernandez-Montes G, Portillo-Bobadilla T, Resendis-Antonio O. Host-microbiome interaction and cancer: potential application in precision medicine. *Frontiers in Physiology*. 2016;7:606. doi: 10.3389/fphys.2016.00606. PubMed PMID: PMC5145879.

154. Baxter NT, Koumpouras CC, Rogers MAM, Ruffin MT, Schloss PD. DNA from fecal immunochemical test can replace stool for detection of colonic lesions using a microbiota-based model. *Microbiome*. 2016;4:59. doi: 10.1186/s40168-016-0205-y. PubMed PMID: PMC5109736.

155. Flemer B, Gaci N, Borrel G, Sanderson IR, Chaudhary PP, Tottey W, O'Toole PW, Brugere JF. Fecal microbiota variation across the lifespan of the healthy laboratory rat. *Gut Microbes*. 2017:0. Epub 2017/06/07. doi: 10.1080/19490976.2017.1334033. PubMed PMID: 28586297.

156. Dewhirst FE, Chen T, Izard J, Paster BJ, Tanner ACR, Yu W-H, Lakshmanan A, Wade WG. The human oral microbiome. *Journal of Bacteriology*. 2010;192(19):5002-17. doi: 10.1128/JB.00542-10. PubMed PMID: PMC2944498.

157. Signat B, Roques C, Poulet P, Duffaut D. *Fusobacterium nucleatum* in periodontal health and disease. *Current Issues in Molecular Biology*. 2011;13(2):25-36. Epub 2011/01/12. PubMed PMID: 21220789.

158. Castellarin M, Warren RL, Freeman JD, Dreolini L, Krzywinski M, Strauss J, Barnes R, Watson P, Allen-Vercoe E, Moore RA, Holt RA. *Fusobacterium nucleatum* infection is prevalent in human colorectal carcinoma. *Genome Research*. 2012;22(2):299-306. doi: 10.1101/gr.126516.111. PubMed PMID: PMC3266037.

159. Mima K, Sukawa Y, Nishihara R, Qian ZR, Yamauchi M, Inamura K, Kim SA, Masuda A, Nowak JA, Nosho K, Kostic AD, Giannakis M, Watanabe H, Bullman S, Milner DA, Harris CC, Giovannucci E, Garraway LA, Freeman GJ, Dranoff G, Chan AT, Garrett WS, Huttenhower C, Fuchs CS, Ogino S. *Fusobacterium nucleatum* and T cells in colorectal carcinoma. *JAMA Oncology*. 2015;1(5):653-61. Epub 2015/07/17. doi: 10.1001/jamaoncol.2015.1377. PubMed PMID: 26181352; PMCID: PMC4537376.

160. Ray K. Colorectal cancer: *Fusobacterium nucleatum* found in colon cancer tissue could an infection cause colorectal cancer? Nature Reviews Gastroenterology & Hepatology. 2011;8(12):662-.
161. Ou J, Carbonero F, Zoetendal EG, DeLany JP, Wang M, Newton K, Gaskins HR, O'Keefe SJD. Diet, microbiota, and microbial metabolites in colon cancer risk in rural Africans and African Americans. The American Journal of Clinical Nutrition. 2013;98(1):111-20. doi: 10.3945/ajcn.112.056689. PubMed PMID: PMC3683814.
162. Li M, Rao M, Chen K, Zhou J, Song J. Selection of reference genes for gene expression studies in heart failure for left and right ventricles. Gene. 2017;620:30-5. Epub 2017/04/10. doi: 10.1016/j.gene.2017.04.006. PubMed PMID: 28390990.
163. Xu K, Jiang B. Analysis of mucosa-associated microbiota in colorectal cancer. Medical Science Monitor: international medical journal of Experimental & Clinical Research. 2017;23:4422-30. doi: 10.12659/MSM.904220. PubMed PMID: PMC5609654.
164. Shoemaker AR, Moser AR, Midgley CA, Clipson L, Newton MA, Dove WF. A resistant genetic background leading to incomplete penetrance of intestinal neoplasia and reduced loss of heterozygosity in *Apc*^{(Min)/+} mice. Proceedings of the National Academy of Sciences of the United States of America. 1998;95(18):10826-31. PubMed PMID: PMC27980.
165. Cheung AF, Carter AM, Kostova KK, Woodruff JF, Crowley D, Bronson RT, Haigis KM, Jacks T Complete deletion of *Apc* results in severe polyposis in mice. Oncogene. 2010;29(12), 1857-1864. doi:10.1038/onc.2009.457.
166. Truett GE, Heeger P, Mynatt RL, Truett AA, Walker JA, Warman ML. Preparation of PCR-quality mouse genomic DNA with hot sodium hydroxide and tris (HotSHOT). BioTechniques. 2000;29(1):52, 4. Epub 2000/07/25. PubMed PMID: 10907076.
167. Irving AA, Young LB, Pleiman JK, Konrath MJ, Marzella B, Nonte M, Cacciatore J, Ford MR, Clipson L, Amos-Landgraf JM, Dove WF. A simple, quantitative method using alginate gel to determine rat colonic tumor volume in vivo. Comparative Medicine. 2014;64(2):128-34. Epub 2014/03/29. PubMed PMID: 24674588; PMCID: PMC3997291.
168. Schneider CA, Rasband WS, Eliceiri KW. NIH Image to ImageJ: 25 years of image analysis. Nature Methods. 2012;9(7):671-5. Epub 2012/08/30. PubMed PMID: 22930834.
169. Langille MG. Exploring linkages between taxonomic and functional profiles of the human microbiome. mSystems. 2018;3(2)e00163-17. doi: <https://doi.org/10.1128/mSystems.00163-17>.

170. Yu J, Chen Y, Fu X, Zhou X, Peng Y, Shi L, Chen T, Wu Y. Invasive *Fusobacterium nucleatum* may play a role in the carcinogenesis of proximal colon cancer through the serrated neoplasia pathway. *International Journal of Cancer*. 2016;139(6):1318-26. Epub 2016/05/01. doi: 10.1002/ijc.30168. PubMed PMID: 27130618.
171. Tahara T, Yamamoto E, Suzuki H, Maruyama R, Chung W, Garriga J, Jelinek J, Yamano HO, Sugai T, An B, Shureiqi I, Toyota M, Kondo Y, Estecio MR, Issa JP. *Fusobacterium* in colonic flora and molecular features of colorectal carcinoma. *Cancer Research*. 2014;74(5):1311-8. Epub 2014/01/05. doi: 10.1158/0008-5472.can-13-1865. PubMed PMID: 24385213; PMCID: PMC4396185.
172. Gur C, Ibrahim Y, Isaacson B, Yamin R, Abed J, Gamliel M, Enk J, Bar-On Y, Stanietsky-Kaynan N, Copenhagen-Glazer S, Shussman N, Almogy G, Cuapio A, Hofer E, Mevorach D, Tabib A, Ortenberg R, Markel G, Miklic K, Jonjic S, Brennan CA, Garrett WS, Bachrach G, Mandelboim O. Binding of the Fap2 protein of *Fusobacterium nucleatum* to human inhibitory receptor TIGIT protects tumors from immune cell attack. *Immunity*. 2015;42(2):344-55. Epub 2015/02/15. doi: 10.1016/j.immuni.2015.01.010. PubMed PMID: 25680274; PMCID: PMC4361732.
173. Bullman S, Peadarallu CS, Sicinska E, Clancy TE, Zhang X, Cai D, Neuberger D, Huang K, Guevara F, Nelson T, Chipashvili O, Hagan T, Walker M, Ramachandran A, Diosdado B, Serna G, Mulet N, Landolfi S, Ramon YCS, Fasani R, Aguirre AJ, Ng K, Elez E, Ogino S, Taberner J, Fuchs CS, Hahn WC, Nuciforo P, Meyerson M. Analysis of *Fusobacterium* persistence and antibiotic response in colorectal cancer. *Science*. 2017;358(6369):1443-8. Epub 2017/11/25. doi: 10.1126/science.aal5240. PubMed PMID: 29170280; PMCID: PMC5823247.
174. Akin H, Tozun N. Diet, microbiota, and colorectal cancer. *Journal of Clinical Gastroenterology*. 2014;48 Suppl 1:S67-9. Epub 2014/10/08. doi: 10.1097/mcg.0000000000000252. PubMed PMID: 25291132.
175. Su T, Liu R, Lee A, Long Y, Du L, Lai S, Chen X, Wang L, Si J, Owyang C, Chen S. Altered intestinal microbiota with increased abundance of *Prevotella* is associated with high risk of diarrhea-predominant irritable bowel syndrome. *Gastroenterology Research & Practice*. 2018;2018:6961783. doi: 10.1155/2018/6961783. PubMed PMID: PMC6008816.
176. Allali I, Boukhatem N, Bouguenouch L, Hardi H, Boudouaya HA, Cadenas MB, Ouldin K, Amzazi S, Azcarate-Peril MA, Ghazal H. Gut microbiome of Moroccan colorectal cancer patients. *Medical Microbiology & Immunology*. 2018; 207(3), 211-225. doi:10.1007/s00430-018-0542-5
177. Kim HS, Lee DS, Chang YH, Kim MJ, Koh S, Kim J, Seong JH, Song SK, Shin HS, Son JB, Jung MY, Park SN, Yoo SY, Cho KW, Kim DK, Moon S, Kim D, Choi Y, Kim BO, Jang HS, Kim CS, Kim C, Choe SJ, Kook JK. Application of *rpoB* and zinc protease gene for use in molecular discrimination of *Fusobacterium nucleatum*

subspecies. *Journal of Clinical Microbiology*. 2010;48(2):545-53. Epub 2009/12/04. doi: 10.1128/jcm.01631-09. PubMed PMID: 19955278; PMCID: PMC2815611.

178. Komiya Y, Shimomura Y, Higurashi T, Sugi Y, Arimoto J, Umezawa S, Uchiyama S, Matsumoto M, Nakajima A. Patients with colorectal cancer have identical strains of *Fusobacterium nucleatum* in their colorectal cancer and oral cavity. *Gut*. 2018. Jun 22. pii: gutjnl-2018-316661. doi: 10.1136/gutjnl-2018-316661.

179. Viljoen KS, Dakshinamurthy A, Goldberg P, Blackburn JM. Quantitative profiling of colorectal cancer-associated bacteria reveals associations between *Fusobacterium* spp., enterotoxigenic *Bacteroides fragilis* (ETBF) and clinicopathological features of colorectal cancer. *PLOS One*. 2015;10(3):e0119462. Epub 2015/03/10. doi: 10.1371/journal.pone.0119462. PubMed PMID: 25751261; PMCID: PMC4353626.

180. Al-hebshi NN, Nasher AT, Maryoud MY, Homeida HE, Chen T, Idris AM, Johnson NW. Inflammatory bacteriome featuring *Fusobacterium nucleatum* and *Pseudomonas aeruginosa* identified in association with oral squamous cell carcinoma. *Scientific Reports*. 2017;7(1):1834. doi: 10.1038/s41598-017-02079-3.

181. Shang FM, Liu HL. *Fusobacterium nucleatum* and colorectal cancer: a review. *World Journal of Gastrointestinal Oncology*. 2018;10(3), 71-81. doi:10.4251/wjgo.v10.i3.71. PubMed PMID: 29564037.

182. Han YW, Ikegami A, Rajanna C, Kawsar HI, Zhou Y, Li M, Sojar HT, Genco RJ, Kuramitsu HK, Deng CX. Identification and characterization of a novel adhesin unique to oral *Fusobacteria*. *Journal of Bacteriology*. 2005;187(15):5330.

183. Copenhagen-Glazer S, Sol A, Abed J, Naor R, Zhang X, Han YW, Bachrach G. Fap2 of *Fusobacterium nucleatum* is a galactose-inhibitable adhesin involved in coaggregation, cell adhesion, and preterm birth. *Infection & Immunity*. 2015;83(3):1104-13. doi: 10.1128/IAI.02838-14. PubMed PMID: PMC4333458.

184. de Theije CG, Wopereis H, Ramadan M, van Eijndthoven T, Lambert J, Knol J, Garssen J, Kraneveld AD, Oozeer R. Altered gut microbiota and activity in a murine model of autism spectrum disorders. *Brain, Behavior & Immunity*. 2014;37:197-206. Epub 2013/12/18. doi: 10.1016/j.bbi.2013.12.005. PubMed PMID: 24333160.

185. Nguyen TL, Vieira-Silva S, Liston A, Raes J. How informative is the mouse for human gut microbiota research? *Disease Models & Mechanisms*. 2015;8(1):1-16. Epub 2015/01/07. doi: 10.1242/dmm.017400. PubMed PMID: 25561744; PMCID: PMC4283646.

186. Org E, Mehrabian M, Lusic AJ. Unraveling the environmental and genetic interactions in atherosclerosis: central role of the gut microbiota. *Atherosclerosis*. 2015;241(2):387-99. Epub 2015/06/15. doi: 10.1016/j.atherosclerosis.2015.05.035. PubMed PMID: 26071662; PMCID: PMC4510029.

187. Palau-Rodriguez M, Tulipani S, Isabel Queipo-Ortuno M, Urpi-Sarda M, Tinahones FJ, Andres-Lacueva C. Metabolomic insights into the intricate gut microbial-host interaction in the development of obesity and type 2 diabetes. *Frontiers in Microbiology*. 2015;6:1151. Epub 2015/11/19. doi: 10.3389/fmicb.2015.01151. PubMed PMID: 26579078; PMCID: PMC4621279.
188. Amos-Landgraf JM, Kwong LN, Kendzioriski CM, Reichelderfer M, Torrealba J, Weichert J, Haag JD, Chen KS, Waller JL, Gould MN, Dove WF. A target-selected Apc-mutant rat kindred enhances the modeling of familial human colon cancer. *Proceedings of the National Academy of Sciences of the United States of America*. 2007;104(10):4036-41. Epub 2007/03/16. doi: 10.1073/pnas.0611690104. PubMed PMID: 17360473; PMCID: PMC1805486.
189. Bashir A, Miskeen AY, Bhat A, Fazili KM, Ganai BA. *Fusobacterium nucleatum*: an emerging bug in colorectal tumorigenesis. *European Journal of Cancer Prevention: the official journal of the European Cancer Prevention Organisation (ECP)*. 2015;24(5):373-85. Epub 2015/01/09. doi: 10.1097/cej.000000000000116. PubMed PMID: 25569450.
190. Repass J. Replication study: *Fusobacterium nucleatum* infection is prevalent in human colorectal carcinoma. *eLife* 2018;7:e25801 doi: 10.7554/eLife.25801.
191. Flanagan L, Schmid J, Ebert M, Soucek P, Kunicka T, Liska V, Bruha J, Neary P, Dezeeuw N, Tommasino M, Jenab M, Prehn JH, Hughes DJ. *Fusobacterium nucleatum* associates with stages of colorectal neoplasia development, colorectal cancer and disease outcome. *European Journal of Clinical Microbiology & Infectious Diseases: official publication of the European Society of Clinical Microbiology*. 2014;33(8):1381-90. Epub 2014/03/07. doi: 10.1007/s10096-014-2081-3. PubMed PMID: 24599709.
192. Han YW. *Fusobacterium nucleatum*: a commensal-turned pathogen. *Current Opinion in Microbiology*. 2015;23:141-7. Epub 2015/01/13. doi: 10.1016/j.mib.2014.11.013. PubMed PMID: 25576662; PMCID: PMC4323942.
193. Keku TO, McCoy AN, Azcarate-Peril AM. *Fusobacterium* spp. and colorectal cancer: cause or consequence? *Trends in Microbiology*. 2013;21(10):506-8. Epub 2013/09/14. doi: 10.1016/j.tim.2013.08.004. PubMed PMID: 24029382; PMCID: PMC3836616.
194. Rubinstein MR, Wang X, Liu W, Hao Y, Cai G, Han YW. *Fusobacterium nucleatum* promotes colorectal carcinogenesis by modulating E-cadherin/beta-catenin signaling via its FadA adhesin. *Cell Host & Microbe*. 2013;14(2):195-206. Epub 2013/08/21. doi: 10.1016/j.chom.2013.07.012. PubMed PMID: 23954158; PMCID: PMC3770529.
195. Yu YN, Yu TC, Zhao HJ, Sun TT, Chen HM, Chen HY, An HF, Weng YR, Yu J, Li M, Qin WX, Ma X, Shen N, Hong J, Fang JY. Berberine may rescue *Fusobacterium nucleatum*-induced colorectal tumorigenesis by modulating the tumor microenvironment. *Oncotarget*. 2015;6(31):32013-26. Epub 2015/09/24. doi: 10.18632/oncotarget.5166. PubMed PMID: 26397137; PMCID: PMC4741656.

196. Mandal S, Mandal A, Park MH. Depletion of the polyamines spermidine and spermine by overexpression of spermidine/spermine N(1)-acetyltransferase1 (SAT1) leads to mitochondria-mediated apoptosis in mammalian cells. *The Biochemical Journal*. 2015;468(3):435-47. doi: 10.1042/BJ20150168. PubMed PMID: PMC4550555.
197. Blachier F, Davila AM, Benamouzig R, Tome D. Channelling of arginine in NO and polyamine pathways in colonocytes and consequences. *Frontiers in Bioscience (Landmark edition)*. 2011;16:1331-43. Epub 2011/01/05. PubMed PMID: 21196235.
198. Loser C, Folsch UR, Paprotny C, Creutzfeldt W. Polyamines in colorectal cancer. Evaluation of polyamine concentrations in the colon tissue, serum, and urine of 50 patients with colorectal cancer. *Cancer*. 1990;65(4):958-66. Epub 1990/02/15. PubMed PMID: 2297664.
199. Wishart DS, Mandal R, Stanislaus A, Ramirez-Gaona M. Cancer metabolomics and the human metabolome database. *Metabolites*. 2016;6(1):10. doi: 10.3390/metabo6010010. PubMed PMID: PMC4812339.
200. Zhao T, Mu X, You Q. Succinate: An initiator in tumorigenesis and progression. *Oncotarget*. 2017;8(32):53819-28. doi: 10.18632/oncotarget.17734. PubMed PMID: PMC5581152.
201. Zhang D, Wang W, Xiang B, Li N, Huang S, Zhou W, Sun Y, Wang X, Ma J, Li G, Li X, Shen S. Reduced succinate dehydrogenase B expression is associated with growth and de-differentiation of colorectal cancer cells. *Tumour Biology: the journal of the International Society for Oncodevelopmental Biology & Medicine*. 2013;34(4):2337-47. Epub 2013/05/07. doi: 10.1007/s13277-013-0781-4. PubMed PMID: 23645213.
202. Tseng P-L, Wu W-H, Hu T-H, Chen C-W, Cheng H-C, Li C-F, Tsai W-H, Tsai H-J, Hsieh M-C, Chuang J-H, Chang W-T. Decreased succinate dehydrogenase B in human hepatocellular carcinoma accelerates tumor malignancy by inducing the Warburg effect. *Scientific Reports*. 2018;8(1):3081. doi: 10.1038/s41598-018-21361-6.
203. Garrigue P, Bodin-Hullin A, Balasse L, Fernandez S, Essamet W, Dignat-George F, Pacak K, Guillet B, Taieb D. The evolving role of succinate in tumor metabolism: an (18)F-FDG-based study. *Journal of Nuclear Medicine: official publication, Society of Nuclear Medicine*. 2017;58(11):1749-55. Epub 2017/06/18. doi: 10.2967/jnumed.117.192674. PubMed PMID: 28619735.
204. Esquivel-Elizondo S, Ilhan ZE, Garcia-Peña EI, Krajmalnik-Brown R. Insights into butyrate production in a controlled fermentation system via gene predictions. *mSystems*. 2017;2(4):e00051-17. doi: 10.1128/mSystems.00051-17. PubMed PMID: PMC5516221.
205. Falony G, Verschaeren A, De Bruycker F, De Preter V, Verbeke K, Leroy F, De Vuyst L. In vitro kinetics of prebiotic inulin-type fructan fermentation by butyrate-producing colon bacteria: implementation of online gas chromatography for quantitative analysis of carbon dioxide and hydrogen gas production. *Applied & Environmental*

- Microbiology. 2009; Sep;75(18):5884-92. doi: 10.1128/AEM.00876-09. Epub 2009 Jul 24.
206. Dwidar M, Park J-Y, Mitchell RJ, Sang B-I. The future of butyric acid in industry. *The Scientific World Journal*. 2012;2012:471417. doi: 10.1100/2012/471417. PubMed PMID: PMC3349206.
207. Hibberd AA, Lyra A, Ouwehand AC, Rolny P, Lindegren H, Cedgård L, Wettergren Y. Intestinal microbiota is altered in patients with colon cancer and modified by probiotic intervention. *BMJ Open Gastroenterology*. 2017;4(1):e000145. doi: 10.1136/bmjgast-2017-000145. PubMed PMID: PMC5609083.
208. Tian Y, Wang K, Ji G. *Faecalibacterium prausnitzii* prevents tumorigenesis in a model of colitis-associated colorectal cancer. *Gastroenterology*. 2017;152(5):S354-S5. doi: 10.1016/S0016-5085(17)31445-2.
209. Le Leu RK, Hu Y, Brown IL, Woodman RJ, Young GP. Synbiotic intervention of *Bifidobacterium lactis* and resistant starch protects against colorectal cancer development in rats. *Carcinogenesis*. 2010;31(2):246-51. Epub 2009/08/22. doi: 10.1093/carcin/bgp197. PubMed PMID: 19696163.
210. Thomas AM, Jesus EC, Lopes A, Aguiar S, Jr., Begnami MD, Rocha RM, Carpinetti PA, Camargo AA, Hoffmann C, Freitas HC, Silva IT, Nunes DN, Setubal JC, Dias-Neto E. Tissue-associated bacterial alterations in rectal carcinoma patients revealed by 16S rRNA community profiling. *Frontiers in Cellular & Infection Microbiology*. 2016;6:179. Epub 2016/12/27. doi: 10.3389/fcimb.2016.00179. PubMed PMID: 28018861; PMCID: PMC5145865.
211. Wang X, Wang J, Rao B, Deng L. Gut flora profiling and fecal metabolite composition of colorectal cancer patients and healthy individuals. *Experimental & Therapeutic Medicine*. 2017;13(6):2848-54. doi: 10.3892/etm.2017.4367. PubMed PMID: PMC5450625.
212. Shaw KA, Bertha M, Hofmekler T, Chopra P, Vatanen T, Srivatsa A, Prince J, Kumar A, Sauer C, Zwick ME, Satten GA, Kostic AD, Mulle JG, Xavier RJ, Kugathasan S. Dysbiosis, inflammation, and response to treatment: a longitudinal study of pediatric subjects with newly diagnosed inflammatory bowel disease. *Genome Medicine*. 2016;8(1):75. doi: 10.1186/s13073-016-0331-y.
213. Marquet P, Duncan SH, Chassard C, Bernalier-Donadille A, Flint HJ. Lactate has the potential to promote hydrogen sulphide formation in the human colon. *FEMS Microbiology Letters*. 2009;299(2):128-34. doi: 10.1111/j.1574-6968.2009.01750.x.
214. Zhao L, Zhang X, Zuo T, Yu J. the composition of colonic commensal bacteria according to anatomical localization in colorectal cancer. *Engineering*. 2017;3(1):90-7. doi: <https://doi.org/10.1016/J.ENG.2017.01.012>.

215. Kverka M, Zakostelska Z, Klimesova K, Sokol D, Hudcovic T, Hrnčir T, Rossmann P, Mrazek J, Kopecny J, Verdu EF, Tlaskalova-Hogenova H. Oral administration of *Parabacteroides distasonis* antigens attenuates experimental murine colitis through modulation of immunity and microbiota composition. *Clinical & Experimental Immunology*. 2011;163(2):250-9. doi: 10.1111/j.1365-2249.2010.04286.x.
216. Moens F, Verce M, De Vuyst L. Lactate- and acetate-based cross-feeding interactions between selected strains of *Lactobacilli*, *Bifidobacteria* and colon bacteria in the presence of inulin-type fructans. *International Journal of Food Microbiology*. 2017;241:225-36. Epub 2016/11/05. doi: 10.1016/j.ijfoodmicro.2016.10.019. PubMed PMID: 27810444.
217. Wu YC, Wang XJ, Yu L, Chan FKL, Cheng ASL, Yu J, Sung JJY, Wu WKK, Cho CH. Hydrogen sulfide lowers proliferation and induces protective autophagy in colon epithelial cells. *PLOS One*. 2012;7(5):e37572. doi: 10.1371/journal.pone.0037572.
218. Bashir A, Miskeen AY, Hazari YM, Asrafuzzaman S, Fazili KM. *Fusobacterium nucleatum*, inflammation, and immunity: the fire within human gut. *Tumour Biology: the journal of the International Society for Oncodevelopmental Biology & Medicine*. 2016;37(3):2805-10. Epub 2016/01/01. doi: 10.1007/s13277-015-4724-0. PubMed PMID: 26718210.
219. Brennan CA, Garrett WS. Gut microbiota, inflammation, and colorectal cancer. *Annual Review of Microbiology*. 2016;70:395-411. Epub 2016/09/09. doi: 10.1146/annurev-micro-102215-095513. PubMed PMID: 27607555; PMCID: PMC5541233.
220. Yu T, Guo F, Yu Y, Sun T, Ma D, Han J, Qian Y, Kryczek I, Sun D, Nagarsheth N, Chen Y, Chen H, Hong J, Zou W, Fang JY. *Fusobacterium nucleatum* promotes chemoresistance to colorectal cancer by modulating autophagy. *Cell*. 2017;170(3):548-63.e16. Epub 2017/07/29. doi: 10.1016/j.cell.2017.07.008. PubMed PMID: 28753429; PMCID: PMC5767127.
221. Nabhani AZ, Eberl G. GAPS in early life facilitate immune tolerance. *Science Immunology*. 2017;2(18). Epub 2017/12/17. doi: 10.1126/sciimmunol.aar2465. PubMed PMID: 29246947.
222. Knoop KA, Gustafsson JK, McDonald KG, Kulkarni DH, Coughlin PE, McCrate S, Kim D, Hsieh CS, Hogan SP, Elson CO, Tarr PI, Newberry RD. Microbial antigen encounter during a preweaning interval is critical for tolerance to gut bacteria. *Science Immunology*. 2017;2(18). Epub 2017/12/17. doi: 10.1126/sciimmunol.aao1314. PubMed PMID: 29246946; PMCID: PMC5759965.
223. Nepelska M, de Wouters T, Jacouton E, Béguet-Crespel F, Lapaque N, Doré J, Arulampalam V, Blottière HM. Commensal gut bacteria modulate phosphorylation-dependent PPAR γ transcriptional activity in human intestinal epithelial cells. *Scientific Reports*. 2017;7:43199. doi: 10.1038/srep43199. PubMed PMID: PMC5339702.

224. Pianta A, Arvikar S, Strle K, Drouin EE, Wang Q, Costello CE, Steere AC. Evidence for immune relevance of *Prevotella copri*, a gut microbe, in patients with rheumatoid arthritis. *Arthritis & Rheumatology (Hoboken, NJ)*. 2017;69(5):964-75. doi: 10.1002/art.40003. PubMed PMID: PMC5406252.
225. Larsen JM. The immune response to *Prevotella* bacteria in chronic inflammatory disease. *Immunology*. 2017;151(4):363-74. doi: 10.1111/imm.12760. PubMed PMID: PMC5506432.
226. Yang L, Liu H, Zhang L, Hu J, Chen H, Wang L, Yin X, Li Q, Qi Y. Effect of IL-17 in the development of colon cancer in mice. *Oncology Letters*. 2016;12(6):4929-36. doi: 10.3892/ol.2016.5329. PubMed PMID: PMC5228117.
227. Amicarella F, Muraro MG, Hirt C, Cremonesi E, Padovan E, Mele V, Governa V, Han J, Huber X, Droeser RA, Zuber M, Adamina M, Bolli M, Rosso R, Lugli A, Zlobec I, Terracciano L, Tornillo L, Zajac P, Eppenberger-Castori S, Trapani F, Oertli D, Iezzi G. Dual role of tumour-infiltrating T helper 17 cells in human colorectal cancer. *Gut*. 2017;66(4):692-704. doi: 10.1136/gutjnl-2015-310016. PubMed PMID: PMC5529969
228. Benatar T, Cao MY, Lee Y, Lightfoot J, Feng N, Gu X, Lee V, Jin H, Wang M, Wright JA, Young AH. IL-17E, a proinflammatory cytokine, has antitumor efficacy against several tumor types in vivo. *Cancer Immunology, Immunotherapy*. 2010;59(6):805-17. Epub 2009/12/17. doi: 10.1007/s00262-009-0802-8. PubMed PMID: 20012860.
229. Bishehsari F, Mahdavinia M, Vacca M, Malekzadeh R, Mariani-Costantini R. Epidemiological transition of colorectal cancer in developing countries: Environmental factors, molecular pathways, and opportunities for prevention. *World Journal of Gastroenterology*. 2014;20(20):6055-72. doi: 10.3748/wjg.v20.i20.6055. PubMed PMID: PMC4033445.
230. Clark, M. E., R. E. Edelman, M. L. Duley, J. D. Wall and M. W. Fields. Biofilm formation in *Desulfovibrio vulgaris* Hildenborough is dependent upon protein filaments. *Environmental Microbiology*. 2007;9(11): 2844-2854. doi: 10.1111/j.1462-2920.2007.01398.x. PubMed PMID: 17922767.
231. Chung L, Thiele Orberg E, Geis AL, Chan JL, Fu K, DeStefano Shields CE, Dejea CM, Fathi P, Chen J, Finard BB, Tam AJ, McAllister F, Fan H, Wu X, Ganguly S, Lebid A, Metz P, Van Meerbeke SW, Huso DL, Wick EC, Pardoll DM, Wan F, Wu S, Sears CL, Housseau F. *Bacteroides fragilis* toxin coordinates a pro-carcinogenic inflammatory cascade via targeting of colonic epithelial cells. *Cell Host & Microbe*. 2018;23(2):203-14.e5. Epub 2018/02/06. doi: 10.1016/j.chom.2018.01.007. PubMed PMID: 29398651; PMCID: PMC5954996.
232. Zou S, Fang L, Lee M-H. Dysbiosis of gut microbiota in promoting the development of colorectal cancer. *Gastroenterology Report*. 2018;6(1):1-12. doi: 10.1093/gastro/gox031. PubMed PMID: PMC5806407.

233. Beaumont M, Andriamihaja M, Lan A, Khodorova N, Audebert M, Blouin JM, Grauso M, Lancha L, Benetti PH, Benamouzig R, Tome D, Bouillaud F, Davila AM, Blachier F. Detrimental effects for colonocytes of an increased exposure to luminal hydrogen sulfide: The adaptive response. *Free Radical Biology & Medicine*. 2016;93:155-64. Epub 2016/02/07. doi: 10.1016/j.freeradbiomed.2016.01.028. PubMed PMID: 26849947.
234. Sobhani I, Amiot A, Le Baleur Y, Levy M, Auriault M-L, Van Nhieu JT, Delchier JC. Microbial dysbiosis and colon carcinogenesis: could colon cancer be considered a bacteria-related disease? *Therapeutic Advances in Gastroenterology*. 2013;6(3):215-29. doi: 10.1177/1756283X12473674. PubMed PMID: PMC3625019.
235. Thursby E, Juge N. Introduction to the human gut microbiota. *Biochemical Journal*. 2017;474(11):1823-36. doi: 10.1042/BCJ20160510. PubMed PMID: PMC5433529.
236. Chen LA, Van Meerbeke S, Albesiano E, Goodwin A, Wu S, Yu H, Carroll K, Sears C. Fecal detection of enterotoxigenic *Bacteroides fragilis*. *European Journal of Clinical Microbiology & Infectious Diseases: official publication of the European Society of Clinical Microbiology*. 2015;34(9):1871-7. Epub 2015/07/16. doi: 10.1007/s10096-015-2425-7. PubMed PMID: 26173688; PMCID: PMC5001496.
237. Arthur JC, Perez-Channona E, Mühlbauer M, Tomkovich S, Uronis JM, Fan TJ. Alterations in the intestinal microbiota promote colorectal cancer. *Cancer Discovery*. 2012;2(10):866. doi: 10.1158/2159-8290.cd-rw2012-138.
238. Garrett WS, Punit S, Gallini CA, Michaud M, Zhang D, Sigrist KS, Lord GM, Glickman JN, Glimcher LH. Colitis-associated colorectal cancer driven by T-bet deficiency in dendritic cells. *Cancer Cell*. 2009;16(3):208-19. doi: <http://dx.doi.org/10.1016/j.ccr.2009.07.015>.
239. Konno-Shimizu M, Yamamichi N, Inada K, Kageyama-Yahara N, Shiogama K, Takahashi Y, Asada-Hirayama I, Yamamichi-Nishina M, Nakayama C, Ono S, Kodashima S, Fujishiro M, Tsutsumi Y, Ichinose M, Koike K. Cathepsin E is a marker of gastric differentiation and signet-ring cell carcinoma of stomach: a novel suggestion on gastric tumorigenesis. *PLOS One*. 2013;8(2):e56766. Epub 2013/03/02. doi: 10.1371/journal.pone.0056766. PubMed PMID: 23451082; PMCID: PMC3579941.
240. Washio J, Sato T, Koseki T, Takahashi N. Hydrogen sulfide-producing bacteria in tongue biofilm and their relationship with oral malodour. *Journal of Medical Microbiology*. 2005;54(Pt 9):889-95. Epub 2005/08/11. doi: 10.1099/jmm.0.46118-0. PubMed PMID: 16091443.
241. Cakmak YO. Provitella-derived hydrogen sulfide, constipation, and neuroprotection in Parkinson's disease. *Movement Disorders: official journal of the Movement Disorder Society*. 2015;30(8):1151. Epub 2015/05/15. doi: 10.1002/mds.26258. PubMed PMID: 25970839.

242. Escobar C, Bravo L, Hernandez J, Herrera L. Hydrogen sulfide production from elemental sulfur by *Desulfovibrio desulfuricans* in an anaerobic bioreactor. *Biotechnology & Bioengineering*. 2007;98(3):569-77. Epub 2007/04/11. doi: 10.1002/bit.21457. PubMed PMID: 17421040.
243. Carbonero F, Benefiel AC, Alizadeh-Ghamsari AH, Gaskins HR. Microbial pathways in colonic sulfur metabolism and links with health and disease. *Frontiers in Physiology*. 2012;3. doi: 10.3389/fphys.2012.00448. PubMed PMID: 23226130; PMCID: Pmc3508456.
244. Stewart JA, Chadwick VS, Murray A. Carriage, quantification, and predominance of methanogens and sulfate-reducing bacteria in faecal samples. *Letters in Applied Microbiology*. 2006;43(1):58-63. Epub 2006/07/13. doi: 10.1111/j.1472-765X.2006.01906.x. PubMed PMID: 16834722.
245. Hansen EE, Lozupone CA, Rey FE, Wu M, Guruge JL, Narra A, Goodfellow J, Zaneveld JR, McDonald DT, Goodrich JA, Heath AC, Knight R, Gordon JI. Pan-genome of the dominant human gut-associated archaeon, *Methanobrevibacter smithii*, studied in twins. *Proceedings of the National Academy of Sciences of the United States of America*. 2011;108(Supplement 1):4599-606. doi: 10.1073/pnas.1000071108.
246. Rey FE, Gonzalez MD, Cheng J, Wu M, Ahern PP, Gordon JI. Metabolic niche of a prominent sulfate-reducing human gut bacterium. *Proceedings of the National Academy of Sciences of the United States of America*. 2013;110(33):13582.
247. Gillings MR, Paulsen IT, Tetu SG. Ecology and evolution of the human microbiota: fire, farming and antibiotics. *Genes*. 2015;6(3):841-57. doi: 10.3390/genes6030841. PubMed PMID: PMC4584332.
248. Mangalam A, Shahi SK, Luckey D, Karau M, Marietta E, Luo N, Choung RS, Ju J, Sompallae R, Gibson-Corley K, Patel R, Rodriguez M, David C, Taneja V, Murray J. Human gut-derived commensal bacteria suppress CNS inflammatory and demyelinating disease. *Cell Reports*. 2017;20(6):1269-77. doi: <https://doi.org/10.1016/j.celrep.2017.07.031>.
249. Chakraborty R, Wu CH, Hazen TC. Systems biology approach to bioremediation. *Current Opinion in Biotechnology*. 2012;23(3):483-90. doi: <https://doi.org/10.1016/j.copbio.2012.01.015>.
250. Santegoeds CM, Ferdelman TG, Muyzer G, de Beer D. Structural and functional dynamics of sulfate-reducing populations in bacterial biofilms. *Applied & Environmental Microbiology*. 1998;64(10):3731-9.
251. Clark ME, He Q, He Z, Huang KH, Edelmann RE, Alm EJ, Wan ZF, Duley ML, Wall JD, Fields MW. Temporal transcriptomic analysis as *Desulfovibrio vulgaris* Hildenborough transitions into stationary phase during electron donor depletion. *Applied Environmental Microbiology*. 2006; 72(8), 5578-5588. doi:10.1128/aem.00284-06

252. Busi SB, Leon KBD, Wall JD, Amos-Landgraf JM. Abstract 4987: Biofilm-producing sulfate-reducing bacteria suppress tumor burden in a rat model of colon cancer. *Cancer Research*. 2018;78(13 Supplement): 4987.
253. Li MZ, Elledge SJ. Harnessing homologous recombination in vitro to generate recombinant DNA via SLIC. *Nature Methods*. 2007;4(3):251.
254. Davis RW BD, Roth JR. A manual for genetic engineering: advanced bacterial genetics. In: Davis RW BD, Roth JR editor. *A Manual for Genetic Engineering: Advanced Bacterial Genetics*. Cold Spring Harbor, New York: Cold Spring Harbor; 1990.
255. Santana M, Crasnier-Mednansky M. The adaptive genome of *Desulfovibrio vulgaris* Hildenborough, *FEMS Microbiology Letters*. 2006; 260(2): 127-133. doi: <https://doi.org/10.1111/j.1574-6968.2006.00261.x>
256. De León KB, Zane GM, Trotter VV, Krantz GP, Arkin AP, Butland GP, Walian PJ, Fields MW, Wall JD. Unintended laboratory-driven evolution reveals genetic requirements for biofilm formation by *Desulfovibrio vulgaris* Hildenborough. *MBIO*. 2017;8(5).
257. Ausubel FM BR, Kingston RE, Moore DD, Seidman JG, Smith JA, Struhl K. *Current Protocols in Molecular Biology*. Current Protocols in Molecular Biology. New York, NY: John Wiley & Sons; 1994.
258. Keller KL, Bender KS, Wall JD. Development of a markerless genetic exchange system for *Desulfovibrio vulgaris* Hildenborough and its use in generating a strain with increased transformation efficiency. *Applied & Environmental Microbiology*. 2009;75(24):7682-91.
259. Montonye DR, Ericsson AC, Busi SB, Lutz C, Wardwell K, Franklin CL. Acclimation and institutionalization of the mouse microbiota following transportation. *Frontiers in Microbiology*. 2018;9:1085. doi: 10.3389/fmicb.2018.01085. PubMed PMID: PMC5985407.
260. Altschul SF, Gish W, Miller W, Myers EW, Lipman DJ. Basic local alignment search tool. *Journal of Molecular Biology*. 1990;215(3):403-10. Epub 1990/10/05. doi: 10.1016/s0022-2836(05)80360-2. PubMed PMID: 2231712.
261. Hart ML, Meyer A, Johnson PJ, Ericsson AC. Comparative evaluation of DNA extraction methods from feces of multiple host species for downstream next-generation sequencing. *PLOS One*. 2015;10(11):e0143334. doi: 10.1371/journal.pone.0143334.
262. Quast C, Pruesse E, Yilmaz P, Gerken J, Schweer T, Yarza P, Peplies J, Glöckner FO. The SILVA ribosomal RNA gene database project: improved data processing and web-based tools. *Nucleic Acids Research*. 2013;41(Database issue):D590-D6. doi: 10.1093/nar/gks1219. PubMed PMID: PMC3531112.

263. Langille MGI, Zaneveld J, Caporaso JG, McDonald D, Knights D, Reyes JA, Clemente JC, Burkepille DE, Vega Thurber RL, Knight R, Beiko RG, Huttenhower C. Predictive functional profiling of microbial communities using 16S rRNA marker gene sequences. *Nature Biotechnology*. 2013;31:814. doi: 10.1038/nbt.2676 <https://www.nature.com/articles/nbt.2676#supplementary-information>.
264. Abubucker S, Segata N, Goll J, Schubert AM, Izard J, Cantarel BL, Rodriguez-Mueller B, Zucker J, Thiagarajan M, Henrissat B, White O, Kelley ST, Methe B, Schloss PD, Gevers D, Mitreva M, Huttenhower C. Metabolic reconstruction for metagenomic data and its application to the human microbiome. *PLOS Computational Biology*. 2012;8(6):e1002358. Epub 2012/06/22. doi: 10.1371/journal.pcbi.1002358. PubMed PMID: 22719234; PMCID: PMC3374609.
265. Segata N, Izard J, Waldron L, Gevers D, Miropolsky L, Garrett WS, Huttenhower C. Metagenomic biomarker discovery and explanation. *Genome Biology*. 2011;12(6):R60-R. doi: 10.1186/gb-2011-12-6-r60. PubMed PMID: PMC3218848.
266. Puchtler H, Waldrop FS, Conner HM, Terry MS. Carnoy fixation: practical and theoretical considerations. *Histochemie Histochemistry Histochemie*. 1968;16(4):361-71. Epub 1968/01/01. PubMed PMID: 4179106.
267. Rossetti ML, Gordon BS. The role of androgens in the regulations of muscle oxidative capacity following aerobic exercise training. *Applied Physiology, Nutrition & Metabolism*. 2017;42:1001-1007, <https://doi.org/10.1139/apnm-2017-0230>.
268. Mark Welch JL, Hasegawa Y, McNulty NP, Gordon JI, Borisy GG. Spatial organization of a model 15-member human gut microbiota established in gnotobiotic mice. *Proceedings of the National Academy of Sciences of the United States of America*. 2017. Oct 24;114(43):E9105-E9114. doi: 10.1073/pnas.1711596114. Epub 2017 Oct 9.
269. Cline JD. Spectrophotometric determination of hydrogen sulfide in natural waters. *Limnology & Oceanography*. 1969;14(3):454-8. doi: doi:10.4319/lo.1969.14.3.0454.
270. Ulrich GA, Krumholz LR, Suflita JM. A rapid and simple method for estimating sulfate reduction activity and quantifying inorganic sulfides. *Applied & Environmental Microbiology*. 1997;63(4):1627-30. PubMed PMID: PMC1389563.
271. Yang G, Pei Y, Cao Q, Wang R. MicroRNA-21 represses human cystathionine gamma-lyase expression by targeting at specificity protein-1 in smooth muscle cells. *Journal of Cellular Physiology*. 2012;227(9):3192-200. doi: 10.1002/jcp.24006.
272. Cord-Ruwisch R. A quick method for the determination of dissolved and precipitated sulfides in cultures of sulfate-reducing bacteria. *Journal of Microbiological Methods*. 1985;4(1):33-6. doi: [http://dx.doi.org/10.1016/0167-7012\(85\)90005-3](http://dx.doi.org/10.1016/0167-7012(85)90005-3).
273. Barber RD, Harmer DW, Coleman RA, Clark BJ. GAPDH as a housekeeping gene: analysis of GAPDH mRNA expression in a panel of 72 human tissues.

Physiological Genomics. 2005;21(3):389-95. Epub 2005/03/17. doi: 10.1152/physiolgenomics.00025.2005. PubMed PMID: 15769908.

274. Rocha DJ, Santos CS, Pacheco LG. Bacterial reference genes for gene expression studies by RT-qPCR: survey and analysis. *Antonie van Leeuwenhoek*. 2015;108(3):685-93. Epub 2015/07/08. doi: 10.1007/s10482-015-0524-1. PubMed PMID: 26149127.

275. Simko TWaV. R package "corrplot": visualization of a correlation matrix 2017.

276. Team RC. R: A language and environment for statistical computing 2018.

277. Tomasova L, Konopelski P, Ufnal M. Gut bacteria and hydrogen sulfide: the new old players in circulatory system homeostasis. *Molecules*. 2016;21(11). Epub 2016/11/22. doi: 10.3390/molecules21111558. PubMed PMID: 27869680.

278. Awano N, Wada M, Mori H, Nakamori S, Takagi H. Identification and functional analysis of *Escherichia coli* cysteine desulfhydrases. *Applied & Environmental Microbiology*. 2005;71(7):4149-52. PubMed PMID: 16000837.

279. Peck HD, Jr. Enzymatic basis for assimilatory and dissimilatory sulfate reduction. *Journal of Bacteriology*. 1961;82:933-9. Epub 1961/12/01. PubMed PMID: 14484818; PMCID: PMC279279.

280. Krekeler D, Teske A, Cypionka H. Strategies of sulfate-reducing bacteria to escape oxygen stress in a cyanobacterial mat. *FEMS Microbiology Ecology*. 1998;25(2):89-96. doi: 10.1111/j.1574-6941.1998.tb00462.x.

281. Cani PD, Jordan BF. Gut microbiota-mediated inflammation in obesity: a link with gastrointestinal cancer. *Nature Reviews Gastroenterology & Hepatology*. 2018. Epub 2018/05/31. doi: 10.1038/s41575-018-0025-6. PubMed PMID: 29844585.

282. Chen J, Vitetta L. Inflammation-modulating effect of butyrate in the prevention of colon cancer by dietary fiber. *Clinical Colorectal Cancer*. 2018. Epub 2018/06/06. doi: 10.1016/j.clcc.2018.05.001. PubMed PMID: 29866614.

283. Ijssennagger N, Belzer C, Hooiveld GJ, Dekker J, van Mil SW, Muller M, Kleerebezem M, van der Meer R. Gut microbiota facilitates dietary heme-induced epithelial hyperproliferation by opening the mucus barrier in colon. *Proceedings of the National Academy of Sciences of the United States of America*. 2015;112(32):10038-43. Epub 2015/07/29. doi: 10.1073/pnas.1507645112. PubMed PMID: 26216954; PMCID: PMC4538683.

284. Mendes MCS, Paulino DS, Brambilla SR, Camargo JA, Persinoti GF, Carnevalheira JBC. Microbiota modification by probiotic supplementation reduces colitis associated colon cancer in mice. *World Journal of Gastroenterology*. 2018;24(18):1995-2008. Epub 2018/05/16. doi: 10.3748/wjg.v24.i18.1995. PubMed PMID: 29760543; PMCID: PMC5949713.

285. Mima K, Nishihara R, Qian ZR, Cao Y, Sukawa Y, Nowak JA, Yang J, Dou R, Masugi Y, Song M, Kostic AD, Giannakis M, Bullman S, Milner DA, Baba H, Giovannucci EL, Garraway LA, Freeman GJ, Dranoff G, Garrett WS, Huttenhower C, Meyerson M, Meyerhardt JA, Chan AT, Fuchs CS, Ogino S. *Fusobacterium nucleatum* in colorectal carcinoma tissue and patient prognosis. *Gut*. 2016;65(12):1973-80. Epub 2015/08/28. doi: 10.1136/gutjnl-2015-310101. PubMed PMID: 26311717; PMCID: PMC4769120.
286. Redelman-Sidi G, Binyamin A, Gaeta I, Palm W, Thompson CB, Romesser PB, Lowe SW, Bagul M, Doench JG, Root DE, Glickman MS. The canonical Wnt pathway drives macropinocytosis in cancer. *Cancer Research*. 2018. Epub 2018/06/07. doi: 10.1158/0008-5472.can-17-3199. PubMed PMID: 29871936.
287. Lee K, Hwang H, Nam KT. Immune response and the tumor microenvironment: how they communicate to regulate gastric cancer. *Gut & Liver*. 2014;8(2):131-9. Epub 2014/03/29. doi: 10.5009/gnl.2014.8.2.131. PubMed PMID: 24672653; PMCID: PMC3964262.
288. Chen GY. The role of the gut microbiome in colorectal cancer. *Clinics in Colon & Rectal Surgery*. 2018; 31(03): 192-198. doi: 10.1055/s-0037-1602239. PubMed PMID: 29720905.
289. Dejea CM, Sears CL. Do biofilms confer a pro-carcinogenic state? *Gut Microbes*. 2016;7(1):54-7. Epub 2016/03/05. doi: 10.1080/19490976.2015.1121363. PubMed PMID: 26939852; PMCID: PMC4856444.
290. Le DT, Hubbard-Lucey VM, Morse MA, Heery CR, Dwyer A, Marsilje TH, Brodsky AN, Chan E, Deming DA, Diaz LA, Jr., Fridman WH, Goldberg RM, Hamilton SR, Housseau F, Jaffee EM, Kang SP, Krishnamurthi SS, Lieu CH, Messersmith W, Sears CL, Segal NH, Yang A, Moss RA, Cha E, O'Donnell-Tormey J, Roach N, Davis AQ, McAbee K, Worrall S, Benson AB. A blueprint to advance colorectal cancer immunotherapies. *Cancer Immunology Research*. 2017;5(11):942-9. Epub 2017/10/19. doi: 10.1158/2326-6066.cir-17-0375. PubMed PMID: 29038296.
291. Mima K, Cao Y, Chan AT, Qian Zr, Nowak JA, Masugi Y, Shi Ya, Song M, da Silva A, Gu M, Wanwan L, Hamada T, Kosumi K, Hanyuda A, Liu L, Kostic A, Giannakis M, Bullman S, Brenna CA, Milner DA, Baba H, Garraway LA, Meyerhardt JA, Garrett WS, Huttenhower C, Meyerson C, Giovannucci EL, Fuchs CS, Nihihara R, Ogino S. *Fusobacterium nucleatum* in colorectal carcinoma tissue according to tumor location. *Clinical & Translational Gastroenterology*. 2016;7,e200. Epub 2018/03/14doi:10.1038/ctg.2016.53.
292. Tlaskalova-Hogenova H, Stepankova R, Kozakova H, Hudcovic T, Vannucci L, Tuckova L, Rossmann P, Hrnecir T, Kverka M, Zakostelska Z, Klimesova K, Pribylova J, Bartova J, Sanchez D, Fundova P, Borovska D, Srutkova D, Zidek Z, Schwarzer M, Drastich P, Funda DP. The role of gut microbiota (commensal bacteria) and the mucosal barrier in the pathogenesis of inflammatory and autoimmune diseases and cancer:

contribution of germ-free and gnotobiotic animal models of human diseases. *Cellular & Molecular Immunology*. 2011;8(2):110-20. Epub 2011/02/01. doi: 10.1038/cmi.2010.67. PubMed PMID: 21278760; PMCID: PMC4003137.

293. Wong SH, Zhao L, Zhang X, Nakatsu G, Han J, Xu W, Xiao X, Kwong TNY, Tsoi H, Wu WKK, Zeng B, Chan FKL, Sung JJY, Wei H, Yu J. Gavage of fecal samples from patients with colorectal cancer promotes intestinal carcinogenesis in germ-free and conventional mice. *Gastroenterology*. 2017;153(6):1621-33.e6. Epub 2017/08/22. doi: 10.1053/j.gastro.2017.08.022. PubMed PMID: 28823860.

294. Yang H, Wang W, Romano KA, Gu M, Sanidad KZ, Kim D, Yang J, Schmidt B, Panigrahy D, Pei R, Martin DA, Ozay EI, Wang Y, Song M, Bolling BW, Xiao H, Minter LM, Yang GY, Liu Z, Rey FE, Zhang G. A common antimicrobial additive increases colonic inflammation and colitis-associated colon tumorigenesis in mice. *Science Translational Medicine*. 2018;10(443). Epub 2018/06/01. doi: 10.1126/scitranslmed.aan4116. PubMed PMID: 29848663.

295. Abed J, Maalouf N, Parhi L, Chaushu S, Mandelboim O, Bachrach G. Tumor targeting by *Fusobacterium nucleatum*: a pilot study and future perspectives. *Frontiers in Cellular & Infection Microbiology*. 2017; 7: 295-295. doi: 10.3389/fcimb.2017.00295. PubMed PMID: 28713780; PMCID: PMC5492862.

296. Flynn KJ, Baxter NT, Schloss PD. Metabolic and community synergy of oral bacteria in colorectal cancer. *mSphere*. 2016;1(3). Epub 2016/06/16. doi: 10.1128/mSphere.00102-16. PubMed PMID: 27303740; PMCID: PMC4888883.

297. Shepherd ES, DeLoache WC, Pruss KM, Whitaker WR, Sonnenburg JL. An exclusive metabolic niche enables strain engraftment in the gut microbiota. *Nature*. 2018;557(7705):434-8. Epub 2018/05/11. doi: 10.1038/s41586-018-0092-4. PubMed PMID: 29743671; PMCID: PMC6126907.

298. Hildebrandt MA, Hoffmann C, Sherrill-Mix SA, Keilbaugh SA, Hamady M, Chen YY, Knight R, Ahima RS, Bushman F, Wu GD. High-fat diet determines the composition of the murine gut microbiome independently of obesity. *Gastroenterology*. 2009;137(5):1716-24.e1-2. Epub 2009/08/27. doi: 10.1053/j.gastro.2009.08.042. PubMed PMID: 19706296; PMCID: PMC2770164.

299. Kashyap PC, Marcobal A, Ursell LK, Larauche M, Duboc H, Earle KA, Sonnenburg ED, Ferreyra JA, Higginbottom SK, Million M, Tache Y, Pasricha PJ, Knight R, Farrugia G, Sonnenburg JL. Complex interactions among diet, gastrointestinal transit, and gut microbiota in humanized mice. *Gastroenterology*. 2013;144(5):967-77. Epub 2013/02/06. doi: 10.1053/j.gastro.2013.01.047. PubMed PMID: 23380084; PMCID: PMC3890323.

300. Wu GD. Diet, the gut microbiome and the metabolome in IBD. *Nestle Nutrition Institute Workshop Series*. 2014;79:73-82. Epub 2014/09/18. doi: 10.1159/000360686. PubMed PMID: 25227296.

301. Zarrinpar A, Chaix A, Yooseph S, Panda S. Diet and feeding pattern affect the diurnal dynamics of the gut microbiome. *Cell Metabolism*. 2014;20(6):1006-17. Epub 2014/12/04. doi: 10.1016/j.cmet.2014.11.008. PubMed PMID: 25470548; PMCID: PMC4255146.
302. Morris LM, Klanke CA, Lang SA, Lim FY, Crombleholme TM. TdTomato and EGFP identification in histological sections: insight and alternatives. *Biotechnic & Histochemistry: official publication of the Biological Stain Commission*. 2010;85(6):379-87. Epub 2010/01/30. doi: 10.3109/10520290903504753. PubMed PMID: 20109099.
303. Syverud BC, Gumucio JP, Rodriguez BL, Wroblewski OM, Florida SE, Mendias CL, Larkin LM. A transgenic tdTomato rat for cell migration and tissue engineering applications. *Tissue Engineering Part C, Methods*. 2018;24(5):263-71. Epub 2018/03/02. doi: 10.1089/ten.TEC.2017.0406. PubMed PMID: 29490563; PMCID: PMC5946766.
304. Mukherjee S, Brothers KM, Shanks RMQ, Kadouri DE. Visualizing *Bdellovibrio bacteriovorus* by using the tdTomato fluorescent protein. *Applied & Environmental Microbiology*. 2016;82(6):1653-61. doi: 10.1128/aem.03611-15.
305. Singer JT, Phennicie RT, Sullivan MJ, Porter LA, Shaffer VJ, Kim CH. Broad-host-range plasmids for red fluorescent protein labeling of gram-negative bacteria for use in the Zebrafish model system. *Applied & Environmental Microbiology*. 2010;76(11):3467-74. doi: 10.1128/aem.01679-09.
306. Acuna N, Ortega-Morales BO, Valadez-Gonzalez A. Biofilm colonization dynamics and its influence on the corrosion resistance of austenitic UNS S31603 stainless steel exposed to Gulf of Mexico seawater. *Marine Biotechnology*. 2006;8(1):62-70. Epub 2006/02/03. doi: 10.1007/s10126-005-5145-7. PubMed PMID: 16453199.
307. Dang H, Lovell CR. Microbial surface colonization and biofilm development in marine environments. *Microbiology & Molecular Biology Reviews*. 2016;80(1):91-138. doi: 10.1128/mnbr.00037-15.
308. Uccello M, Malaguarnera G, Basile F, D'agata V, Malaguarnera M, Bertino G, Vacante M, Drago F, Biondi A. Potential role of probiotics on colorectal cancer prevention. *BMC Surgery*. 2012;12(Suppl 1):S35-S. doi: 10.1186/1471-2482-12-S1-S35. PubMed PMID: PMC3499195.
309. Shen XJ, Rawls JF, Randall T, Burcal L, Mpande CN, Jenkins N, Jovov B, Abdo Z, Sandler RS, Keku TO. Molecular characterization of mucosal adherent bacteria and associations with colorectal adenomas. *Gut Microbes*. 2010;1(3):138-47. Epub 2010/08/27. doi: 10.4161/gmic.1.3.12360. PubMed PMID: 20740058; PMCID: PMC2927011.
310. Tomkovich S, Yang Y, Winglee K, Gauthier J, Mühlbauer M, Sun X, Mohamadzadeh M, Liu X, Martin P, Wang GP, Oswald E, Fodor AA, Jobin C. Locoregional effects of microbiota in a preclinical model of colon carcinogenesis. *Cancer*

Research. 2017;77(10):2620-32. doi: 10.1158/0008-5472.CAN-16-3472. PubMed PMID: PMC5468752.

311. Feng Q, Liang S, Jia H, Stadlmayr A, Tang L, Lan Z, Zhang D, Xia H, Xu X, Jie Z, Su L, Li X, Li X, Li J, Xiao L, Huber-Schönauer U, Niederseer D, Xu X, Al-Aama JY, Yang H, Wang J, Kristiansen K, Arumugam M, Tilg H, Datz C, Wang J. Gut microbiome development along the colorectal adenoma–carcinoma sequence. *Nature Communications*. 2015;6:6528. doi: 10.1038/ncomms7528 <https://www.nature.com/articles/ncomms7528#supplementary-information>.

312. Sun T, Liu S, Zhou Y, Yao Z, Zhang D, Cao S, Wei Z, Tan B, Li Y, Lian Z, Wang S. Evolutionary biologic changes of gut microbiota in an ‘adenoma-carcinoma sequence’ mouse colorectal cancer model induced by 1, 2-Dimethylhydrazine. *Oncotarget*. 2017;8(1):444-57. doi: 10.18632/oncotarget.13443. PubMed PMID: PMC5352133.

313. Zackular JP, Rogers MAM, Ruffin MT, Schloss PD. The human gut microbiome as a screening tool for colorectal cancer. *Cancer Prevention Research*. 2014;7(11):1112-21. doi: 10.1158/1940-6207.CAPR-14-0129. PubMed PMID: PMC4221363.

314. Morgan JLW, Acheson JF, Zimmer J. Structure of a Type-1 secretion system ABC transporter. *Structure*. 2017;25(3):522-9. Epub 2017/02/22. doi: 10.1016/j.str.2017.01.010. PubMed PMID: 28216041.

315. Abby SS, Cury J, Guglielmini J, Néron B, Touchon M, Rocha EPC. Identification of protein secretion systems in bacterial genomes. *Scientific Reports*. 2016;6:23080. doi: 10.1038/srep23080 <https://www.nature.com/articles/srep23080#supplementary-information>.

316. Delepelaire P. Type I secretion in Gram-negative bacteria. *Biochimica et Biophysica Acta*. 2004;1694(1):149-61. doi: <https://doi.org/10.1016/j.bbamcr.2004.05.001>.

317. Green ER, Meccas J. Bacterial secretion systems – an overview. *Microbiology Spectrum*. 2016;4(1):10.1128/microbiolspec.VMBF-0012-2015. doi: 10.1128/microbiolspec.VMBF-0012-2015. PubMed PMID: PMC4804464.

318. Vigil PD, Wiles TJ, Engstrom MD, Prasov L, Mulvey MA, Mobley HLT. The Repeat-In-Toxin family member TosA mediates adherence of *Escherichia coli* and survival during bacteremia. *Infection & Immunity*. 2012;80(2):493.

319. Bauer ME, Welch RA. Association of RTX toxins with erythrocytes. *Infection & Immunity*. 1996;64(11):4665-72. PubMed PMID: PMC174429.

320. Sasaki H, Kawamoto E, Tanaka Y, Sawada T, Kunita S, Yagami K-i. Identification and characterization of hemolysin-like proteins similar to RTX toxin in *Pasteurella pneumotropica*. *Journal of Bacteriology*. 2009;191(11):3698.

321. Jin Y, Tang S, Li W, Ng SC, Chan MW, Sung JJ, Yu J. Hemolytic *E. coli* promotes colonic tumorigenesis in females. *Cancer Research*. 2016;76(10):2891-900. Epub 2016/03/26. doi: 10.1158/0008-5472.can-15-2083. PubMed PMID: 27013198.
322. Chowdhury P, Pore D, Mahata N, Karmakar P, Pal A, Chakrabarti MK. Thermostable direct hemolysin downregulates human colon carcinoma cell proliferation with the involvement of E-cadherin, and beta-catenin/Tcf-4 signaling. *PLOS One*. 2011;6(5):e20098. Epub 2011/06/01. doi: 10.1371/journal.pone.0020098. PubMed PMID: 21625458; PMCID: PMC3098874.
323. Welch C, Fan N, Brown R, Talaga M, Fueri A, Driscoll K, Lawry K, Vizurraga A, Rekhi R, Bandyopadhyay P, Dam T. A novel hemolysin with anti-cancer and anti-fungal properties binds to serum glycoproteins and cholesterol. *The FASEB Journal*. 2017;31(1_supplement):953.4-4. doi: 10.1096/fasebj.31.1_supplement.953.4.
324. Leavitt WD, Venceslau SS, Pereira IA, Johnston DT, Bradley AS. Fractionation of sulfur and hydrogen isotopes in *Desulfovibrio vulgaris* with perturbed DsrC expression. *FEMS Microbiology Letters*. 2016;363(20). Epub 2016/11/01. doi: 10.1093/femsle/fnw226. PubMed PMID: 27702753.
325. Feng Y, Stams AJM, de Vos WM, Sánchez-Andrea I. Enrichment of sulfidogenic bacteria from the human intestinal tract. *FEMS Microbiology Letters*. 2017;364(4):fnx028-fnx. doi: 10.1093/femsle/fnx028.
326. Ritz NL, Lin DM, Wilson MR, Barton LL, Lin HC. Sulfate-reducing bacteria slow intestinal transit in a bismuth-reversible fashion in mice. *Neurogastroenterology & Motility: the official journal of the European Gastrointestinal Motility Society*. 2017;29(1). Epub 2016/08/02. doi: 10.1111/nmo.12907. PubMed PMID: 27477318.
327. Landry AP, Ballou DP, Banerjee R. Modulation of catalytic promiscuity during hydrogen sulfide oxidation. *ACS Chemical Biology*. 2018;13(6):1651-8. Epub 2018/05/02. doi: 10.1021/acscchembio.8b00258. PubMed PMID: 29715001.
328. Yadav V, Gao XH, Willard B, Hatzoglou M, Banerjee R, Kabil O. Hydrogen sulfide modulates eukaryotic translation initiation factor 2alpha (eIF2alpha) phosphorylation status in the integrated stress-response pathway. *The Journal of Biological Chemistry*. 2017;292(32):13143-53. Epub 2017/06/24. doi: 10.1074/jbc.M117.778654. PubMed PMID: 28637872; PMCID: PMC5555178.
329. Heidelberg JF, Seshadri R, Haveman SA, Hemme CL, Paulsen IT, Kolonay JF, Eisen JA, Ward N, Methe B, Brinkac LM, Daugherty SC, Deboy RT, Dodson RJ, Durkin AS, Madupu R, Nelson WC, Sullivan SA, Fouts D, Haft DH, Selengut J, Peterson JD, Davidsen TM, Zafar N, Zhou L, Radune D, Dimitrov G, Hance M, Tran K, Khouri H, Gill J, Utterback TR, Feldblyum TV, Wall JD, Voordouw G, Fraser CM. The genome sequence of the anaerobic, sulfate-reducing bacterium *Desulfovibrio vulgaris* Hildenborough. *Nature Biotechnology*. 2004;22(5):554-9. Epub 2004/04/13. doi: 10.1038/nbt959. PubMed PMID: 15077118.

330. Taniguchi S, Kang L, Kimura T, Niki I. Hydrogen sulphide protects mouse pancreatic β -cells from cell death induced by oxidative stress, but not by endoplasmic reticulum stress. *British Journal of Pharmacology*. 2011;162(5):1171-8. doi: 10.1111/j.1476-5381.2010.01119.x.
331. Tyagi N, Moshal KS, Sen U, Vacek TP, Kumar M, Hughes WM, Jr., Kundu S, Tyagi SC. H₂S protects against methionine-induced oxidative stress in brain endothelial cells. *Antioxidants & Redox Signaling*. 2009;11(1):25-33. Epub 2008/10/08. doi: 10.1089/ars.2008.2073. PubMed PMID: 18837652; PMCID: Pmc2742910.
332. Dufton N, Natividad J, Verdu EF, Wallace JL. Hydrogen sulfide and resolution of acute inflammation: A comparative study utilizing a novel fluorescent probe. *Scientific Reports*. 2012;2:499. doi: 10.1038/srep00499.
333. Whiteman M, Winyard PG. Hydrogen sulfide and inflammation: the good, the bad, the ugly and the promising. *Expert Review of Clinical Pharmacology*. 2011;4(1):13-32. Epub 2011/11/26. doi: 10.1586/ecp.10.134. PubMed PMID: 22115346.
334. Wallace JL, Vong L, McKnight W, Dickey M, Martin GR. Endogenous and exogenous hydrogen sulfide promotes resolution of colitis in rats. *Gastroenterology*. 2009;137(2):569-78, 78.e1. Epub 2009/04/21. doi: 10.1053/j.gastro.2009.04.012. PubMed PMID: 19375422.
335. Wallace JL, Dickey M, McKnight W, Martin GR. Hydrogen sulfide enhances ulcer healing in rats. *The FASEB Journal*. 2007;21(14):4070-6. Epub 2007/07/20. doi: 10.1096/fj.07-8669com. PubMed PMID: 17634391.
336. Lee M, Sparatore A, Del Soldato P, McGeer E, McGeer PL. Hydrogen sulfide-releasing NSAIDs attenuate neuroinflammation induced by microglial and astrocytic activation. *Glia*. 2010;58(1):103-13. Epub 2009/06/23. doi: 10.1002/glia.20905. PubMed PMID: 19544392.
337. Magierowski M, Magierowska K, Kwiecien S, Brzozowski T. Gaseous mediators nitric oxide and hydrogen sulfide in the mechanism of gastrointestinal integrity, protection and ulcer healing. *Molecules*. 2015;20(5):9099-123. Epub 2015/05/23. doi: 10.3390/molecules20059099. PubMed PMID: 25996214.
338. Ianaro A, Cirino G, Wallace JL. Hydrogen sulfide-releasing anti-inflammatory drugs for chemoprevention and treatment of cancer. *Pharmacological Research*. 2016;111:652-8. Epub 2016/08/01. doi: 10.1016/j.phrs.2016.07.041. PubMed PMID: 27475881.
339. Kodela R, Nath N, Chattopadhyay M, Nesbitt DE, Velazquez-Martinez CA, Kashfi K. Hydrogen sulfide-releasing naproxen suppresses colon cancer cell growth and inhibits NF-kappaB signaling. *Drug Design, Development & Therapy*. 2015;9:4873-82. Epub 2015/09/09. doi: 10.2147/dddt.s91116. PubMed PMID: 26346117; PMCID: PMC4554424.

340. Paul-Clark M, Elsheikh W, Kirkby N, Chan M, Devchand P, Agbor TA, Flannigan KL, Cheadle C, Freydin M, Ianaro A, Mitchell JA, Wallace JL. Profound chemopreventative effects of a hydrogen sulfide-releasing nsaid in the *APC^{Min/+}* mouse model of intestinal tumorigenesis. *PLOS One*. 2016;11(2):e0147289. Epub 2016/02/26. doi: 10.1371/journal.pone.0147289. PubMed PMID: 26910063; PMCID: PMC4766010.
341. Dar SA, Yao L, van Dongen U, Kuenen JG, Muyzer G. Analysis of diversity and activity of sulfate-reducing bacterial communities in sulfidogenic bioreactors using 16S rRNA and *dsrB* genes as molecular markers. *Applied Environmental Microbiology*. 2007;73 (2) 594-604; doi: 10.1128/AEM.01875-06.
342. Cai WJ, Wang MJ, Ju LH, Wang C, Zhu YC. Hydrogen sulfide induces human colon cancer cell proliferation: role of Akt, ERK and p21. *Cell Biology International*. 2010;34(6):565-72. Epub 2010/02/27. doi: 10.1042/cbi20090368. PubMed PMID: 20184555.
343. Untereiner AA, Pavlidou A, Druzhyna N, Papapetropoulos A, Hellmich MR, Szabo C. Drug resistance induces the upregulation of H₂S-producing enzymes in HCT116 colon cancer cells. *Biochemical Pharmacology*. 2018;149:174-85. Epub 2017/10/25. doi: 10.1016/j.bcp.2017.10.007. PubMed PMID: 29061341; PMCID: PMC5866167.
344. Predmore BL, Lefer DJ, Gojon G. hydrogen sulfide in biochemistry and medicine. *Antioxidants & Redox Signaling*. 2012;17(1):119-40. doi: 10.1089/ars.2012.4612. PubMed PMID: 22432697; PMCID: Pmc3342665.
345. Ramasamy S, Singh S, Taniere P, Langman MJ, Eggo MC. Sulfide-detoxifying enzymes in the human colon are decreased in cancer and upregulated in differentiation. *American Journal of Physiology Gastrointestinal & Liver Physiology*. 2006;291(2):G288-96. Epub 2006/02/28. doi: 10.1152/ajpgi.00324.2005. PubMed PMID: 16500920.
346. Bir SC, Kolluru GK, McCarthy P, Shen X, Pardue S, Pattillo CB, Kevil CG. Hydrogen sulfide stimulates ischemic vascular remodeling through nitric oxide synthase and nitrite reduction activity regulating hypoxia-inducible factor-1alpha and vascular endothelial growth factor-dependent angiogenesis. *Journal of the American Heart Association*. 2012;1(5):e004093. Epub 2013/01/15. doi: 10.1161/jaha.112.004093. PubMed PMID: 23316304; PMCID: PMC3541625.
347. Bianco S, Mancardi D, Merlino A, Bussolati B, Munaron L. Hypoxia and hydrogen sulfide differentially affect normal and tumor-derived vascular endothelium. *Redox Biology*. 2017;12:499-504. doi: <https://doi.org/10.1016/j.redox.2017.03.015>.
348. Szabo C. Hydrogen sulphide and its therapeutic potential. *Nature Reviews Drug Discovery*. 2007;6(11):917-35. Epub 2007/10/20. doi: 10.1038/nrd2425. PubMed PMID: 17948022.

349. Leschelle X, Gubern M, Andriamihaja M, Blottiere HM, Couplan E, Gonzalez-Barroso MD, Petit C, Pagniez A, Chaumontet C, Mignotte B, Bouillaud F, Blachier F. Adaptive metabolic response of human colonic epithelial cells to the adverse effects of the luminal compound sulfide. *Biochimica et Biophysica Acta*. 2005;1725(2):201-12. Epub 2005/07/06. doi: 10.1016/j.bbagen.2005.06.002. PubMed PMID: 15996823.
350. Bernaudin M, Tang Y, Reilly M, Petit E, Sharp FR. Brain genomic response following hypoxia and re-oxygenation in the neonatal rat: identification of genes that might contribute to hypoxia-induced ischemic tolerance. *Journal of Biological Chemistry*. 2002;277(42):39728-38. doi: 10.1074/jbc.M204619200.
351. Diebold I, Petry A, Hess J, Gorlach A. The NADPH oxidase subunit NOX4 is a new target gene of the hypoxia-inducible factor-1. *Molecular Biology of the Cell*. 2010;21(12):2087-96. Epub 2010/04/30. doi: 10.1091/mbc.E09-12-1003. PubMed PMID: 20427574; PMCID: PMC2883952.
352. Mittal M, Roth M, König P, Hofmann S, Dony E, Goyal P, Selbitz A-C, Schermuly RT, Ghofrani HA, Kwapiszewska G, Kummer W, Klepetko W, Hoda MAR, Fink L, Hänze J, Seeger W, Grimminger F, Schmidt HHHW, Weissmann N. Hypoxia-dependent regulation of nonphagocytic NADPH oxidase subunit NOX4 in the pulmonary vasculature. *Circulation Research*. 2007;101(3):258-267. doi: 10.1161/CIRCRESAHA.107.148015 PubMed PMID: 17585072.
353. Wang D, DuBois RN. The Role of COX-2 in Intestinal Inflammation and Colorectal Cancer. *Oncogene*. 2010;29(6):781-8. doi: 10.1038/onc.2009.421. PubMed PMID: PMC3181054.
354. Ng K, Meyerhardt JA, Chan AT, Sato K, Chan JA, Niedzwiecki D, Saltz LB, Mayer RJ, Benson AB, 3rd, Schaefer PL, Whittom R, Hantel A, Goldberg RM, Venook AP, Ogino S, Giovannucci EL, Fuchs CS. Aspirin and COX-2 inhibitor use in patients with stage III colon cancer. *Journal of the National Cancer Institute*. 2015;107(1):345. Epub 2014/11/30. doi: 10.1093/jnci/dju345. PubMed PMID: 25432409; PMCID: PMC4271076.
355. Lobo Prabhu KC, Vu L, Chan SK, Phang T, Gown A, Jones SJ, Wiseman SM. Predictive utility of cyclo-oxygenase-2 expression by colon and rectal cancer. *American Journal of Surgery*. 2014;207(5):712-6. Epub 2014/05/06. doi: 10.1016/j.amjsurg.2013.12.019. PubMed PMID: 24791632.
356. Wiesner GL, Platzer P, Buxbaum S, Lewis S, MacMillen M, Olechnowicz J, Willis J, Chakravarti A, Elston RC, Markowitz SD. Testing for colon neoplasia susceptibility variants at the human COX2 locus. *Journal of the National Cancer Institute*. 2001;93(8):635-9. Epub 2001/04/20. PubMed PMID: 11309440.
357. Cox DG, Pontes C, Guino E, Navarro M, Osorio A, Canzian F, Moreno V. Polymorphisms in prostaglandin synthase 2/cyclooxygenase 2 (PTGS2/COX2) and risk of colorectal cancer. *British Journal of Cancer*. 2004;91:339. doi: 10.1038/sj.bjc.6601906.

358. Habib P, Dang J, Slowik A, Victor M, Beyer C. Hypoxia-induced gene expression of aquaporin-4, cyclooxygenase-2 and hypoxia-inducible factor 1alpha in rat cortical astroglia is inhibited by 17beta-estradiol and progesterone. *Neuroendocrinology*. 2014;99(3-4):156-67. Epub 2014/04/02. doi: 10.1159/000362279. PubMed PMID: 24685982.
359. Bocca C, Bozzo F, Cannito S, Parola M, Miglietta A. Celecoxib inactivates epithelial-mesenchymal transition stimulated by hypoxia and/or epidermal growth factor in colon cancer cells. *Molecular Carcinogenesis*. 2012;51(10):783-95. Epub 2011/09/02. doi: 10.1002/mc.20846. PubMed PMID: 21882253.
360. Roberts HR, Smartt HJ, Greenhough A, Moore AE, Williams AC, Paraskeva C. Colon tumour cells increase PGE(2) by regulating COX-2 and 15-PGDH to promote survival during the microenvironmental stress of glucose deprivation. *Carcinogenesis*. 2011;32(11):1741-7. Epub 2011/09/20. doi: 10.1093/carcin/bgr210. PubMed PMID: 21926111.
361. Jackson SP, Bartek J. The DNA-damage response in human biology and disease. *Nature*. 2009;461(7267):1071-8. doi: 10.1038/nature08467. PubMed PMID: PMC2906700.
362. Zhou BB, Elledge SJ. The DNA damage response: putting checkpoints in perspective. *Nature*. 2000;408(6811):433-9. Epub 2000/12/02. doi: 10.1038/35044005. PubMed PMID: 11100718.
363. Yang X, Hao D, Zhang H, Liu B, Yang M, He B. Treatment with hydrogen sulfide attenuates sublesional skeletal deterioration following motor complete spinal cord injury in rats. *Osteoporosis International: a journal established as result of cooperation between the European Foundation for Osteoporosis & the National Osteoporosis Foundation of the USA*. 2017;28(2):687-95. Epub 2016/09/07. doi: 10.1007/s00198-016-3756-7. PubMed PMID: 27591786.
364. Chattopadhyay M, Kodela R, Olson KR, Kashfi K. NOSH-aspirin (NBS-1120), a novel nitric oxide- and hydrogen sulfide-releasing hybrid is a potent inhibitor of colon cancer cell growth in vitro and in a xenograft mouse model. *Biochemical & Biophysical Research Communications*. 2012;419(3):523-8. Epub 2012/03/01. doi: 10.1016/j.bbrc.2012.02.051. PubMed PMID: 22366248.
365. Foster KR, Schluter J, Coyte KZ, Rakoff-Nahoum S. The evolution of the host microbiome as an ecosystem on a leash. *Nature*. 2017;548:43. doi: 10.1038/nature23292.
366. Zeng Q, Wu S, Sukumaran J, Rodrigo A. Models of microbiome evolution incorporating host and microbial selection. *Microbiome*. 2017;5(1):127. doi: 10.1186/s40168-017-0343-x.
367. Davenport ER, Sanders JG, Song SJ, Amato KR, Clark AG, Knight R. The human microbiome in evolution. *BMC Biology*. 2017;15:127. doi: 10.1186/s12915-017-0454-7. PubMed PMID: PMC5744394.

368. Hensler ME. *Streptococcus gallolyticus*, infective endocarditis, and colon carcinoma: new light on an intriguing coincidence. *The Journal of Infectious Diseases*. 2011;203(8):1040-2. Epub 2011/04/01. doi: 10.1093/infdis/jiq170. PubMed PMID: 21450993.
369. Hold GL. Gastrointestinal microbiota and colon cancer. *Digestive Diseases*. 2016;34(3):244-50. Epub 2016/03/31. doi: 10.1159/000443358. PubMed PMID: 27028619.
370. Johnson CH, Spilker ME, Goetz L, Peterson SN, Siuzdak G. Metabolite and microbiome interplay in cancer immunotherapy. *Cancer Research*. 2016;76(21):6146-52. Epub 2016/11/03. doi: 10.1158/0008-5472.can-16-0309. PubMed PMID: 27729325; PMCID: PMC5093024.
371. Raisch J, Buc E, Bonnet M, Sauvanet P, Vazeille E, de Vallee A, Dechelotte P, Darcha C, Pezet D, Bonnet R, Bringer MA, Darfeuille-Michaud A. Colon cancer-associated B2 *Escherichia coli* colonize gut mucosa and promote cell proliferation. *World Journal of Gastroenterology*. 2014;20(21):6560-72. Epub 2014/06/11. doi: 10.3748/wjg.v20.i21.6560. PubMed PMID: 24914378; PMCID: PMC4047342.
372. Khan SR, Gaines J, Roop RM, Farrand SK. Broad-host-range expression vectors with tightly regulated promoters and their use to examine the influence of TraR and TraM expression on Ti plasmid quorum sensing. *Applied & Environmental Microbiology*. 2008;74(16):5053-62.
373. Heindl JE, Crosby D, Brar S, Merenich D, Buechlein AM, Bruger EL, Waters CM, Fuqua C. Reciprocal control of motility and biofilm formation by the PdhS2 two-component sensor kinase of *Agrobacterium tumefaciens*. *bioRxiv*. 2017:148429.
374. Dolla A, Fu R, Brumlik M, Voordouw G. Nucleotide sequence of dcrA, a *Desulfovibrio vulgaris* Hildenborough chemoreceptor gene, and its expression in *Escherichia coli*. *Journal of Bacteriology*. 1992;174(6):1726-33.
375. Mittal VK, Bhullar JS, Jayant K. Animal models of human colorectal cancer: current status, uses and limitations. *World Journal of Gastroenterology*. 2015;21(41):11854-61. Epub 2015/11/12. doi: 10.3748/wjg.v21.i41.11854. PubMed PMID: 26557009; PMCID: PMC4631983.
376. Johnson RL, Fleet JC. Animal models of colorectal cancer. *Cancer and Metastasis Reviews*. 2013;32(0):39-61. doi: 10.1007/s10555-012-9404-6. PubMed PMID: PMC3572245.
377. De-Souza ASC, Costa-Casagrande TA. Animal models for colorectal cancer. *Arquivos Brasileiros de Cirurgia Digestiva*. 2018;31(2):e1369. doi: 10.1590/0102-672020180001e1369. PubMed PMID: PMC6044195.

378. Tong Y, Yang W, Koeffler HP. Mouse models of colorectal cancer. *Chinese Journal of Cancer*. 2011;30(7):450-62. doi: 10.5732/cjc.011.10041. PubMed PMID: PMC4013420.
379. Vannucci L, Stepankova R, Kozakova H, Fiserova A, Rossmann P, Tlaskalova-Hogenova H. Colorectal carcinogenesis in germ-free and conventionally reared rats: different intestinal environments affect the systemic immunity. *International Journal of Oncology*. 2008;32(3):609-17. Epub 2008/02/23. PubMed PMID: 18292938.
380. Jobin C. Human intestinal microbiota and colorectal cancer: moving beyond associative studies. *Gastroenterology*. 2017;153(6):1475-8. doi: 10.1053/j.gastro.2017.10.030.
381. Arthur JC, Perez-Chanona E, Muhlbauer M, Tomkovich S, Uronis JM, Fan TJ, Campbell BJ, Abujamel T, Dogan B, Rogers AB, Rhodes JM, Stintzi A, Simpson KW, Hansen JJ, Keku TO, Fodor AA, Jobin C. Intestinal inflammation targets cancer-inducing activity of the microbiota. *Science*. 2012;338(6103):120-3. Epub 2012/08/21. doi: 10.1126/science.1224820. PubMed PMID: 22903521; PMCID: PMC3645302.
382. Arthur JC, Gharaibeh RZ, Mühlbauer M, Perez-Chanona E, Uronis JM, McCafferty J, Fodor AA, Jobin C. Microbial genomic analysis reveals the essential role of inflammation in bacteria-induced colorectal cancer. *Nature Communications*. 2014;5:4724. doi: 10.1038/ncomms5724
<https://www.nature.com/articles/ncomms5724#supplementary-information>.
383. Cougnoux A, Dalmaso G, Martinez R, Buc E, Delmas J, Gibold L, Sauvanet P, Darcha C, Déchelotte P, Bonnet M, Pezet D, Wodrich H, Darfeuille-Michaud A, Bonnet R. Bacterial genotoxin colibactin promotes colon tumour growth by inducing a senescence-associated secretory phenotype. *Gut*. 2014;63(12):1932.
384. Uronis JM, Muhlbauer M, Herfarth HH, Rubinas TC, Jones GS, Jobin C. Modulation of the intestinal microbiota alters colitis-associated colorectal cancer susceptibility. *PLOS One*. 2009;4(6):e6026. Epub 2009/06/25. doi: 10.1371/journal.pone.0006026. PubMed PMID: 19551144; PMCID: PMC2696084.
385. Wu S, Rhee K-J, Albesiano E, Rabizadeh S, Wu X, Yen H-R, Huso DL, Brancati FL, Wick E, McAllister F, Housseau F, Pardoll DM, Sears CL. A human colonic commensal promotes colon tumorigenesis via activation of T helper type 17 T cell responses. *Nature Medicine*. 2009;15:1016. doi: 10.1038/nm.2015
<https://www.nature.com/articles/nm.2015#supplementary-information>.
386. Stehr M, Greweling MC, Tischer S, Singh M, Blocker H, Monner DA, Muller W. Charles River altered Schaedler flora (CRASF) remained stable for four years in a mouse colony housed in individually ventilated cages. *Laboratory Animals*. 2009;43(4):362-70. Epub 2009/06/19. doi: 10.1258/la.2009.0080075. PubMed PMID: 19535393.
387. Dewhirst FE, Chien CC, Paster BJ, Ericson RL, Orcutt RP, Schauer DB, Fox JG. Phylogeny of the defined murine microbiota: altered Schaedler flora. *Applied &*

Environmental Microbiology. 1999;65(8):3287-92. Epub 1999/07/31. PubMed PMID: 10427008; PMCID: PMC91493.

388. Wannemuehler MJ, Overstreet A-M, Ward DV, Phillips GJ. Draft genome sequences of the Altered Schaedler Flora, a defined bacterial community from gnotobiotic mice. *Genome Announcements*. 2014 Apr 10;2(2). pii: e00287-14. doi: 10.1128/genomeA.00287-14.

389. Hammer O, Harper DAT, Ryan PD. PAST: Paleontological statistics software package for education and data analysis. *Palaeontological Electronica*. 2001;4(1):9pp.

390. Biggs MB, Medlock GL, Moutinho TJ, Lees HJ, Swann JR, Kolling GL, Papin JA. Systems-level metabolism of the altered Schaedler flora, a complete gut microbiota. *The ISME Journal*. 2016;11:426. doi: 10.1038/ismej.2016.130 <https://www.nature.com/articles/ismej2016130#supplementary-information>.

391. Savage DC, McAllister JS. Cecal enlargement and microbial flora in suckling mice given antibacterial drugs. *Infection & Immunity*. 1971;3(2):342-9. PubMed PMID: PMC416153.

392. Thompson GR, Trexler PC. Gastrointestinal structure and function in germ-free or gnotobiotic animals. *Gut*. 1971;12(3):230-5. PubMed PMID: PMC1411593.

393. Savage DC, Dubos R. Alterations in the mouse cecum and its flora produced by antibacterial drugs. *The Journal of Experimental Medicine*. 1968;128(1):97-110. Epub 1968/07/01. PubMed PMID: 5662019; PMCID: PMC2138511.

394. McNally L, Brown SP. Building the microbiome in health and disease: niche construction and social conflict in bacteria. *Philosophical Transactions of the Royal Society of London Series B, Biological Sciences*. 2015;370(1675). Epub 2015/07/08. doi: 10.1098/rstb.2014.0298. PubMed PMID: 26150664; PMCID: PMC4528496.

395. Knights D, Lassen KG, Xavier RJ. Advances in inflammatory bowel disease pathogenesis: linking host genetics and the microbiome. *Gut*. 2013;62(10):1505-10. Epub 2013/09/17. doi: 10.1136/gutjnl-2012-303954. PubMed PMID: 24037875; PMCID: PMC3822528.

396. Holmes E, Li JV, Marchesi JR, Nicholson JK. Gut microbiota composition and activity in relation to host metabolic phenotype and disease risk. *Cell Metabolism*. 2012;16(5):559-64. Epub 2012/11/13. doi: 10.1016/j.cmet.2012.10.007. PubMed PMID: 23140640.

397. Feehley T, Nagler CR. Cellular and molecular pathways through which commensal bacteria modulate sensitization to dietary antigens. *Current Opinion in Immunology*. 2014;31:79-86. Epub 2014/12/03. doi: 10.1016/j.coi.2014.10.001. PubMed PMID: 25458998; PMCID: PMC4255329.

398. Ericsson AC, Gagliardi J, Bouhan D, Spollen WG, Givan SA, Franklin CL. The influence of caging, bedding, and diet on the composition of the microbiota in different regions of the mouse gut. *Scientific Reports*. 2018;8(1):4065. doi: 10.1038/s41598-018-21986-7.
399. Wang S, Chen L, He M, Shen J, Li G, Tao Z, Wu R, Lu L. Different rearing conditions alter gut microbiota composition and host physiology in Shaoxing ducks. *Scientific Reports*. 2018;8(1):7387. doi: 10.1038/s41598-018-25760-7.
400. Rausch P, Basic M, Batra A, Bischoff SC, Blaut M, Clavel T, Gläsner J, Gopalakrishnan S, Grassl GA, Günther C, Haller D, Hirose M, Ibrahim S, Loh G, Mattner J, Nagel S, Pabst O, Schmidt F, Siegmund B, Strowig T, Volynets V, Wirtz S, Zeissig S, Zeissig Y, Bleich A, Baines JF. Analysis of factors contributing to variation in the C57BL/6J fecal microbiota across German animal facilities. *International Journal of Medical Microbiology*. 2016;306(5):343-55. doi: <https://doi.org/10.1016/j.ijmm.2016.03.004>.
401. Kers JG, Velkers FC, Fischer EAJ, Hermes GDA, Stegeman JA, Smidt H. Host and environmental factors affecting the intestinal microbiota in chickens. *Frontiers in Microbiology*. 2018;9(235). doi: 10.3389/fmicb.2018.00235.
402. Sivaprakasam S, Gurav A, Paschall AV, Coe GL, Chaudhary K, Cai Y, Kolhe R, Martin P, Browning D, Huang L, Shi H, Sifuentes H, Vijay-Kumar M, Thompson SA, Munn DH, Mellor A, McGaha TL, Shiao P, Cutler CW, Liu K, Ganapathy V, Li H, Singh N. An essential role of Ffar2 (Gpr43) in dietary fibre-mediated promotion of healthy composition of gut microbiota and suppression of intestinal carcinogenesis. *Oncogenesis*. 2016;5(6):e238. Epub 2016/06/28. doi: 10.1038/oncsis.2016.38. PubMed PMID: 27348268; PMCID: PMC4945739.
403. Ma W, Chen J, Meng Y, Yang J, Cui Q, Zhou Y. Metformin alters gut microbiota of healthy mice: implication for its potential role in gut microbiota homeostasis. *Frontiers in Microbiology*. 2018;9:1336. Epub 2018/07/11. doi: 10.3389/fmicb.2018.01336. PubMed PMID: 29988362; PMCID: PMC6023991.
404. Ou J, Carbonero F, Zoetendal EG, DeLany JP, Wang M, Newton K, Gaskins HR, O'Keefe SJ. Diet, microbiota, and microbial metabolites in colon cancer risk in rural Africans and African Americans. *The American Journal of Clinical Nutrition*. 2013;98(1):111-20. Epub 2013/05/31. doi: 10.3945/ajcn.112.056689. PubMed PMID: 23719549; PMCID: PMC3683814.
405. Bonnet M, Buc E, Sauvanet P, Darcha C, Dubois D, Pereira B, Dechelotte P, Bonnet R, Pezet D, Darfeuille-Michaud A. Colonization of the human gut by *E. coli* and colorectal cancer risk. *Clinical Cancer Research: an official journal of the American Association for Cancer Research*. 2014;20(4):859-67. Epub 2013/12/18. doi: 10.1158/1078-0432.ccr-13-1343. PubMed PMID: 24334760.
406. Gagniere J, Bonnin V, Jarrousse AS, Cardamone E, Agus A, Uhrhammer N, Sauvanet P, Dechelotte P, Barnich N, Bonnet R, Pezet D, Bonnet M. Interactions

between microsatellite instability and human gut colonization by *Escherichia coli* in colorectal cancer. *Clinical Science*. 2017;131(6):471-85. Epub 2017/01/18. doi: 10.1042/cs20160876. PubMed PMID: 28093453.

407. Link A, Balaguer F, Shen Y, Nagasaka T, Lozano JJ, Boland CR, Goel A. Fecal microRNAs as novel biomarkers for colon cancer screening. *Cancer Epidemiology Biomarkers & Prevention*. 2010 Jul;19(7):1766-74. doi: 10.1158/1055-9965.EPI-10-0027. Epub 2010 Jun 15.

408. Wang T, Cai G, Qiu Y, Fei N, Zhang M, Pang X, Jia W, Cai S, Zhao L. Structural segregation of gut microbiota between colorectal cancer patients and healthy volunteers. *The ISME Journal*. 2012;6(2):320-9. Epub 2011/08/19. doi: 10.1038/ismej.2011.109. PubMed PMID: 21850056; PMCID: PMC3260502.

409. Sze MA, Baxter NT, Ruffin MT, Rogers MAM, Schloss PD. Normalization of the microbiota in patients after treatment for colonic lesions. *Microbiome*. 2017;5(1):150. Epub 2017/11/18. doi: 10.1186/s40168-017-0366-3. PubMed PMID: 29145893; PMCID: PMC5689185.

410. Reddy BS, Weisburger JH, Wynder EL. Effects of high risk and low risk diets for colon carcinogenesis on fecal microflora and steroids in man. *The Journal of Nutrition*. 1975;105(7):878-84. doi: 10.1093/jn/105.7.878.

411. Wilson WR, Martin WJ, Wilkowske CJ, Washington JA, 2nd. Anaerobic bacteremia. *Mayo Clinic Proceedings*. 1972;47(9):639-46. Epub 1972/09/01. PubMed PMID: 5073944.

412. Leung A, Tsoi H, Yu J. *Fusobacterium* and *Escherichia*: models of colorectal cancer driven by microbiota and the utility of microbiota in colorectal cancer screening. *Expert Review of Gastroenterology & Hepatology*. 2015;9(5):651-7. Epub 2015/01/15. doi: 10.1586/17474124.2015.1001745. PubMed PMID: 25582922.

413. Watne AL, Lai H-YL, Mance T, Core S. Fecal steroids and bacterial flora in patients with polyposis coli. *The American Journal of Surgery*. 1976;131(1):42-6. doi: [https://doi.org/10.1016/0002-9610\(76\)90418-9](https://doi.org/10.1016/0002-9610(76)90418-9).

414. Kamada N, Chen GY, Inohara N, Núñez G. Control of Pathogens and Pathobionts by the Gut Microbiota. *Nature Immunology*. 2013;14(7):685-90. doi: 10.1038/ni.2608. PubMed PMID: PMC4083503.

415. Kitazawa S, Ebara S, Ando A, Baba Y, Satomi Y, Soga T, Hara T. Succinate dehydrogenase B-deficient cancer cells are highly sensitive to bromodomain and extra-terminal inhibitors. *Oncotarget*. 2017;8(17):28922-38. Epub 2017/04/21. doi: 10.18632/oncotarget.15959. PubMed PMID: 28423651; PMCID: PMC5438703.

416. Cao Y, Zhang R, Sun C, Cheng T, Liu Y, Xian M. fermentative succinate production: an emerging technology to replace the traditional petrochemical processes.

BioMed Research International. 2013;2013:723412. doi: 10.1155/2013/723412. PubMed PMID: PMC3874355.

417. Zhang F, Zhang Y, Zhao W, Deng K, Wang Z, Yang C, Ma L, Openkova MS, Hou Y, Li K. Metabolomics for biomarker discovery in the diagnosis, prognosis, survival and recurrence of colorectal cancer: a systematic review. *Oncotarget*. 2017;8(21), 35460-35472. doi:10.18632/oncotarget.16727

418. Wishart DS. Emerging applications of metabolomics in drug discovery and precision medicine. *Nature Reviews Drug Discovery*. 2016;15(7):473-84. Epub 2016/03/12. doi: 10.1038/nrd.2016.32. PubMed PMID: 26965202.

419. Boroughs LK, DeBerardinis RJ. Metabolic pathways promoting cancer cell survival and growth. *Nature Cell Biology*. 2015;17(4):351-9. doi: 10.1038/ncb3124. PubMed PMID: PMC4939711.

420. Upp JR, Saydjari R, Townsend CM, Singh P, Barranco SC, Thompson JC. Polyamine levels and gastrin receptors in colon cancers. *Annals of Surgery*. 1988;207(6):662-9. PubMed PMID: PMC1493553.

421. Goodwin AC, Shields CED, Wu S, Huso DL, Wu X, Murray-Stewart TR, Hacker-Prietz A, Rabizadeh S, Woster PM, Sears CL. Polyamine catabolism contributes to enterotoxigenic *Bacteroides fragilis*-induced colon tumorigenesis. *Proceedings of the National Academy of Sciences of the United States of America*. 2011;108(37), 15354-15359. doi:10.1073/pnas.1010203108. PubMed PMID: 21876161.

422. Vujcic S, Diegelman P, Bacchi CJ, Kramer DL, Porter CW. Identification and characterization of a novel flavin-containing spermine oxidase of mammalian cell origin. *Biochemical Journal*. 2002;367(3):665-75.

423. McIntyre RE, Buczacki SJA, Arends MJ, Adams DJ. Mouse models of colorectal cancer as preclinical models. *Bioessays*. 2015;37(8):909-20. doi: 10.1002/bies.201500032. PubMed PMID: PMC4755199.

424. Rust JH. Animal models for human diseases. *Perspectives in Biology & Medicine*. 1982;25(4):662-72. Epub 1982/01/01. PubMed PMID: 7167364.

425. Vandamme TF. Use of rodents as models of human diseases. *Journal of Pharmacy & Bioallied Sciences*. 2014;6(1):2-9. doi: 10.4103/0975-7406.124301. PubMed PMID: PMC3895289.

426. Tilg H, Adolph TE, Gerner RR, Moschen AR. The intestinal microbiota in colorectal cancer. *Cancer Cell*. 2018;33(6), 954-964. doi:https://doi.org/10.1016/j.ccell.2018.03.004

427. Fukugaiti MH, Ignacio A, Fernandes MR, Ribeiro Junior U, Nakano V, Avila-Campos MJ. High occurrence of *Fusobacterium nucleatum* and *Clostridium difficile* in the intestinal microbiota of colorectal carcinoma patients. *Brazilian Journal of*

Microbiology: publication of the Brazilian Society for Microbiology. 2015;46(4):1135-40. Epub 2015/12/23. doi: 10.1590/s1517-838246420140665. PubMed PMID: 26691472; PMCID: PMC4704648.

428. Kostic AD, Chun E, Meyerson M, Garrett WS. Microbes and inflammation in colorectal cancer. *Cancer Immunology Research*. 2013;1(3):150-7. Epub 2014/04/30. doi: 10.1158/2326-6066.cir-13-0101. PubMed PMID: 24777677.

429. McCoy AN, Araujo-Perez F, Azcarate-Peril A, Yeh JJ, Sandler RS, Keku TO. *Fusobacterium* is associated with colorectal adenomas. *PLOS One*. 2013;8(1):e53653. Epub 2013/01/22. doi: 10.1371/journal.pone.0053653. PubMed PMID: 23335968; PMCID: PMC3546075.

430. Siegel RL, Miller KD, Jemal A. Cancer statistics, 2016. *CA: a Cancer Journal for Clinicians*. 2016;66(1):7-30. Epub 2016/01/09. doi: 10.3322/caac.21332. PubMed PMID: 26742998.

431. Chen X, Halberg RB, Ehrhardt WM, Torrealba J, Dove WF. Clusterin as a biomarker in murine and human intestinal neoplasia. *Proceedings of the National Academy of Sciences of the United States of America*. 2003; 100(16), 9530-9535. doi:10.1073/pnas.1233633100. PubMed PMID: 12886021.

432. Washington MK, Powell AE, Sullivan R, Sundberg JP, Wright N, Coffey RJ, Dove WF. Pathology of rodent models of intestinal cancer: progress report and recommendations. *Gastroenterology*. 2013;144(4):705-17. doi: <https://doi.org/10.1053/j.gastro.2013.01.067>.

433. Ward DG, Suggett N, Cheng Y, Wei W, Johnson H, Billingham LJ, Ismail T, Wakelam MJO, Johnson PJ, Martin A. Identification of serum biomarkers for colon cancer by proteomic analysis. *British Journal of Cancer*. 2006;94:1898. doi: 10.1038/sj.bjc.6603188.

434. Volmer MW, Stühler K, Zapatka M, Schöneck A, Klein-Scory S, Schmiegel W, Meyer HE, Schwarte-Waldhoff I. Differential proteome analysis of conditioned media to detect Smad4 regulated secreted biomarkers in colon cancer. *Proteomics*. 2005;5(10):2587-601. doi: doi:10.1002/pmic.200401188.

435. Brown DG, Rao S, Weir TL, O'Malia J, Bazan M, Brown RJ, Ryan EP. Metabolomics and metabolic pathway networks from human colorectal cancers, adjacent mucosa, and stool. *Cancer & Metabolism*. 2016;4(1):11. doi: 10.1186/s40170-016-0151-y.

436. Johnson CH, Ivanisevic J, Siuzdak G. Metabolomics: beyond biomarkers and towards mechanisms. *Nature Reviews Molecular Cell Biology*. 2016;17:451. doi: 10.1038/nrm.2016.25 <https://www.nature.com/articles/nrm.2016.25#supplementary-information>.

437. Hirayama A, Kami K, Sugimoto M, Sugawara M, Toki N, Onozuka H, Kinoshita T, Saito N, Ochiai A, Tomita M, Esumi H, Soga T. Quantitative metabolome profiling of colon and stomach cancer microenvironment by capillary electrophoresis time-of-flight mass spectrometry. *Cancer Research*. 2009;69(11):4918.
438. Davis CD, Milner J. Frontiers in nutrigenomics, proteomics, metabolomics and cancer prevention. *Mutation Research/Fundamental & Molecular Mechanisms of Mutagenesis*. 2004;551(1):51-64. doi: <https://doi.org/10.1016/j.mrfmmm.2004.01.012>.
439. Glunde K, Serkova NJ. Therapeutic targets and biomarkers identified in cancer choline phospholipid metabolism. *Pharmacogenomics*. 2006;7(7):1109-23. doi: 10.2217/14622416.7.7.1109.
440. Moore WEC, Holdeman LV. Discussion of current bacteriological investigations of the relationships between intestinal flora, diet, and colon cancer. *Cancer Research*. 1975;35(11 Part 2):3418.
441. Bultman SJ. Interplay between diet, gut microbiota, epigenetic events, and colorectal cancer. *Molecular Nutrition & Food Research*. 2016;61(1):1500902. doi: 10.1002/mnfr.201500902.
442. Hansen AK, Friis Hansen CH, Krych L, Nielsen DS. Impact of the gut microbiota on rodent models of human disease. *World Journal of Gastroenterology*. 2014;20(47):17727-36. doi: 10.3748/wjg.v20.i47.17727. PubMed PMID: PMC4273123.
443. Hörmannspurger G, Schaubeck M, Haller D. Intestinal microbiota in animal models of inflammatory diseases. *ILAR Journal*. 2015;56(2):179-91. doi: 10.1093/ilar/ilv019.
444. Gagnière J, Raisch J, Veziat J, Barnich N, Bonnet R, Buc E, Bringer M-A, Pezet D, Bonnet M. Gut microbiota imbalance and colorectal cancer. *World Journal of Gastroenterology*. 2016;22(2):501-18. doi: 10.3748/wjg.v22.i2.501. PubMed PMID: PMC4716055.
445. Oke S, Martin A. Insights into the role of the intestinal microbiota in colon cancer. *Therapeutic Advances in Gastroenterology*. 2017;10(5):417-28. doi: 10.1177/1756283X17694832. PubMed PMID: PMC5415097.
446. Gkouskou KK, Deligianni C, Tsatsanis C, Eliopoulos AG. The gut microbiota in mouse models of inflammatory bowel disease. *Frontiers in Cellular & Infection Microbiology*. 2014;4:28. doi: 10.3389/fcimb.2014.00028. PubMed PMID: PMC3937555.
447. Li Y, Kundu P, Seow SW, de Matos CT, Aronsson L, Chin KC, Kärre K, Pettersson S, Greicius G. Gut microbiota accelerate tumor growth via c-jun and STAT3 phosphorylation in *Apc^{Min/+}* mice. *Carcinogenesis*. 2012;33(6):1231-8. doi: 10.1093/carcin/bgs137.

448. Huang G, Khan I, Li X, Chen L, Leong W, Ho LT, Hsiao WLW. Ginsenosides Rb3 and Rd reduce polyps formation while reinstate the dysbiotic gut microbiota and the intestinal microenvironment in *Apc^{Min/+}* mice. *Scientific Reports*. 2017;7(1):12552. Epub 2017/10/04. doi: 10.1038/s41598-017-12644-5. PubMed PMID: 28970547; PMCID: PMC5624945.
449. Yang Y, Jobin C. Microbial imbalance and intestinal pathologies: connections and contributions. *Disease Models & Mechanisms*. 2014;7(10):1131-1142. doi:10.1242/dmm.016428. PubMed PMID: 25256712.
450. Kawajiri K, Kobayashi Y, Ohtake F, Ikuta T, Matsushima Y, Mimura J, Pettersson S, Pollenz RS, Sakaki T, Hirokawa T, Akiyama T, Kurosumi M, Poellinger L, Kato S, Fujii-Kuriyama Y. Aryl hydrocarbon receptor suppresses intestinal carcinogenesis in *Apc^{Min/+}* mice with natural ligands. *Proceedings of the National Academy of Sciences of the United States of America*. 2009;106(32):13481-6. doi: 10.1073/pnas.0902132106. PubMed PMID: 19651607.
451. Park CH, Eun CS, Han DS. Intestinal microbiota, chronic inflammation, and colorectal cancer. *Intestinal Research*. 2018;16(3), 338-345. doi:10.5217/ir.2018.16.3.338.
452. Holmes E, Li JV, Athanasiou T, Ashrafiyan H, Nicholson JK. Understanding the role of gut microbiome in host metabolic signal disruption in health and disease. *Trends in Microbiology*. 19(7):349-59. doi: 10.1016/j.tim.2011.05.006.
453. Pope JL, Tomkovich S, Yang Y, Jobin C. Microbiota as a mediator of cancer progression and therapy. *Translational Research: the journal of Laboratory & Clinical Medicine*. 2017;179:139-54. Epub 2016/08/25. doi: 10.1016/j.trsl.2016.07.021. PubMed PMID: 27554797; PMCID: PMC5674984.
454. Lustrì BC, Sperandio V, Moreira CG. Bacterial chat: intestinal metabolites and signals in host-microbiota-pathogen interactions. *Infection & Immunity*. 2017;85(12). pii: e00476-17. doi: 10.1128/iai.00476-17.
455. Wikoff WR, Anfora AT, Liu J, Schultz PG, Lesley SA, Peters EC, Siuzdak G. Metabolomics analysis reveals large effects of gut microflora on mammalian blood metabolites. *Proceedings of the National Academy of Sciences of the United States of America*. 2009;106(10):3698-703.
456. J.J. D. Metabolomics of *Apc^{Min/+}* mice genetically susceptible to intestinal cancer. *BMC Systems Biology*. 2014;8(72). doi:10.1186/1752-0509-8-72. PubMed PMID: 24954394.
457. Yoshie T, Nishiumi S, Izumi Y, Sakai A, Inoue J, Azuma T, Yoshida M. Regulation of the metabolite profile by an APC gene mutation in colorectal cancer. *Cancer Science*. 2012;103(6):1010-21. doi: 10.1111/j.1349-7006.2012.02262.x. PubMed PMID: 22380946.

458. Avula B, Wang Y-H, Isaac G, Yuk J, Wrona M, Yu K, Khan IA. Metabolic profiling of hoodia, chamomile, terminalia species and evaluation of commercial preparations using ultrahigh-performance liquid chromatography quadrupole-time-of-flight mass spectrometry. *Planta Medica*. 2017;83(16):1297-308. Epub 28.04.2017. doi: 10.1055/s-0043-109239.
459. Lei Z, Jing L, Qiu F, Zhang H, Huhman D, Zhou Z, Sumner LW. Construction of an ultrahigh pressure liquid chromatography-tandem mass spectral library of plant natural products and comparative spectral analyses. *Analytical Chemistry*. 2015;87(14):7373-81. doi: 10.1021/acs.analchem.5b01559.
460. Schooling CM. Could androgens be relevant to partly explain why men have lower life expectancy than women? *Journal of Epidemiological & Community Health*. 2016;70:324-328. <http://dx.doi.org/10.1136/jech-2015-206336>. PubMed PMID: 26659456.
461. Peña-Llopis S, Brugarolas J. Simultaneous isolation of high-quality DNA, RNA, miRNA and proteins from tissues for genomic applications. *Nature Protocols*. 2013;8(11):2240-55. doi: 10.1038/nprot.2013.141. PubMed PMID: PMC4211643.
462. Frey KG, Herrera-Galeano JE, Redden CL, Luu TV, Servetas SL, Mateczun AJ, Mokashi VP, Bishop-Lilly KA. Comparison of three next-generation sequencing platforms for metagenomic sequencing and identification of pathogens in blood. *BMC Genomics*. 2014;15:96-. doi: 10.1186/1471-2164-15-96. PubMed PMID: PMC3922542.
463. Trapnell C, Roberts A, Goff L, Pertea G, Kim D, Kelley DR, Pimentel H, Salzberg SL, Rinn JL, Pachter L. Differential gene and transcript expression analysis of RNA-seq experiments with TopHat and Cufflinks. *Nature Protocols*. 2012;7(3):562-78. Epub 2012/03/03. doi: 10.1038/nprot.2012.016. PubMed PMID: 22383036; PMCID: PMC3334321.
464. Bolger AM, Lohse M, Usadel B. Trimmomatic: a flexible trimmer for Illumina sequence data. *Bioinformatics*. 2014;30(15):2114-20. Epub 2014/04/04. doi: 10.1093/bioinformatics/btu170. PubMed PMID: 24695404; PMCID: PMC4103590.
465. Love MI, Huber W, Anders S. Moderated estimation of fold-change and dispersion for RNA-seq data with DESeq2. *Genome Biology*. 2014;15(12):550. Epub 2014/12/18. doi: 10.1186/s13059-014-0550-8. PubMed PMID: 25516281; PMCID: PMC4302049.
466. Xia J, Sinelnikov IV, Han B, Wishart DS. MetaboAnalyst 3.0-making metabolomics more meaningful. *Nucleic Acids Research*. 2015;43(W1):W251-7. Epub 2015/04/22. doi: 10.1093/nar/gkv380. PubMed PMID: 25897128; PMCID: PMC4489235.
467. Smith CA, Want EJ, O'Maille G, Abagyan R, Siuzdak G. XCMS: processing mass spectrometry data for metabolite profiling using nonlinear peak alignment,

- matching, and identification. *Analytical Chemistry*. 2006;78(3):779-87. Epub 2006/02/02. doi: 10.1021/ac051437y. PubMed PMID: 16448051.
468. Zhang Z, Castelló A. Principal components analysis in clinical studies. *Annals of Translational Medicine*. 2017;5(17):351. doi: 10.21037/atm.2017.07.12. PubMed PMID: PMC5599285.
469. Dixon P. VEGAN, a package of R functions for community ecology. *Journal of Vegetation Science*. 2003;14(6):927-30.
470. Deng L, Chang D, Foshaug RR, Eisner R, Tso VK, Wishart DS, Fedorak RN. Development and validation of a high-throughput mass spectrometry based urine metabolomic test for the detection of colonic adenomatous polyps. *Metabolites*. 2017;7(3). doi: 10.3390/metabo7030032. PubMed PMID: 28640228; PMCID: PMC5618317.
471. Sumner LW, Lei Z, Nikolau BJ, Saito K. Modern plant metabolomics: advanced natural product gene discoveries, improved technologies, and future prospects. *Natural Product Reports*. 2015;32(2):212-29. doi: 10.1039/C4NP00072B.
472. Anil Bhatia SJS, Zhentian Lei, and Lloyd W. Sumner. UHPLC-QTOF-MS/MS-SPE-NMR is a solution to the metabolomics grand challenge of higher-throughput, confident metabolite identifications. *Methods in Molecular Biology*. Submitted 31 Aug 2018.
473. Hornbrook MC, Goshen R, Choman E, O'Keeffe-Rosetti M, Kinar Y, Liles EG, Rust KC. Early colorectal cancer detected by machine learning model using gender, age, and complete blood count data. *Digestive Diseases & Sciences*. 2017;62(10):2719-27. Epub 2017/08/25. doi: 10.1007/s10620-017-4722-8. PubMed PMID: 28836087.
474. Roadknight C, Aickelin U, Qiu G, Scholefield J, Durrant L, editors. Supervised learning and anti-learning of colorectal cancer classes and survival rates from cellular biology parameters. 2012 IEEE International Conference on Systems, Man, & Cybernetics (SMC); 2012 14-17 Oct. 2012.
475. Ajouz H, Mukherji D, Shamseddine A. Secondary bile acids: an underrecognized cause of colon cancer. *World Journal of Surgical Oncology*. 2014;12:164-. doi: 10.1186/1477-7819-12-164. PubMed PMID: PMC4041630.
476. Farhana L, Nangia-Makker P, Arbit E, Shango K, Sarkar S, Mahmud H, Hadden T, Yu Y, Majumdar APN. Bile acid: a potential inducer of colon cancer stem cells. *Stem Cell Research & Therapy*. 2016;7:181. doi: 10.1186/s13287-016-0439-4. PubMed PMID: PMC5134122.
477. Chaplin MF. Review: Bile acids, fibre and colon cancer: the story unfolds. *Journal of the Royal Society of Health*. 1998;118(1):53-61. doi: 10.1177/146642409811800111.

478. Bayerdorffer E, Mannes GA, Richter WO, Ochsenkuhn T, Wiebecke B, Kopcke W, Paumgartner G. Increased serum deoxycholic acid levels in men with colorectal adenomas. *Gastroenterology*. 1993;104(1):145-51. Epub 1993/01/01. PubMed PMID: 8419237.
479. Nagengast FM, Grubben MJ, van Munster IP. Role of bile acids in colorectal carcinogenesis. *European Journal of Cancer*. 1995;31a(7-8):1067-70. Epub 1995/07/01. PubMed PMID: 7576993.
480. Glinghammar B, Inoue H, Rafter JJ. Deoxycholic acid causes DNA damage in colonic cells with subsequent induction of caspases, COX-2 promoter activity and the transcription factors NF-kB and AP-1. *Carcinogenesis*. 2002;23(5):839-45. Epub 2002/05/23. PubMed PMID: 12016158.
481. Ridlon JM, Bajaj JS. The human gut sterolbiome: bile acid-microbiome endocrine aspects and therapeutics. *Acta Pharmaceutica Sinica B*. 2015;5(2):99-105. doi: 10.1016/j.apsb.2015.01.006. PubMed PMID: PMC4629220.
482. Kure I, Nishiumi S, Nishitani Y, Tanoue T, Ishida T, Mizuno M, Fujita T, Kutsumi H, Arita M, Azuma T, Yoshida M. Lipoxin A(4) reduces lipopolysaccharide-induced inflammation in macrophages and intestinal epithelial cells through inhibition of nuclear factor-kappaB activation. *The Journal of Pharmacology & Experimental Therapeutics*. 2010;332(2):541-8. Epub 2009/10/23. doi: 10.1124/jpet.109.159046. PubMed PMID: 19846590.
483. Janakiram NB, Mohammed A, Rao CV. Role of lipoxins, resolvins, and other bioactive lipids in colon and pancreatic cancer. *Cancer and Metastasis Reviews*. 2011;30(3-4):507-23. Epub 2011/10/22. doi: 10.1007/s10555-011-9311-2. PubMed PMID: 22015691.
484. Janakiram NB, Rao CV. Role of lipoxins and resolvins as anti-inflammatory and proresolving mediators in colon cancer. *Current Molecular Medicine*. 2009;9(5):565-79. Epub 2009/07/16. PubMed PMID: 19601807.
485. Huang ES, Strate LL, Ho WW, Lee SS, Chan AT. A prospective study of aspirin use and the risk of gastrointestinal bleeding in men. *PLOS One*. 2011;5(12):e15721. doi: 10.1371/journal.pone.0015721.
486. Chan AT, Giovannucci EL, Meyerhardt JA, Schernhammer ES, Curhan GC, Fuchs CS. Long-term use of aspirin and nonsteroidal anti-inflammatory drugs and risk of colorectal cancer. *Journal of the American Medical Association*. 2005;294(8):914-23. doi: 10.1001/jama.294.8.914.
487. Rothwell PM, Wilson M, Elwin CE, Norrving B, Algra A, Warlow CP, Meade TW. Long-term effect of aspirin on colorectal cancer incidence and mortality: 20-year follow-up of five randomised trials. *Lancet*. 2010;376(9754):1741-50. Epub 2010/10/26. doi: 10.1016/s0140-6736(10)61543-7. PubMed PMID: 20970847.

488. Ishikawa H, Mutoh M, Suzuki S, Tokudome S, Saida Y, Abe T, Okamura S, Tajika M, Joh T, Tanaka S, Kudo SE, Matsuda T, Iimuro M, Yukawa T, Takayama T, Sato Y, Lee K, Kitamura S, Mizuno M, Sano Y, Gondo N, Sugimoto K, Kusunoki M, Goto C, Matsuura N, Sakai T, Wakabayashi K. The preventive effects of low-dose enteric-coated aspirin tablets on the development of colorectal tumours in Asian patients: a randomised trial. *Gut*. 2014;63(11):1755-9. Epub 2014/02/04. doi: 10.1136/gutjnl-2013-305827. PubMed PMID: 24488498.
489. Femia AP, Luceri C, Lodovici M, Crucitta S, Caderni G. Gene expression profile of colon mucosa after cytotoxic insult in wt and apc-mutated pirc rats: possible relation to resistance to apoptosis during carcinogenesis. *BioMed Research International*. 2016;8. doi: 10.1155/2016/1310342. PubMed PMID: 27840820.
490. Femia AP, Luceri C, Soares PV, Lodovici M, Caderni G. Multiple mucin depleted foci, high proliferation and low apoptotic response in the onset of colon carcinogenesis of the Pirc rat, mutated in Apc. *International Journal of Cancer*. 2015;136(6):E488-95. Epub 2014/09/27. doi: 10.1002/ijc.29232. PubMed PMID: 25257656.
491. Femia AP, Soares PV, Luceri C, Lodovici M, Giannini A, Caderni G. Sulindac, 3,3'-diindolylmethane and curcumin reduce carcinogenesis in the Pirc rat, an Apc-driven model of colon carcinogenesis. *BMC Cancer*. 2015;15(1):611. doi: 10.1186/s12885-015-1627-9.
492. Makar KW, Poole EM, Resler AJ, Seufert B, Curtin K, Kleinstein SE, Duggan D, Kulmacz RJ, Hsu L, Whitton J, Carlson CS, Rimorin CF, Caan BJ, Baron JA, Potter JD, Slattery ML, Ulrich CM. COX-1 (PTGS1) and COX-2 (PTGS2) polymorphisms, NSAID interactions, and risk of colon and rectal cancer in two independent populations. *Cancer Causes & Control: CCC*. 2013;24(12):2059-75. doi: 10.1007/s10552-013-0282-1. PubMed PMID: PMC3913564.
493. Dixon DA, Blanco FF, Bruno A, Patrignani P. Chapter 2: Mechanistic ASPECTS of COX-2 expression in colorectal neoplasia. *Recent Results in Cancer Research: Fortschritte der Krebsforschung Progres dans les Recherches sur le Cancer*. 2013;191:7-37. doi: 10.1007/978-3-642-30331-9_2. PubMed PMID: PMC3477597.
494. Habermann N, Ulrich CM, Lundgreen A, Makar KW, Poole EM, Caan B, Kulmacz R, Whitton J, Galbraith R, Potter JD, Slattery ML. PTGS1, PTGS2, ALOX5, ALOX12, ALOX15, and FLAP SNPs: interaction with fatty acids in colon cancer and rectal cancer. *Genes & Nutrition*. 2013;8(1):115-26. Epub 2012/06/09. doi: 10.1007/s12263-012-0302-x. PubMed PMID: 22678777; PMCID: PMC3534991.
495. Che XH, Chen CL, Ye XL, Weng GB, Guo XZ, Yu WY, Tao J, Chen YC, Chen X. Dual inhibition of COX-2/5-LOX blocks colon cancer proliferation, migration and invasion in vitro. *Oncology Reports*. 2016;35(3):1680-8. Epub 2015/12/29. doi: 10.3892/or.2015.4506. PubMed PMID: 26707712.

496. Mashima R, Okuyama T. The role of lipoxygenases in pathophysiology; new insights and future perspectives. *Redox Biology*. 2015;6:297-310. doi: <https://doi.org/10.1016/j.redox.2015.08.006>.
497. Swan R, Alnabulsi A, Cash B, Alnabulsi A, Murray GI. Characterisation of the oxysterol metabolising enzyme pathway in mismatch repair proficient and deficient colorectal cancer. *Oncotarget*. 2016;7(29):46509-27. doi: 10.18632/oncotarget.10224. PubMed PMID: PMC5216813.
498. Tsuei J, Chau T, Mills D, Wan Y-JY. Bile acid dysregulation, gut dysbiosis, and gastrointestinal cancer. *Experimental Biology & Medicine*. 2014;239(11):1489-504. doi: 10.1177/1535370214538743. PubMed PMID: PMC4357421.
499. Ridlon JM, Kang DH, Hylemon PB. Bile salt transformation by human intestinal bacteria. *Journal of Lipid Research*. 2006;47(2):241-59. doi: 10.1194/jlr.R500013-JLR200. PubMed PMID: 16299351.
500. Kundu S, Kumar S, Bajaj A. Cross-talk between bile acids and gastrointestinal tract for progression and development of cancer and its therapeutic implications. *IUBMB Life*. 2015;67(7):514-23. Epub 2015/07/17. doi: 10.1002/iub.1399. PubMed PMID: 26177921.
501. Aymeric L, Donnadiou F, Mulet C, du Merle L, Nigro G, Saffarian A, Berard M, Poyart C, Robine S, Regnault B, Trieu-Cuot P, Sansonetti PJ, Dramsi S. Colorectal cancer specific conditions promote *Streptococcus gallolyticus* gut colonization. *Proceedings of the National Academy of Sciences of the United States of America*. 2018;115(2):E283-e91. Epub 2017/12/28. doi: 10.1073/pnas.1715112115. PubMed PMID: 29279402; PMCID: PMC5777054.
502. Cao L, Che Y, Meng T, Deng S, Zhang J, Zhao M, Xu W, Wang D, Pu Z, Wang G, Hao H. Repression of intestinal transporters and FXR-FGF15 signaling explains bile acids dysregulation in experimental colitis-associated colon cancer. *Oncotarget*. 2017;8(38):63665-79. doi: 10.18632/oncotarget.18885. PubMed PMID: PMC5609951.
503. Berridge MJ, Lipp P, Bootman MD. The versatility and universality of calcium signalling. *Nature Reviews Molecular Cell Biology*. 2000;1(1):11-21. Epub 2001/06/20. doi: 10.1038/35036035. PubMed PMID: 11413485.
504. Roderick HL, Cook SJ. Ca²⁺ signalling checkpoints in cancer: remodelling Ca²⁺ for cancer cell proliferation and survival. *Nature Reviews Cancer*. 2008;8(5):361-75. Epub 2008/04/25. doi: 10.1038/nrc2374. PubMed PMID: 18432251.
505. Irving AA, Plum LA, Blaser WJ, Ford MR, Weng C, Clipson L, DeLuca HF, Dove WF. Cholecalciferol or 25-hydroxycholecalciferol neither prevents nor treats adenomas in a rat model of familial colon cancer. *The Journal of Nutrition*. 2015;145(2):291-8. doi: 10.3945/jn.114.204396. PubMed PMID: PMC4304025.

506. Wactawski-Wende J, Kotchen JM, Anderson GL, Assaf AR, Brunner RL, O'Sullivan MJ, Margolis KL, Ockene JK, Phillips L, Pottern L, Prentice RL, Robbins J, Rohan TE, Sarto GE, Sharma S, Stefanick ML, Van Horn L, Wallace RB, Whitlock E, Bassford T, Beresford SA, Black HR, Bonds DE, Brzyski RG, Caan B, Chlebowski RT, Cochrane B, Garland C, Gass M, Hays J, Heiss G, Hendrix SL, Howard BV, Hsia J, Hubbell FA, Jackson RD, Johnson KC, Judd H, Kooperberg CL, Kuller LH, LaCroix AZ, Lane DS, Langer RD, Lasser NL, Lewis CE, Limacher MC, Manson JE. Calcium plus vitamin D supplementation and the risk of colorectal cancer. *The New England Journal of Medicine*. 2006;354(7):684-96. Epub 2006/02/17. doi: 10.1056/NEJMoa055222. PubMed PMID: 16481636.
507. Han C, Shin A, Lee J, Lee J, Park JW, Oh JH, Kim J. Dietary calcium intake and the risk of colorectal cancer: a case control study. *BMC Cancer*. 2015;15:966. doi: 10.1186/s12885-015-1963-9. PubMed PMID: PMC4682267.
508. Cho E, Smith-Warner SA, Spiegelman D, Beeson WL, van den Brandt PA, Colditz GA, Folsom AR, Fraser GE, Freudenheim JL, Giovannucci E, Goldbohm RA, Graham S, Miller AB, Pietinen P, Potter JD, Rohan TE, Terry P, Toniolo P, Virtanen MJ, Willett WC, Wolk A, Wu K, Yaun SS, Zeleniuch-Jacquotte A, Hunter DJ. Dairy foods, calcium, and colorectal cancer: a pooled analysis of 10 cohort studies. *Journal of the National Cancer Institute*. 2004;96(13):1015-22. Epub 2004/07/09. PubMed PMID: 15240785.
509. Dai Q, Shrubsole MJ, Ness RM, Schlundt D, Cai Q, Smalley WE, Li M, Shyr Y, Zheng W. The relation of magnesium and calcium intakes and a genetic polymorphism in the magnesium transporter to colorectal neoplasia risk. *The American Journal of Clinical Nutrition*. 2007;86(3):743-51. Epub 2007/09/08. doi: 10.1093/ajcn/86.3.743. PubMed PMID: 17823441; PMCID: PMC2082111.
510. Baron JA, Beach M, Mandel JS, van Stolk RU, Haile RW, Sandler RS, Rothstein R, Summers RW, Snover DC, Beck GJ, Bond JH, Greenberg ER. Calcium supplements for the prevention of colorectal adenomas. Calcium Polyp Prevention Study Group. *The New England Journal of Medicine*. 1999;340(2):101-7. Epub 1999/01/14. doi: 10.1056/nejm199901143400204. PubMed PMID: 9887161.
511. Geng J, Song Q, Tang X, Liang X, Fan H, Peng H, Guo Q, Zhang Z. Co-occurrence of driver and passenger bacteria in human colorectal cancer. *Gut Pathogens*. 2014;6:26-. doi: 10.1186/1757-4749-6-26. PubMed PMID: PMC4080773.
512. Scanlan PD, Shanahan F, Marchesi JR. Culture-independent analysis of desulfovibrios in the human distal colon of healthy, colorectal cancer and polypectomized individuals. *FEMS Microbiology Ecology*. 2009;69(2):213-21. doi: 10.1111/j.1574-6941.2009.00709.x.
513. Pearson, T., J. G. Caporaso, M. Yellowhair, N. A. Bokulich, D. J. Roe, B. C. Wertheim, M. Linhart, J. A. Martinez, C. Bilagody, H. Hornstra, D. S. Alberts, P. Lance

and P. A. Thompson. Lack of evidence that ursodeoxycholic acid's effects on the gut microbiome influence colorectal adenoma risk. bioRxiv. 2017. doi: 10.1101/237495.

VITA

Susheel Bhanu Busi was born in Salur in the state of Andhra Pradesh in India on a midsummer's day. After his schooling in various cities, he received his degree in Bachelor of Science majoring in Microbiology from Madras Christian College, Chennai, India in 2008. It was at this time that Google Inc. recruited Susheel out of college to work as an AdWords Representative. Despite the liberal and thriving environment, he chose to pursue his passion of research and science. This quest led him on his journey to Hood College, Frederick, MD, where he received his Master's degree in Biomedical Science. It was also during this time that Susheel Busi worked concurrently with a company, manufacturing and researching the probiotic bacteria, *Pediococcus acidilactici* under Dr. J.J.Lin. His work in developing a strain that could withstand extremely high temperatures and a low pH environment simultaneously was granted a Patent through the United States Patent and Trademarks Office in 2013.

The desire to understand the mechanisms by which probiotic strains provide beneficial effects to mammalian hosts drove Susheel to then attend University of Missouri. His pursuit for answers was supported through the Molecular Pathogenesis and Therapeutics program offered by the MMI (Molecular Microbiology and Immunology) and the VPB (Veterinary Pathobiology) departments at the School of Medicine and the School of Veterinary Medicine. Under the able and very knowledgeable mentorship of Dr. James Amos-Landgraf and Dr. Craig Franklin, he sought to unravel the role of bacteria in the gastrointestinal tract and their effect on the development of colon cancer. Some of his findings and consequent reflections are presented within this body of research.

Susheel continues to have a strong interest in research and hopes to one day share the enthusiasm for research with the next generation of scientists through teaching and mentorship. Throughout his fledgling research career, Susheel has learnt many a lesson from his students, peers, and mentors. He expresses his gratitude to his family, and hopes to acknowledge every being that made a difference in his life at some point or the other. He hopes to continue sharing these stories and create an environment whereupon, all members of the scientific community may benefit from his ideas and research. Susheel hopes to unravel the complex interactions that exist between a host, its environment and the concurrent processes that affect vice versa. He wishes to continue in Academia, slowly, but steadily teasing apart the complexity of microbiological research, thus continuing to make an impact on improving human health one day at a time.